Xavier Prats i Menéndez

Contributions to the optimisation of aircraft noise abatement procedures

Doctoral Thesis

VIII abertis Prize - Honorable mention

UPC cátedra abertis

Xavier Prats i Menéndez

Contributions to the optimisation of aircraft noise abatement procedures

Doctoral Thesis

VIII abertis Prize - Honorable mention

cátedra abertis

Primera edición: mayo de 2011

càtedra abertis de Gestión de Infraestructuras del Transporte
Universitat Politècnica de Catalunya
Jordi Girona 1-3, edificio B1 - 101
08034 Barcelona
tel.: 93 4015655, Fax: 93 4017264
catedra.abertis@upc.edu
www.catedrasabertis.com

Maquetación: Vicenç Marco Design
Producción: GR Impressors - Gráficas Rotativas, S.A.

Pórtico

El modelo de colaboración entre universidad y empresa iniciado en 2003 por **abertis** y la Universitat Politècnica de Catalunya para la creación de la **cátedra abertis**-UPC ha demostrado ser una propuesta de éxito que ha sido validada tanto por la cantidad como por la calidad de las actividades desarrolladas por la cátedra en ámbitos como la investigación, la formación o la divulgación de contenidos relacionados con la gestión de infraestructuras para la movilidad y las comunicaciones.

La experiencia acumulada durante todos estos años ha inspirado proyectos similares con otras universidades y centros de excelencia en países donde el grupo **abertis** desarrolla su actividades. Cada una de estas iniciativas se centra en la investigación y en la formación en diferentes aspectos que afectan a la gestión de las infraestructuras. Todas ellas, enmarcadas dentro de la Responsabilidad Social Corporativa de **abertis**, facilitan la transferencia de conocimiento entre universidad y empresa, además de reforzar la implicación de nuestro Grupo en la sociedad que lo acoge.

En esta línea, en Francia se ha dado un paso más en esta dirección al crearse la **chaire abertis** conjuntamente con l'École des Ponts ParisTech (ENPC) y el Institut Français des Sciences et Technologies des Transports, de l'Aménagement et des Réseaux (IFSTTAR). Este mismo año, la **cátedra abertis**-UPC y la **chaire abertis**-ENPC-IFSTTAR convocan el primer Premio **abertis** internacional de investigación en gestión de infraestructuras de transporte, alcanzando así un nuevo hito en la internacionalización de las cátedras **abertis** que refuerza además la vocación europea del Grupo, desarrollando a su vez una experiencia pionera de trabajo en red que posibilita el trabajo conjunto, el intercambio de experiencias y la generación de sinergias entre los expertos de universidades y centros de excelencia con los gestores de las infraestructuras de los distintos países.

El lector encontrará más información sobre las actividades de las cátedras en la web:
www.catedrasabertis.com

abertis

fundación abertis

Presentación

La **cátedra abertis** de la Universidad Politécnica de Cataluña (UPC) promueve la realización de seminarios y conferencias y la investigación sobre la gestión de infraestructuras del transporte estructurada en seis ejes de actividad de la corporación: carreteras y autopistas, aparcamientos, seguridad vial, logística, aeropuertos y sistemas de transporte inteligentes.

Asimismo, con objeto de potenciar el interés de los universitarios españoles, incluyendo estudiantes de titulaciones regladas y de máster y doctorado, la **cátedra abertis** establece anualmente el Premio **abertis**, al mejor trabajo de investigación inédito en gestión del transporte (tesis doctoral, tesina, trabajo tutelado, etc.) realizado por estudiantes en España.

En la octava convocatoria de 2010, se presentaron quince candidatos, todos ellos de elevada calidad, con contribuciones como: viabilidad de un mercado de futuros y opciones sobre franjas horarias aeroportuarias, estimación de matrices de movilidad mediante datos de telefonía móvil, análisis del sector de los operadores logísticos, minimización del ruido de las aeronaves gestionando las trayectorias de aproximación, análisis de la longitud de los carriles de deceleración en carreteras, estimación del tiempo de viaje en autopista con fusión de datos, guía para la elaboración de Planes Urbanos de Moderación del Tráfico, robustez en logística aplicada al transporte ferroviario de pasajeros, mejora de la seguridad en carretera en intersecciones, efectos de la implantación de tarifación dinámica sobre la equidad, análisis de la distancia de visibilidad de adelantamiento, relaciones entre infraestructura y territorio, rentabilidad económica y social del Bicing y un análisis del flujo peatonal de las estaciones ferroviarias .

Ha resultado ganador de un Accésit al **VIII Premio abertis 2010** en la categoría de Tesis Doctorales, la tesis del Dr. **Xavier Prats i Menéndez**, Ingeniero Aeronáutico y de Telecomunicaciones por la Universitat Politècnica de Catalunya con su tesis "Contributions to the optimization of aircraft noise abatement procedures".

La tesis trata de minimizar el sonido generado por las operaciones de las aeronaves, asumiendo al mismo tiempo la creciente demanda de vuelos. En los próximos años se esperan nuevos sistemas de aviónica y conceptos de gestión del tráfico aéreo que permitirán mejorar el diseño de estos procedimientos, permitiendo la definición de procedimientos de vuelo óptimos desde un punto de vista de impacto acústico. La tesis propone una metodología para diseñar estos procedimientos de forma automática o semi-automática para un sistema experto basado en técnicas de optimización multi-objetivo. La metodología se ha aplicado con éxito a un escenario real y complejo donde se optimizan las salidas hacia el este de la pista 02 del aeropuerto de Girona.

Prof. **Francesc Robusté**
Director de la **cátedra abertis**-UPC

Contributions to the Optimisation of Aircraft Noise Abatement Procedures

XAVIER PRATS I MENÉNDEZ

Aeronautical Engineer
Telecommunications Engineer

Advisers
DR. JOSEBA QUEVEDO CASIN
DR. VICENÇ PUIG I CAYUELA

Doctorate program in Aerospace Science and Technology
Technical School of Castelldefels
Technical University of Catalonia

Programa de doctorat en Ciència i Tecnologia Aeroespacial
Escola Politècnica Superior de Castelldefels (EPSC)
Universitat Politècnica de Catalunya (UPC)

A dissertation submitted for the degree of
European Doctor of Philosophy
January 2010

Contributions to the Optimisation of Aircraft Noise Abatement Procedures

Doctorate program in Aerospace Science and Technology
Technical University of Catalonia
January 2010

PhD. Thesis made in:
Technical School of Castelldefels
Esteve Terradas, 5.
08860 Castelldefels
Catalonia (Spain)

A la meva família,
que tant a prop tinc.

Contents

List of Figures

Figures in Appendices

List of Tables

Tables in Appendices

List of Publications

The list of publications resulting from this PhD. work is given in inverse chronological order as follows:

Journal Papers

- PRATS, XAVIER, PUIG, VICENÇ, QUEVEDO, JOSEBA, & NEJJARI, FATIHA. 2009. Multi-objective optimisation for aircraft departure trajectories minimising noise annoyance. *Journal of Transportation Research - Part C*. Accepted for publication.
- PRATS, XAVIER, PUIG, VICENÇ, QUEVEDO, JOSEBA, & NEJJARI, FATIHA. 2009. Lexicographic optimisation for optimal departure aircraft trajectories. *Aerospace Science and Technology*. In press. D.O.I: 10.1016/j.ast.2009.11.003
- PRATS, XAVIER, QUEVEDO, JOSEBA, FATIHA, NEJJARI, & PUIG, VICENÇ. 2007. Optimisation of aircraft trajectories in order to minimise noise nuisances modelled with fuzzy logic – Optimización de trayectorias de aviones para minimizar la molestia acústica modelizada mediante lógica borrosa. *Revista iberoamericana de automática e informática industrial*, ISSN 1697-7912 **4**(2), 43–51. (in Spanish).

Conference Proceedings

- PRATS, XAVIER, PUIG, VICENÇ, QUEVEDO, JOSEBA, & NEJJARI, FATIHA. 2009 (Sept.). Equitable noise abatement departure procedures. *In: Proceedings of the 9th AIAA Aviation Technology, Integration, and Operations (ATIO) conference*. AIAA, Hilton Head, South Carolina (USA).
- PRATS, XAVIER, QUEVEDO, JOSEBA, & PUIG, VICENÇ. 2009 (Mar.). Trajectory management for aircraft noise mitigation. *In: Proceedings of the ENRI International Workshop on ATM/CNS (EIWAC)*. Electronic Navigation Research Institute (ENRI), Tokyo (Japan). **Invited conference.**
- PRATS, XAVIER, PUIG, VICENÇ, QUEVEDO, JOSEBA, & NEJJARI, FATIHA. 2008 (Sept.). Hierarchical and sensitivity analysis for noise abatement departure procedures. *In: Proceedings of the 8th AIAA Aviation Technology, Integration, and Operations (ATIO) conference*. AIAA, Anchorage, Alaska (USA).

- PRATS, XAVIER, PUIG, VICENÇ, QUEVEDO, JOSEBA, & NEJJARI, FATIHA. 2008 (Jun.). Optimal departure aircraft trajectories minimising population annoyance. *Pages 421–428 of: Proceedings of the 3rd international congress on research in air transportation (ICRAT)*. EUROCONTROL & George Mason University, Fairfax, Virginia (USA). **Best paper in track award.**

- PRATS, XAVIER, QUEVEDO, JOSEBA, PUIG, VICENÇ, & NEJJARI, FATIHA. 2007 (Aug.). Planning of aircraft departure trajectories by using fuzzy logic and lexicographic optimisation. *In: Proceedings of the 36th congress and exposition on noise control engineering*. Turkish AcoTurkish Acoustical Society; IZOCAM, Istanbul (Turkey).

- QUEVEDO, JOSEBA, PRATS, XAVIER, NEJJARI, FATIHA, & PUIG, VICENÇ. 2007 (May). Aircraft annoyance minimization around urban airports based on fuzzy logic. *In: Proceedings of the conference on systems and control (CSC)*. GERAD,École Polytechnique de Montreal & Cadi Ayyad University, Marrakesh, Morocco.

- PRATS, XAVIER, NEJJARI, FATIHA, PUIG, VICENÇ, QUEVEDO, JOSEBA, & MORA-CAMINO, FELIX. 2006 (Jun.). A framework for RNAV trajectory generation minimising noise nuisances. *Pages 19–28 of: Proceedings of the 2nd international congress on research in air transportation (ICRAT)*. EUROCONTROL & Faculty of Transport and Traffic Engineering of Belgrade University, Belgrade (Serbia). **Best paper in track award.**

- PRATS, XAVIER, QUEVEDO, JOSEBA, NEJJARI, FATIHA, & PUIG, VICENÇ. 2006 (Jun.). Noise nuisance model for optimising flight trajectories around airports. *In: Proceedings of the 8th international symposium in transport noise and vibration*. East European Acoustical Association, St. Petersburg (Russia).

- NEJJARI, FATIHA, PRATS, XAVIER, PUIG, VICENÇ, QUEVEDO, JOSEBA, POLIT, MONIQUE, OUATTARA, BABA, ACHAIBOU, KARIM, & MORA-CAMINO, FELIX. 2005 (Aug.). Containing aircraft noise levels at take-off: a mathematical programming approach. *In: Proceedings of the 34th congress and exposition on noise control engineering*. International Institute of Noise Control Engineering (I-INCE), Brazilian Acoustical Society (SOBRAC) & Iberoamerican Federation of Acoustic, Rio de Janeiro (Brazil).

Agraïments

Tot va començar amb un dinar. Minuts abans, el Dr. Joseba Quevedo havia impartit una conferència exposant les línies i projectes de recerca que es duien a terme al grup SAC (Sistemes Avançats de Control) de la UPC. O això suposo, ja que vaig arribar tard. La sort però, es que el Dr. Quevedo es va guardar la millor part pel final: va parlar d'avions i molèsties acústiques, de trajectòries i d'optimització. El tema em va agradar. Com dèiem, la conferència va continuar amb un dinar on ponent i audiència podien seguir discutint en un ambient més distès i informal. Tot plegat, organitzat per l'Ignasi Casanova, coordinador en aquell temps del programa de doctorat en Ciència i Tecnologia Aeroespacial (DoCTA). L'Ignasi, a part d'organitzar fantàstics seminaris-dinar, va ser la primera persona amb qui vaig treballar només d'arribar a la UPC, un parell d'anys abans de l'esmentat dinar. Sempre he valorat el seu punt de vista en molts aspectes i des d'aquí voldria expressar-li el meu agraïment per la seva ajuda, suport i valuós consell durant aquells primers mesos a la universitat com a investigador. En aquest sentit, gràcies també a en Josep Fenollosa, del Departament d'Enginyeria Mecànica pel seu savi consell.

Aquells dos primers anys a la UPC vaig estar col·laborant amb el grup d'Astronomia i GEomàtica (gAGE). La meva estada a gAGE va ser d'allò més positiva i vull expressar la meva més sincera gratitud a en Manuel Hernández-Pajares, Miguel Juan i Jaume Sanz. Tot el que vaig aprendre amb vosaltres –des d'anar a reunions a Eurocontrol fins a elaborar rebuscats *scripts* Linux que *ho fan tot*– va sedimentar en forma de robustos fonaments per la meva formació com a investigador. Gràcies als tres també pel vostre agradable tracte personal, proper, planer i acollidor.

Dit això, tornem al famós dinar. De l'àpat, va seguir una visita als laboratoris del grup SAC a Terrassa. De la visita, una oferta per fer una tesi doctoral amb un tema un xic nou per a tots, però molt engrescador. De l'oferta, l'acceptació per part meva i de l'acceptació, a la tesi que el lector té ara mateix entre les mans. El camí però, no ha estat gens fàcil. Han estat uns quants anys de bons i mals moments i amb molta gent que d'una manera o altra m'han ajudat a tirar endavant. A tots ells moltes gràcies. Serà difícil, per no dir impossible, anomenar a tothom. Però ho intentaré.

Primer de tot, agrair de tot cor l'esforç dels meus dos directors de tesi: Joseba Quevedo i Vicenç Puig. Gràcies pel vostre temps i dedicació. Gràcies per ajudar-me a ser un millor investigador. Gràcies Joseba per la teva visió i optimisme. Gràcies Vicenç per la teva lucidesa i per tants viatges amb cotxe plegats! Gràcies també a la Fatiha i a la resta de companys del SAC, que encara que ens hàgim vist poc, sempre m'heu tractat com un dels vostres. Dir també, que aquesta tesi ha estat parcialment finançada per dos subvencions de recerca de la Generalitat de Catalunya. En

un inici, pel projecte SONORA, finançat pel DURSI en el marc de les Comunitats de Treball dels Pirineus (CTP) i en una segona fase per l'ajuda de Grup de Recerca de Qualitat i Consolidat del Pla de Recerca de Catalunya (codi 2005SGR00537).

Tots aquests anys han estat també els anys de posta en marxa de la titulació d'Enginyeria Tècnica Aeronàutica a l'Escola Politècnica Superior de Castelldefels (EPSC). És a l'EPSC on he passat la majoria del meu temps i on he tingut l'oportunitat de conèixer de prop a gent molt especial. Gràcies a Eduard Bertran i Miguel Valero per la vostra confiança i savis consells. Gràcies també a Ricard González per la teva magnífica gestió com a subdirector d'aeronàutica. Gràcies a tota la gent d'ICARUS, molt especialment a l'Enric Pastor i a la Cristina Barrado pel vostre suport moral i optimisme. Gràcies al grup d'*aeros* de l'EPSC (Adeline, Dago, Jorge, Lucas, Luís, Pep i Santi) i a la millor PAS del campus (Consol!!) pel *vostre pa de cada dia*.

Gràcies al Departament d'Arquitectura de Computadors (DAC) per donar-me accés als seus *clústers*. Gràcies a l'Ángel Sánchez i en David Pino pels seus consells en acústica i mecànica, respectivament. *Je tiens à remercier Félix Mora-Camino pour votre avis toujours créatif et critique. Thank you, as well, to Dries Visser for your time and invaluable advice.* Gràcies a en Ferran Pous per ser tan crack, a l'Àngela Aragón per la teva energia i pel teu suport matemàtic, a en Gerard Prats per la teva genialitat creativa (que te la vas quedar tota tu!), a en Marcos Pérez pel cop de mà amb el Google Earth *and finally, thanks to Celeste for your English support*.

Una tesi són uns quants anys d'una dedicació constant, on t'adones de la gent que tens realment a prop i que et dona suport *incondicional*, encara que no entenguin ben bé el què fas i per què ho fas. Parlo dels amics i la família, que a part de donar-los les gràcies, els vull demanar també perdó pels meus moments de mal humor i per no estar moltes vegades tant per ells com es mereixerien durant aquests anys.

Gràcies als companys del gAGE Júnior: Miquel, Raül i Àngela per tants somriures i tant de *Radiohead*. Gràcies al *DoCTA team* per compartir tantes coses junts: Jordi, Mercè i evidentment l'Eli. Gràcies a tots els *Teleconguitos* i molt especialment a en Xavi, Francesc i Víctor per aguantar-me i escoltar-me. Gràcies a l'Hugo i a l'Enric també per escoltar-me i animar-me amb el vostre estil tant peculiar i únic. Gràcies a la colla Gironina (Polo, Àlex, Jordi, Xevi i Gerard) per tants Pirineus, ratafies i Risks plegats. *Merci aux colocataires les plus incroyables de Toulouse pour bien m'aider à finir (??!!) cette thèse: Cat et Chiara!!*. Gràcies a la Marta i en JP, que per més lluny que vagin a viure sempre els tindré a prop. Gràcies també a uns *aeros* molt especials: Mireia, Xavi, Inés, Chelu i Albert Ramírez.

Així doncs, les meves últimes paraules són per la meva família. Tot i ser les últimes, no vol dir que siguin les menys importants, ans al contrari. Mai hauria arribat on sóc sinó hagués tingut uns pares com els que tinc. Sempre heu estat presents quan us necessitava i sempre m'heu fet costat amb totes les decisions que he pres (encara que tots sabem que el més fàcil era fer enginyeria industrial a Girona). Gràcies a en Gerard, que a part d'un gran professional i amic, tinc la sort que siguis també el meu germà. Gràcies a la meva tia Glòria per tot el que m'has donat. Gràcies als avis i avies tant fantàstics que tinc i dels que també molt he après. Gràcies també als meus tius, cosins i a la Cunyàààà Laia. Finalment, gràcies a l'Ester, la meva *dona* que m'ha fet tant de costat i que m'estima tant. A tots vosaltres, moltes gràcies per ser com sou, n'estic orgullós. Aquesta tesi també és vostra.

Castelldefels, Desembre de 2009
Xavier Prats i Menéndez

Resum

Tot i que en les últimes dècades la reducció del soroll emès pels avions ha estat substancial, el seu impacte a la població ubicada a prop dels aeroports és un problema que encara persisteix. Contenir el soroll generat per les operacions d'aeronaus, tot assumint al mateix temps la creixent demanda de vols, és un dels principals desafiaments a que s'enfronten les autoritats aeroportuàries, els proveïdors de serveis per a la navegació aèria i els operadors de les aeronaus. A part de millorar la seva aerodinàmica o el nivell d'emissions sonores, l'impacte acústic de les operacions aèries es pot reduïr també gràcies a la definició de nous procediments de vol més òptims. Aquests procediments s'anomenen generalment Procediments d'Atenuació de Soroll (PAS) i poden estar formats per rutes preferencials de vol, a fi d'evitar les zones poblades, i/o també perfils verticals de vol optimitzats.

Els procediments que existeixen avui en dia per reduïr el soroll de les operacions aèries són lluny de ser els més òptims. De fet, la seva optimització no és possible a causa de les limitacions actuals en els mètodes de navegació, els equips d'aviònica i la complexitat present en certs espais aeris. D'altra banda, molts PAS es dissenyen de forma manual per un grup d'experts i amb l'ajuda de diverses iteracions. Tot i això, en els propers anys s'esperen nous sistemes d'aviònica i conceptes de gestió del trànsit aeri que permetin millorar el disseny d'aquests procediments, fent que siguin més flexibles. A més a més, en els pocs casos on s'optimitzen PAS, se sol utilitzar una mètrica acústica en l'elaboració de les diferents funcions objectiu i per tant, no es tenen en compte les molèsties sonores reals. La molèstia sonora és un concepte subjectiu, complexe i que depèn del context en que s'usa. La seva integració en l'optimització de trajectòries segueix essent un aspecte a estudiar.

La motivació principal de la present tesi doctoral es basa en el fet que en un futur pròxim serà possible definir trajectòries d'aeronaus més flexibles i precises. D'aquesta manera es permetrà la definició de procediments de vol òptims des d'un punt de vista mediambiental. Així doncs, es considera una situació en que aquest tipus de procediments poden ser dissenyats de forma automàtica o semiautomàtica per un sistema expert basat en tècniques d'optimització i de raonament aproximat. Això serviria com una eina de presa de decisions per planificadors de l'espai aeri i dissenyadors de procediments de navegació aèria.

Així doncs, en aquest treball es desenvolupa una eina completa pel càlcul òptim de procediments d'atenuació de soroll per aeronaus. Això inclou un conjunt de models no lineals que tenen en compte la dinàmica de les aeronaus, les limitacions de la trajectòria i les funcions objectiu a op-

timitzar. La molèstia causada pel soroll es modela utilitzant tècniques de lògica difusa en funció del nivell màxim de so percebut, l'hora del dia i el tipus de zona a sobrevolar. Llavors, s'identifica i es formula formalment el problema com un de control òptim multi-criteri. Per resoldre'l es proposa un mètode de transcripció directa per tal de transformar-lo en un problema de programació no lineal. A continuació s'avaluen una sèrie de tècniques d'optimització multi-objectiu i entre elles es destaca el mètode d'escalarització, el més utilitzat en la literatura. No obstant això, s'exploren diverses tècniques alternatives que permeten superar certs inconvenients que l'escalarització presenta. En aquest sentit, es presenten i proven tècniques d'optimització lexicogràfica, jeràrquica, igualitària (o min-max) i per objectius. D'aquest anàlisi es desprenen certes conclusions que permeten aprofitar les millors característiques de cada tècnica i formar finalment una tècnica composta d'optimització multi-objectiu. Aquesta última estratègia s'aplica amb èxit a un escenari real i complexe, on s'optimitzen les sortides cap a l'Est de la pista 02 de l'aeroport de Girona. En aquest exemple, dos tipus diferents d'aeronaus volant a diferents períodes del dia són simulats obtenint, conseqüentment, trajectòries òptimes diferents.

Abstract

Despite the substantial reduction of the emitted aircraft noise in the last decades, the noise impact on communities located near airports is a problem that still lingers. Containing the sound generated by aircraft operations, while meeting the increasing demand for aircraft transportation, is one of the major challenges that airport authorities, air traffic service providers and aircraft operators may deal with. Aircraft noise can be reduced by improving the aerodynamics of the aircraft, the engine noise emissions but also in designing new optimised flight procedures. These procedures are generally called Noise Abatement Procedures (NAP) and may include preferential routings (in order to avoid populated areas) and also schedule optimised vertical flight path profiles.

Present noise abatement procedures are far from being optimal in regards to minimising noise nuisances. In general, their optimisation is not possible due to the limitations of navigation methods, current avionic equipments and the complexity present at some terminal airspaces. Moreover, NAP are often designed manually by a group of experts and several iterations are needed. However, in the forthcoming years, new avionic systems and new Air Traffic Management concepts are expected to significantly improve the design of flight procedures. This will make them more flexible, and therefore will allow them to be more environmental friendly. Furthermore, in the few cases where NAP are optimised, an acoustical metric is usually used when building up the different optimisation functions. Therefore, the actual noise annoyance is not taken into account in the optimisation process. The annoyance is a subjective, complex and context-dependent concept. Even if sophisticated (and more accurate) noise annoyance models are already available today, their integration into an trajectory optimisation framework is still something to be further explored.

This dissertation is mainly focused on the fact that those precise and more flexible trajectories will enable the definition of optimal flight procedures regarding the noise annoyance impact, especially in the arrival and departure phases of flights. In addition, one can conceive a situation where these kinds of procedures can be designed automatically or semi-automatically by an expert system, based on optimisation techniques and approximate reasoning. This would serve as a decision making tool for airspace planners and procedure designers.

A complete framework for computing optimal NAP is developed in this work. This includes a set of nonlinear models which take into account aircraft dynamics, trajectory constraints and objective functions. The noise annoyance is modelled by using fuzzy logic techniques in function of the perceived maximum sound level, the hour of the day and the type of over-flown zone.

The problem tackled, formally identified and formulated as a multi-criteria optimal control problem, uses a direct transcription method to transform it into a Non Linear Programming problem. Then, an assessment of different multi-objective optimisation techniques is presented. Among these techniques, scalarisation methods are identified as the most widely used methodologies in the present day literature. Yet, in this dissertation several alternative techniques are explored in order to overcome some known drawbacks of this technique. In this context, lexicographic, hierarchical, egalitarian (or min-max) and goal optimisation strategies are presented and tested. From this analysis some conclusions arise allowing us to take advantage of the best features of each optimisation technique aimed at building a final compound multi-objective optimisation strategy. Finally, this strategy is applied successfully to a complex and real scenario, where the East departures of runway 02 at the airport of Girona (Catalonia, Spain) are optimised. Two aircraft types are simulated at different periods of the day obtaining different optimal trajectories.

Notation

Throughout this dissertation and as a general rule, scalars and vectors are denoted either with lower or upper case letters. Vectors are noted with the conventional overhead arrow, like for example $\vec{a}$ or $\vec{\psi}$. Sets are denoted using caligraphic fonts, like for example $\mathcal{A}$, $\mathcal{B}$ or $\mathcal{X}$, while matrices use the same font but in bold series, like $\boldsymbol{\mathcal{R}}$. The time derivative of magnitude $a(t)$ is simple expressed by $\frac{\mathrm{d}a(t)}{\mathrm{d}t}$. Finally, if not otherwise noted, all vectors are column vectors and a transposed vector is denoted by $[\cdot]^T$. Next, the principal symbols that are used throughout this dissertation are shown along with their meaning. The reader should note that this list is not exhaustive.

$\mathbb{R}$	set of real numbers
$\times$	Cartesian product
$\mathbb{R}^m$	$\underbrace{\mathbb{R} \times \mathbb{R} \times \cdots \times \mathbb{R}}_{m \text{ times}}$
a	aerodynamic coefficient a
a_0	a value in clean flap/slat configuration
a_i	a value for the i-th flap/slat configuration
A	noise annoyance function
A_i^*	optimal noise annoyance value at the i-th noise sensitive location
$A_i^\star$	ideal annoyance value at the i-th noise sensitive location
$\bar{A}_i$	aspiration level (goal) at the i-th noise sensitive location
$\bar{A}$	threshold level for the noise annoyance
$\mathbf{A}$	Air reference frame
b	aerodynamic coefficient b
b_0	b value in clean flap/slat configuration
b_i	b value for the i-th flap/slat configuration
$\mathbf{B}$	Body reference frame
$\mathcal{B}$	set of blocked locations
c_{ij}^σ	thrust polynomial coefficients for thrust setting σ
C_a	airliner cost (cost for the aircraft operator)
C_f	fuel cost
C_t	time cost
C_D	drag coefficient

C_L	lift coefficient
CI	cost index
χ	aerodynamic heading angle
χ_{RWY}	runway heading
D	aerodynamic drag force
$\Delta a_{i\to j}$	a increment when transitioning from i-th to j-th flap/slat configuration
$\Delta b_{i\to j}$	b increment when transitioning from i-th to j-th flap/slat configuration
Δt	sampling time
Δ^P_{MA}	maximum noise deviation from ideal values for prioritisation P
Δ^P_{MR}	maximum relative noise deviation from ideal values for prioritisation P
Δ^P_{AA}	average noise deviation from ideal values for prioritisation P
Δ^P_{AR}	average relative noise deviation from ideal values for prioritisation P
Δ_i	annoyance deviation at the i-th noise sensitive location
Δ^*_i	optimal value for the annoyance deviation at the i-th location
$\Delta^\mathfrak{h}_i$	annoyance deviation at the i-th location at hour of the day $\mathfrak{h}$
$\urcorner_i$	optimal noise annoyance deviation at the i-th step
e	eastward position coordinate
$\vec{\eta}$	functions defining the event constraints
$\vec{\eta}_L$	bounds for the lower event constraints
$\vec{\eta}_U$	bounds for the upper event constraints
e_f	final eastward position coordinate
ε	tolerance value for hierarchical optimisation
$\vec{f}$	equations of the aircraft dynamics
FF	fuel flow
FF_{TOGA}	fuel flow in *Take-off–Go Around* configuration
FF_{CL}	fuel flow in *Climb* configuration
$\mathcal{F}$	set of free (non-blocked) locations
g	gravity vector module
$\mathbf{G}$	Ground reference frame
$\mathcal{G}$	set of objectives with aspiration levels
γ	aerodynamic flight path angle
γ_2	aerodynamic flight path angle when flying at V_2
Γ	elevation contribution in the INM lateral attenuation factor
h	height position coordinate
$\mathfrak{h}$	hour of the day
h_f	final height position coordinate
$h_f^{\min}$	minimum height at final point
$h_f^{\max}$	maximum height at final point
h_c	thrust cutback height
HI	height index
$\boldsymbol{\mathcal{I}}$	identity matrix
J_i	i-th objective optimisation function
J_i^*	optimal value for the i-th objective optimisation function
$J_i^\star$	ideal value for the i-th objective optimisation function
$\bar{J}_i$	aspiration level (goal) for the i-th objective optimisation function
$\mathcal{J}$	set of optimisation objectives
$k_{i\to j}$	steepness constant for flap/slat transition from i-th to j-th configuration
l	sideline distance
L	aerodynamic lift force
$\mathrm{L}_{\max}$	maximum perceived sound level
L_{EQ}	equivalent sound level

L_i	L_{max} at the i-th location
L_i^P	L_{max} at the i-th location for prioritisation P
L_i^a	background noise at the i-th location
L_i^*	optimal L_{max} at the i-th location
$L_i^\star$	ideal L_{max} at the i-th location
$\mathcal{L}$	set of noise sensitive locations
λ_i	i-th eigenvalue
Λ	sideline distance contribution for INM lateral attenuation
m	mass of the aircraft
$\mathcal{M}$	set of fine mesh grid points
μ	aerodynamic bank angle
n	northward position coordinate
n_e	number of engines
n_f	final northward position coordinate
n_G	number of aspiration levels (goals)
n_L	number of noise sensitive locations
n_M	number of grid points in the fine mesh
n_J	number of optimisation objectives e
n_p	number of control parameters
n_P	number prioritisations
n_u	number of control variables
n_x	number of state variables
n_z	dimension of the set of feasible trajectories
$\mathsf{n_z}$	vertical load factor
N	number of discretisation points
N_i	sound pressure level at the i-th location
N^L	INM lateral attenuation adjustment factor
N^{NTD}	sound pressure level extracted from the INM NTD tables
O_G	ground reference frame origin
O_B	centre of mass of the aircraft
$\mathcal{O}$	feasible objective region
P	prioritisation
$\vec{p}$	vector of control parameters
$\vec{p}_L$	lower bounds for the vector of control parameters
$\vec{p}_U$	upper bounds for the vector of control parameters
$\vec{\psi}$	functions defining the path constraints
$\vec{\psi}_L$	lower bounds for the path constraints
$\vec{\psi}_U$	upper bounds for the path constraints
ψ	yaw angle
φ	total number of flap/slats configurations
ρ	air density
ρ_0	air density at sea level
s	procedure design gradient
S	total wing surface
σ	thrust setting
t	time
t_0	initial time
t_f	final time
t_k	k-th time sample
T	total net thrust force
T_{TOGA}	total net thrust in *Take-off–Go Around* configuration

T_{CL}	total net thrust in *Climb* configuration
τ_{max}	time constant of the fastest dynamic mode
$\vec{u}$	control vector
$\vec{u}_L$	lower bounds for the control vector
$\vec{u}_U$	upper bounds for the control vector
v	true airspeed (TAS)
$v_{i \to j}$	airspeed for flap/slat transition from i-th to j-th configuration
V_2	minimum climb safe speed
V_{max}	maximum airspeed
w_i	weight for the i-th objective
$\vec{W}$	wind velocity vector
W_n	northward local wind component
W_e	eastward local wind component
W_h	vertical local wind component
$\vec{x}$	state vector
$\vec{x}_L$	lower bounds for the state vector
$\vec{x}_U$	upper bounds for the state vector
ξ	elevation angle
$\vec{z}$	decision variables vector (aircraft trajectory)
$\vec{z}^*$	solution of the optimisation problem (aircraft trajectory)
Z	Type of zone
$\mathcal{Z}$	admissible set of decision variables

List of Acronyms

ABAS	Airborne Based Augmentation System
ACDA	Advanced Continuous Descent Approach
ADF	Automatic Direction Finder
ANSP	Air Navigation Service Provider
APU	Auxiliary Power Unit
ARINC	Aeronautical Radio INC.
ATC	Air Traffic Control
ATM	Air Traffic Management
CDA	Continuous Descent Approach
CF	Course to a Fix
DENL	Day Evening Night Level
DNL	Day Night Level
DME	Distance Measurement Equipment
ECAC	European Civil Aviation Conference
EGNOS	European Geostationary Navigation Overlay System
EPN	Effective Perceived Noise
ESRA	Eurocontrol Statistical Reference Area
FICAN	Federal Interagency Committee on Aviation Noise
FIR	Flight Information Region
FMS	Flight Management System
FPA	Flight Path Angle
GBAS	Ground Based Augmentation System
GIS	Geographic Information System
GNSS	Global Navigation Satellite System
GPS	Global Positioning System
GS	Glide Slope
GTF	Geared TurboFan
IAS	Indicated Air Speed
ICAO	International Civil Aviation Organisation
IFR	Instrumental Flight Rules
ILS	Instrumental Landing System
INM	Integrated Noise Model

ISA	International Standard Atmosphere
LDLP	Low Drag Low Power
LLZ	Localizer
MTDDA	Modified Three Degree Decelerating Approach
NAI	Normalised Annoyance Index
NAP	Noise Abatement Procedure
NADP	Noise Abatement Departure Procedure
NDB	Non Directional Beacon
NLP	NonLinear Programming
NTD	Noise Thrust Distance
NPR	Noise Preferential Route
PANS-OPS	Procedures for Air Navigation Services – OPerationS
PBN	Performance Based Navigation
(P-)RNAV	(Precise) Area Navigation
RF	Radius to a Fix
SARPs	Standard And Recommended Practices
SBAS	Satellite Based Augmentation System
SEL	Sound Exposure Level
SENEL	Single Event Noise Exposure Level
SESAR	Single European Sky ATM Research
SID	Standard Instrumental Departure
STAR	Standard Terminal Arrival Route
TA	Time Above
TAS	True Air Speed
TDDA	Three Degree Decelerating Approach
TF	Track between Fixes
TMA	Terminal Manoeuvring Area
TOD	Take-off Distance
TODA	Take-off Distance Available
TOGA	Take-Off–Go Around
TORA	Take-Off Run Available
UIR	Upper Information Region
VFR	Visual Flight Rules
VHF	Very High Frequency
VOR	VHF Omnidirectional Range
WAAS	Wide Area Augmentation System

The economic and technological triumphs of the past few years have not solved as many problems as we thought they would, and, in fact, have brought us new problems we did not foresee.

— Henry Ford

Music is the silence between the notes.

— Claude Debussy

I

Introduction

Air transportation is one of the most important services in the world, contributing greatly to the advancement of modern society. The use of commercial aviation has grown more than seven-fold since the first jet airliner flight in 1949, and is unmatched by any other major form of transportation. Modern aircraft have transformed international travel from a luxury for a few into an affordable option for most of us. Today, the air transportation business is global, involving plenty of different stake-holders, such as aircraft manufacturers; engine manufacturers; aircraft components suppliers and associated industry; airline operators; airports and ground facilities industry; fuel suppliers; local, regional and international authorities, organisations and regulatory bodies; etc. By any measure, it is an economic force and a source of enormous wealth.

However, air transportation has a local and a global impact on the environment. Aircraft emissions represent approximately 4% of the world's man-made atmospheric emissions, according to (Intergovernmental Panel on Climate Change, 1999). These emissions impact significantly on the Climate Change (the green house effect) and the local and regional air quality levels. The other important environmental issue is aircraft noise.

As it is well known, noise disturbs or annoys us. In particular, the presence of environmental noise interferes with activities that we may be undertaking, such as communicating, listening to music, relaxing, sleeping, reading, working, studying, etc. Complaints about global noise exposure are one of the most, if not the most, frequently reported complaints among populations living in large cities (Martin-Houssart & Rizk, 2002). For example, according to (Roy, 2003), in the year 2001, 51% of French citizens admit being annoyed by environmental noise. In this context, noise is the most important annoyance being reported for people living in large cities like Paris. Among this 51% of noise annoyed people, 66% claim road traffic as the main source of annoyance, while air traffic represents only 17%. Logically, road noise becomes even more important if only large

cities are regarded, yet aircraft noise becomes very significant, despite road noise, if small communities (towns of less than 2000 inhabitants) are taken into account. Furthermore, according to (The Parliamentary Office of Science and Technology, 2003), aircraft noise has the potential to affect the quality of life of at least half a million people living close to the United Kingdom airports. 80% of these people are living close to the major airports in the southeast of England. In addition, the United States General Accounting Office has reported noise as the greatest environmental concern for 29 of the 50 busiest US airports (GAO, 2000).

Aircraft noise is an unwanted sound in the vicinity of airports that disturbs the routine activities and peace of the people inhabitting these areas and it is recognized as a major barrier in the expansion of airport operations. While there has been progress in aircraft noise reduction, further reductions become harder to achieve. The problem is made more difficult by the anticipated increase in noise due to the growth in aircraft operations. In this context, the forecast of flights in the Eurocontrol Statistical Reference Area (ESRA) for 2030 is between 1.7 and 2.9 times the traffic of 2007 (Eurocontrol, 2008). Therefore, an average growth of 2.3% to 3.5% per year is expected. Business aviation and general aviation are also expected to rise in demand in a long term basis at an average of 1.8% a year through to 2025 (FAA, 2009a). Moreover, aircraft manufacturers are (obviously) slightly more *optimistic* and predict bigger figures. Airbus, for example, forecasts a threefold increase in air traffic worldwide by 2025 (Airbus, 2007), while Boeing predicts an average of 4.8% annual air traffic growth over the next 20 years (Boeing, 2008). Both aircraft manufacturers also estimate that the demand for flight frequency between destinations will more than double over the next 20 year period.

I.1 Strategies for aircraft noise reduction

Containing the sound generated by aircraft operations, while meeting the increasing demand for aircraft flights, is one of the major challenges for the air transportation stake-holders. Generally speaking, noise can be mitigated by acting at three different levels: reducing noise at source, improving the propagation conditions and improving the receiver conditions.

- **Noise reduction at source**: Since the beginning of the jet age, aircraft noise has been reduced by some 20 dB (see Figure I-1). The most important factor in this reduction has been the introduction of high bypass ratio turbofan engines and, thereafter, the steady increase in bypass ratios until the ratio they are now. The incorporation of other specific noise reducing devices into the engine has also played an important part. The progressive reduction of aircraft noise at source has been matched by the tightening of international regulations and even by the introduction of local regulations specific to particular airports, which sometimes are more stringent than the international rules.

  As outlined before, the reduction of engine emissions is the other sticking point in the progress to a more environmentally friendly aviation. The next break-through in engine emissions is expected with the development of open-rotor propulsion systems and Geared TurboFans (GTF). Open-rotor technology promises considerable fuel reductions, but at the expense of noise. On the other hand, GTF may provide noise reduction but the fuel efficiency is substantially lower if compared wit the open-rotors (Thomas, 2008).

- **Improve the propagation conditions**: Once the aircraft, and the associated power plant is manufactured, the way that it is operated also plays a crucial role in the total amount of perceived noise by the affected population. The aircraft's trajectory (considering both lateral and vertical paths) determines the distance between the noise source (the aircraft) and the receivers (the population).

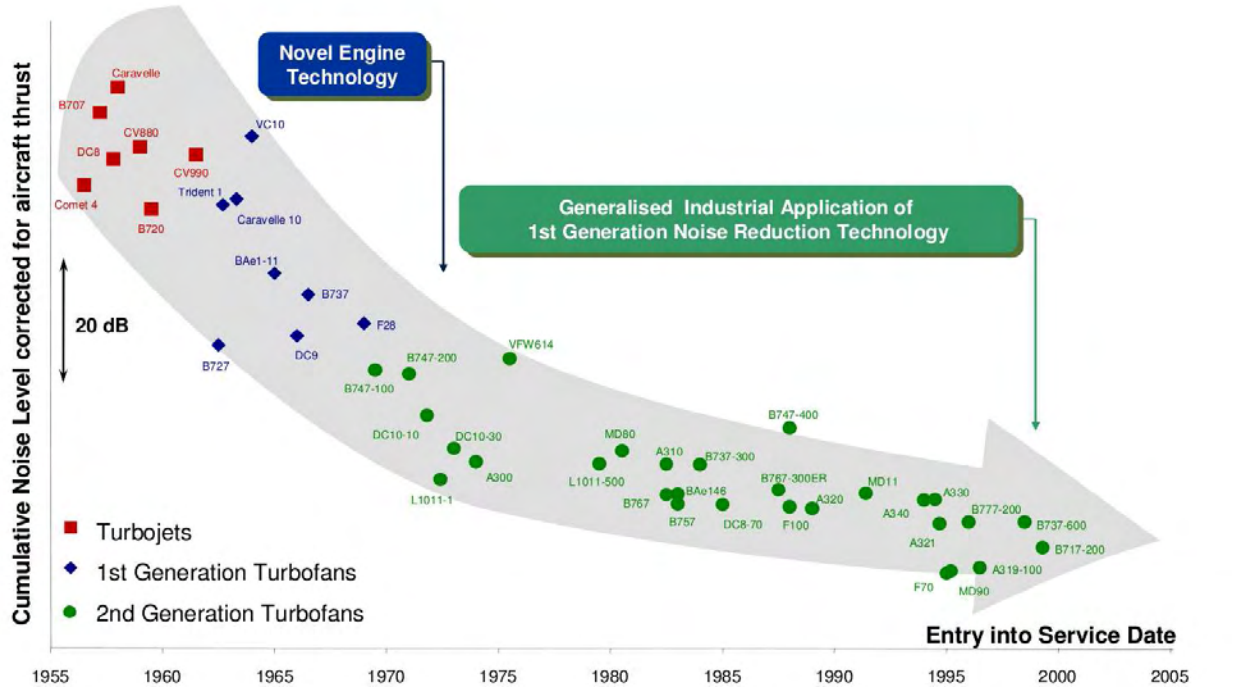

Figure I-1: *Progress in noise reduction.*

Source: (ICCAIA, 2005). Printed with permission

A convenient definition of Noise Preferential Routes (NPR) and Noise Abatement Procedures (NAP) is paramount for keeping noise away from populated areas. NPR will establish a set of flight legs to follow in order to avoid over-flying populated areas. On the other hand, NAP could also schedule specific speed, altitude and thrust profiles during the procedure.

- **Improve the receiver conditions**: Land use planning near airports is vital if the noise reductions already achieved are not to be offset by people moving closer to airports. Keeping populations a certain distance away from airports and maintaining a quiet buffer zone which is kept free of residential, or other noise-sensitive development areas, is also important (IATA, 2000). Specialised programs on the acoustical isolation of dwellings are also carried out in existing populated areas suffering from aircraft noise.

I.2 Noise policies and regulations

Standards And Recommended Practices (SARPs) for Aircraft Noise were first adopted on the 2nd of April, 1971 pursuant to the provisions of Article 37 of the Convention on International Civil Aviation (ICAO, 2000) and designated as Annex 16 to the Convention (ICAO, 1993a). This ICAO Annex sets the framework for the noise classification of aircraft, reflecting the size of the aircraft and their engine type, and is linked to a reduction in noise as technology evolves. With this in place, the Annex also contains Standards, Recommended Practices and guidelines for noise certification of aircraft engaged in international civil air navigation. In addition, this Annex contains Recommended Practices and guidance material for use by States with a view of promoting uniformity in the measurement of noise for monitoring purposes, the use of an international noise exposure reference unit for land use planning, and the establishment of noise abatement operating procedures. The details for designing such procedures can be found in the first volume of the Procedures for Air Navigation Services – Aircraft Operations (PANS-OPS) document (ICAO, 2006a).

The Annex 16 classifications are internationally recognised for their use in certifying aircraft noise levels. However, there are no global regulations concerning the maximum levels of perceived noise in inhabited areas around airports. Nowadays ICAO is recommending a *Balanced Approach* for noise management, considering aircraft noise as one of a suite of measures including land use management, operational procedures and flight restrictions (ICAO, 2008).

In Europe, among numerous policies, two Directives from the European Union have been edicted in 2002. The first one is the D2002/30 (European Parliament, 2002a) which is specifically devoted to air traffic noise and is inspired by the *Balanced Approach* concept adopted by ICAO. The second is the D2002/49 (European Parliament, 2002b) dealing with environmental noise in general and specifying which noise metrics should be used for assessing perceived noise levels, with the objective harmonising strategic noise maps in Europe.

At local level, noise restrictions are often reflected in limits on the airport licence to operate in certain conditions. For instance, there may exist limits on the number of movements or the total permitted noise. This can lead to the use of preferential runways and routes, partial or complete curfew during night periods, mandatory phase-out of noisy aircraft, prohibition of engine testing, prohibition of using engine reverses at landing, prohibition of using Auxiliary Power Units (APU) on the ground or even the definition of differential landing charges on aircraft to reflect differences in the noise generated (Williams, 2007). For example, in the UK, a system of night noise quotas is used (DfT, 2003), where each aircraft and engine configuration has been allocated a quota count. Aircraft with *high* quota counts cannot be scheduled to take off or land after 23h and before 7h. Moreover, in Madrid Barajas (Spain) different departure procedures are published for day and night periods (AENA, 2009b). Finally, in Amsterdam Schipol (The Netherlands) specific noise abatement procedures for arrival and departures are also published (Air Traffic Control the Netherlands, 2009a). For a recent and extensive comparison of policies and strategies of noise mitigation, the reader should refer to (Girvin, 2009).

I.3 Motivation of this PhD thesis

Despite the combined efforts to substantially reduce the impact of noise on populations living around airports, the noise problem still lingers. According to (Greener by Design, 2005), the downward trend in noise exposure around airports of past years (mainly due to the significant reduction of emitted engine noise as seen in Figure I-1) has now flattened out at major airports. In other words, even if all the older aircraft are phased out and the continued fleet renewal introduces progressively quieter types, these benefits will be less appreciable due to the increasing number of aircraft operations.

Present noise abatement procedures are far from being the optimal ones minimising noise nuisances. Most of the time optimisation is not possible due to the limitations of current navigation methods and the complexity present at some terminal airspaces. Moreover, noise preferential routes are often designed manually by a group of experts and several iterations are needed.

However, in the forthcoming years, new avionic systems and new Air Traffic Management (ATM) concepts are expected to significantly improve the design of flight procedures. This will make them more flexible, and therefore allow them to be more environmental friendly. Thus, this PhD thesis is mainly motivated by the fact that these precise and more flexible trajectories will enable the definition of *optimal* flight procedures regarding noise impact, especially in the arrival and departing phases of the flight. In addition, one can conceive a situation where these kind of procedures can be designed automatically or semi-automatically by an expert system, based on optimisation techniques, that would serve as a decision making tool for airspace planners and procedure designers.

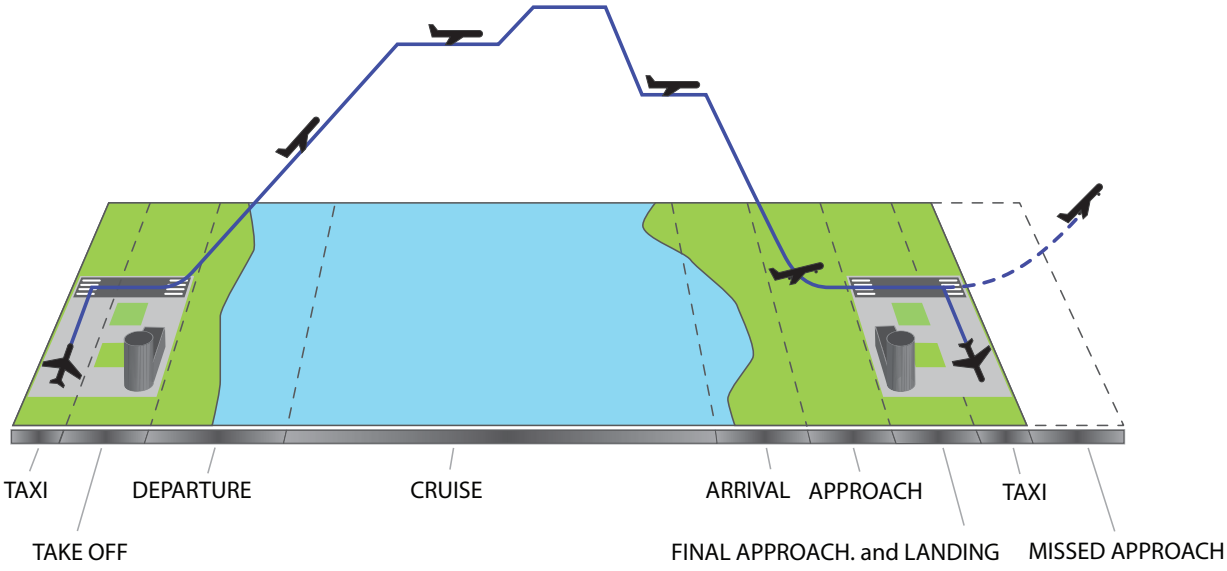

Figure I-2: *Different flight phases in a IFR flight*

I.3.1 Flight procedures

Commercial civil aviation typically operates under Instrumental Flight Rules (IFR). This means that aircraft use several navigation instruments and systems which provide the necessary guidance to follow a certain route. These routes have been previously studied, designed and published by the competent authorities and are called procedures (for airport departure, arrival and approach manoeuvres) or airways (for the en-route phase). Figure I-2 shows the usual division of the different flight phases and the standardised procedures associated with them. IFR departures are usually named Standard Instrumental Departures (SID) while the arrivals are Standard Terminal Arrival Routes (STAR). The design of procedures and airways guarantee obstacle clearance by means of a minimum safe flight altitude, as well as a minimum separation between aircraft using different procedures or airways in the vicinity. Obviously, this kind of organisation of the airspace helps in managing and controlling the air traffic. Each flight phase has some particularities that makes it different from the other phases. Besides a particular route to follow, depending on the phase, the aircraft will follow different configurations, speeds and altitude profiles. All IFR flights are mandated to fly these procedures (if published), except if the air traffic control authorises to skip or override the existing procedure.

During the last decades, navigation within continental airspace has been based on over-flying a set of radionavigation aids. Specific bearings can be followed in relation to these aids, either towards or away from them. This kind of navigation results in non-efficient and inflexible routes causing sometimes flight congestion or environmental issues, and hence non efficient flights. Although, with the introduction of computerised and digital avionics, along with an important onboard integration of different systems, new solutions have arisen to overcome the major drawbacks in conventional navigation. The first step into new navigation techniques was introduced with the *Area Navigation (RNAV)* concept. Aircraft equipped with suitable RNAV systems can fly routes that can be defined between arbitrary waypoints and therefore, not necessarily placed over radionavigation aids, as in conventional navigation. This flexibility is one of the key enablers for the definition of more environmental friendly flight procedures and therefore, will be considered thoroughly in this PhD thesis. More background on air navigation, radionavigation systems and flight procedures is found in Appendix A of this thesis.

I.3.2 Air Traffic Management for next decades

Two ground breaking initiatives aiming at improving the Air Traffic Management (ATM) system are currently being undertaken throughout Europe and the United States of America: SESAR[1] and NEXTGEN[2] respectively.

SESAR stands for the Single European Sky ATM Research programme. For the first time in European ATM history, all the stake-holders in the ATM world are involved in defining, committing to and implementing a pan-European programme, and supporting the Single European Sky legislation. The objectives of SESAR are to eliminate the fragmented approach to ATM and to transform the European ATM system. In the United States the fragmentation of ATM technologies and methodologies does not exist. However, it is also needed to endeavour an evolution of the present ATM systems in order to cope with the air traffic forecasts expected in the near future. In 2008, the SESAR definition phase was completed and the actions needed were identified to transition from research to implementation phases in order to achieve SESAR goals. According to these objectives, the European ATM network will be re-engineered towards a more efficient, better integrated, more cost-efficient and safer network (SESAR Consortium, 2006). In this context, high precision 4D trajectories will be one of the most important elements in future ATM.

A 4D trajectory is a precise description of the flight path of an aircraft as a 4 dimensional continuum, from its current position to the point at which it touches down at its destination. Thus, every point on a 4D Trajectory is precisely associated with a time (Wilson, 2007). 4D trajectories are expected to play a significant role in the improvement of the ATM scenario in the future, but also in the definition of environmental optimised procedures. For further reading on this topic see, for instance (de Jonge, 2002; le Tallec & Joulia, 2007; Kuenz *et al.* , 2008) and the references therein.

I.3.3 Noise annoyance modelling

Aircraft noise disturbs the normal activities of airport neighbours, their conversation, sleep, and relaxation, and degrades their quality of life. Depending on the use of land contiguous to an airport, noise may also affect education, health services, and other public activities. One of the most important aspects when dealing with an optimisation problem is the definition of the optimisation objective itself. In the case of noise abatement procedures it seems obvious, at least *a priori*, that the objective function might be the perceived noise. However, there are several metrics that express in a different way the magnitude of a particular noise event. Besides loudness, these metrics try to take into account other factors (such as the duration of the event or the presence of certain tones) in order to better express the annoyance perceived by humans. Some background on aircraft noise and measurement metrics is given in Appendix B of this work.

Furthermore, the noise annoyance not only depends on acoustical elements but also on a list of other, sometimes vague or subjective, factors. In this context, (Skånberg & Öhrström, 2002), affirm that it is currently believed that noise exposure alone can only explain about the 30% of the total noise annoyance. According to this study, one possible reason for the low correlation between annoyance and noise exposure is the lack of assessment of individual noise-dose immission. Several authors have addressed in detail the effects of noise in humans by using different methodologies. A wide number of noise annoyance models have been published ranging from very simplistic deterministic equations to more sophisticated methods, but very few of them have been applied in the definition of noise abatement procedures.

[1] http://www.sesarju.eu
[2] http://www.faa.gov/nextgen

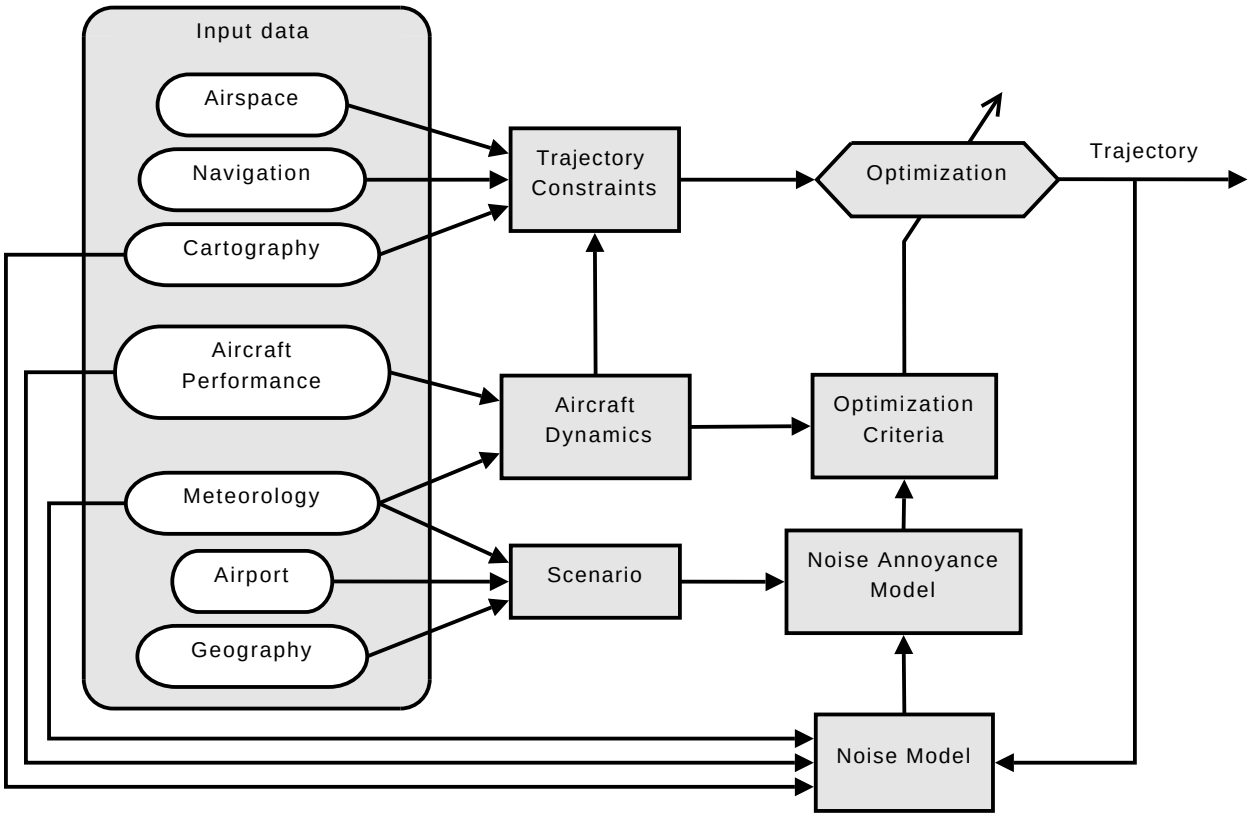

Figure I-3: *Trajectory optimisation framework for noise abatement procedures*

I.4 Objectives of this PhD thesis

During the departure, arrival and approach phases, an aircraft is flying at a relatively low altitude and it is during these phases that aircraft noise becomes more significant over the populated areas. Therefore, a thorough design of SIDs, STARs and standard approach procedures is paramount when aircraft noise needs to be mitigated. Based on the discussions presented thus far, the main objective of this work is the development of an optimisation framework aimed at minimising the noise annoyance to communities located near airports by designing **optimal flight procedures**. This will allow to define **optimal Noise Preferential Routes (NPR)** or more generally, **optimal Noise Abatement Procedures (NAP)**.

Figure I-3 depicts a block diagram for the proposed optimisation framework. The airport of study, along with the surrounding cartographical, geographical and meteorological conditions, will form a *scenario* which will be used to compute several *noise annoyance* criteria as a function of the *perceived aircraft noise* along the flight trajectory. Therefore, the impact of aircraft noise will depend on this scenario definition and would be completely different in another airport environment. Thus, this strategy is intended to be used by the Air Navigation Service Provider (ANSP), or the corresponding local authority in charge of the design of the operational procedures at the airport of study.

The annoyance values will be extracted from ad-hoc or existing annoyance models. Along with some fuel and/or time economic considerations, they will define a set of *optimisation criteria*. Then, an *optimisation algorithm* will compute the best departing or approaching trajectory minimising the criteria while at the same time, a set of *trajectory constraints* are satisfied. In turn, these constraints will depend on the dynamics of the aircraft, possible navigation constraints, 4D constraints and airspace constraints. The optimisation algorithm will tackle with more than one optimisation functions at the same time. Therefore, besides the optimisation itself, a decision making process will be needed in order to trade-off among all the objectives and select a final

trajectory.

Summing up, the objectives of this PhD thesis can be outlined as follows:

- Give a complete and exhaustive review of the state of the art in noise abatement procedures and noise annoyance modelling.
- Build all the necessary models needed for the optimisation of noise abatement procedures. In particular, the model for aircraft dynamics, which presents nonlinear equations and different modes as a function of discrete variables such as flaps/slats configuration and thrust settings.
- Propose a mechanism to integrate complex noise annoyance models into the optimisation framework by investigating knowledge reasoning methods such as fuzzy logic techniques.
- Explore and test different multi-criteria optimisation techniques that go beyond the classical approaches dealing with this type of multi-objective problems.
- Apply and test the optimisation framework in a real and complex scenario environment with different kinds of populated areas.

I.5 Scope and limitations of this PhD thesis

The proposed research will be focused on a single over-flight problem, *i.e.* the annoyance produced by several operations will not be taken into account. As it will be seen in Chapter III, the proposed methodology is generic enough to consider different aircraft types, different noise metrics as well as landing and take-off operations. However, the scope of the presented research only considers take-off procedures for two types of aeroplanes. Moreover, no assessment will be done regarding different aircraft payloads (which influence on the take-off mass of the aircraft and therefore, on its climbing performances). Cartographical constraints will not consider the actual obstacle distribution under the flight path and will be simple expressed by means of minimum climb gradients (conservative approach).

On the other hand, no assessment will be done regarding which metrics and/or weighting scales (or combination of them) are better to express the noise annoyance. Only the maximum A-weighted sound level will be considered in this work as noise metric. Furthermore, it is out of the scope of this PhD thesis to develop a detailed and validated fuzzy model describing noise annoyance. Our goal is to show how these models would be integrated in the optimisation framework that we are proposing.

Finally, it should be noted that one of the most important issues when dealing with optimisation problems is the difficulty to obtain a globally optimal solution. Real world problems often involve nonlinear equations and are in consequence, non-convex optimisation problems. For an optimisation problem this means that several local optima may exist. Nowadays, global optimisation methods require a computational burden that is prohibitive for many applications. As it will be seen throughout this dissertation, the optimisation problem we tackle involves hundreds of thousands variables and equations which can not be afforded by the state of the art on global optimisation packages and algorithms. In fact, in the worst case, the computational time of these algorithms grows exponentially with the number of optimisation variables. Therefore, the proposed methodology in this work involves the use of local optimisation algorithms. However, some strategies aimed at mitigating local optima are also given in this dissertation.

I.6 Outline of this PhD thesis

The material in the present document is organised in seven Chapters and five Appendices which are summarised as follows:

- **Chapter II** presents the state of the art in noise abatement procedures and in noise annoyance modelling.
- **Chapter III** contains the models that have been developed or adapted for this work. In particular, the model describing the dynamics of the aircraft is given along with the chosen noise computation methodology. Finally, a fuzzy model is presented aimed at modelling the noise annoyance.
- **Chapter IV** defines formally the optimisation problem and the methodology for solving it is described. Moreover, some fundamentals in multi-objective optimisation are given and the techniques that will be explored later are outlined.
- **Chapter V** shows the results of applying lexicographic and hierarchical optimisation in a hypothetical scenario with only few noise sensitive locations. This Chapter allows us to proof the proposed optimisation framework and some conclusions in the use of these multi-objective optimisation techniques are drawn.
- **Chapter VI** tackles the computation of optimal depart trajectories for a real and complex scenario where multiple areas of population are found. A multi-criteria optimisation technique is proposed, taking advantage of the methodologies explored in previous Chapter. There, *optimality* and *fairness* of the final trajectories are assessed and the annoyance models are considered as optimisation functions.
- **Chapter VII** gives the conclusions that are drawn from this work and points out some future work that could be done in the direction of the presented research.
- **Appendix A** gives some background in aircraft navigation, radionavigation systems and procedures. This material is recommended for those readers which are not familiar with all these concepts.
- **Appendix B** gives an overview on aircraft noise and summarises the existing noise metrics aimed at evaluating the aircraft noise impact.
- **Appendix C** contains the detailed model of the aircraft dynamics. This material is placed out of the main text for the sake of simplicity.
- **Appendix D** gives some basic background in fuzzy sets and fuzzy logic applied to fuzzy rule-based systems. Recommended Appendix for those readers which are not familiar with this discipline.
- **Appendix E** summarises the list of noise measurement locations that have been used in the real case application example of Chapter VI.

Little by little you fill the sink.

— Catalan Proverb

What a big book would be written with all that the humanity knows.

— Jules Verne

II

State of the Art

By the end of the 1920s, the new concept of *standard departure route* arose at Croydon airfield, in the United Kingdom. Surprisingly, these routes were not for traffic separation purposes but were created as noise abatement procedures following complaints from local residents (Baumgartner, 2007). This is a curious paradox: when Standard Instrumental Departures (SID) started to be widely used in the second half of the 20th century, the main reason for their definition was traffic separation issues in the more and more congested Terminal Manoeuvring Areas (TMA) and not for noise mitigation strategies. Then, at the end of the 20th century noise exposure to populations became a major concern and SIDs, along with STARs and approach procedures, were regarded again as a major key enablers for the redesign of new procedures aimed at reducing the noise impact around the airports. This Chapter gives an overview of the current state of the art in the design of such procedures, ranging from simple and very specific operational strategies to improve some noise conditions to more sophisticated and global techniques where mathematical optimisation of the procedures is performed. Moreover, the last part of this Chapter is devoted to give a review on noise annoyance models and techniques that try to take into account not only the acoustical magnitudes of noise but also all the other non-acoustical factors that have a significant impact on the final perceived annoyance.

II.1 Noise abatement procedures (NAPs)

Early studies in noise abatement procedures can be found for instance in (Zalovcik & Shaefer, 1967), showing the feasibility of increasing the final approach slope to about 6^o. In this study, it was found that with these steepened procedures, the prime source of

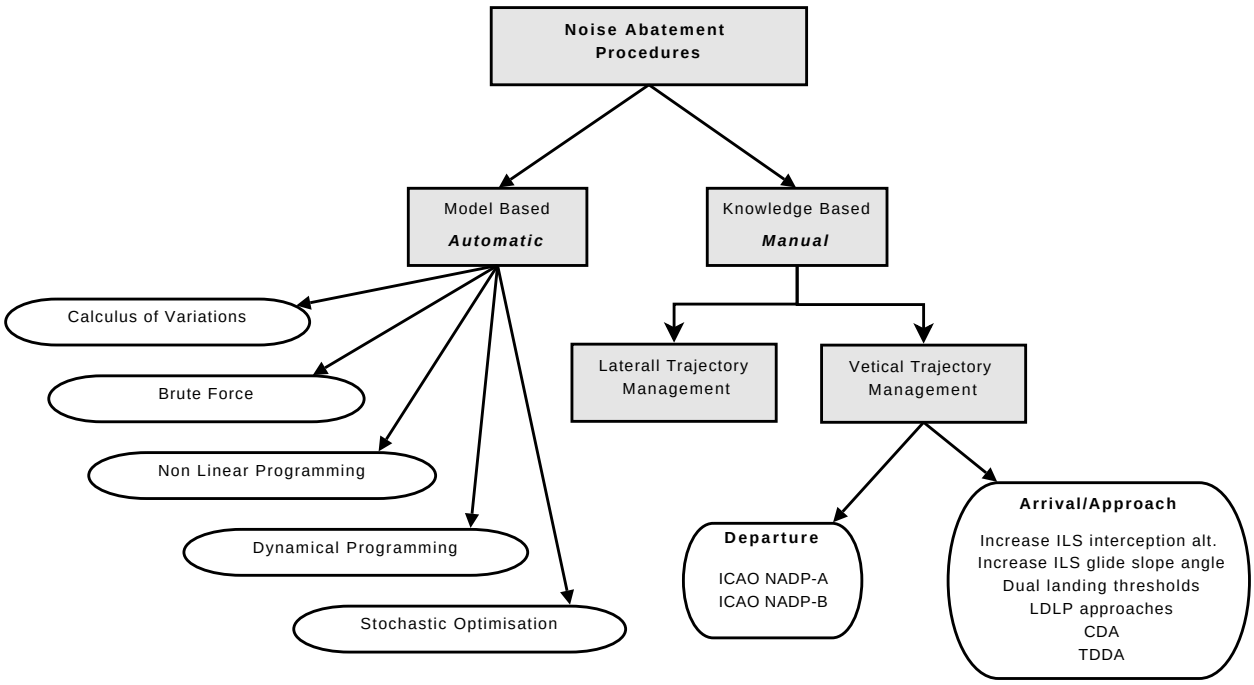

Figure II-1: *Different Strategies for the design of Noise Abatement Procedures*

noise reduction was the power cut-back of flying the new glide path. However, it was highlighted that some improvements were required concerning the engine response time needed to guarantee a safe landing at this inclined approach. In addition, the necessity of having improved displays for the pilots was also outlined. In (Paullin, 1970), the concerns caused by aircraft noise were identified as a major problem and some solutions were already proposed. These, include thrust reduction in departures, noise preferential runways and even runway redesign and reorientation. In addition, this paper already highlighted the problems in airport capacity that noise friendly procedures may cause, identifying that noise abatement procedures and airport or airspace capacity were conflicting objectives.

More recent noise abatement flight procedures around airports are based on avoiding over-flying densely populated areas. For example, the construction of Noise Preferential Routes (NPR) by modifying the horizontal (or lateral) flight path. In addition to lateral adjustments, the vertical path (climbing or descending profiles) can also be improved, or at least modified, minimising the noise footprint even more. Figure II-1 summarises several mechanisms for designing NAPs. We split them in two big families: those strategies that are performed *manually* by one or several experts according to empiric data, previous experience and knowledge and those methods that are based in mathematical methods and can compute *automatically* or *semi-automatically* optimal noise abatement procedures. The first group contains specific and in general, partial solutions. However, most of them are already being applied in an operational context. On the other hand, the model based strategies are generally a subject of on-going research and although they provide mathematically an optimal solution, their operational implementation is still not straightforward. Next, a extensive review on these different strategies is presented.

II.1.1 Lateral Trajectory Management

Conventional navigation, which is based on over-flying a set of radionavigation aids, has shown some limitations in the last years due to the increase of air traffic. The concept of Area Navigation (RNAV) provides flexibility not only in the procedure design but also the flown tracks turnout to be more accurate, giving a much lower dispersion around the nominal track than in conventional

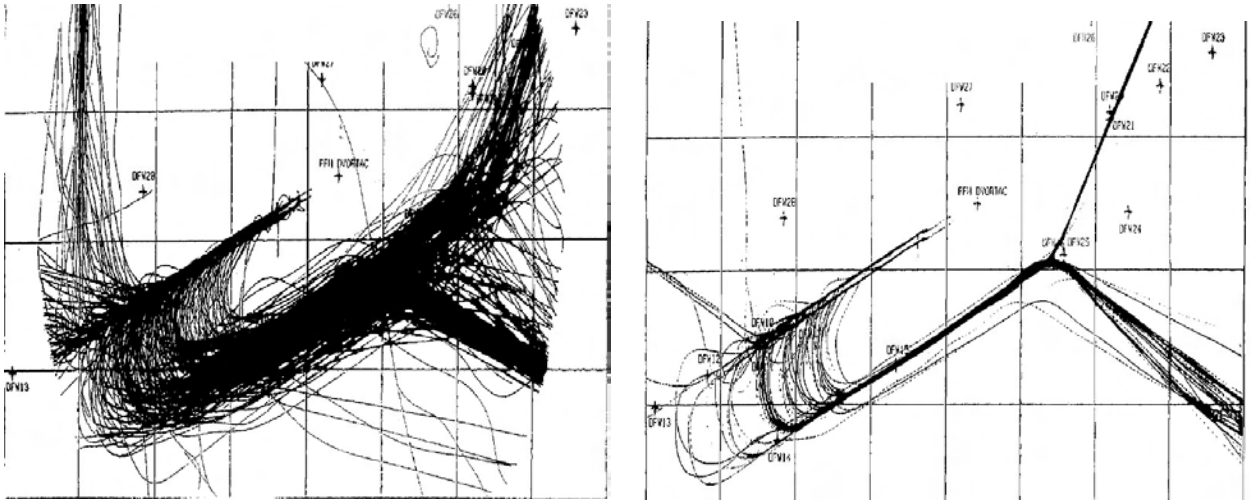

(a) Conventional procedures (b) RNAV procedures

Figure II-2: *Example of flight tracks corresponding to arrival procedures in Frankfurt (Germany).*

Source: (SOURDINE II Consortium, 2003)

navigation. Figure II-2 shows an example of the flight tracks corresponding to a STAR at Frankfurt airport, in Germany. Left figure shows the flight tracks corresponding to a STAR based on conventional navigation means, while in the right figure the tracks correspond to the same procedure when flown by RNAV equipped aircraft. It is obvious that RNAV navigation is one of the main keys enabling the new noise-friendly aircraft procedures. Since RNAV navigation is possible with only GNSS (Global Navigation Satellite System) positioning, new RNAV procedures could be designed in secondary airports where nowadays there does not exist a significant set of radionavigation aids permitting enough flexibility for the procedure design. See, for instance, the early experiments at Nice airport showing how the future European Geostationary Navigation Overlay Service (EGNOS) system would significantly improve the flexibility when designing NAPs (de Lépinay, 2002).

Yet, despite RNAV procedures being implemented gradually worldwide, not all aircraft are equally equipped and, for compatibility issues, conventional procedures are still widely used in major airports. Furthermore, RNAV implementation is not as easy as the concept seams to be. As procedures were implemented at different locations, it was identified almost immediately that aircraft equipped with different Flight Management Systems (FMS) were not all flying the same ground paths and nor were they turning or descending at the same point in space. The result is that aircraft tracks are not as predictable as expected. There are four primary elements that contribute to variations in the aircraft RNAV ground tracks: FMS equipment installed on the aircraft, procedure coding into FMS databases, aircraft to FMS interfaces and associated aircraft performance capabilities, and flight crew procedures. See (Herndon *et al.* , 2007; Herndon *et al.* , 2008) or (Herndon *et al.* , 2006) for an interesting study showing how several FMSs perform differently when flying the same procedure.

The interpretation of a published procedure into a format that the FMS of the aircraft can interpret is a critical issue: in RNAV navigation the pilot is no longer flying “a chart” but it is the FMS which is flying “a database”. To facilitate this interpretation there is a database standard published by Aeronautical Radio, Inc. (ARINC): the standard 424 (ARINC, 2000). This document details how navigation databases for FMSs are to be coded. One of the most important elements of this coding is that of Path Terminators, which provide the means to translate terminal area procedures, such as SIDs, STARs and approach procedures, into FMS readable code. In short, a Path terminator defines a specific flight path and a specific type of termination for that flight path.

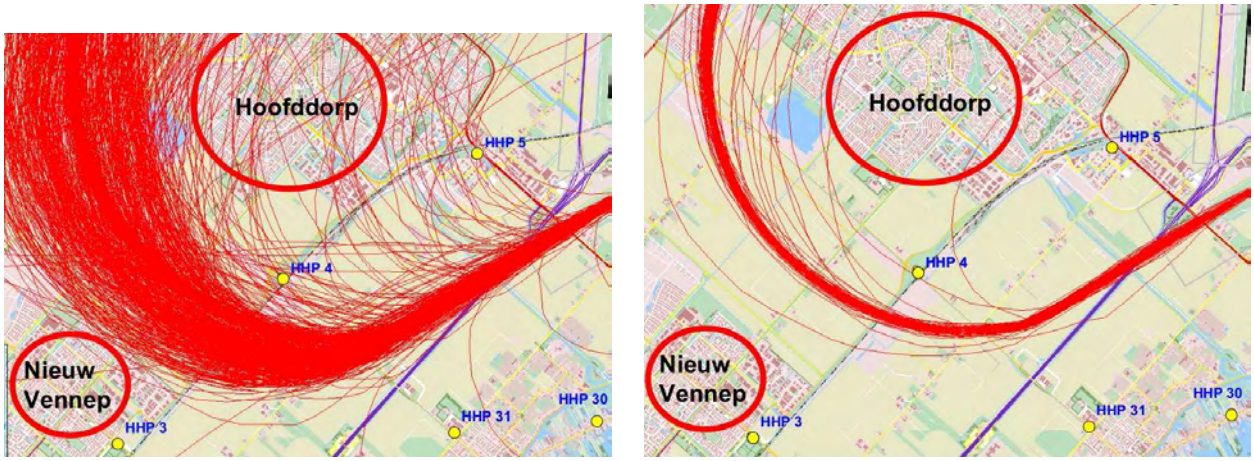

(a) Subset of aircraft using conventional and RNAV navigation with no RF leg capability

(b) Subset of aircraft (KLM B737) using RNAV navigation upgraded with RF legs capability

Figure II-3: *Example of flight tracks corresponding to the initial turn of the Spijkerboor departure in Schiphol (The Netherlands)*

Courtesy of Theo van de Ven, KLM. Printed with permission

See Appendix A for more information concerning Path Terminators and RNAV implementation.

Track between Fixes (TF) is the basic and recommended Path Terminator for procedure designers as all FMS implementations can perform it. However, as explained before, different aircraft, equipped with different FMS, flying at different speeds with different wind conditions, all will compute different distance turn anticipation values for the same turn in a given fly-by waypoint. This will produce a certain ground track dispersion that may turn ineffective a carefully designed noise abatement procedure. Knowing this, the Radius to a Fix (RF) Path Terminator offers higher containment regarding track dispersion and therefore, becomes significantly attractive for the design of NAPs. Due to the fact that the aircraft is continuously adjusting the bank angle when performing a turn with a constant radius, during a RF leg much higher accuracy throughout the turn is achieved. However, nowadays this Path Terminator is still a recommended function for P-RNAV equipments and is not implemented in all FMS (JAA, 2005).

Figure II-3 a) shows the flight tracks corresponding to the beginning of the SPIJKERBOOR (SPY) departure from runway 24 at Schiphol airport in The Netherlands. At 4NM after the take-off, the aircraft may perform a right turn of an almost 180^o course change. For aircraft equipped with RNAV systems this turn corresponds to a Track between Fixes (TF) leg after a turning fly-by waypoint. For conventionally equipped aircraft the turn is performed once reaching 4NM after the take-off (Air Traffic Control the Netherlands, 2009b). The nominal path of this procedure passes in between two populated areas: Niew Vennep and Hoofdorp. However, due to aircraft flying with conventional radionavigation means and due to the different turn anticipation distances for RNAV equipped aircraft, the dispersion of ground tracks during the right turn is quite significant in having a negative impact on the noise footprint over the populated areas. On the other hand, Figure II-3 b) shows the same procedure when the right turn has been coded as a RF leg instead of TF leg. These experimental results were conducted by KLM in a pilot project aimed at showing the benefits of the RF Path Terminator for noise abatement procedures. As seen in the Figure, the dispersion of the aircraft flying this leg type is significantly smaller.

Unfortunately, RF legs are not widely available in all FMS flying nowadays and there are still few airports that enforce their use to aircraft operators. An example of current RF procedures for noise abatement purposes (as well as for not over-flying restricted airspace) are these published at Ronald Regan National Airport, in Washington DC (USA). Figure II-4 shows the approach to runway 19. As it can be seen, to ensure that aircraft fly over the Potomac River as much as possible,

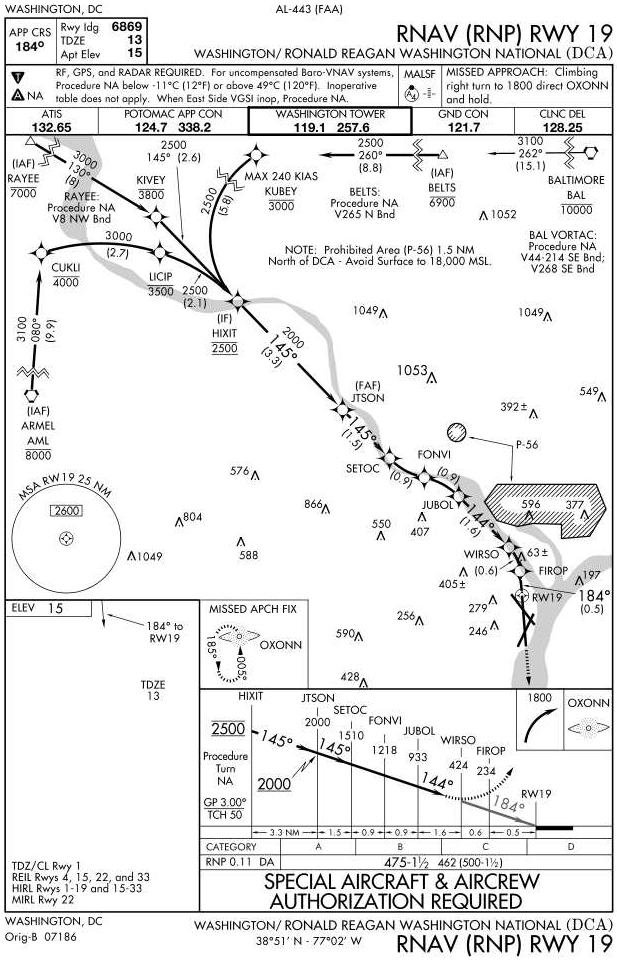

Figure II-4: *Example of an RNAV approach with RF legs at Ronald Regan National Airport (Washington DC, USA)*

Source: (FAA, 2009b)

a configuration of RF legs is published after the SETOC waypoint.

II.1.2 Vertical Trajectory Management

If lateral adjustments are not possible and the trajectory must over-fly certain populated regions, acting in the vertical plane is also a very efficient method to mitigate aircraft noise. There are several ways to improve the noise footprint if the vertical profile is optimised. Unlike lateral trajectory modifications, a given vertical trajectory profile will closely relate thrust settings with flight path angles and aircraft speed during the procedure. Some vertical trajectory improvements have been used extensively in the past, while other techniques are still undergoing testing or validation phases. Some are further awaiting new technological improvements in aircraft and ATM systems. Following is a summary of existing and forthcoming NAPs for both departure and arrival/approach phases.

Concerning the departure phase, the most widely used procedures for mitigating noise are the so called ICAO Noise Abatement Departure Procedures (NADP) defined in (ICAO, 2006a). The NADP-A procedure is designed to protect areas located close to the airport, while the NADP-B procedure is designed to protect distant areas to the airport. Each procedure specifies the airspeed profile that should be maintained during the initial climb as well as the points (altitudes)

where thrust/power reduction may be done. The difference between NADP-A and NADP-B procedures resides in the fact that the first one gives more importance to climb as fast as possible and then accelerate and gain airspeed while the second tries to accelerate first and then climb.

The main problem of these procedures is that they are generic procedures and not always fit into the specific problems or environment that a certain airport may suffer from. For example, they do not allow for consideration of the actual population distribution around the airport. This is due to several factors, such as the impossibility to define a general procedure satisfying the specific problems that may affect each particular airport, air traffic management and airport capacity constraints or even the limitations of current installed on-board technology equipping the majority of the FMS.

On the other hand, several and different techniques are being used in order to reduce noise during the approach or arrival phases. Nowadays, the final approach segment into the landing runway is straight and aligned with the extended runway centreline, albeit in non-precision approaches a very small misalignment is permitted (ICAO, 2006b). Current approach operations in major airports are based on an Instrumental Landing System (ILS) providing lateral and vertical guidance during this final segment (see Appendix A for more details in radionavigation aids and approach types). Therefore, in this phase very few improvements can be obtained in the trajectory in order to improve the noise footprint. On the other hand, the arrival phase and the initial approach phase offer more flexibility in the design of vertical (an lateral) paths. The principal solutions that have been identified for these phases are summarised next.

II.1.2.1 Increase the ILS interception altitude

ILS glide-slopes are usually intercepted after a flat segment (the intermediate approach segment) at altitudes ranging between 2 000 to 3 000 ft. Increasing this interception altitude will maintain a higher vertical distance from the ground during these flat segments, where higher thrust is normally required. This technique is already being applied in many airports and does not impact, in general, on the airspace capacity, although the ATC (Air Traffic Control) should give attention to monitor traffic on longer final approaches (SOURDINE I Consortium, 2001). In addition, it is worth mentioning that in some cases this strategy may lead to ILS signal coverage problems due to the increased distance from the emitting antennae to the point where the interception is done.

II.1.2.2 Higher ILS glide-slope angle

The standard ILS interception angle is 3^o and according to the ICAO PANS-OPS document (ICAO, 2006b), the maximum angle is 3.5^o for CAT-I approaches and remains 3^o for CAT-II or CAT-III approaches. In exceptional cases this angle can be increased, like for example in London City Airport (LCACC, 2009). The main reason for increasing these angles is generally to allow the required obstacle clearance in the final approach segment. Thus, the potential noise reduction remains as a collateral benefit from these procedures. A major drawback to this technique however is the requirement for special crew training and aircraft certification issues. Evidently, a higher ILS glide-slope angle may improve noise conditions directly underneath the path due to a higher slant range between the aircraft and the population. Yet, the corridor of high intensity noise may actually increase due to reduced lateral attenuation effects (the aircraft will be seen with higher elevation angles and therefore the lateral attenuation will be lower).

II.1.2.3 Dual landing thresholds

Dual landing threshold allows the overall noise contour to be shifted towards the airport by enabling light and medium aircraft to perform approaches at a displaced threshold. This in turn reduces the final approach spacing and runway occupancy time, thus increasing arrival capacity.

However, dual landing thresholds require a dedicated implementation study for suitable runways (Fraport, 2009).

II.1.2.4 Low Drag Low Power (LDLP) approaches

Currently, this technique is widely used and drives the aircraft in clean configuration (*i.e.* with flaps and slats retracted) and with the landing gear up for as long as possible. Aerodynamic noise produced by these elements is reduced, even if the aircraft are required to fly at higher speeds which increase aerodynamic noise (to a lesser extent). The extension of the landing gear is one of the biggest sources of noise because, besides aerodynamic noise, the extra drag has to be compensated by increasing the engine thrust too. This procedure has some minor disadvantages regarding capacity and ATC aspects. In fact, reduced flap settings during the final approach leads to a higher final approach speed, which in some cases, may result in a reduction of airport capacity due to increasing runway occupancy time (SOURDINE II Consortium, 2003).

II.1.2.5 Continuous Descent Approaches

During a Continuous Descent Approach (CDA) the aircraft performs a thrust-idle flight until a point before ILS-Localiser interception, considerably reducing the noise footprint during the descent. With current flight guidance systems, two main different types of CDA can be flown: fixing speed profiles (leaving free the vertical profile) or fixing the vertical profile (leaving free the speed profile). There exists a third type of CDA where speed and vertical profiles are fixed but the thrust configuration can not always be set to the idle position. All CDA procedures reduce significantly noise levels during the approach, yet they also impact heavily on air traffic control operations and airport capacity due to the higher separation values required for aircraft flying CDAs. In (Erkelens, 1999) an overview can be found discussing the implementation of CDAs in The Netherlands, one of the first European states to introduce such procedures. On the other hand, in (Macke & Koenig, 2007; Koenig & Macke, 2008), the benefits of combining CDA approaches with LDLP strategies are shown.

A large disadvantage of the CDA procedure however, is that once the idle descent has commenced, it is hardly possible to react on air traffic control instructions. Both the shortening and the extension of the lateral paths would decrease fuel efficiency as well as noise emissions. In addition, allowing aircraft to fly their preferred speed and vertical profiles on a joined lateral path could result in a suboptimal separation causing a break-in of capacity. Therefore, in major airports, these approaches are only flown in low traffic periods (such as night operations) where the required higher separations are not an issue in regards to the capacity. This is explored in the study conducted by (Wubben & Busink, 2000), where the benefits of the CDAs implemented in Schiphol airport (The Netherlands) are highlighted. The study further shows the constraints in airport capacity resulting in their application for night only operations. Moreover, some flight tests involving 12 to 14 Boeing B757-200 and B767-300 night flights are described in (Clarke *et al.* , 2006). The results from these tests demonstrate the consistency of the procedure, the measurements in noise reduction, fuel burnt, emissions, and flight time.

Several papers assess the separation issues that arise when mixing CDA with non-CDA traffic. See, for instance (Ren & Clarke, 2007) or (Elmer, 2008). On the other hand, an Advanced CDA (ACDA) is a CDA that is enhanced with future infrastructure, ATC tools and crew tools in order to meet demands of capacity and safety. During an ACDA procedure, the requirements for ATC speed control may be relaxed or even removed, and additional constraints may be added. For example, in executing a part of the approach with thrust idle or to follow a certain fixed vertical flight path. In (Gomez Comendador, 2004), a study of the compatibility of new ACDA procedures combined with conventional procedures in Madrid TMA is presented. The study concludes that in certain circumstances such compatibility is possible while keeping airport capacity within ac-

ceptable levels. Furthermore, in (Kuenz *et al.* , 2007), the trade-off between ACDAs and airport capacity is assessed, highlighting 4D navigation as a major key enabler for maintaining compatibility of these green trajectories in dense TMAs.

II.1.2.6 Three Degree Decelerating Approaches

Clarke *et al.* proposed a significant improvement on conventional CDA approaches by defining the *Three Degree Decelerating Approach* (TDDA) showing improvements on better noise abatement, while maintaining acceptable airport (or TMA) capacity levels (Clarke & Hansman, 1997). In this procedure, the aircraft starts to descend towards to the runway along a three degree glide slope (the same angle as in the ILS approach) yet at a higher altitude and at higher speeds than the normal ILS approach. This initial descent, which can be straight or curved, is out of the coverage of the ILS system. Furthermore, the aircraft is supposed to be guided in the vertical plane by an RNAV capable FMS. The speed reductions that are usually performed during the intermediate approach segment can be achieved during the descent by reducing the thrust to idle while maintaining a constant three degree flight path angle. Due to this constant glide path descent angle during the entire procedure, TDDAs are more user-friendly from a pilot's point of view than CDA approaches. However a special cockpit display for flying such procedures is still recommended as explained in (de Beer *et al.* , 2008).

Further work involving this concept led to the Modified TDDA (MTDDA), providing the same noise benefits as the TDDA with little or no loss in capacity relative to conventional approach procedures (Ren *et al.* , 2003). In this case, the initial speed is maintained during a certain period of time after the descent point, reducing in this way, the dispersion of aircraft around this point and enabling more reduced separation distances between aircraft.

II.1.3 Optimisation of NAPs

So far, different noise abatement procedures have been presented as a list of techniques or strategies that have been proved to reduce the noise footprint during an aircraft depart or approach. However, it is not clear how all these methods should be used together or how they will perform in a specific scenario. In other words, it would be conceivable to design the optimal procedure for each specific problem, not only dealing with noise criteria but also with existing capacity or ATM constraints. At research level, some work in theoretical optimal trajectories minimising the noise impact in depart or approach procedures is also found in the literature. For example, in (Zaporozhets & Tokarev, 1998b), a trajectory optimisation problem was identified and formulated. This work also shows how noise can be spread by using more than one possible trajectory and allocating, in this way, the noise exposure optimally. Other works showing noise allocation concepts can be found in (Heblij *et al.* , 2007) or (Netjasov, 2006).

As it will be explained in Chapter IV, the optimisation of an aircraft trajectory, as a 4 dimensional continuum, is a *constrained optimal control problem*. This kind of problems is not easy to solve, specially when nonlinear functions appear in the definition of the optimisation objective and/or the constraints. One way to solve this kind of problems is with the *calculus of variations* (also called the *Maximum Principle of Pontryagin*). Analytically this kind of solutions is only possible to obtain for small and simplified problems which, unfortunately, is not the case in the optimisation of an aircraft trajectory (Bryson & Ho, 1975). Therefore, besides simple or more *academic* problems, no real applications in the optimisation of noise abatement procedures use this kind of formulation.

However, a numerical solution is conceivable if complex problems are tackled. See for instance (Visser, 1990), where fuel-optimal flight profiles are computed. However, even if solved numerically, this methodology presents some inconveniences that will be discussed in section IV.1.3.

With the availability of more powerful computers, other numeric alternatives become more

popular in the late 90's requiring much more computational burden, but overcoming the limitations of the previous formulation. In Figure II-1 we have identified the most important ones. The following sections summarise the most relevant contributions that have tackled the optimisation of NAPs by using one or several of these numerical approaches. For an interesting survey of numerical methods for trajectory optimisation the reader can refer to (Betts, 1998).

II.1.3.1 Brute force approaches

Early attempts to optimise specific flight procedures are found for example in (Norgia, 1999), where ten different take-off profiles were used for simulation at Rome airport, in Italy. In this case, the *optimal* trajectory was chosen among ten different *a priori* designed flight profiles. In (Capozzi *et al.* , 2002), a noise aware decision support tool is presented, where actual flight tracks (from radar data) can be displayed over a map containing the location of noise sensitive areas. Then, flight trajectories can be modified manually in order to construct a flight path avoiding these areas. More recently, in (Reynolds *et al.* , 2007), a combination of CDA and LDLP techniques are merged to define specific noise abatement procedures in Nottingham East Midlands Airport, in UK.

On the other hand, the SOURDINE I project was funded by the European commission under the transport RTD (Research and Technology development and Demonstration) programme of the 4th framework programme (SOURDINE I Consortium, 2001). There, an effort to improve take-off procedures was done and some simulations with specific aircraft types were carried out. In this study, optimal take-off procedures were obtained involving a progressive increase in thrust (which is not feasible with present technology) and low airspeeds during the whole departure which could be a problem regarding airport capacity. Those procedures were derived from ICAO NADP-A and NADP-B procedures and optimisation involved changes in values for engine cut-off, acceleration and climb points (altitudes). Further work was done in SOURDINE II project, this time a RTD of the competitive and sustainable growth programme funded by the European commission (SOURDINE II Consortium, 2006). In this project, the take-off procedures were refined selecting a grid of speed/thrust combinations and altitudes where thrust cut-off were performed. In this case, more than 30 different simulations were carried out but any further optimisation was not done.

Finally, in (Clarke & Hansman, 1997) and (Clarke, 2000), a tool is presented that combines a Flight Simulator, a Noise Model, and a Geographic Information System (GIS). This tool allows to create a unique rapid prototyping environment in which the user can simulate aircraft operations in existing and potential guidance and navigation environments, while simultaneously evaluating the aircraft's noise impact.

II.1.3.2 Non Linear Programming

These methods consist of a convenient discretisation of the differential equations in order to transform the initial continuous problem into a Non Linear Programming (NLP) problem. NLP is the process of determining a finite set of variables that should be arranged in order to maximise/minimise an objective function under a set of finite constraints on the decision variables. Either the objective or constraint functions may be nonlinear in this kind of problems (Vajda, 1974). If the problem is not convex (due, to the nonlinearities) one cannot guarantee that a global optimal solution is attained with this technique. In fact, the final solution is quite sensitive to the initial variable values (or *guesses*) that are given at the beginning of the optimisation.

The contributions of Visser *et al.* are particularly significant in the application of these methods in the optimisation of noise abatement procedures. In (Visser & Wijnen, 2001), optimal noise departures are optimised by using a tool combining a noise computation model, a Geographical Information System (GIS) and a dynamic trajectory optimisation algorithm using direct collo-

cation methods. In (Visser & Wijnen, 2003), the same methodology is applied for noise optimal arrival trajectories. Furthermore, (Visser, 2005) identifies that current procedures do not generally take into account the actual population density and distribution at a specific airport site. This is due to the fact that most current noise abatement procedures (like those explained in previous sections) are local adaptations of generic procedures aimed at optimising aircraft noise footprint. In addition, it is shown how different criteria affecting the optimisation trajectories are not compatible: improving one objective means to reduce the performance on other objectives. In this context, the difficulty of finding a compromise solution satisfying all criteria is clearly highlighted. Furthermore, the sensitivity of these trade-off between objectives is initially explored showing a significant variation in the computed optimal trajectory. Exploiting the multi-stage capability of this tool, (Hogenhuis *et al.* , 2008) show how RNAV procedures can be optimised, offering the possibility to calculate routes that can be programmed into FMS currently available in most aircraft cockpits. On the other hand, in (Heblij & Visser, 2008) only the vertical profile of an existing RNAV flight procedure is optimised. Lateral path is not taken into account for noise abatement purposes in order to overcome capacity and ATC issues.

In (Suzuki *et al.* , 2009) and (Tsuchiya *et al.* , 2009) another real time algorithm, based again in a direct collocation methods, is defined. Moreover, in (Suzuki & Yanagida, 2008; Masui *et al.* , 2008), it is shown how this methodology is implemented and tested on-board an aircraft.

II.1.3.3 Dynamic programing

With dynamic programing, a complex problem can be solved by breaking it down into simpler subproblems. Then the problem is solved in a recursive manner and, as explained previously, a local optimal solution will be generally found if the problem is non convex (Bellman, 2003).

An application of this methodology for aircraft fuel optimisation is presented in (Hagelauer & Mora-Camino, 1998). Xue *et al.* performed important contributions in the noise minimisation of runway independent aircraft operations by using dynamic programing techniques. See for instance (Xue & Atkins, 2003; Xue & Atkins, 2006a; Atkins & Xue, 2004) or for a deeper insight on this field, (Xue, 2006). On the other hand, a real-time and adaptative algorithm for noise abatement optimal trajectories is presented in (Zou & Clarke, 2003; Zou, 2004), where dynamic programming techniques are also used. The main limitation of this technique, if compared with the previous case, is the computational cost when dealing with complex scenarios, with a large number of objectives and variables.

II.1.3.4 Stochastic optimisation

These methods incorporate random elements, either in the objective functions and/or constraints and/or decision variables and/or in the algorithm itself (Spall, 2003). One of the most used algorithms are genetic algorithms, where a stochastic search method is performed inspired on the process of natural Darwinian evolution (Gen & Cheng, 1997). Other methods include simulated annealing, ant colony, bees algorithms etc., and are often inspired in biological or physical processes. This family of techniques aims at finding a global optimum. However, once a optimal solution has been found, it is almost not possible to prove that it corresponds to the global optimum indeed.

In (Vormer, 2005; Vormer *et al.* , 2006), a multi-objective genetic algorithm was developed that provides a way to optimise arrival trajectories. The scheduling algorithm considers four objectives: throughput, deviation from altitude and speed profiles of a three-degree decelerated approach, and noise impact on community. In this work, the trajectory is optimised from an existing reference trajectory, obtaining flexible variations of it, but a global trajectory optimisation is not performed. On the other hand, in (Xue & Atkins, 2006b; Xue, 2006) a simulated annealing algo-

rithm is used for the minimisation of noise in runway independent aircraft operations. Albeit the results are quite interesting, the computational burden for more realistic and complex scenarios seems again to be not affordable.

II.2 Noise annoyance modelling

According to (Verkeyn, 2004), the history of modern community noise annoyance modelling started in 1978, when Schultz re-analysed the English language data from several social surveys dealing with the perception of airway, railway and road traffic noise (Schultz., 1978). In this study, the annoyance levels as a function of the sound exposure were plotted. Moreover he computed the percentage of people that were *highly annoyed* for each dose. Several authors followed him with more surveys and with refinements on the meta-analysis methodology. More recently, one of the largest database coming from 45 surveys has been compiled by (Miedema & Vos, 1998; Miedema & Oudshoorn, 2001). From this analysis, they acknowledge three different dose-response relationships, one for airway, railway and road traffic, and assume a linear relationship with normal distributed random component between the measured noise exposure and the experienced degree of annoyance. In (Vallet, 2006; Vos, 2000) it is also reported that for similar noise exposure levels, aircraft noise is more annoying than other sources of noise such as train or road traffic. This points out the complexity that exists between noise exposure and noise annoyance.

In 1982, three noise abatement procedures were tested in John Wayne airport, in Santa Ana (California, USA) followed by telephonic surveys before and after the application of these new procedures (Fidell *et al.* , 1982). The analysis of the results showed a bad correlation of different dosage-response curves. Even if the noise exposure had decreased significantly after the application of the noise abatement procedures, the community reported to be still annoyed.

Although widely accepted, these kinds of dose-response relationships assume two important restrictions (Kryter, 1994): average noise metrics are usually used and non-acoustic factors are also averaged out. Average noise metrics take into account the noise exposure during a large period (*i.e.* a day) and therefore the context of the affected individuals when the noise event occurs is not taken into account. Therefore, this kind of meta-analysis approach is only suitable for modelling the annoyance impact on large groups or neighbourhoods.

II.2.1 Effects of aircraft noise

Several studies in the psychological and medical fields have also been carried out in order to better understand the effects of noise on humans. For example, (Muzet, 2007) explains the effects of sleep disturbance due to noise which can be appreciated physiologically and also psychologically. As immediate consequence, noise can delay the sleep onset and can lead to early final awakenings or nocturnal awakenings. The body would produce vegetative or hormonal responses to noise and the sleep structure will change. As a secondary effect of these sleep disturbances the performance of the affected people would decrease and the daytime behaviour will change. On the other hand, the Federal Interagency Committee on Aviation Noise (FICAN) recommends a dose-response curve for predicting awakenings, based on field data gathered after several years of research (FICAN, 1997). As it can be seen in Figure II-5, this relationship represents the worst-case bound on the number of people likely to awake because of the perceived indoor sound exposure level. As a consequence, chronic partial sleep deprivation induces marked tiredness, increases a low vigilance state, and reduces both daytime performance and the overall quality of life (Öhrström & Griefahn, 1993).

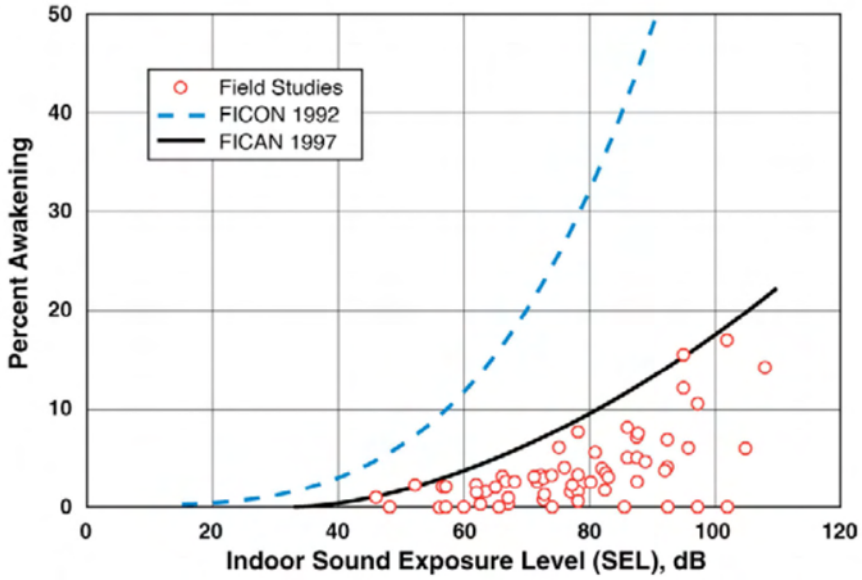

Figure II-5: *Sleep disturbance dose-response curve proposed by FICAN*

Source: (FICAN, 1997)

But noise not only affects the quality of the sleep. It produces speech interference, hearing loss, lack of concentration and cognitive deterioration. Even the animals are sensible to noise and, for example milk production in dairy cattle may decrease because of aircraft flyovers or negative effects on wild animals reproduction can be also a consequence of noise exposure. For a very complete review of the effects of aircraft noise on wildlife and humans see (Pepper *et al.* , 2003) or (Berglund & Lindvall, (Eds.) 1995). On the other hand, for studies analysing the effects of aircraft noise in particular scenarios the reader should refer, for instance, to (Hiramatsu *et al.* , 2004; Hiramatsu *et al.* , 1997).

II.2.2 Fuzzy models for noise annoyance

As explained before, annoyance is usually qualitatively assessed with social surveys. See for instance (Berglund & Lindvall, (Eds.) 1995; Rylander & Björkman, 1997) or (Fields *et al.* , 2001). As a subjective, complex and context-dependent concept, noise annoyance can be studied qualitatively by using *fuzzy logic sets* rather than quantitatively by using exact models or formulae. Fuzzy set theory is a generalisation of traditional set theory and provides a powerful means for the representation of imprecision and vagueness.

In (Botteldooren & Verkeyn, 2002), an interesting comparison between classical noise annoyance models and fuzzy ones is shown. Classical models try to quantify the relation between exposure and annoyance, but they do not take into account the modifiers that may influence this relation. The proposed fuzzy model focuses on the cognitive processes involved in general in the judgement of noise annoyance. Moreover, (Botteldooren *et al.* , 2003) provides the theoretical background for building fuzzy rule based models aimed at expressing the noise annoyance. In addition, it is shown how this way of thinking about noise effect modelling can be used in practice both in management support as a noise *annoyance advisor* and in social science for testing hypotheses such as the effect of noise sensitivity or the degree of urbanisation. The translation of linguistic terms into different languages is assessed in (Verkeyn & Botteldooren, 2004), where 21 adverbs in 9 different languages are tested. Finally, the reader should refer as well to (Verkeyn, 2004) for a detailed description on how to build such a fuzzy system, capable of judging the impact of noise on a individual person.

Other works, conducted by Zaheeruddin *et al.* are also devoted to model the effects of noise by using fuzzy models. For example in (Zaheeruddin *et al.* , 2003), the human work efficiency in noise environment is modelled by using fuzzy logic where noise exposure, its duration and the working task complexity are considered as input variables. On the other hand, in (Zaheeruddin & Vinod, 2006), a fuzzy prediction of the effects on sleep disturbance by noise is presented as a function of noise exposure, age, and duration of its occurrence. Furthermore in (Zaheeruddin *et al.* , 2006), the noise exposure, its duration and the socio-economic status of the affected people are identified as the more relevant aspects for the fuzzy modelling of noise annoyance.

II.3 Concluding discussion

All the results and conclusions arisen from the above-mentioned works are encouraging and will set the basis for new noise abatement procedures. The research done in the field of trajectory optimisation is very promising, especially if we take into account the forthcoming wide implementation of RNAV or CDA/TDDA procedures. As commented before, this will allow more flexible trajectories, not bounded to over-flying conventional radionavigation aids, leading to a significant capacity to implement noise optimal procedures.

Although multi-criteria optimisation is a discipline that has been analysed for more than a century, the multi-criteria nature in noise abatement procedures is a topic that has not been deeply assessed in the literature. Several strategies are available aimed at dealing with several conflicting optimisation objectives, like fore example fuel and noise or different conflicting noise criteria. However, in all the above-mentioned works, the objectives are multiplied by a weighting factor and summed up to build a single *weighted average function* to be minimised. This technique is known as scalarisation and presents some drawbacks as we will comment in Chapter IV.

On the other hand, more complex (and therefore, more accurate) noise annoyance models are already available nowadays but their integration into an trajectory optimisation framework is still something to be further explored. Recalling the above-mentioned works in the optimisation of NAPs, almost all of them use a noise metric for building the optimisation functions. Exceptionally, (Xue, 2006) gives different weights to the noise sensitive areas as a function of the population density and the work done by Visser *et al.* considers night awakenings (according to the FICAN studies) as the objective function to be minimised in their trajectory optimisation algorithm (Visser & Wijnen, 2001; Visser & Wijnen, 2003; Wijnen & Visser, 2003). In this way, annoyance is, somehow, taken into account instead of just considering the acoustical metrics as the majority of similar works do.

As stated in the introduction of this thesis, among other issues, in this work we will try to focus on these two existing *gaps* in the trajectory optimisation for noise abatement procedures: explore alternatives to deal with the multi-criteria optimisation and the consideration of noise annoyance models in the optimisation objectives.

If people do not believe that mathematics is simple, it is only because they do not realize how complicated life is.

— John von Neumann

Have no fear of perfection. You will never reach it.

— Salvador Dalí

III Modelling

In this Chapter, the different models needed for setting up the optimisation framework are presented. First, the considered input data and the modelling of a given scenario are explained. Then, the model for the aircraft dynamics and the rest of optimisation constraints are presented. In addition, the noise model that has been adopted for this work is outlined. Finally, this Chapter ends with the construction of a basic noise annoyance model based on fuzzy logic reasoning and aimed at being used as optimisation function in the following Chapters. Although the general methodology presented in this PhD thesis is valid for the optimisation of either departure or arrival procedures, only departure trajectories will be assessed in this dissertation. Thus, the presented models and methodologies are generic and valid for departure or approach unless otherwise stated.

III.1 Input data and scenario definition

Different sources of data are required to run the optimisation framework presented in Figure I-3. These are grouped as follows:

- **Airspace data**: airspace characteristics of the studied area, restricted areas and airspace structure organisation. In addition, the departure final point or arrival initial point defining, respectively, the final or initial conditions of the problem.
- **Navigation data**: possible navigation constraints such as RNAV or Performance Based Navigation (PBN) and procedure design criteria. In addition, time constraints at waypoints may also be considered, taking into account eventual 4D trajectory designs.

- **Cartographical data**: terrain elevations and obstacle identification, needed to safely define flight procedures in accordance with RNAV procedure design criteria. In addition, this information will be used by the noise model.
- **Aircraft performance data**: including aerodynamic and power plant related data of the studied aircraft that is needed to build up the aircraft dynamic model as well as the noise model.
- **Meteorological data**: general data and winds, in particular, that will affect available runway configuration, the noise propagation model and the aircraft ground trajectory.
- **Airport data**: location of the airport, the type of procedure, available runway configuration etc.
- **Geographical data**: airport's surrounding areas, such as the location, type and characteristics of the inhabited areas.

III.1.1 Scenario definition

The airport configuration, the present meteorological and the relevant geographical data around the airport will define the scenario where the trajectory should be optimised. The annoyance caused by the departing/approaching aircraft along the trajectory will be determined in function of the scenario. Therefore, this module should provide information about:

- the runway in use and the type of procedure (depart or arrival/approach),
- the time of day that the procedure will be take place,
- the location and shape of the inhabited areas surrounding the airport,
- the type of the inhabited areas (industrial zones, residential zones, etc.),
- an estimated value of the background noise at each zone (taking into account the presence of noisy elements, such as motorways, harbours, etc. that could mask partially or totally the perceived aircraft noise),
- the location of eventual high-sensitive areas such as environmentally protected zones, hospitals etc.

III.2 Model of the aircraft dynamics

The dynamics of the aircraft can be described by a set of nonlinear differential equations. When studying the trajectory of a civil aircraft during the take-off phase, it is natural to study the movement of its centre of mass. Therefore, only translational motion is considered, neglecting the angular motion of the aircraft. This kind of model has been widely used in aircraft performance optimisation studies, see for instance (Roskam, 2001), (Stevens & Lewis, 1992) or (Berton, 2003).

In fact, this assumption means that only the guidance dynamics of the aircraft are considered since it is assumed that the aircraft of interest is equipped with basic auto-pilots which deal efficiently with its fast dynamics and therefore, the body attitude (pitch, bank and yaw angles) and the regime of the engines are controlled. It is also assumed that turn manoeuvres are achieved in a coordinated way (the sideslip angle remaining approximately null) and the aircraft is assumed to fly in a standard atmosphere, over a locally flat non-rotating Earth and with a constant aircraft mass during the procedure. Appendix C contains some flight mechanics theory and the details of the modelling methodology that leads to the final kinematic and dynamic equations used in this work. These, are just summarised in what follows.

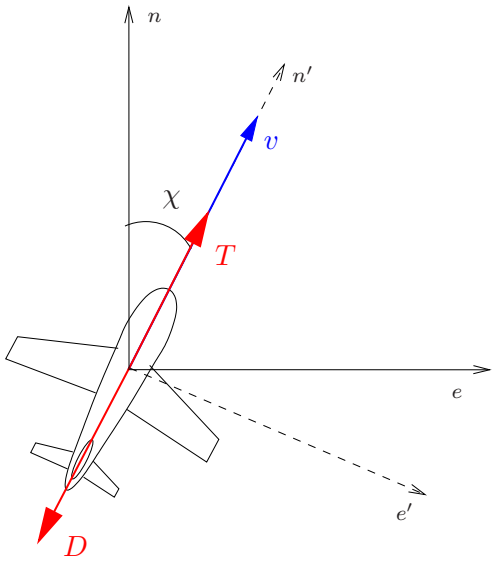

Figure III-1: *Reference frames and magnitudes of a climbing and turning aircraft: n-e plane*

III.2.1 Reference frames and main magnitudes

Two different reference frames are used to describe the aircraft equations of motion. A *Ground* reference frame which will be used as inertial frame and an *Air* reference frame where the aerodynamic forces are easily expressed. These two reference frames are defined as:

- **Ground reference frame**: $\mathbf{G} = [O_G; e, n, h]$. East, North, Height (or Up) conventional right handed frame on the surface of the Earth with a given origin O_G. The h axis points upwards following the local vertical direction (*i.e.* with the same direction of the local gravity vector, $\vec{g}$ but in the opposite sense) and the n-e plane is tangent to the Earth's surface at O_G. The e axis points Eastwards and therefore the n axis points to the North.
- **Air reference frame**: $\mathbf{A} = [O_B; x_A, y_A, z_A]$. Conventional right handed frame with origin O_B, the centre of mass of the aeroplane. The x_A axis is always aligned with the relative velocity vector between the air and the aeroplane. y_A axis is perpendicular to x_A and starboard aligned while z_A axis goes down the aircraft and it is perpendicular to the x_A-y_A plane.

The three angular rotations relating these two reference frames are (rotation sequence starting from reference frame **G**):

- First rotation about the h axis, nose right (aerodynamic heading angle χ)
- Second rotation about the new e' axis, nose up (aerodynamic flight path angle γ)
- Third rotation about the new n'' axis (x_A axis), right wing down (aerodynamic bank angle μ)

Figures III-1 and III-2 show these reference frames and angles as well as the main magnitudes that will appear in the dynamic model of the aircraft. Namely, L is the aircraft lift force, D is the drag force, T is the total net thrust force generated by all the engines of the aircraft, m is the mass of the aircraft, g the module of the local gravity vector, $\mathsf{n_z}$ the vertical load factor and v the relative air to aircraft speed, also known as the *True Air Speed* (TAS).

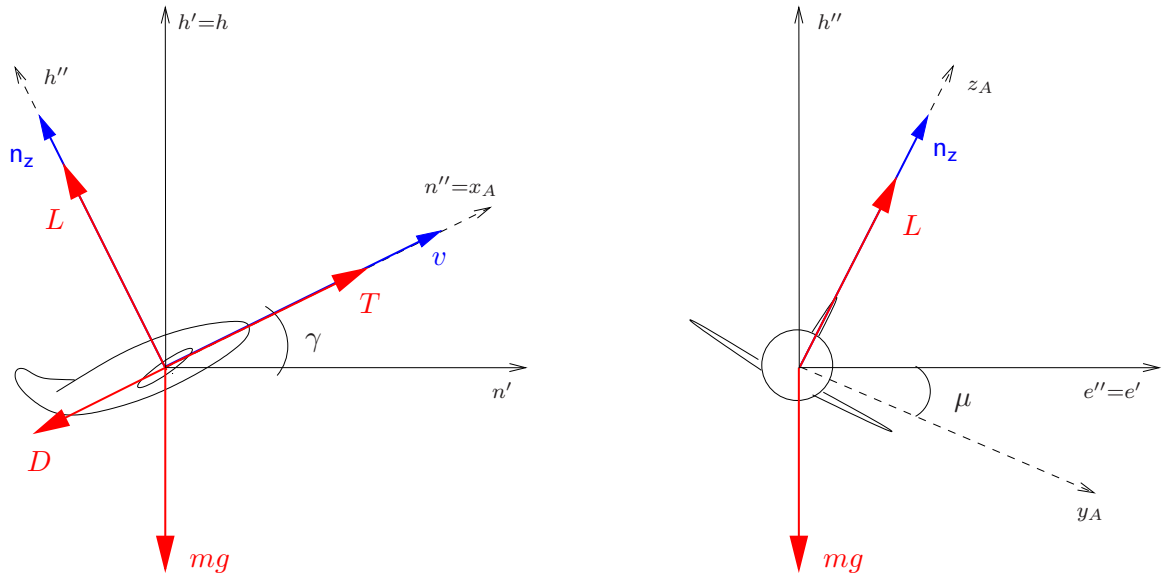

(a) h'-n' plane (b) h''-e'' plane

Figure III-2: *Reference frames and magnitudes of a climbing and turning aircraft*

III.2.2 State representation of aircraft dynamics

Using this relative-wind axes formulation, the aircraft dynamic and cinematic equations of movement can be derived and merged in a state-space representation. For the sake of clarity, the complete deduction of these equations is given in Appendix C. Then, the state-space representation of the flight guidance equations, chosen for this dissertation, is:

$$\begin{bmatrix} \frac{\mathrm{d}v}{\mathrm{d}t} \\ \frac{\mathrm{d}\chi}{\mathrm{d}t} \\ \frac{\mathrm{d}\gamma}{\mathrm{d}t} \\ \frac{\mathrm{d}e}{\mathrm{d}t} \\ \frac{\mathrm{d}n}{\mathrm{d}t} \\ \frac{\mathrm{d}h}{\mathrm{d}t} \end{bmatrix} = \begin{bmatrix} \frac{1}{m}\left[T(v(t),h(t),h_c) - D(\mathsf{n_z}(t),v(t),h(t)) - mg\sin\gamma(t)\right] \\ \frac{g}{v(t)}\frac{\sin\mu(t)}{\cos\gamma(t)}\mathsf{n_z}(t) \\ \frac{g}{v(t)}\left[\mathsf{n_z}(t)\cos\mu(t) - \cos\gamma(t)\right] \\ v(t)\sin\chi\cos\gamma(t) + W_e \\ v(t)\cos\chi\cos\gamma(t) + W_n \\ v(t)\sin\gamma(t) + W_h \end{bmatrix} \tag{III.1}$$

where the nomenclature adopted is described in Table III-1.

The wind flow field is supposed to be known and steady during the take-off or approach procedure. In addition, Lift and Drag forces are supposed to remain in the plane of symmetry of the aircraft (plane $x_A - z_A$) and the trust vector, in a first approximation, is assumed to be aligned with the airspeed vector.

Moreover, aerodynamic Drag force D is denoted by (see Appendix C):

$$D(\mathsf{n_z}(t),v(t),h(t)) = \frac{1}{2}\rho(t)Sa(t)v^2(t) + \frac{2b(t)}{\rho(t)S}\left[\frac{\mathsf{n_z}(t)mg}{v(t)}\right]^2 \tag{III.2}$$

where S is the total wing surface and $\rho(t)$ is the air density which is altitude dependant according to the International Standard Atmosphere. The value of aerodynamic coefficients $a(t)$ and $b(t)$

Table III-1: *Notation used in the state space representation of the aircraft dynamics*

t :	Time
v :	Module of the relative air to aircraft velocity (or *True Air Speed*)
χ :	Aerodynamic heading angle
γ :	Aerodynamic flight path angle
e :	Eastward coordinate
n :	Northward coordinate
h :	Height coordinate
$\mathsf{n_z}$:	Vertical load factor (defined as $\mathsf{n_z} = \frac{L}{mg}$)
μ :	Aerodynamic bank angle
m :	Mass of the aircraft
g :	Local gravity vector module
W_e :	Eastwards local wind component
W_n :	Northwards local wind component
W_h :	Vertical local wind component

depend on the aircraft *flaps* and/or *slats* configuration, being the transition from one configuration to another usually executed at given operational speeds:

$$a(t) = a(v(t)) = \begin{cases} a_\varphi & \text{if} \quad v(t) \leq v_{\varphi\to\varphi-1} \\ a_{\varphi-1} & \text{if} \quad v_{\varphi\to\varphi-1} < v(t) \leq v_{\varphi-1\to\varphi-2} \\ \vdots & \\ a_1 & \text{if} \quad v_{2\to1} < v(t) \leq v_{1\to0} \\ a_0 & \text{if} \quad v(t) > v_{1\to0} \end{cases} \tag{III.3}$$

where a_i is the constant aerodynamic coefficient corresponding to flap/slat configuration i, the operational speed where the transition from configuration i to j is performed is denoted by $v_{i\to j}$ and φ is the total amount of flap/slats different configurations. Aerodynamic coefficient $b(t)$ could be expressed as a function of the same operational speeds in a similar way.

On the other hand, for a take-off procedure, the total net thrust, as a function of time, can be expressed by:

$$T(v(t), h(t), h_c) = \begin{cases} T_{TOGA}(v(t), h(t)) & \text{if} \quad h(t) < h_c \\ T_{CL}(v(t), h(t)) & \text{if} \quad h(t) \geq h_c \end{cases} \tag{III.4}$$

where T_{TOGA} is the thrust in *Take-off–Go Around* setting, while T_{CL} corresponds to the *Climb* setting. Since we are dealing with a take-off, we suppose that in the whole procedure the *Auto-Thrust* system is providing the maximum available thrust at a given speed and altitude for each thrust setting. In addition, h_c denotes the height where a thrust cut-back is performed. When the aircraft reaches h_c, the initial *Take-off–Go Around* setting is commuted to *Climb* thrust setting. In this way, we take into account current take-off operational procedures, where the pilot applies a single cut-back at a specified altitude or height. We could think about more futuristic procedures where the value of the thrust can be continuously controlled by the FMS. In that case the function $T(t)$ would be left *free* as a set of decision variables (as a function of the time). However, this is not considered in this dissertation and the equation (III.4) will be used instead.

Then, for each thrust setting ($\sigma = TOGA$ or $\sigma = CL$), the thrust function is modelled by a

third order polynomial approximation:

$$T_\sigma(v(t),h(t)) \simeq n_e \sum_{i=0}^{3}\sum_{j=0}^{3} c_{ij}^{\sigma} v^i(t) h^j(t) \tag{III.5}$$

where n_e is the number of engines and c_{ij}^{σ} are the 16 different polynomial coefficients for thrust setting σ that can be obtained from the typical aircraft performance data tables by using least mean squares curve fitting techniques.

On the other hand, for an aircraft departure fuel consumption is modelled as:

$$FF(v(t),h(t),h_c) = \begin{cases} FF_{TOGA}(v(t),h(t)) & \text{if} \quad h(t) < h_c \\ FF_{CL}(v(t),h(t)) & \text{if} \quad h(t) \geq h_c \end{cases} \tag{III.6}$$

where FF_{TOGA} is the fuel flow in *Take-off–Go Around* configuration, while FF_{CL} corresponds to the fuel consumption in *Climb* configuration, being h_c the thrust cut-back height. Following the same methodology as for the thrust model, described in equation (III.5), fuel consumption at each thrust setting σ is also modelled by a third order polynomial approximation.

In the case of studying arrival and approach procedures, the total net thrust and fuel consumption for these phases could be also modelled in a similar way. There, the appropriate engine cruise and idle performance data would be used instead of the take-off and climb settings.

III.2.3 Variable bounds and constraints

In a departure procedure, the initial position of the aircraft is obviously the end of the departing runway. Usually, such a procedure is intended to drive the aircraft to a particular navigation fix where the en-route airway structure will be joined. Therefore, the horizontal final coordinates (n_f and e_f) will also be fixed and chosen by the procedure designer. On the other hand, the altitude at this final point is not usually fixed, but it is constrained to be higher than a minimum safe altitude $h_f^{\min}$ and usually, due to air traffic management criteria, lower than a maximum altitude $h_f^{\max}$. Moreover, the initial take-off phase going from ground level to a height of 120 m (400 ft) will not be considered in the optimisation process since the standard operational regulations almost restrict all degrees of freedom during this particular phase, see (ICAO, 2006a) and (JAA, 2003). In this initial phase, the aircraft follows a straight trajectory, following the departing runway heading χ_{RWY}, at a constant speed V_2, which depends on the aerodynamics and the weight of the aircraft. For the sake of simplicity initial horizontal coordinates are set to zero at the point where the aircraft reaches a height of 120 m above the runway if not otherwise specified. Moreover, during a normal take-off, the landing gear has been completely retracted when passing 120 m, and consequently, aircraft configurations featuring an extended gear are not considered in the simulations.

Taking all considerations above into account, the constraints that apply at initial and final points for a departure procedure are:

$$\begin{array}{lll} v(t_0) = V_2 & \chi(t_0) = \chi_{RWY} & \gamma(t_0) = \gamma_2 \\ n(t_0) = 0 & e(t_0) = 0 & h(t_0) = 120\,\text{m} \\ n(t_f) = n_f & e(t_f) = e_f & h_f^{\min} \leq h(t_f) \leq h_f^{\max} \end{array} \tag{III.7}$$

Here, γ_2 is the flight path angle that results when the aircraft is flying at V_2 speed while applying *Take-off–Go Around* thrust settings. All variables not listed in equation (III.7) are considered *free* and will be determined by the optimisation itself (including the time at the final point, t_f).

In addition, and for operational reasons, it is enforced that the speed and altitude of the aircraft should not decrease during the whole departure procedure. Moreover, a minimum procedure design gradient must be guaranteed. ICAO Document 8168 (ICAO, 2006a) specifies a default gradient of $s = 3.3\,\%$, which can be higher for obstacle clearance reasons. This gradient is not intended as an operational limitation for those operations assessing departure obstacles in relation to aircraft performance. Thus, the value of the minimum climb gradient s will be chosen in function of the scenario and the aircraft operator. Summing up, these three path constraints can be written as:

$$\frac{\mathrm{d}v(t)}{\mathrm{d}t} \geq 0\,; \qquad \frac{\mathrm{d}h(t)}{\mathrm{d}t} \geq 0\,; \qquad h(t) \geq h(t_0) + s\sqrt{n^2(t) + e^2(t)} \tag{III.8}$$

Finally, some variables should be bounded in order to ensure existing operational or safety requirements for a given aircraft. Therefore, the following bounding constraints are defined for this work:

$$\begin{array}{rcccl} V_2 & \leq & v(t) & \leq & V_{\max} \\ 0.85 & \leq & n_z(t) & \leq & 1.15 \\ -25^o & \leq & \mu(t) & \leq & 25^o \\ 244\,\mathrm{m} & \leq & h_c & \leq & 1\,000\,\mathrm{m} \end{array} \tag{III.9}$$

The maximum velocity $V_{\max}$ may be limited either by an aircraft related limit (maximum operating airspeed) or eventual ATC constraints. On the other hand, in (ICAO, 2006a) is specified that thrust cut-back height should be greater than $244\,\mathrm{m}$ ($800\,\mathrm{ft}$) for noise abatement purposes. Finally, the load factor ($\mathrm{n_z}$), bank angle (μ) and maximum thrust cut-back height (h_c) bounding values correspond to typical values applied by aircraft operators (Pratt, 2000).

III.3 Noise model

When aircraft noise is studied, several metrics exist. Moreover, taking into account the human sensitivity to different frequencies, some ponderation (or weighting) scales have been proposed by experts in acoustics. The models and optimisation techniques developed in this work are independent from the used scales and metrics. Appendix B gives some background in aircraft noise and some metrics and ponderation scales are introduced.

The maximum A-weighted sound level (LAMAX or $\mathrm{L_{max}}$) will be considered as the base metric throughout this work. Therefore, all noise magnitudes will be expressed in dB(A). From now on, this maximum sound level at a given location i will be denoted as L_i and it is simply defined by:

$$L_i = \max_t \; [N_i(t)] \tag{III.10}$$

where $N_i(t)$ is the sound pressure level at location i as a function of the time t.

Despite all results of this PhD thesis will be derived from these L_i values expressed in dB(A), it would suffice to change the noise model block if other metrics or ponderation scales are desired to be taken into account.

III.3.1 The Integrated Noise Model (INM)

The noise model implemented in this study is based on the methodology employed by the Integrated Noise Model (INM) program. INM is developed by the Federal Aviation Administration[1] and has been adopted as the standard package for noise studies and assessments in many countries. INM deals with several noise metrics and, in particular, noise levels are computed at a given point by selecting and interpolating appropriate noise values from a noise-thrust-distance (NTD) table, which is derived from empirical measurements at some specific reference conditions for each aircraft type. To compute the actual noise at a given distance a number of noise level adjustments need to be made as a function of the reference NTD values. Another concept for noise calculation is proposed by (Zaporozhets & Tokarev, 1998a), where the noise radius is used instead of the NTD table.

A detailed description of how INM models aircraft noise and how several metrics are computed is found in the INM technical manual, see (Olmstead *et al.* , 2002). Moreover, the basis for the aircraft noise computation are, in fact, defined in SAE-AIR-1845 standard (SAE – Comitee A-21, Aircraft Noise., 1986). Next, this noise computation procedure is outlined.

III.3.2 INM noise computation

INM contains an acoustic database of noise versus thrust versus distance (NTD) values. The NTD data for an aircraft consists of a set of A-weighted decibel levels for various combinations of aircraft engine power states and distances from the noise measurement point to the aircraft. NTD data consist of two or more noise curves which, in turn, are associated with an engine power parameter, an operational attribute (either departure or approach) and noise levels at the following ten distances: 200, 400, 630, 1 000, 2 000, 4 000, 6 300, 10 000, 16 000 and 25 000 feet. To obtain noise levels that lie between thrust values or between distance values, linear interpolation of thrust and logarithmic interpolation on distance may be used. Extrapolation is used to obtain levels outside of the bounding thrust or distances values. The interpolation/extrapolation is a piece-wise linear process between the engine power setting and the base-10 logarithm of the distance. Finally, being noise levels dependent on the engine thrust settings, INM proposes an approximated method to compute thrust by using a quadratic function fitting similar to equation (III.5).

Noise levels in the NTD tables assume standard reference day conditions (temperature of 27^{o}C, pressure of 1 013 hPa, 70% relative humidity and an altitude at mean sea level) and measurement conditions according to (SAE – Comitee A-21, Aircraft Noise., 1986). Thus, the values issued from the interpolation/extrapolation from NTD values may be adjusted to take into account the actual conditions. The adjustments implemented in INM for the computation of maximum noise level metrics are summarised as follows:

- **Atmospheric absorption adjustment:** taking into account atmospheric absorption due to the effects of temperature and relative humidity according to (SAE. Comitee A-21, Aircraft Noise., 1975).
- **Acoustic impedance adjustment:** defined as the product of the density of air and the speed of sound, and being a function of temperature atmospheric pressure and indirectly the altitude. This component takes into account non-reference day conditions or the effects of the observer (noise measurement point) elevation.
- **Lateral attenuation adjustment:** taking into account the over-ground propagation. This term is derived from field measurements and takes into account ground reflection effects, refraction effects and aeroplane shielding effects as well as other ground and engine/aircraft installation effects according to (SAE – Comitee A-21, Aircraft Noise., 1981).

[1] http://www.faa.org

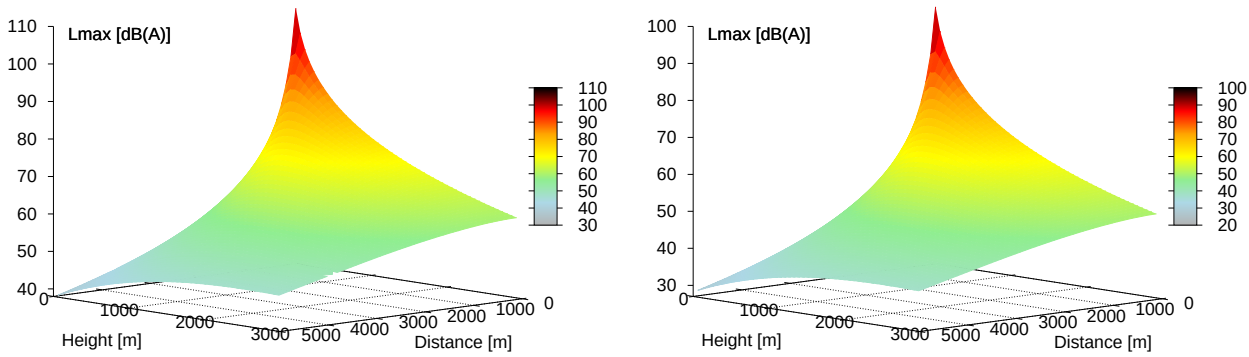

(a) Thrust = 25000 lb $\simeq$ 111 210 N (b) Thrust = 14000 lb $\simeq$ 62 275 N

Figure III-3: *Noise curve (L_{max}) for the Airbus A321 computed according to the INM methodology*

It is out of scope of this thesis to study accurately a specific airport during a specific time period. Therefore, reference day conditions will be assumed and only the lateral attenuation will be considered among the previous three adjustments. Then, the sound pressure level at location i as a function of the time will be computed as:

$$N_i(t) = N_i^{NTD}(t) - N_i^L(t) \quad \text{[dB(A)]} \tag{III.11}$$

where N_i^{NTD} is the perceived noise at location i in dB(A), extracted from the NTD tables, and $N_i^L(t)$ is the lateral attenuation adjustment which takes into account the lateral attenuation in case the trajectory is not over-flying vertically the location i. This lateral attenuation is modelled as:

$$N_i^L(t) = \frac{1}{13.86}\Gamma_i(t)\Lambda_i(t) \quad \text{[dB]} \tag{III.12}$$

with

$$\Lambda_i(t) = \begin{cases} 15.09\left[1 - e^{-0.00274 l_i(t)}\right] & \text{for} \quad 0 < l_i(t) < 914\,\text{m} \\ 13.86 & \text{for} \quad l_i(t) > 914\,\text{m} \end{cases} \quad \text{[dB]} \tag{III.13}$$

and

$$\Gamma_i(t) = \begin{cases} 3.96 - 0.066\xi(t) + 9.9e^{-0.13\xi(t)} & \text{for} \quad 0 < \xi(t) < 60^o \\ 0 & \text{for} \quad 60^o < \xi(t) < 90^o \end{cases} \quad \text{[dB]} \tag{III.14}$$

where $l_i(t)$ (in meters) and $\xi(t)$ (in degrees) are, respectively, the sideline distance from the flight path segment to the observer and the elevation angle formed by the aircraft and the horizontal plane of the the observer location. It is worth mentioning that the previous lateral attenuation model is taken from the INM version 5. In the more recent versions of this program, this model has been refined and slightly modified as explained in (FAA, 2006) and (He *et al.* , 2007).

Figure III-3 shows graphically the maximum A-weighted noise levels that can be computed according to the previous explanation. These L_{max} values are given as a function of different horizontal distances and heights to the noise source (the aircraft) for the Airbus A321 flying at two different thrust settings.

III.4 Noise annoyance model

All noise metrics and weighting scales try to model the way the sound is perceived by humans. However, these metrics are not sufficient measurements defining completely the annoyance that a particular noise is producing. The annoyance or perception of the acoustic noise describes the relation between a given acoustic situation and a given individual or set of persons affected by the noise and how cognitively or emotionally they evaluate this situation. In addition to acoustic elements, such as the loudness, the intensity, the spectra distribution and duration of the noise there is a list of non-acoustic elements that should be taken into account to define a global annoyance figure. According to several studies (Schomer, 2001; Lim *et al.* , 2007; Rylander, 2004; Kuwano & Namba, 1996; Hume *et al.* , 2003) the following factors are identified to have a significant influence in the perception of the noise annoyance, besides the acoustical magnitudes of the sound event:

- the existing background noise;
- the time of the day when the noise event occurs (day, evening, night);
- the type of day when the noise event occurs (working day, weekend, holiday period...);
- the period of time between two consecutive flights;
- the types of affected zones (rural zones, residential zones, industrial zones, hospitals, schools, markets,...);
- personal elements (emotional moods, apprehension and irritability to noise, personal health, size of the family,...); and
- socio-economic aspects (age, habits, education level, economic level, ...).

III.4.1 Knowledge reasoning and fuzzy sets

As we have already discussed earlier in this PhD thesis, annoyance is a subjective, complex and context-dependent concept. In this work we propose to model the annoyance produced by aircraft noise by using fuzzy sets theory.

In short, fuzzy sets are sets whose elements have degrees of membership, instead of the classical notion of binary membership expressing an element either belongs or does not belong to the set. In this way, statements can be represented with different degrees of truthfulness and/or falsehood. While variables in mathematics usually take numerical values, in fuzzy logic applications the non-numeric linguistic variables are often used to facilitate the expression of rules and facts. Then, many-valued logic can be extended to allow for fuzzy premises from which graded conclusions may be drawn. Rule-based systems are used in artificial intelligence to make predictions based on expert knowledge and classical logic reasoning. A fuzzy rule based model extends classical logic and reasoning to non-crisp variables. A typical example of such fuzzy quantities is the level of noise annoyance indicated by a word: a *linguistic term*. In this way, fuzzy rules have the advantage of allowing a suitable management of vague and uncertain knowledge being more understandable for humans.

The main paradigm of a fuzzy model is that it is based on knowledge, the essential concepts of which are derived from fuzzy logic. Thus, the fuzzy system is an expert knowledge-based system that contains the fuzzy algorithm in a simple rule-base providing a natural tool to model and process uncertainty.

As shown in Figure III-4, a fuzzy system is mainly composed of four parts (Benítez *et al.* , 1997):

- The **fuzzifier**, which converts real valued inputs into fuzzy values according to the member-

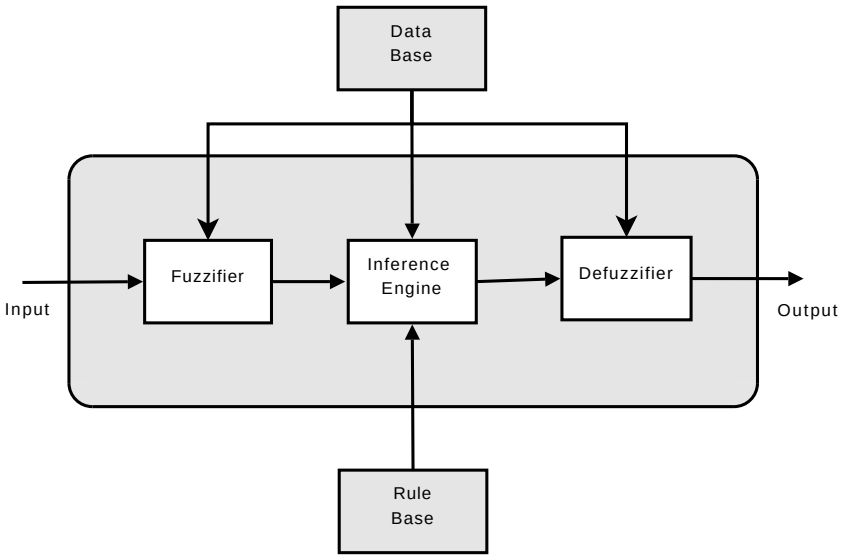

Figure III-4: *Block diagram for a fuzzy expert system*

ship functions of the linguistic terms defined for the input variables.

- The **knowledge base**, composed by:
  - a **data base**, containing the membership functions of the linguistic terms; and
  - a **rule base**, which specifies a set of rules than can represent in a natural way causality relationships between inputs and outputs of a system, corresponding to the usual linguistic construction of *IF a set of conditions are satisfied, THEN a set of consequences are inferred*.
- The **inference engine** which computes fuzzy output from fuzzy inputs using fuzzy implication functions established by the rule base.
- The **defuzzifier** yielding real-value outputs from the inferred fuzzy output.

Systems using fuzzy rules map n-dimensional spaces into m-dimensional spaces. For more background on fuzzy sets and systems the reader should refer to Appendix D of this work and the references therein.

III.4.2 A simple fuzzy model for noise annoyance

Essentially, the annoyance component can be regarded as a black box that produces as a output the degree of annoyance, drawn from the input data by the inference mechanism. Internally, the domain specific intelligence combines a database and a rule base. This pool of knowledge could come from several sources, such as the result of detailed studies carried out by experts in noise annoyance, the data treatment coming from social surveys or, ideally, a combination of both.

Next, a simple annoyance model, using fuzzy reasoning, is described. The derived annoyance nonlinear functions will be used as optimisation objectives for the design of optimal noise abatement procedures.

III.4.2.1 Input and output variables

In this simple model, the annoyance that an aircraft trajectory generates will be computed from three different inputs, which are:

- the Noise Level, in function of the maximum sound level (L_{max}) metric and the A-weighted

ponderation scale;

- the Period of the Day when the procedure is supposed to be flown, in function of the hour of the day; and
- the Type of Zone that the procedure will over-fly, in function of the activity that is undertaken in the zone.

On the other hand, only one output variable will be used:

- the Annoyance that will derive with a numerical output variable: a Normalised Annoyance Index (NAI).

III.4.2.2 Linguistic values: fuzzification and defuzzification

The previous inputs and output are the basis of the definition of the corresponding linguistic variables with their associated linguistic values expressed in the form of fuzzy sets. The Noise Level is fuzzyfied from the maximum sound level in six different linguistic values, ranging from *Null* noise to *Very High* noise. On the other hand, for the Period of the Day, after the fuzzification of the hour of the day we will consider *Morning*, *Afternoon* and *Night* periods. For the Type of Zone we will differentiate among *Residential Zones*, *Industrial Zones*, *Schools* and *Hospitals*. This last variable does not come from the fuzzification of input variables because, in general, is relatively simple to identify and label unequivocally these kind of zones in a map. As it will be seen later in the application example of Chapter VI, *Industrial* and *Residential Zones* will be delimited by polygons while *Hospitals* and *Schools* will be represented as singular points. Finally, the Annoyance will be expressed with five linguistic values, ranging from *Null* to *Extreme* annoyance.

Table III-2 shows the system input and output variables, along with the associated fuzzy linguistic variables and with their respective linguistic values. On the other hand, the fuzzy sets defining the linguistic values of the Noise level, Period of Day and Annoyance are defined by means of fuzzy membership functions, as shown in Figure III-5.

For the input variables simple triangular membership shapes have been used to establish these functions. Triangular functions are the simplest ones and they are the most widely used set-membership functions to describe fuzzy sets in fuzzy control. They are appropriate because the fuzzy reasoning and tuning process is simplified and they are more computational friendly too (Tanaka, 1997; Verkeyn, 2004).

A maximum A-weighted noise level of 50 dB(A) is considered purely a *Very Low* noise. Then, the membership function decreases linearly in both sides of this peak and a level of 60 dB(A) or 40 dB(A) is no longer considered a *Very Low* noise (see Figure III-5(c)). The same membership function is repeated for *Low*, *Medium* and *High* noises at a 10 dB(A) interval. For *Null* and *Very High* noise the membership function is no longer triangular and all values below 40 dB(A) are considered as a *Null* noise, while all values above 90 dB(A) are considered equally as a *Very High* noise. As an example, a noise event with a maximum sound level of 80 dB(A) will be labelled only as a *High Noise* while a 77 dB(A) event would be treated a 70% of *High Noise* and a 30% of *Medium Noise*.

A similar reasoning is done for the membership functions of the Period of Day, where the relationship with the hour of the day is established (see Figure III-5(a)). Finally, the Annoyance variable is simply modelled as a crisp variable, where each linguistic value takes a unique normalised annoyance index value. Hence, *Extreme* annoyance corresponds to a output value of 1.00, *High* annoyance takes 0.75, *Moderate* annoyance corresponds to 0.50, *Small* annoyance to 0.25 and finally, *Null* annoyance corresponds to 0.00 (see Figure III-5(b)).

Table III-2: *Fuzzy Input/Output linguistic variables with their respective linguistic values*

	System variables	Linguistic Variables	Linguistic Values
Inputs	L_{max} in dB(A)	Noise level	*Null (NN)* *Very Low (VL)* *Low Noise (LO)* *Medium (ME)* *High (HI)* *Very High (VH)*
	Hour of the day	Period of Day	*Morning (M)* *Afternoon (A)* *Night (N)*
	Zone activity	Type of Zone	*Industrial Zone (IZ)* *Residential Zone (RZ)* *School (SZ)* *Hospital (HZ)*
Output	Normalised Annoyance Index	Annoyance	*Null (NA)* *Small (SA)* *Moderate (MA)* *High (HA)* *Extreme (EA)*

III.4.2.3 Rule base

After the definition of all the input/outputs of the fuzzy system, a rule base can be established to represent the annoyance of a particular event in the form of `IF-THEN` rules.

As explained in Chapter I, it is out of the scope of this PhD thesis to determine an accurate fuzzy model for noise annoyance. Then, a simple way to establish the rule base is proposed here. A *Residential Zone*, in the *Afternoon* is chosen as the *baseline* situation where a *Very High* noise produces an *Extreme* annoyance, *High* noise produces *High* annoyance, *Medium* noise corresponds to *Moderated* annoyance, *Low* noise to *Small* annoyance and *Very Low* noise and *Null* noise to *Null* annoyance. In other words, this could be written with the following rules:

`IF` [Type of Zone `IS` *Residential Zone* `AND` Period of Day `IS` *Afternoon* `AND` Noise Level `IS` *Very High*] `THEN` Annoyance `IS` *Extreme*

`IF` [Type of Zone `IS` *Residential Zone* `AND` Period of Day `IS` *Afternoon* `AND` Noise Level `IS` *High*] `THEN` Annoyance `IS` *High*

`IF` [Type of Zone `IS` *Residential Zone* `AND` Period of Day `IS` *Afternoon* `AND` Noise Level `IS` *Medium*] `THEN` Annoyance `IS` *Moderated*

`IF` [Type of Zone `IS` *Residential Zone* `AND` Period of Day `IS` *Afternoon* `AND` Noise Level `IS` *Low*] `THEN` Annoyance `IS` *Small*

`IF` [Type of Zone `IS` *Residential Zone* `AND` Period of Day `IS` *Afternoon* `AND` Noise Level `IS` (*Very Low* `OR` *Null*)] `THEN` Annoyance `IS` *Null*

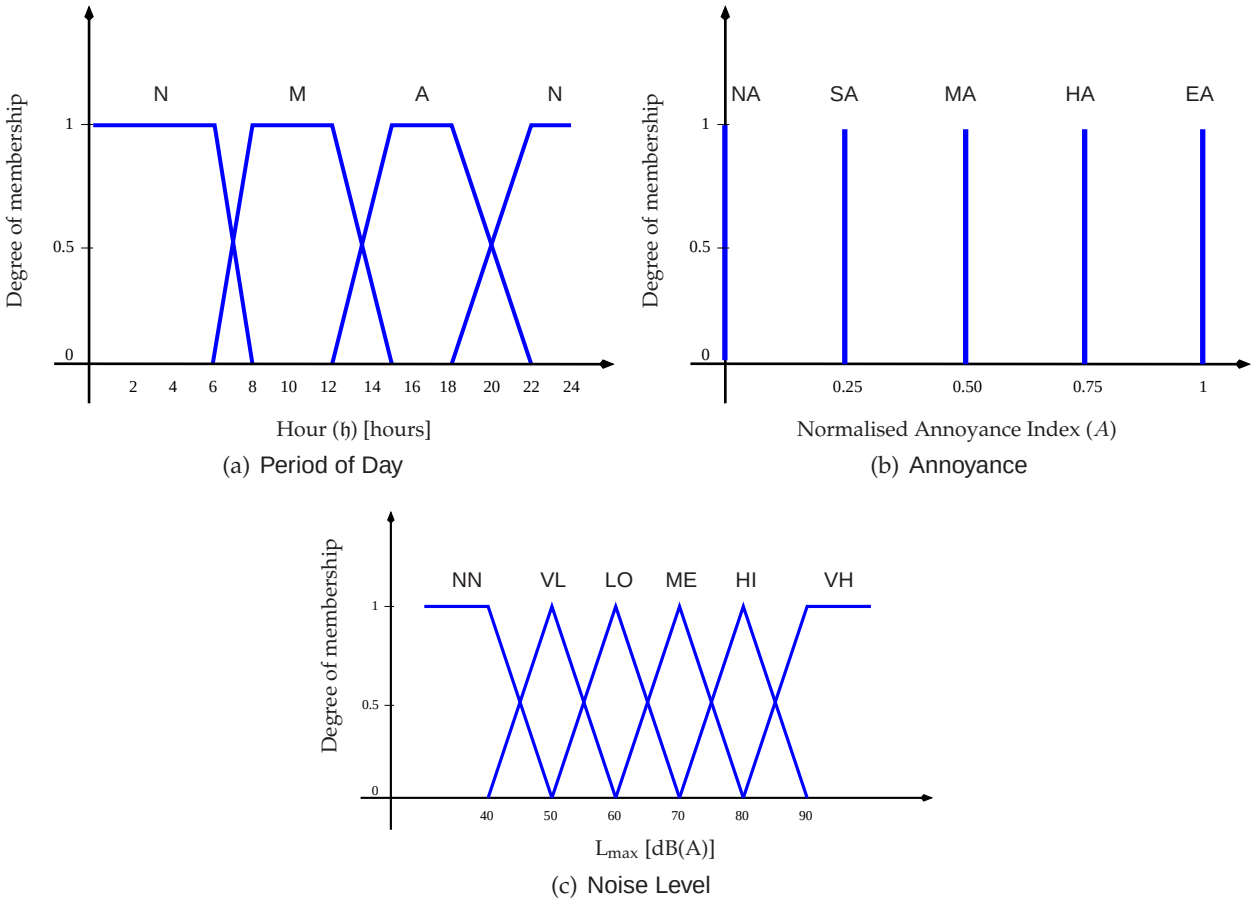

(a) Period of Day (b) Annoyance

(c) Noise Level

Figure III-5: *Membership functions defining the different linguistic values*

The same *Residential Zone* but during the *Night* period is more sensitive to the Noise Level and, consequently, the Annoyance linguistic values from the rule base have been shifted to one higher position vis-à-vis the *baseline* case (the *Afternoon* period). On the other hand, it makes sense supposing that the *Residential Zone* during the *Morning* period is less annoyed for a same Noise Level if compared with the *Afternoon* or the *Night*. In addition, environmental noise tends to be higher during the *Morning*. Therefore, the Annoyance linguistic values have been shifted to one lower position vis-à-vis the *baseline* case.

Being a *Industrial Zone* noisier than a *Residential* one, for this Type of Zone the Annoyance linguistic values have been shifted one lower position during the *Afternoon*, two positions during the *Night* and three positions during the *Morning* in the rule base. Similarly, and based on this simple reasoning, the remaining set of rules are established when the over-flown Type of Zone is an *Hospital* or a *School* for each Period of Day and Noise Level. Obviously in a *Hospital* the Annoyance produced is more important than in a *Residential Zone*, regardless of the Period of Day and in a *School*, the Annoyance is *Null* during *Night* periods because of the lack of activity in that location. Table III-3 summarises all the `IF-THEN` rules that form the rule base proposed for this work.

This kind of reasoning could be done by a group of experts in noise annoyance which would establish the different logic implications that the input variables have with the final perceived annoyance. They would build up a set of rules, similar to the previous ones, which would be much more easy to construct if using linguistic elements instead of numerical values. In addition, the output of a population survey, asking for the annoyance produced by the airport, would be easily used to construct the rule set because the type of formulated questions and answers are closer to the fuzzy reasoning principle. This kind of surveys could also be used for tuning the

Table III-3: Annoyance *rule base summary in function of the* Noise Level*, the* Period of Day *and the* Type of Zone

	Residential Zone			*Industrial Zone*		
	Morning	*Afternoon*	*Night*	*Morning*	*Afternoon*	*Night*
Null	*NA*	*NA*	*NA*	*NA*	*NA*	*NA*
Very Low	*NA*	*NA*	*SA*	*NA*	*NA*	*NA*
Low	*NA*	*SA*	*MA*	*NA*	*NA*	*NA*
Medium	*SA*	*MA*	*HA*	*NA*	*SA*	*SA*
High	*MA*	*HA*	*EA*	*SA*	*MA*	*MA*
Very High	*HA*	*EA*	*EA*	*MA*	*HA*	*HA*

	Hospital			*School*		
	Morning	*Afternoon*	*Night*	*Morning*	*Afternoon*	*Night*
Null	*NA*	*NA*	*NA*	*NA*	*NA*	*NA*
Very Low	*SA*	*SA*	*MA*	*NA*	*NA*	*NA*
Low	*MA*	*MA*	*HA*	*SA*	*SA*	*NA*
Medium	*HA*	*HA*	*EA*	*MA*	*MA*	*NA*
High	*EA*	*EA*	*EA*	*HA*	*HA*	*NA*
Very High	*EA*	*EA*	*EA*	*EA*	*EA*	*NA*

membership functions of the linguistic variables, as explained in (Verkeyn, 2004).

For this work we have used the *Larsen* implication for the inference of fuzzy rules along with the *sum* method for the aggregation process and the *centroid* method for the defuzzification process. Appendix D define and give more details about these methodologies. In addition, a practical case of the presented model, involving a fuzzification, approximate reasoning using the rule base and the consequent defuzzification, is exemplified in section D.2 of the same Appendix.

After this defuzzification process, we can compute a group of different nonlinear *annoyance functions* $A(L_i(t), \mathfrak{h}) : \mathbb{R}^2 \rightarrow \mathbb{R}$ mapping a maximum noise level $L_i(t)$, for a given location i at hour of the day $\mathfrak{h}$, to a Normalised Annoyance Index value. Figure III-6 shows graphically these functions for the four types of inhabited zones considered in this work. Finally, at a given hour of the day $\mathfrak{h}$, a fourth order polynomial approximation of the Noise Annoyance Index as a function of the maximum A-weighted sound level is performed. Is this new function, $A(L_i(t)) : \mathbb{R} \rightarrow \mathbb{R}$, that will be used as optimisation function in the following Chapters. Figure III-7 shows a couple of examples of this simple polynomial fitting which allows us to avoid the original and non-differentiable triangular shaped functions.

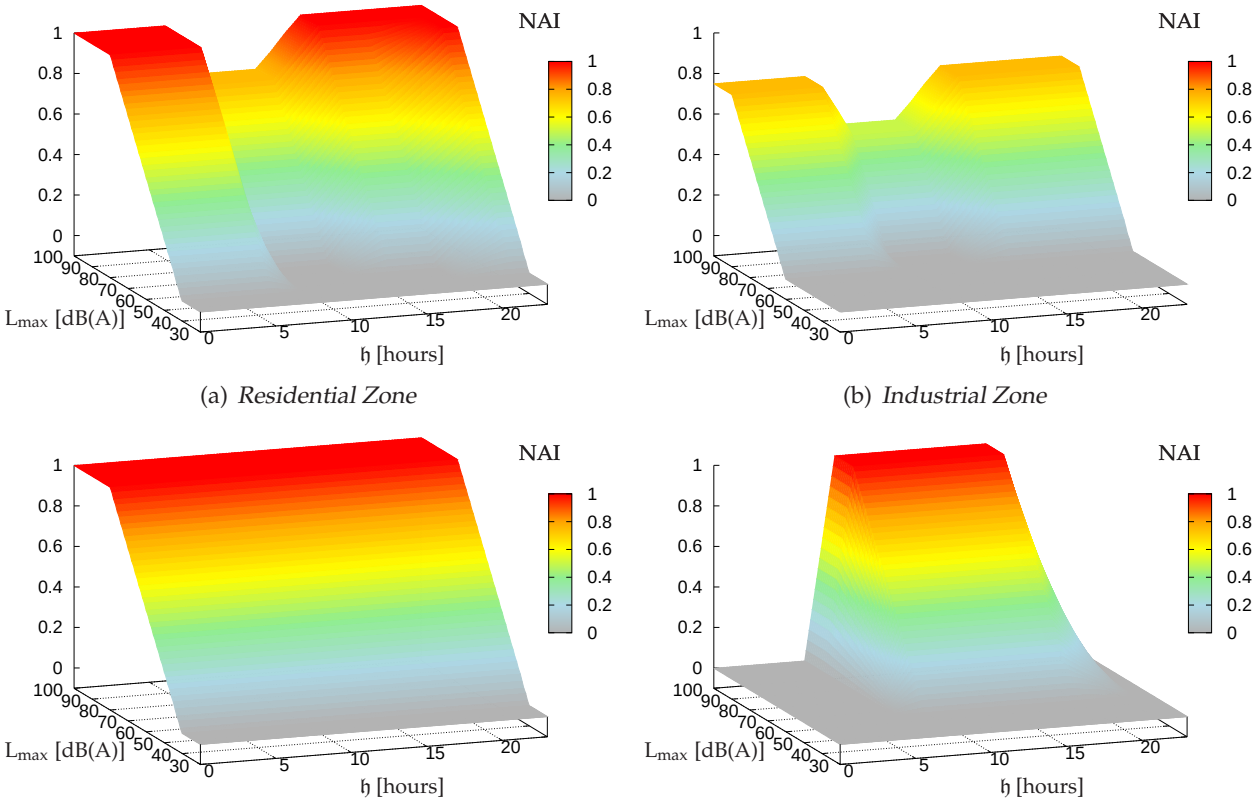

(a) *Residential Zone* (b) *Industrial Zone*

(c) *Hospital* (d) *School*

Figure III-6: *Representation of the Normalised Annoyance Index (NAI) as a function of the input variables*

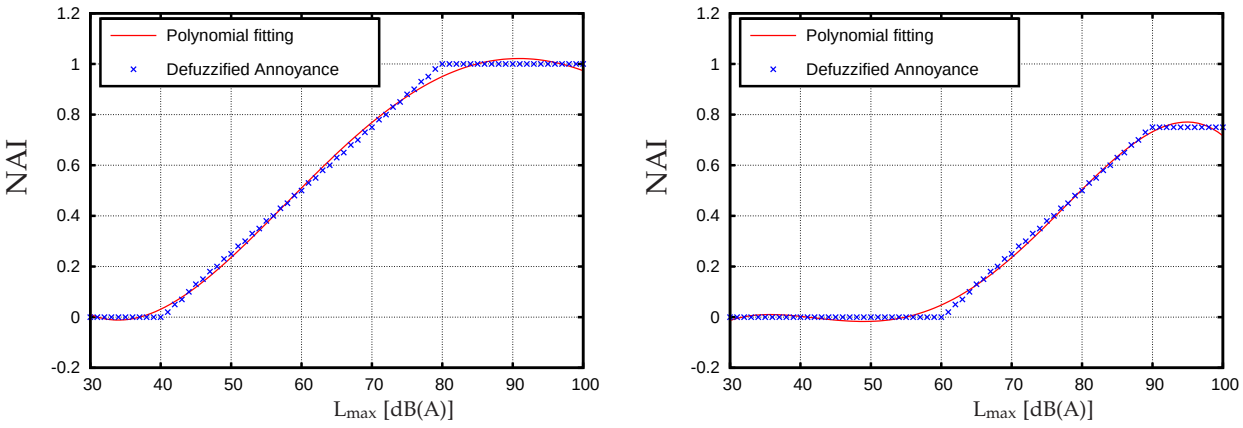

(a) *Hospital* at ħ =04h (b) *Residential Zone* at ħ =10h

Figure III-7: *Fourth order polynomial approximation for the defuzzified Noise Annoyance Index (NAI)*

Solving an optimal control problem is not easy. Pieces of the puzzle are found scattered throughout many different disciplines.

— John T. Betts

Nothing is more difficult, and therefore more precious, than to be able to decide.

— Napoleon Bonaparte

IV

Multi-objective Optimal Control

This Chapter is devoted to explaining the methodology that is proposed to solve the optimisation problem proposed in this PhD thesis, which can be formally written as a *constrained multi-objective optimal control problem*. The problem we tackle is non-feasible analytically due to its complexity and nonlinearity. Then a discretisation approach is presented in order to solve it numerically. Although the methodology presented here would be valid for the optimisation of departure or arrival and approach procedures only the departure case will be finally studied in this work. On the other hand, the optimisation of several conflicting criteria (such as different noise sensitive locations and airline associated costs) is not a straightforward task. The issues arising from this multi-objective optimisation nature are also addressed in this Chapter.

IV.1 Optimal control problem

Let the time $t \in \mathbb{R}$ be the independent variable for this problem and $[t_0, t_f] \subset \mathbb{R}$ be a given time interval where t_0 and t_f are respectively, the values for the initial and final time of the optimal trajectory. The value of t_f is left *free* during the optimisation, meaning that this value is a decision variable itself and will be fixed by the optimisation algorithm. Let $\vec{x}(t) \in \mathbb{R}^{n_x}$ be the state vector describing the trajectory of the aircraft over the time. The control vector $\vec{u}(t) \in \mathbb{R}^{n_u}$ contains those variables that lead to a specific trajectory and $\vec{p} \in \mathbb{R}^{n_p}$ is a set of control parameters not dependent on t. Thence, the set of decision variables $\vec{z}(t) = [\vec{x}(t), \vec{u}(t), \vec{p}, t_f]^T$ define an unique aircraft trajectory.

The dynamic equations of the aircraft were presented in section III.2 and, according to equa-

tion (III.1), the state vector is chosen as:

$$\vec{x}(t) = [v(t)\ \chi(t)\ \gamma(t)\ n(t)\ e(t)\ h(t)]^T \tag{IV.1}$$

being $v(t)$ the module of the *True Airspeed* (TAS), $\chi(t)$ the *aerodynamic yaw* angle and $\gamma(t)$ the *Flight Path Angle (FPA)*. Vector $\vec{r}(t) = [n(t)\ e(t)\ h(t)]^T$ represents the aircraft centre of mass position.

Similarly, the control vector is chosen as:

$$\vec{u}(t) = [\mathsf{n_z}(t)\ \mu(t)]^T \tag{IV.2}$$

where $\mathsf{n_z}(t)$ is the vertical load factor and $\mu(t)$ is the aerodynamic bank angle. If we consider a departure, the control parameter vector is formed by just one component which is the height at which the trust cut-back is performed: $\vec{p} = [h_c]$.

As outlined in Chapter II, a RNAV trajectory is formed by a set of waypoints and path terminators (see also Appendix A for further information). This means that the trajectory is actually formed by a consecutive list *straight* or *curved* segments that are flown sequentially by the on-board Flight Management System (FMS). According to this implementation, the optimal control problem that we are formulating should be split in a (unknown) number of phases in order to represent the different RNAV segments as done, for example in (Hogenhuis *et al.* , 2008). As seen in this work, the differences between an RNAV and completely *free* trajectories are minimal, but the phase formulation of the optimal control problem adds more complexity and computational burden. Therefore, in this dissertation we propose to optimise the trajectory as a continuous (and *free*) function of the time. In this way, we suppose that the coding process into a RNAV readable trajectory that might follow the optimisation will not be an issue.

Being $n_z = n_x + n_u + n_p + 1$, the goal of the optimisation process is to find the best trajectory $\vec{z}(t)$ that minimises a given optimisation function $\vec{J} : \mathbb{R}^{n_z} \to \mathbb{R}^{n_J}$, where $n_J < \infty$ is the number of different single objective functions. These real valued functions $J_i : \mathbb{R}^n \to \mathbb{R}$ form the vector of objective functions $\vec{J} = [J_1, J_2, ..., J_{n_J}]^T$. Moreover, the decision variables $\vec{z}(t)$ shall belong to the *feasible* or *admissible* set $\mathcal{Z} \subseteq \mathbb{R}^{n_z}$, where $\mathbb{R}^{n_z}$ is also called the decision variable space.

Then, we write this optimisation problem as:

$$\min_{\vec{z}(t)\in\mathcal{Z}} \{J_1(\vec{z}(t)), J_2(\vec{z}(t)), \cdots, J_{n_J}(\vec{z}(t))\} \tag{IV.3}$$

Next, the optimisation functions for our problem will be described, as well as the *constraint functions* that form the admissible set $\mathcal{Z}$.

IV.1.1 Optimisation criteria

Different objective functions will take into account noise (or annoyance) magnitudes and also other costs associated with the aircraft operations and the efficiency of the air traffic management. If the maximum noise level is considered as optimisation criterion, equation (III.10) will be used as optimisation function at each noise sensitive location i being considered. On the other hand, in the case of modelling the noise annoyance, as explained in section III.4, we will use a cut of the annoyance functions $A(L_i(t), \mathfrak{h})$ for a given location i and hour of the day $\mathfrak{h}$.

As it will be explained later in section IV.1.3, the chosen methodology for solving this optimal control problem can not tackle with functions that have discontinuous derivatives. Equation (III.10) defines the maximum sound level by using the $\max(\cdot)$ function which is non-differentiable in all its domain. Therefore, an alternative formulation is given, taken from (Drud, 2000), where equation (III.10) is replaced by the following inequality constraint:

$$L_i(\vec{z}) \geq N_i(\vec{z}(t)) \tag{IV.4}$$

Providing that the objective function will try to minimise $L_i(\vec{z})$, at some time instant this constraint will become binding as equality and $L_i(\vec{z})$ will be indeed the maximum of $N_i(\vec{z}(t))$ at that instant.

Concerning the operation of the aircraft, $Fuel$ and/or $Time$ spent during the trajectory may be considered as optimisation objectives too. Being t_0 and t_f the initial and final time of a given trajectory, fuel cost C_f associated to this trajectory can be computed as:

$$C_f = \pi_c \cdot Fuel = \pi_c \int_{t_0}^{t_f} FF(t)\, dt \tag{IV.5}$$

where π_c is the fuel price and $FF(t)$ is the total fuel flow, which in turn can be expressed as functions of the current thrust setting.

On the other hand, time cost represents the different constant rate costs associated with aircraft operations (insurances, traffic control fees, crew salaries, etc.). This can be easily written as:

$$C_t = \pi_t \cdot Time = \pi_t(t_f - t_0) \tag{IV.6}$$

being π_t the cost attached to one unit of time of delay.

Current Flight Management Systems equipping a wide number of aircraft deal with a compound cost function which involves fuel and time consumption during the flight. A cost index parameter (CI) relates the cost of time delay to the price of the fuel and its value is carefully chosen by the operator prior to each flight. Cost index (CI) is defined as:

$$CI = \frac{\pi_t}{\pi_c} \tag{IV.7}$$

Fuel saving flights are associated with low values of the cost index while more direct and faster flights are associated with high values of this index. As mentioned above, this strategy is currently used in civil aircraft operations giving optimal flight levels and speed settings for all phases of flight.

In this work, where only the departure phase is optimised, it would be incomplete to consider only these magnitudes regardless of the altitude achieved at the end of the procedure. Reaching a low final altitude $h(t_f)$ would lead to small time or fuel consumption figures during the departure but the consumption would increase in the following en-route phase, when trying to gain the altitude required to reach the optimal cruise flight level. Therefore, the final altitude must be also taken into account as an optimisation criterion to be maximised. Following the same philosophy as before, a *Height Index* (HI) is proposed in this work.

Then, the airliner cost compound function is defined as:

$$C_a = Fuel + CI \cdot Time - HI \cdot h(t_f) \tag{IV.8}$$

where, by definition, $CI > 0$ and $HI > 0$.

IV.1.2 Optimisation constraints

In order to guarantee a feasible and acceptable trajectory, as a result of the optimisation process described above, several constraints must be considered. Therefore, different constraint functions will define the set of admissible variables (or trajectories) $\mathcal{Z}$.

Besides aircraft dynamics, airspace organisation will be taken into account, regarding prohibited, dangerous and restricted areas as well as particular airspace sectorisation focusing on the compatibility with other existing flight procedures in the same airspace. By doing this kind of analysis, we will finally identify a portion of *usable airspace* where the obtained trajectories should be contained. Moreover ICAO Document 8168, Volume II (ICAO, 2006b) contains all the rules and methodology for designing visual and instrumental flight procedures. The applicable information will be transformed into the form of trajectory constraints, restricting even more the *usable airspace* defined before. Basically, some constraints might be added in order to guarantee obstacle clearance throughout the trajectory.

Some initial and final conditions on the trajectory will be also specified. If a departure procedure is studied, the final departure point location and possible altitude restrictions will be considered as the trajectory final condition. On the other hand, if an arriving procedure is considered an initial approach fix, along with possible altitude restrictions, will be included as the trajectory initial condition. It should be noted that it is not necessary to define fixed (known) initial or final points since the optimisation algorithm can tackle with non fixed initial or final conditions. Therefore if some of them are left *free* they will become part of the decision variables. Finally, if a 4D trajectory is considered, initial or final time constraints can also be defined at the initial or final points respectively. Time restrictions can also be useful to guarantee a maximum transit time to perform either an approach or a departure and consider, in this way, possible air traffic congestion issues in the terminal airspace being used.

All the constraint functions are grouped and summarised as follows:

- *Dynamic constraints* describing the trajectory of the aircraft:

$$\frac{\mathrm{d}\vec{x}(t)}{\mathrm{d}t} = \dot{\vec{x}}(t) = \vec{f}(\vec{x}(t), \vec{u}(t), \vec{p}) \tag{IV.9}$$

  where function $\vec{f} : \mathbb{R}^{n_x+n_u+n_p} \rightarrow \mathbb{R}^{n_x}$ is the nonlinear function presented in equation (III.1).

- *End point or event constraints* fixing the initial and final boundary conditions:

$$\vec{\eta}_L \leq \vec{\eta}(\vec{x}(t_0), \vec{x}(t_f), t_0, t_f) \leq \vec{\eta}_U \tag{IV.10}$$

  where function $\vec{\eta} : \mathbb{R}^{2(n_x+1)} \rightarrow \mathbb{R}^{n_\eta}$ define the n_η different *event* constraints and vectors $\vec{\eta}_L \in \mathbb{R}^{n_\eta}$ and $\vec{\eta}_U \in \mathbb{R}^{n_\eta}$ are respectively, the *L*ower and *U*pper values which bound all the constraints. These equations will contain, for example, the initial trajectory conditions, which will be actually equality equations (*i.e.* with equal lower and upper bounds) but also eventual final conditions like minimum or maximum altitudes at the final point.

- *Mixed state-control path constraints* allowing to restrict the behaviour of some variables:

$$\vec{\psi}_L \leq \vec{\psi}(\vec{x}(t), \vec{u}(t), t) \leq \vec{\psi}_U \tag{IV.11}$$

  Similarly, as in the previous equation, function $\vec{\psi} : \mathbb{R}^{n_x+n_u+1} \rightarrow \mathbb{R}^{n_\psi}$ define the n_ψ different *path* constraints and vectors $\vec{\psi}_L \in \mathbb{R}^{n_\psi}$ and $\vec{\psi}_U \in \mathbb{R}^{n_\psi}$ are, respectively, the *L*ower and *U*pper constraint values. One path equation could be, for instance, the restriction that speed should always increase, or remain constant, during a departure procedure.

- *Box constraints on the state and control variables* allowing to bound them:

$$\begin{array}{rcl} \vec{x}_L \leq & \vec{x}(t) & \leq \vec{x}_U \\ \vec{u}_L \leq & \vec{u}(t) & \leq \vec{u}_U \\ \vec{p}_L \leq & \vec{p} & \leq \vec{p}_U \end{array} \tag{IV.12}$$

where $\vec{x}_L \in \mathbb{R}^{n_x}$, $\vec{x}_U \in \mathbb{R}^{n_x}$, $\vec{u}_L \in \mathbb{R}^{n_u}$, $\vec{u}_U \in \mathbb{R}^{n_u}$, $\vec{p}_L \in \mathbb{R}^{n_p}$ and $\vec{p}_U \in \mathbb{R}^{n_p}$ are the *L*ower and *U*pper values which bound all states and control variables.

As explained before, all the functions defining the problem constraints must be smooth with smooth derivatives.

The aircraft dynamics, expressed by equation (III.1) contain some parameters that change their value as a function of certain variables. For example, aerodynamic parameters $a(t)$ and $b(t)$ depend directly on the value of the aircraft speed (see the piecewise equation (III.3)). These switching behaviour can be treated with *Mixed Logical Dynamic* resolution techniques, which permit to model this kind of hybrid models by introducing a set of *logical* variables. This variables can dynamically activate/deactivate the different modes of the system in a easy and intuitive way, but introduce important numerical issues (Ocampo-Martínez *et al.* , 2007). A possible roundabout is to translate the piecewise function to a single function by using $\min(\cdot)$ and $\max(\cdot)$ operators (Ovchinnikov, 2002), but like the objective functions, all the constraint functions are required to be smooth with smooth derivatives too.

In this work, the switching behaviour of aerodynamic parameters $a(t)$ and $b(t)$ are modelled with an arctangent function. Therefore, equation (III.3) is rewritten as:

$$a(t) = a(v(t)) = a_0 + \sum_{i=1}^{\varphi} \Delta a_{i\to i-1} \left[\frac{1}{2} - \frac{1}{\pi} \arctan(k_{i\to i-1}(v(t) - v_{i\to i-1})) \right] \tag{IV.13}$$

where a_0 is the coefficient value in clean configuration, $\Delta a_{i\to j}$ denote the increment in the coefficient value when transitioning from configuration i to j and $v_{i\to j}$ is the operational speed where this transition is performed. The value of $k_{i\to j}$ is chosen in order to adjust the steepness of the transition according to the modelled aircraft.

Finally, the piecewise functions described in equations (III.4, III.6, III.13 and III.14) are also rewritten in a similar way.

IV.1.3 Problem resolution

The minimisation of one of the optimisation objectives presented above, $L_i(\vec{z})$ or C_a, under the constraints stated by equations (IV.9 – IV.12) is known as a *constrained optimal control problem*. This section assesses the resolution of a problem with a single objective while Section IV.2 will deal with the multi-criteria aspects of the problem we tackle.

Basically, two different methods are available for solving this kind of optimal control problems:

- *Indirect methods* involving the *calculus of variations* or the *Maximum Principle of Pontryagin*.
- *Direct methods*, which transform the original optimal control problem into a nonlinear programming optimisation (NLP) problem.

Indirect methods date back the XVIIth century, when Sir Isaac Newton introduced them. Since then, the theory has continuously evolved: first order necessary conditions for optimality were formulated by Euler and Lagrange (the so-called Euler-Lagrange equations), then these

conditions were posed in a more clear form by the introduction of the Hamilton function and the Euler-Lagrange equations were extended by the introduction of further necessary conditions such as the Legendre-Clebsch condition, the Jacobi condition, and the Weierstrass condition. Finally, Pontryagin allowed the introduction of constrained variables (the path constraints), which are inevitable in the formulation of technical problems. An excellent summary of all necessary conditions for a very general class of trajectory optimisation problems can be found in (Bryson & Ho, 1975) or (Lewis & Syrmos, 1995).

The solution of single-phase trajectory optimisation problems with indirect methods requires the solution of a two-point boundary value problem using an appropriate, multi-dimensional zero finding algorithm. In a more general setup, a multi-point boundary value problem has to be solved. The major drawback of these methods is the requirement for a detailed mathematical analysis of each single problem. Even slight changes in the dynamics or in the boundary constraints can lead to a completely different solution structure, often requiring a complete revision of any previous derivation of the necessary equations. On the other hand, such an analysis yields to an in-depth insight into the problem. Moreover, major difficulty arises in the requirement of supplying very accurate initial guesses for the adjoint (or costate) variables. Usually, these variables do not have any physical meaning, but the trajectory is highly sensitive to even small changes of these costates. This inevitably leads to solution difficulties when new problems have to be solved and little knowledge is available on the structure of the optimal solution (Gath, 2002).

Direct methods convert the infinite-dimensional original problem into a finite-dimensional optimisation by applying three fundamental steps (Betts, 2001):

- Convert the dynamic system into a problem with a finite set of variables; then
- solve the finite-dimensional problem using a parameter optimisation method (*i.e.* solving a NLP problem); and finally
- assess the accuracy of the finite-dimensional approximation and if necessary repeat the transcription and optimisation steps.

The discretisation is achieved by first dividing the time interval into a prescribed number of subintervals whose endpoints are called nodes. These methods can be divided into two subclasses: shooting methods and transcription (or collocation) methods. Both strategies estimate the optimal control time history by using approximations such as piecewise constant or piecewise linear functions, or even spline approximations.

Shooting methods guess the initial conditions (the value of the states at t_0) and then propagate the differential equations from t_0 to t_f. Then the error in the boundary conditions is evaluated and by using a NLP algorithm the control variables (and the initial guess) are adjusted in order to satisfy the constraints. The multiple shooting methods simple break the problem into shorter steps. A deep insight on direct shooting methods can be found, for instance in (Gath, 2002), (Bulirsch *et al.* , 1993) and the references therein. See also (Virtanen *et al.* , 1999) for an interesting review on existing optimal control software packages.

The direct transcription method provides the time histories of control inputs and state variables as a set of nodal points at each time step. The unknowns are the values of the controls and the states at these nodes, the state and control parameters. The cost function and the state equations can be expressed in terms of these parameters which effectively reduce the optimal control problem to an NLP that can be solved by a standard nonlinear programming code. The time histories of both the control and the state variables can be obtained by using an interpolation scheme (Fahroo & Ross, 2000; Ross & Fahroo, 2002b). The approximation of the state time evolution can be approximated simply with the Euler method, see for instance (Vanderbei, 2000). Other discretisation/interpolation methods include Trapezoidal discretisation, Runge-Kutta or Hermite-Simpson polynomials (Hargraves & Paris, 1987; Jansch & Paus, 1990). Finally, more sophisticated

methods use pseudo-spectral techniques such as the work done by (Ross & Fahroo, 2002a) or (Fahroo & Ross, 2000).

A direct method constructs a sequence of points such as the objective function is minimised. An indirect method attempts to find a root of the necessary condition. Therefore, the direct method only needs to compare values for the objective function, while the indirect method must compute the *slope* of the objective function and decide if it is sufficiently close to zero (Betts, 2001). The advantage of direct methods, if compared with the indirect ones, is the possibility of solving very complex problems with a minimum effort of mathematical analysis. In fact, only the physical equations need to be coded and the necessary conditions do not have to be derived. Thus, the direct methods can be quickly used to solve a number of practical trajectory optimisation problems. However, these methods require an efficient algorithm to solve the constrained nonlinear programming problems with thousands of variables and (nonlinear) constraints. Therefore, the computational burden of direct methods can be, in some cases, a limiting factor. Moreover, for many direct optimisation packages, it is possible to check a posteriori whether the first order necessary conditions of optimality have been satisfied.

Finally, the major advantages of using direct transcription methods, in comparison to a direct multiple shooting method, are a much better run-time performance as long as a relatively small number of collocation intervals is used with a larger convergence radius. The latter advantage can be attributed to the fact that a direct collocation method can be seen as an implicit integration of the dynamic system, while multiple shooting methods are using explicit integration formulas such as a Runge-Kutta method. In that sense, transcription methods are usually using many more "multiple shooting points" (in the sense of collocation intervals) than a multiple shooting method. On the other hand, one of the major advantages of using multiple-shooting methods is the possibility of running them with an ODE solver that includes a step-size control algorithm. Therefore, the algorithm is almost independent of the discretisation grid and will, if it converges, at least deliver a suboptimal solution (Gath, 2002).

IV.1.3.1 Implemented method

In this work a direct transcription method is implemented. Then, the optimal control problem described above, which contains differential and algebraic constraints, is transformed in two steps into a nonlinear programming (NLP) problem with only algebraic constraints. First, differential equations (IV.9) are written in its equivalent integral form:

$$\vec{x}(t) = \vec{x}(t_0) + \int_{t_0}^{t} \vec{f}(\vec{x}(\tau), \vec{u}(\tau), \vec{p})\, \mathrm{d}\tau \tag{IV.14}$$

Then, equation (IV.14) is discretised using a sampling time $\Delta t = t_{k+1} - t_k$ where t_{k+1} and t_k are two consecutive time instants using an explicit numerical integration rule to approximate the above integral. The Euler method is chosen and the following equivalent discrete-time formulation is obtained:

$$\vec{x}(k+1) = \vec{x}(k) + \Delta t \cdot \vec{f}(\vec{x}(k), \vec{u}(k), \vec{p}) \tag{IV.15}$$

Even if more sophisticated (and accurate) methods exist for doing this discretisation (such as Runge-Kutta, Hermite-Simpson etc.), the previous formulation is easier to implement and gives us with enough accuracy for the application being considered (Betts, 1998).

Finally, once the problem is formulated as a NLP, it can be solved using a commercial optimisation software suite. In this thesis, the General Algebraic Modelling System (GAMS)[1] is used to

[1] http://www.gams.com

code and solve the NLP problem. The numerical optimisation method used to solve the problem is a generalised reduced gradient search (see for instance (Drud, 1985)), implemented in the NLP solver CONOPT[2] available in the GAMS optimisation package, which can cater for the nonlinearities of the performance index and constraints.

The CONOPT optimisation algorithm starts by finding a feasible solution; then, an iterative procedure follows, which consists on:

- Finding a search direction, through the use of the Jacobian of the constraints, the selection of a set of basic variables and the computation of the reduced gradient.
- Performing a search in this direction, through a pseudo-Newton process until a convergence criterion is met.

A detailed description of this algorithm and its implementation may be found in (Drud, 1994) and in the manuals available at the GAMS web page. CONOPT has been successfully proved to be an efficient package to solve large problems with thousands of variables and highly nonlinear functions. However, since this package is aimed at solving generic NLP problems, it does not offer the possibility to check, a posteriori, if the solution satisfies the optimal first order necessary conditions. Moreover, the obtained solution will be, in general, a locally optimal solution and special care with this issue should be taken by the user.

IV.1.3.2 Discretisation strategy

As it has been seen in equation (IV.15), the dynamic constraints are discretised using a sampling time Δt. This discretisation time should be judiciously chosen in order to properly model the dynamic behaviour of the system (i.e the aircraft) because control variables are constant over the interval between any two consecutive sampling instants. In control theory, it is widely accepted that the sampling time should be at least on tenth of the fastest dynamic mode of the system (Franklin *et al.* , 2006):

$$\Delta t \lesssim \frac{\tau_{\max}}{10} \tag{IV.16}$$

where $\tau_{\max}$ is the time constant of the fastest dynamic mode.

In a linear problem, we can write a dynamic system as:

$$\dot{\vec{x}}(t) = \boldsymbol{\mathcal{A}} \cdot \vec{x}(t) + \boldsymbol{\mathcal{B}} \cdot \vec{u}(t) \tag{IV.17}$$

by using matrices $\boldsymbol{\mathcal{A}} \in \mathbb{R}^{n_x \times n_x}$ and $\boldsymbol{\mathcal{B}} \in \mathbb{R}^{n_u \times n_x}$.

The eigenvalues of $\boldsymbol{\mathcal{A}}$ (also known of eigenvalues of the system) determine completely the natural response (unforced response) of the system. As explained in (Franklin *et al.* , 2006), given a linear system such as equation (IV.17), the fastest dynamic response of the system is determined by the biggest absolute value among all the real parts of the eigenvalues of $\boldsymbol{\mathcal{A}}$:

$$\tau_{\max} = \max_i \ |\Re(\lambda_i)| \tag{IV.18}$$

for all $i = 1, ..., n$. In turn, the components of the vector $\vec{\lambda} = [\lambda_1, ..., \lambda_n]^T$ (*i.e.* the eigenvalues of the matrix $\boldsymbol{\mathcal{A}}$) can be computed by solving the following system:

$$|\boldsymbol{\mathcal{A}} - \lambda \boldsymbol{\mathcal{I}}| = 0 \tag{IV.19}$$

[2] http://www.aimms.com/aimms/product/solvers/conopt.html

being $\mathcal{I}$, the identity matrix.

In the problem we tackle, where the system being considered is the movement of an aeroplane along its flying trajectory, function $\vec{f}$ is definitely nonlinear. Then, the system should be linearised as a first step if one wants to compute the dynamic modes. Therefore, for different operations points at instants t_k we have:

$$\left.\frac{\mathrm{d}\vec{x}(t)}{\mathrm{d}t}\right|_{t=t_k} = \dot{\vec{x}}(t_k) = \boldsymbol{\mathcal{A}}_k \cdot \vec{x}(t_k) + \boldsymbol{\mathcal{B}}_k \cdot \vec{u}(t_k) \tag{IV.20}$$

where matrices $\boldsymbol{\mathcal{A}}_k$ and $\boldsymbol{\mathcal{B}}_k$ correspond to the linearisation of the system at the operating point k.

On the other hand, being the final time of the flight trajectory, t_f, a free variable of the optimisation process, it is not possible beforehand to fix the Δt value. In this context, the number of discretisation points N are fixed prior to the optimisation and Δt is let free in the optimisation satisfying the following constraint:

$$\Delta t = \frac{t_f}{N} \tag{IV.21}$$

Therefore, after each optimisation equation (IV.16) will be checked in order to guarantee that the discretisation has been done properly. In this process all N discretisation points will be used as different operation points where the system will be linearised according to equation (IV.20).

IV.2 Multi-objective optimisation

The optimisation of noise abatement procedures, as studied in this thesis, involves the optimisation of several objectives at the same time, such as noise, (or annoyance) at different locations, as well as some airliner or ATM considerations. Therefore, the goal of the optimisation process is to find the best trajectory $\vec{z}(t) \in \mathcal{Z}$ that minimises a set of n_J objectives:

$$\min_{\vec{z}\in\mathcal{Z}} \{J_1(\vec{z}), J_2(\vec{z}), \cdots, J_{n_J}(\vec{z})\} \tag{IV.22}$$

where for clarity, the time dependency has been dropped from the notation from now on and $J_i(\vec{z})$ are the scalar valued functions representing each individual optimisation criterion.

The word *minimise* means that all the objective functions may be minimised simultaneously. If there is no conflict between the objective functions, then a solution can be found where every objective function attains its optimum. In this case, no special methods are needed to solve this multi-objective problem, but unfortunately such trivial cases does not correspond with the problem tackled in this thesis. The objective functions are in general conflicting, meaning that a trajectory that produces acceptable values for a given criterion may lead to very poor results on other criteria. Because of the contradiction and possible incommesurability (*i.e.* merging objectives in different units) of the objective functions, it is not possible to find a single solution that would be optimal for all the objectives simultaneously. In addition, there is no natural ordering in the objective space because it is only partially ordered. In a single objective problem it is obvious that solution $J(\vec{z}_1) = 2$ is better that $J(\vec{z}_2) = 3$ because the ordering $J(\vec{z}_1) < J(\vec{z}_2)$ can be easily established. But how to compare, for instance, a two dimensional objective problem with solutions $\vec{J}(\vec{z}_1) = [2, 3]^T$ and $\vec{J}(\vec{z}_2) = [3, 2]^T$?

However, there are some of the objective vectors that can be extracted for examination. Such vectors are those where none of the components can be improved without degrading at least one

of the other components. This definition is usually called *Pareto* optimality, after the economist and sociologist Vilfredo Pareto, who developed it further (Amoroso, 1938).

IV.2.1 The *Pareto* optima

A solution $\vec{z}^*$ of the multi-objective optimisation problem, presented in equation (IV.22), is said to be *Pareto optimal* (or *Pareto efficient*) iff there does not exist another $\vec{z} \in \mathcal{Z}$ such that $J_i(\vec{z}) \leq J_i(\vec{z}^*)$ for all $i \in \{1, \cdots, n_J\}$ and $J_j(\vec{z}) < J_j(\vec{z}^*)$ for at least one index j. In other words, a solution is Pareto optimal if and only if an objective $J_i(\vec{z})$ can be reduced only at the expense of increasing at least one of the other objectives. There may be many Pareto optimal solutions to a multi-objective optimisation problem (usually an infinite number), speaking about a set of Pareto optimal solutions or a Pareto optimal set, which in general, can be non-convex and non-connected.

On the other hand, a decision vector $\vec{z}^*$ is said to be *weakly Pareto optimal* if there does not exist another decision vector $\vec{z} \in \mathcal{Z}$ such that $J_i(\vec{z}) < J_i(\vec{z}^*)$ for all $i \in \{1, \cdots, n_J\}$. It can be proved that the Pareto optimal set is a subset of the weakly Pareto optimal set (Miettinen, 1999).

Moreover, an objective vector minimising each of the objective functions is called an ideal (or perfect) objective vector $\vec{J}^\star = [J_1(\vec{z}_1^\star), J_2(\vec{z}_2^\star), \cdots, J_{n_J}(\vec{z}_{n_J}^\star)]^T$. Mathematically, this vector is obtained by minimising each of the objective functions J_i individually subject to the constraints defined by $\mathcal{Z}$, i. e.:

$$J_i^\star = J_i(\vec{z}^\star) = \min_{\vec{z} \in \mathcal{Z}} J_i(\vec{z}) \quad \forall i \in \{1, \cdots, n_J\} \tag{IV.23}$$

It is obvious that if the ideal objective vector were feasible, it would be the solution of the problem and the Pareto optimal set would be reduced to it. Even thought the ideal objective vector is not attainable, it can be considered as a reference point for some multi-objective optimisation strategies.

Figure IV-1 shows a simplified example corresponding to a hypothetical multi-objective optimisation problem where there are only two criteria to be minimised: J_1 and J_2. In this example, the image of the feasible region $\mathcal{Z}$ is denoted by the feasible objective region $\mathcal{O} \subseteq \mathbb{R}^2$. The thick line illustrates the set of weakly Pareto optimal objective vectors and the fact that the Pareto optimal set (green thick line) is a subset of the weakly Pareto optimal set can also be seen in this Figure. Point A is the ideal objective vector $\vec{J}^\star = [J_1^\star, J_2^\star]^T$ for this example. This point typically falls out of the admissible set of solutions and the decision maker has to choose a point among the infinite Pareto-optimal solutions.

Mathematically, every Pareto optimal solution is an equally acceptable solution of the multi-objective optimisation problem. However, it is generally desirable to obtain one point as a solution. Selecting one out the set of Pareto optimal solutions calls for information that is not contained in the objective functions. This is why, compared to single objective optimisation, a new element is added in the multi-objective optimisation which is a *decision making process*. In general, multi-objective optimisation problems are solved by an scalarisation technique. However, this methodology presents, in some cases, important drawbacks that can be bypassed by using alternative multi-objective optimisation techniques. Next sections are devoted to introduce some of these multi-objective optimisation approaches that will be explored in this thesis for the optimisation of noise abatement procedures. A review in multi-objective optimisation methods can be found in (Marler & Arora, 2004) or (Nakayama, 2005), and for a in-depth analysis of several methods the reader should refer to (Hwang & Massud, 1979) or (Miettinen, 1999).

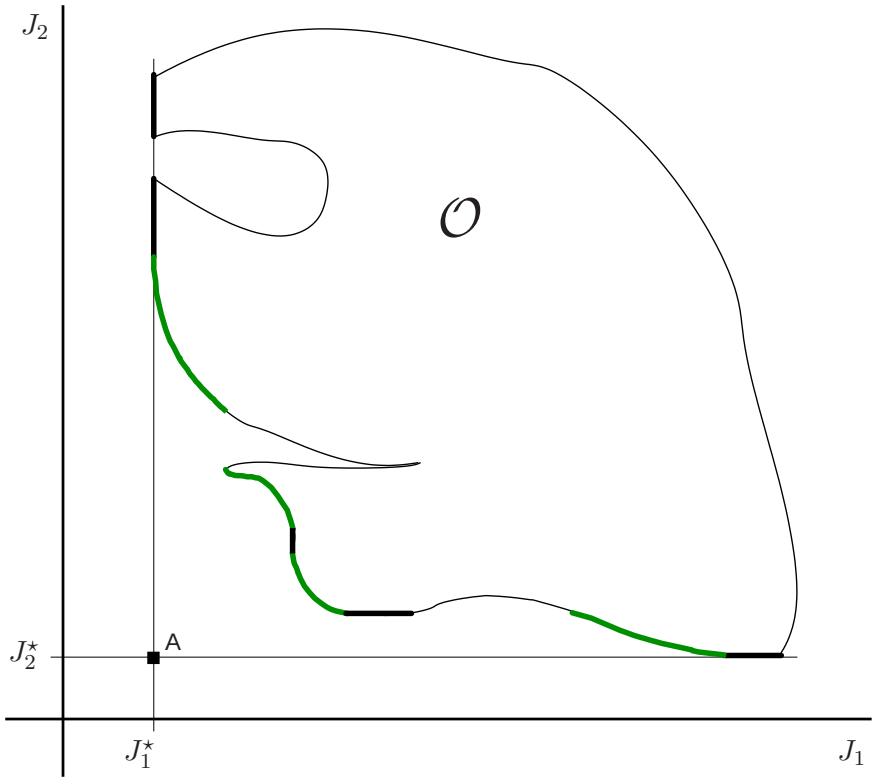

Figure IV-1: *Example of the Pareto region for a two criteria multi-objective minimisation problem*

IV.2.2 Scalarisation approach

Scalarisation is a common approach to solving such multi-objective optimisation problems and, therefore, a technique to choose a solution among all Pareto optimal ones. The multi-objective problem is converted into a single objective optimisation problem by means of a real-valued objective function, termed as the scalarising function which depends on some parameters. One of the most used strategies to obtain a scalar objective function is to form a linearly weighted sum of the objective functions J_i:

$$\min_{\vec{z}\in\mathcal{Z}} \{J_1(\vec{z}), J_2(\vec{z}), \cdots, J_{n_J}(\vec{z})\} = \min_{\vec{z}\in\mathcal{Z}} \sum_{i=1}^{n_J} w_i J_i(\vec{z}) \tag{IV.24}$$

The priority of the objectives are reflected by the weights $w_i \geq 0$ which are real numbers and are generally normalised, i. e. $\sum_{i=1}^{n_J} w_i = 1$, providing that the different objectives are also normalised. It can be proved that the solution of the equation (IV.24) is weakly Pareto optimal. However, choosing the value of the weights is not always a straightforward task. That is why this method is considered in the literature as an *a posteriori* method. It means that the decision maker runs several optimisations by changing the values of the different weights, choosing at the end the best weight vector that better conforms to what he/she thinks is the best solution. Thus, the most obvious problem with weighted formulae is the ad-hoc setting of the weights. This setting is based either on a somewhat vague intuition of the user about the relative importance of different quality criteria or on several trial and error experiments with different weighting values. In addition, altering the weighting vectors linearly does not have to mean that the values of the objective function also change linearly. Therefore, an even spread of weights does not produce an even spread of points on the Pareto curve making it more difficult to assess the selection of the final weights by the decision maker even if several trials are run. Then, in this case it is difficult to

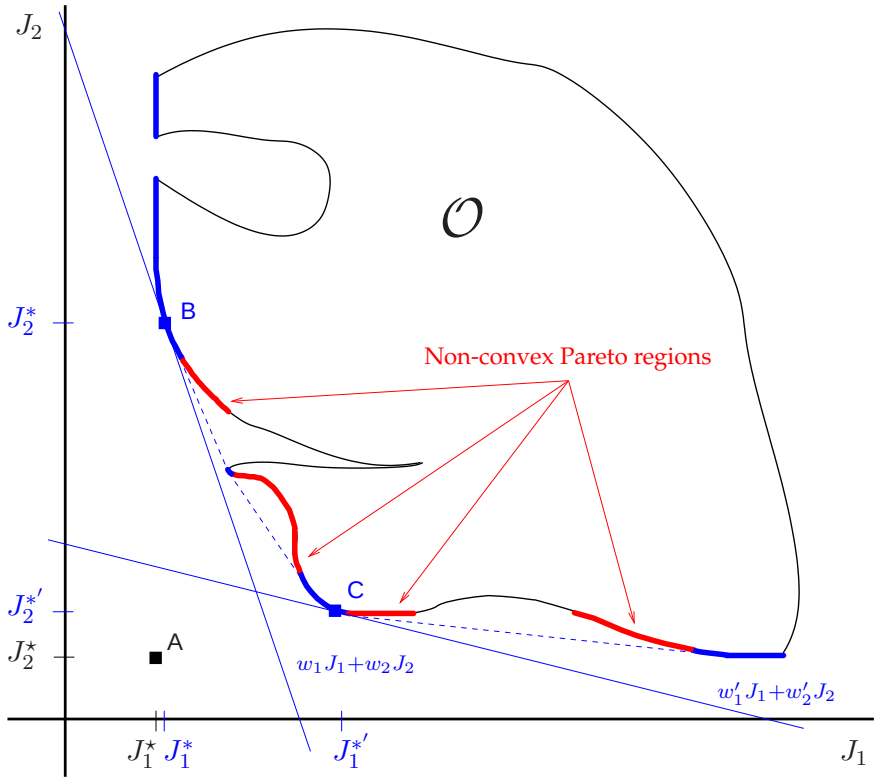

Figure IV-2: *Example of the scalarisation strategy for a two criteria multi-objective minimisation problem*

control the direction of the solutions by the weighting coefficients.

A simple and widely used case, when all the criteria share the same priority or importance, is to assign the same value to all individual weights:

$$w_i = \frac{1}{n_J} \quad \forall i \in \{1, \cdots, n_J\} \tag{IV.25}$$

However, this can still lead to the addition of non-commensurable criteria in the objective function, which does not make any sense at all, regardless of eventual normalisation.

Another drawback with the scalarisation approach is that, once a formula with precise values of weights has been defined, the optimisation algorithm will be effectively trying to find the best model for that particular setting of weights, missing the opportunity to find other solutions that might be actually more interesting to the user, and representing a better trade-off between different quality criteria. In particular, weighted formulae, involving a linear combination of different criteria, have the limitation that they cannot find solutions in a non-convex region of the Pareto front. This problem is particularly serious when the weighted formula involves a summation/subtraction (rather than a multiplication/division) of terms representing different magnitudes, often with very different scales in their units of measurement. This can be dealt by normalising the different quality criteria so that they refer to the same scale. This approach is well-known in the literature and at first glance it is a very satisfactory approach. There is, however, a subtle problem associated with normalisation that is rarely discussed in the literature: in general there are several different ways of normalising, and the decision about which normalisation procedure should be applied tends to be ad-hoc as well. For a deeper insight on scalarisation methods as well as the proofs of the above statements, the reader could refer to (Miettinen, 1999).

Figure IV-2 shows again the two criteria multi-objective minimisation example where two

different Pareto optimal solutions are attained using two different weighting sets. The optimal values $[J_1^*, J_2^*]^T$ are obtained when the scalarisation $J = w_1 J_1 + w_2 J_2$ is applied, being the optimisation result $[J_1^{*'}, J_2^{*'}]^T$ when the scalarisation is $J = w_1' J_1 + w_2' J_2$. As it can be seen in this Figure, the geometrical interpretation of the scalarisation approach is that the solution of the minimisation problem corresponds to that point in the Pareto zone which is tangent to a line with slope $\frac{w_1}{w_2}$. See (Das & Dennis, 1997) for the details of this geometrical interpretation. Therefore, it is not possible to obtain a solution in the *hollow regions* of the Pareto front (*i.e.* the non-convex regions) using this scalarisation technique.

The above mentioned drawbacks may appear when dealing with the optimisation of noise abatement procedures. For example, in (Visser, 2005) noise abatement trajectories are also optimised by using a weighted objective function and the obtained solution is seen to be highly dependent on the chosen weights. On the other hand, the work presented in (Xue, 2006), uses weighting techniques to take into account in the same optimisation process several non-commensurable magnitudes such as noise, fuel consumed and time spent during the trajectory.

As outlined in the introduction of this thesis, the present work aims at exploring different multi-objective optimisation techniques in order to avoid the problems described above. Hence, we will consider lexicographic, hierarchical, egalitarian and goal optimisation. All these strategies are presented next.

IV.2.3 Lexicographic approach

Lexicographic optimisation establishes a hierarchical order among all the optimisation objectives. If such a priority exists, a unique solution exist on the Pareto hyper-surface, see (Kerrigan & Maciejowski, 2002) and the references therein.

Let the objective functions be arranged according to the *lexicographic order* from the most important J_1 to the least important J_{n_J}. A given $\vec{z}^* \in \mathcal{Z}$ is a *lexicographic minimiser* of equation (IV.22) iff there does not exist a $\vec{z} \in \mathcal{Z}$ and a j satisfying $J_j(\vec{z}) < J_j(\vec{z}^*)$ and $J_i(\vec{z}) = J_i(\vec{z}^*)$ for all $i \in \{1, \cdots, j-1\}$. An interpretation of this definition is that a solution is a lexicographic minimum iff an objective J_i can be reduced only at the expense of increasing at least one of the higher-prioritised objectives $\{J_1, ..., J_{(i-1)}\}$. Hence, a lexicographic solution is a special type of Pareto-optimal solution that takes into account the order of the objectives. This hierarchy defines an order on the objective function establishing that a more important objective is infinitely more important that a less important objective. The solution of a lexicographic problem is always Pareto optimal, see (Miettinen, 1999).

A standard method for finding a lexicographic solution is to solve a sequential order of single objective constrained optimisation problems. After ordering, the most important objective function is minimised, subject to the original constraints. If this problem has a unique solution, it is the solution of the whole multi-objective optimisation problem. Otherwise, the second most important objective function is minimised. Now, in addition to the original constraints, a new constraint is added to guarantee that the most important objective function preserves its optimal value. If this problem has a unique solution, it is the solution of the original problem. Otherwise, the process goes on iteratively. More formally, the lexicographic minimum of equation (IV.22) can be found by using Algorithm IV.1.

With this approach, the decision maker must arrange the objective functions according to their relative importance permitting, in this way, sort *a priori* the different optimisation criteria. This method has shown several benefits in favour of the classical weighting methodology. Further investigation, at theoretical level is conducted in (Rentmeesters *et al.* , 1996). Moreover, lexicographic techniques have started to be widely used in control engineering applications. For instance, in (Aggelogiannaki & Sarimveis, 2006) lexicographic ordering is incorporated in an adap-

Algorithm IV.1: $\vec{J}^* = \underset{\vec{z}\in\mathcal{Z}}{lex\ min}\ \{J_1(\vec{z}), J_2(\vec{z}), ..., J_{n_J}(\vec{z})\}$.
Lexicographic multi-objective optimisation with prioritisation 1–2–...–n_J

1: $J_1^* = \min_{\vec{z}\in\mathcal{Z}} [J_1(\vec{z})]$
2: **for** $i = 2$ to n_J **do**
3: $\quad J_i^* = \min_{\vec{z}\in\mathcal{Z}} \left[J_i(\vec{z}) \,|\, J_j(\vec{z}) \leq J_j^*\,, \quad \forall j \in \{1, \cdots, i-1\}\right]$
4: **end for**
5: **return** Lexicographic minimiser set as: $\vec{z}^* = \arg(J_{n_J}^*)$
6: **return** Lexicographic solution as: $\vec{J}^* = [J_1(\vec{z}^*), J_2(\vec{z}^*), \cdots, J_{n_J}(\vec{z}^*)]^T$

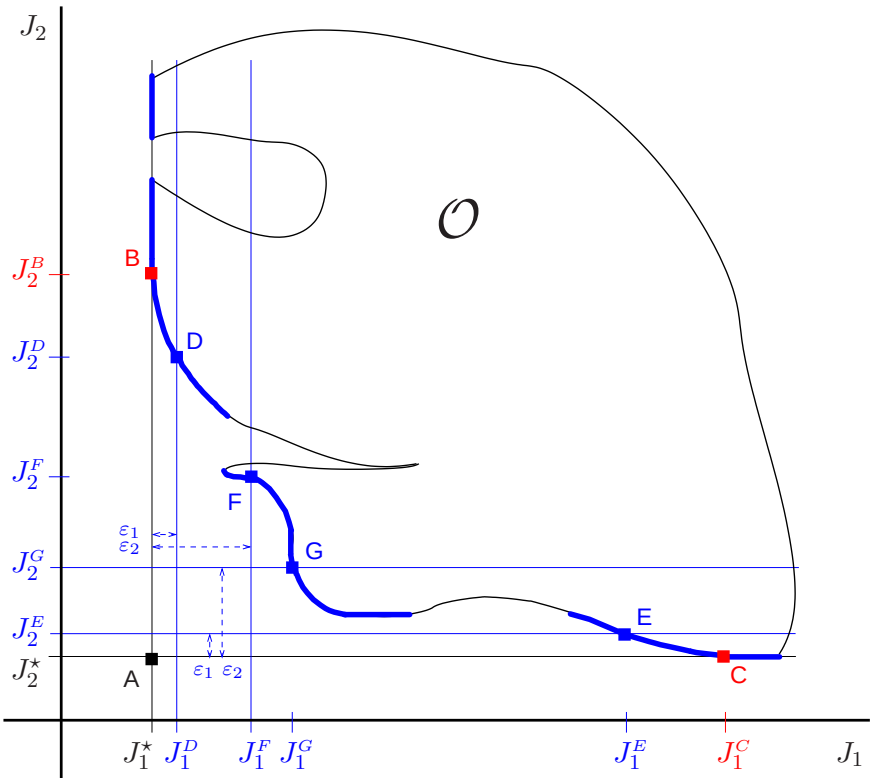

Figure IV-3: *Example of the lexicographic and hierarchic strategies for a two criteria multi-objective minimisation problem*

tive model predictive control framework in order to improve the closed-loop performance in the case of time-varying systems. Instead of weighting the different control goals, the proposed methodology creates a hierarchy according to the importance of each objective and optimises each one separately. A similar formulation is found in (Kerrigan & Maciejowski, 2002). In real world applications, (Ocampo-Martínez *et al.* , 2008) apply the previous methodology to control complex sewer networks and (Weber *et al.* , 2002) into water resources planning.

Recalling again the two criteria minimisation example, Figure IV-3 shows the lexicographic solutions corresponding to prioritisations $\{J_1, J_2\}$ and $\{J_2, J_1\}$. First prioritisation leads to point B where $\vec{J}^* = [J_1^\star, J_2^B]^T$ while second prioritisation leads to point C where $\vec{J}^* = [J_1^C, J_2^\star]^T$.

Lexicographic algorithm is simple and easy to implement. In addition, people usually make decisions successively and the establishment of the priorities can be easily done. However, in some situations the decision maker may have difficulties in putting the objective functions into an absolute order of importance. Note that the lexicographic ordering does not allow a small

Algorithm IV.2: $\vec{J}^* = hie\min_{\vec{z}\in\mathcal{Z}} \{J_1(\vec{z}), J_2(\vec{z}), ..., J_{n_J}(\vec{z})\}$.
Hierarchical multi-objective optimisation with prioritisation 1–2–...–n_J

1: $J_1^* = \min_{\vec{z}\in\mathcal{Z}} [J_1(\vec{z})]$
2: **for** $i = 2$ to n_J **do**
3: $\quad J_i^* = \min_{\vec{z}\in\mathcal{Z}} \left[J_i(\vec{z}) \,|\, J_j(\vec{z}) \leq (1+\varepsilon)J_j^*\,, \quad \forall j \in \{1, \cdots, i-1\}\right]$
4: **end for**
5: **return** Hierarchical minimiser set as: $\vec{z}^* = \arg(J_{n_J}^*)$
6: **return** Hierarchical solution as: $\vec{J}^* = [J_1(\vec{z}^*), J_2(\vec{z}^*), \cdots, J_{n_J}(\vec{z}^*)]^T$

increment of an important objective function to be traded off with a great decrement of a less important objective function. Yet, this kind of trading might often be appealing to the decision maker being it possible with hierarchical optimisation.

IV.2.4 Hierarchical approach

There exist a modification of lexicographic ordering called hierarchical optimisation where the upper bounds obtained when minimising more important objective functions are relaxed by so-called worsening factors ε, with $\varepsilon > 0$. These relaxations allow to trade off higher prioritised objectives in front of lower prioritised ones, exploring in this case, a widest area of the Pareto front containing solutions that can be more interesting to the decision maker. Then, the lexicographic algorithm is slightly modified as shown by Algorithm IV.2. This strategy is also found in the literature for solving engineering problems such as in (Bestle & Eberhard, 1997) where a vehicle design problem is assessed or in (Guo *et al.* , 2006) where hierarchical optimisation is applied at a coking problem. A more high level methodology is presented in (Bower & Kroo, 2008) for aircraft optimisation for minimum cost and emissions.

Figure IV-3 shows the solutions that are achieved when applying this hierarchical methodology to a two criteria minimisation problem. When the allowed relaxation is ε_1 and the prioritisation order is $\{J_1, J_2\}$ the optimisation leads to point D, where $\vec{J}^* = [J_1^D, J_2^D]^T$. With the same relaxation value, but with prioritisation $\{J_2, J_1\}$ the chosen optimal Pareto solution corresponds to point E, where $\vec{J}^* = [J_1^E, J_2^E]^T$. Similarly, point F corresponds to bigger relaxation of ε_2 with priority $\{J_1, J_2\}$ while point G corresponds to the same relaxation but with the opposite priority $\{J_2, J_1\}$. As it can be seen from this Figure in some cases the effect of relaxing a higher priority objective may lead to an important reduction on the other objective. In this case, this solution may appear more interesting to the decision maker (despite the higher priority objective has been worsened) than the original lexicographic solution.

IV.2.5 Egalitarian (or min-max) approach

As said previously, in a multi-objective optimisation problem there exist a set of optimal solutions that are equally acceptable from a mathematical point of view: the Pareto optimal (or Pareto efficient) solutions. Therefore, after the optimisation process, some decision making is needed for choosing one solution among all the possible ones. Let us suppose that all the optimisation objectives share the same importance from a decision making point of view. As it was seen in section IV.2.2, if the scalarisation approach is used for solving the optimisation problem the same weight will be assigned to all the criteria (see equation (IV.25)). In this way, the *average criterion* will be minimised when performing the optimisation described by equation (IV.24). On the other hand, if the lexicographic approach is employed, the user must establish beforehand a certain priority

among the objectives, which is not possible to do if all of them share the same importance. Hierarchical optimisation may help on that by relaxing the constraints related with the higher priorities, by choosing different ε values. Yet, this task would not be straightforward either.

Despite the average (or weighted) optimal solution is Pareto efficient, the main concern is that there is no fairness component embedded in this kind of decision making process. Obviously, the same lack of fairness is observed when the priorities have to be established when using lexicographic and hierarchical optimisation techniques even if the obtained solutions are also Pareto efficient. Therefore, these techniques may lead to solutions in which some criteria are very close to their ideal optimal value while the remaining have a very high values in their objective functions. Actually, if each objective is engaged in minimising its own value, fairness tends to disappear.

Criticism on this kind of solutions dates back 1971 from Rawls' egalitarian principle (Rawls, 2005), being one of the most widely accepted concepts for fairness. This principle states that *the system is no better-off than its worse-off individual*. Therefore, if this principle is applied to solve the multi-objective optimisation problem of equation (IV.22), we have that:

$$\min_{\vec{z}\in\mathcal{Z}} \{J_1(\vec{z}), J_2(\vec{z}), \cdots, J_{n_J}(\vec{z})\} = \min_{\vec{z}\in\mathcal{Z}} \left[\max_{i\in\mathcal{J}} J_i\right] \tag{IV.26}$$

where $\mathcal{J} = \{1, ..., n_J\}$ is the set of the optimisation criteria.

Although equation (IV.26) guarantees fairness, as defined above, the obtained solution is weakly Pareto optimal and one can not guarantee a Pareto optimal solution (Miettinen, 1999). This means that some objectives can be still improved without increasing the optimal value of the solution.

In the literature we find also this optimisation method applied in engineering problems. For example, in (Luss, 1999), it is applied to deal with resource allocation problems, while (Salles & Barria, 2004) and (Sarkar & Tassiulas, 2000) use this egalitarian (or fair) optimisation to build bandwidth allocation strategies in telecommunication applications.

IV.2.6 Goal optimisation

The basic idea in goal optimisation is that the decision maker specifies aspiration levels for some of the objective functions forming *goals*. We can say for example that minimising the noise at a given location is an objective function, but if we want the noise to be less than $60\,$dB(A), it is a a goal.

Let the aspiration level of the objective function $J_i(\vec{z})$ be $\bar{J}_i$ and the set of objective functions with aspiration levels for a given problem be $\mathcal{G} \subseteq \{1, 2, \cdots, n_G\}$. Then, these goals will be simply expressed by adding n_G extra constraints in addition to the existing path constraints of the optimisation (see equation (IV.11)):

$$J_i(\vec{z}) \leq \bar{J}_i \quad \forall i \in \mathcal{G} \tag{IV.27}$$

By using only goal programming, one can find solutions that are not Pareto efficient. To correct this, after defining the desired goals (*i.e.* constraints) the remaining multi-objective optimisation problem shall be solved with other techniques as explained in previous sections (scalarisation, lexicographic, egalitarian, etc.).

A man with one watch knows what time it is; a man with two watches is never quite sure.

— Lee Segall

If a man who cannot count finds a four-leaf clover, is he lucky?

— Stanislaw J. Lec

V

Lexicographic and hierarchical optimisation for NADP

In this Chapter, lexicographic and hierarchical optimisation approaches presented in sections IV.2.3 and IV.2.4 are implemented and aimed at solving optimal minimum noise departure procedures. As a preliminary study, we will use a simple and hypothetical scenario in order to exemplify the use of this technique and assess its potential advantages and inconveniences. Moreover, for this preliminary application we will consider the maximum A-weighted sound level at several noise sensitive locations as noise objective functions. Noise annoyance models will be introduced in next Chapter of this thesis report. Table V-1 summarises the data that define this test scenario and Figure V-1(a) shows the scenario.

According to (ICAO, 2006a), for all trajectories in the TMA below $10\,000\,\text{ft}$, the maximum airspeed is constrained to $250\,\text{kt}$ of Indicated Air Speed (IAS). For this work, a first approximation is done by supposing that this IAS limitation is in fact a TAS limitation. The relationship between

Table V-1: *Relevant data defining the test scenario*

$\chi_{RWY} = 70^o$	$s = 3.3\%$	$h_f^{\min} = 1\,220\,\text{m} \quad (4\,000\,\text{ft})$
$n_f = 20\,\text{km}$	$e_f = 10\,\text{km}$	$h_f^{\max} = 3\,000\,\text{m} \quad (10\,000\,\text{ft})$
$CI = 70$	$HI = 0.5$	$V_{\max} = 128.6\,\text{ms}^{-1} \quad (250\,\text{kt})$
$W_n = 0\,\text{km}^{-1}$	$W_e = 0\,\text{km}^{-1}$	$W_h = 0\,\text{km}^{-1}$

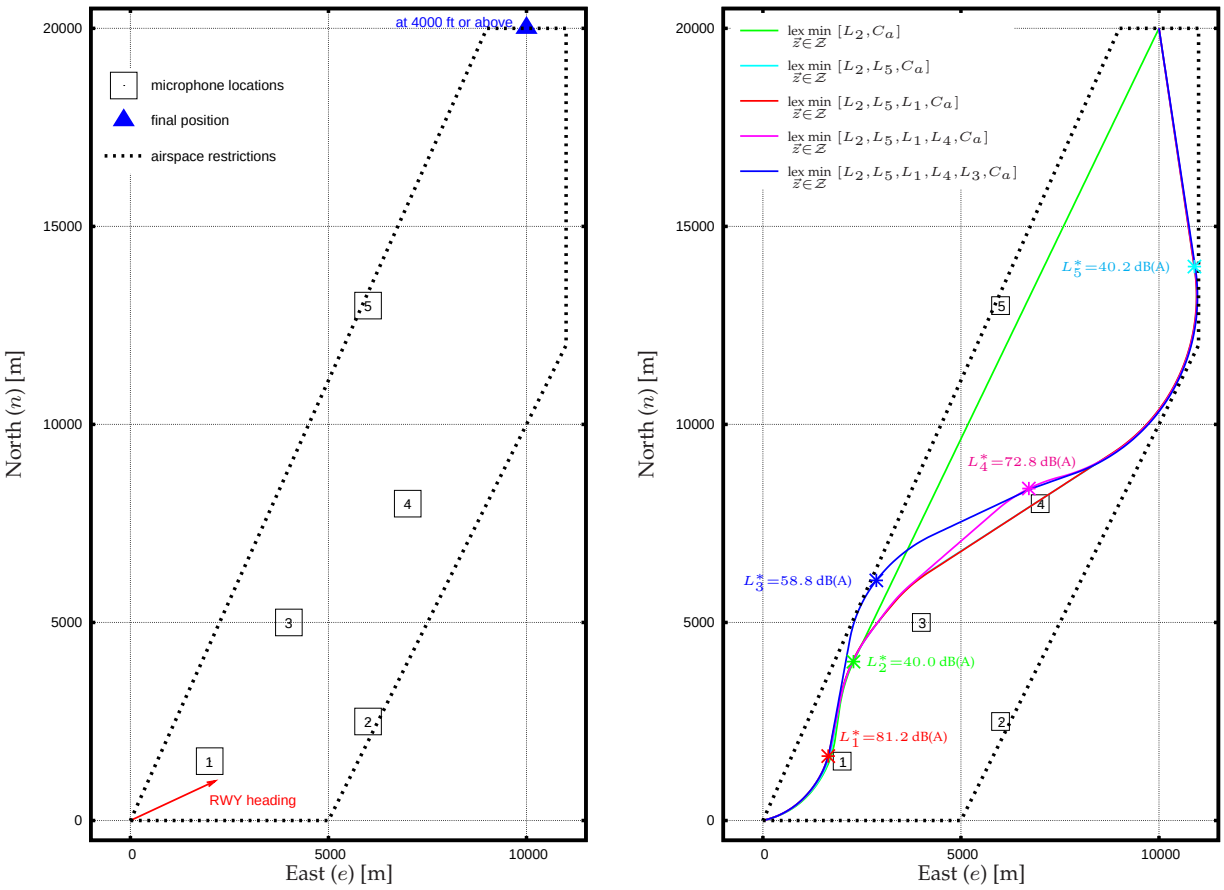

(a) Hypothetical scenario description (b) All lexicographic steps: prioritisation *2-5-1-4-3*

Figure V-1: *Hypothetical scenario environment for the optimisation of noise departure abatement procedures by using lexicographic optimisation strategies. Horizontal track for all lexicographic steps for prioritisation* 2-5-1-4-3.

these two speeds could be written as a function of the air density (*i.e.* the altitude) and the outside air temperature. For a more accurate study these magnitudes should be modeled in order to take into account the actual operational speed limitation given in IAS. In addition, the chosen aircraft for this example corresponds to the Airbus A340-600 equipped with Trent 556 engines and operating at its maximum take-off mass: $m = 368\,000\,\text{kg}$. The take-off is supposed to be performed using CONF3 flaps/slats configuration with $V_2 = 94.1\,\text{ms}^{-1} \simeq 183\,\text{kt}$ (TAS).

Lastly, as seen in Figure V-1(a), five different noise sensitive locations have been placed in the vicinity of the departure runway, with the following coordinates:

$$\begin{array}{lll} \text{Location \#1} & n_1 = 1\,500\,\text{m} & e_1 = 2\,000\,\text{m} \\ \text{Location \#2} & n_2 = 2\,500\,\text{m} & e_2 = 6\,000\,\text{m} \\ \text{Location \#3} & n_3 = 5\,000\,\text{m} & e_3 = 4\,000\,\text{m} \\ \text{Location \#4} & n_4 = 8\,000\,\text{m} & e_4 = 7\,000\,\text{m} \\ \text{Location \#5} & n_5 = 13\,000\,\text{m} & e_5 = 6\,000\,\text{m} \end{array} \tag{V.1}$$

On the other hand, equation (IV.8) is chosen as operator cost function and it is rewritten here for clarity:

$$C_a = Fuel + CI \cdot Time - HI \cdot h(t_f) \tag{V.2}$$

where the cost index CI and height index HI are aircraft operator dependent values selected to weight the consumption of fuel, time and altitude at the final departure point into a single cost function. It should be noted that this cost function C_a is a weighted sum of different criteria summarising the costs related with the operations of the aircraft. This compound cost function will be used together with all noise related objectives in the lexicographic ordering. If desired, the three associated costs (fuel, time and height) could be considered independently and introduced with all other objectives in the lexicographic ordering. This approach, which would analyse airliner operational procedures, is out of the scope of this work since it is focused only in noise optimisation strategies for airspace planners or procedure designers.

V.1 Lexicographic steps

Aimed at better understanding of how the lexicographic optimisation works, the optimisation Algorithm IV.1 will be analysed step by step. Let us choose, as a first example, the prioritisation *2-5-1-4-3* for the different noise sensitive locations. So as the maximum noise at location #2 becomes the most important criterion, followed by noise at locations #5, #1, #4 and finally, location #3.

In order to properly show all intermediate trajectories in the lexicographic process, airliner cost minimisation is performed after each intermediate step in the optimisation. This allows *common sense* trajectories to be obtained after noise has been optimised. It is worth mentioning that this intermediate airliner cost optimisation does not affect the constraints that are progressively established through the lexicographic process. Mathematically this is reflected by Algorithm V.1.

Algorithm V.1: *Modification of Algorithm IV.1 in order to properly show intermediate steps in the lexicographic optimisation sequence (prioritisation* 1–2–3–4–5*).*

$L_1^* = \min_{\vec{z}\in\mathcal{Z}} [L_1(\vec{z})]$
$C_a^* = \min_{\vec{z}\in\mathcal{Z}} [C_a(\vec{z}) \,|\, L_1(\vec{z}) \leq L_1^*]$
return Lexicographic step 1 minimiser set as: $\vec{z}^* = \arg(C_a^*)$
return Lexicographic step 1 solution as: $J_1^* = L_1(\vec{z}^*)$
for $i = 2$ to 5 **do**
    $L_i^* = \min_{\vec{z}\in\mathcal{Z}} \left[L_i(\vec{z}) \,|\, L_j(\vec{z}) \leq L_j^*\,, \quad \forall j \in \{1, \cdots, i-1\}\right]$
    $C_a^* = \min_{\vec{z}\in\mathcal{Z}} \left[C_a(\vec{z}) \,|\, L_j(\vec{z}) \leq L_j^*\,, \quad \forall j \in \{1, \cdots, i\}\right]$
    return Lexicographic step i minimiser set as: $\vec{z}^* = \arg(C_a^*)$
    return Lexicographic step i solution as: $J_i^* = L_i(\vec{z}^*)$
end for
return Lexicographic solution as: $\vec{J}^* = [L_1(\vec{z}^*), L_2(\vec{z}^*), L_3(\vec{z}^*), L_4(\vec{z}^*), L_5(\vec{z}^*), C_a^*]^T$

As it can be seen in Figure V-1(b) and Table V-2, the first optimisation gives a trajectory performing an initial and brief left turn and then proceeding directly to the final departure point. This first step produces an optimal noise value at location #2 of $L_2^* = 40.0\,$dB(A), then the airliner cost C_a is minimised. The second optimisation allows the reduction of the maximum noise at location #5 to $L_5^* = 40.2\,$dB(A) while L_2 is fixed at the previously obtained optimal value. In this case, the trajectory flies eastwards from location #5 avoiding the noise disturbance at this location, as much as possible. In the third step, the problem becomes so constrained by the previous two steps that the noise at location #1 is hardly improved. The fourth and fifth optimisations can still modify the middle segment of the trajectory in order to improve the noise impact at locations #4

Table V-2: *Maximum noise levels, at each noise sensitive location, corresponding to all steps in the lexicographic algorithm with the* 2-5-1-4-3 *prioritisation. Background noise is not considered.*

	L_2^*	L_5^*	L_1^*	L_4^*	L_3^*	C_a^*
$\underset{\vec{z}\in\mathcal{Z}}{\text{lex min}}\,[L_2, C_a]$	**40.0**	68.6	82.7	52.3	64.9	1 127
$\underset{\vec{z}\in\mathcal{Z}}{\text{lex min}}\,[L_2, L_5, C_a]$	**40.0**	**40.2**	82.1	75.2	69.2	1 231
$\underset{\vec{z}\in\mathcal{Z}}{\text{lex min}}\,[L_2, L_5, L_1, C_a]$	**40.0**	**40.2**	**81.2**	75.4	69.4	1 233
$\underset{\vec{z}\in\mathcal{Z}}{\text{lex min}}\,[L_2, L_5, L_1, L_4, C_a]$	**40.0**	**40.2**	**81.2**	**72.8**	69.1	1 234
$\underset{\vec{z}\in\mathcal{Z}}{\text{lex min}}\,[L_2, L_5, L_1, L_4, L_3, C_a]$	**40.0**	**40.2**	**81.2**	**72.8**	**58.8**	1 256

NOTE: L_i^* expressed in dB(A) and C_a^* in kg.

Table V-3: *Maximum noise levels at each noise sensitive location corresponding to all steps in the lexicographic algorithm with* 2-5-1-4-3 *prioritisation. Background noise is modelled.*

	L_2^*	L_5^*	L_1^*	L_4^*	L_3^*	C_a^*
$\underset{\vec{z}\in\mathcal{Z}}{\text{lex min}}\,[L_2, C_a]$	**42.5**	67.3	83.2	55.1	73.0	1 123
$\underset{\vec{z}\in\mathcal{Z}}{\text{lex min}}\,[L_2, L_5, C_a]$	**46.1**	**50.0**	85.2	71.6	82.8	1 146
$\underset{\vec{z}\in\mathcal{Z}}{\text{lex min}}\,[L_2, L_5, L_1, C_a]$	**50.0**	**50.0**	**67.0**	72.9	74.8	1 178
$\underset{\vec{z}\in\mathcal{Z}}{\text{lex min}}\,[L_2, L_5, L_1, L_4, C_a]$	**50.0**	**50.0**	**67.0**	**56.1**	79.7	1 269
$\underset{\vec{z}\in\mathcal{Z}}{\text{lex min}}\,[L_2, L_5, L_1, L_4, L_3, C_a]$	**50.0**	**50.0**	**67.0**	**56.1**	**62.6**	1 309

NOTE: L_i^* expressed in dB(A) and C_a^* in kg.

(with $L_4^* = 72.8\,\text{dB(A)}$) and #3 (with $L_3^* = 58.8\,\text{dB(A)}$) while respecting all optimal values of the higher prioritised locations.

As expected, from this example we see that when the lexicographic algorithm is used, objectives with higher priorities could constrain too much the ones following. Knowing this, if we take into account background noise at each location and set it as a lower bound in the lexicographic constraints, the flexibility in the lexicographic process can be significantly improved.

V.1.1 Considering background noise

Obviously, it is not worth improving the noise perceived at a particular location if in that location ambient (or background) noise is already higher than the noise produced by the over-flying aircraft. This background noise can take on different values depending on the type of location, the hour of the day, the day of the week, etc. According to (Schomer, 2001), background noise values usually range between $40\,\text{dB(A)}$ in the country side to $60\,\text{dB(A)}$ in busy cities.

To simplify the example we tackle in this Chapter, let us imagine that the background noise is the same at all sensitive locations with a value of $50\,\text{dB(A)}$. Then:

$$L_i^a = 50.0\,\text{dB(A)} \quad \forall i \in \{1, \cdots, 5\} \tag{V.3}$$

Therefore, Algorithm V.1 is slightly modified where the constraints that appear at steps 2, 6 and 7 are redefined considering background noise as a lower bound. Then, for steps 2 and 7 we have:

Table V-4: *Different optimal trajectories, according to all different prioritisations*

Trajectory	Number of prioritisations	Prioritisations
A	11	23514, 23541, 25314, 25341, 25431, 52314, 52341, 52431, 54231, 54312, 54321
B	12	12435, 12453, 14235, 14253, 14523, 14532, 41235, 41253, 41523, 41532, 45123, 45132
C	2	14325, 41325
D	9	12543, 15243, 15423, 15432, 51243, 51423, 51432, 54123, 54132
E	17	23415, 23451, 24315, 24351, 24513, 24531, 42315, 42351, 42513, 42531, 43215, 43251, 43521, 45213, 45231, 45312, 45321
F	1	23154
G	40	13245, 13254, 13425, 13452, 13524, 13542, 15324, 15342, 31245, 31254, 31425, 31452, 31524, 31542, 32154, 32145, 32415, 32451, 32514, 32541, 34125, 34152, 34215, 34251, 34512, 34521, 35124, 35142, 35214, 35241, 35412, 35421, 51324, 51342, 53124, 53142, 53214, 53241, 53412, 53421
H	4	23145, 43125, 43152, 43512
I	9	21534, 21543, 25134, 25143, 25413, 52134, 52143, 52413, 54213
J	8	21345, 21354, 21435, 21453, 24135, 24153, 42135, 42153
K	5	12345, 12354, 12534, 15234, 51234
L	2	14352, 41352

$$C_a^* = \min_{\vec{z}\in\mathcal{Z}} \left[C_a(\vec{z}) \,|\, L_j(\vec{z}) \leq \max(L_i^a, L_j^*), \quad \forall j \in \{1, \cdots, i\} \right] \tag{V.4}$$

and similarly for step 6, background noise is considered as follows:

$$L_i^* = \min_{\vec{z}\in\mathcal{Z}} \left[L_i(\vec{z}) \,|\, L_j(\vec{z}) \leq \max(L_i^a, L_j^*), \quad \forall j \in \{1, \cdots, i-1\} \right] \tag{V.5}$$

Taking into account all these considerations, the new algorithm is run and the lexicographic steps which are obtained with this new optimisation are shown in Table V-3 and in Figure V-2(a). As it can be seen, the first step produces an optimal noise value at location #2 of $L_2^* = 42.5$ dB(A), while minimising airliner cost. Now L_2^* is 2.5 dB(A) higher than in previous cases because in step 2 of the lexicographic algorithm there can be a slight improvement in the airliner cost at the expense of this noise increment. However, as this noise value is below the background noise, the actual constraint for location #2 has been set to 50.0 dB(A), meaning that this trajectory is not actually producing any noise disturbance at location #2. The second optimisation allows for the reduction of the maximum noise at location #5 to $L_5^* = 50.0$ dB(A) while L_2 is still under background noise. In this case, the trajectory flies eastwards from location #5 producing no noise disturbance at this location. The third step introduces an initial right turn, followed by a left turn, allowing a significant reduction of the maximum noise at location #1, $L_1^* = 67.0$ dB(A) , while maintaining L_2 and L_5 at background noise levels. The fourth optimisation modifies again the middle segment of the trajectory improving the noise impact at location #4 with $L_4^* = 56.1$ dB(A). Finally, the fifth step can still reduce the maximum noise at location #3 to $L_3^* = 62.6$ dB(A). In this case, the initial segment is shaped as a left turn arc allowing the trajectory to pass in between locations #1 and #3.

On the other hand, Figure V-3 shows the rest of the states and control variables, in function

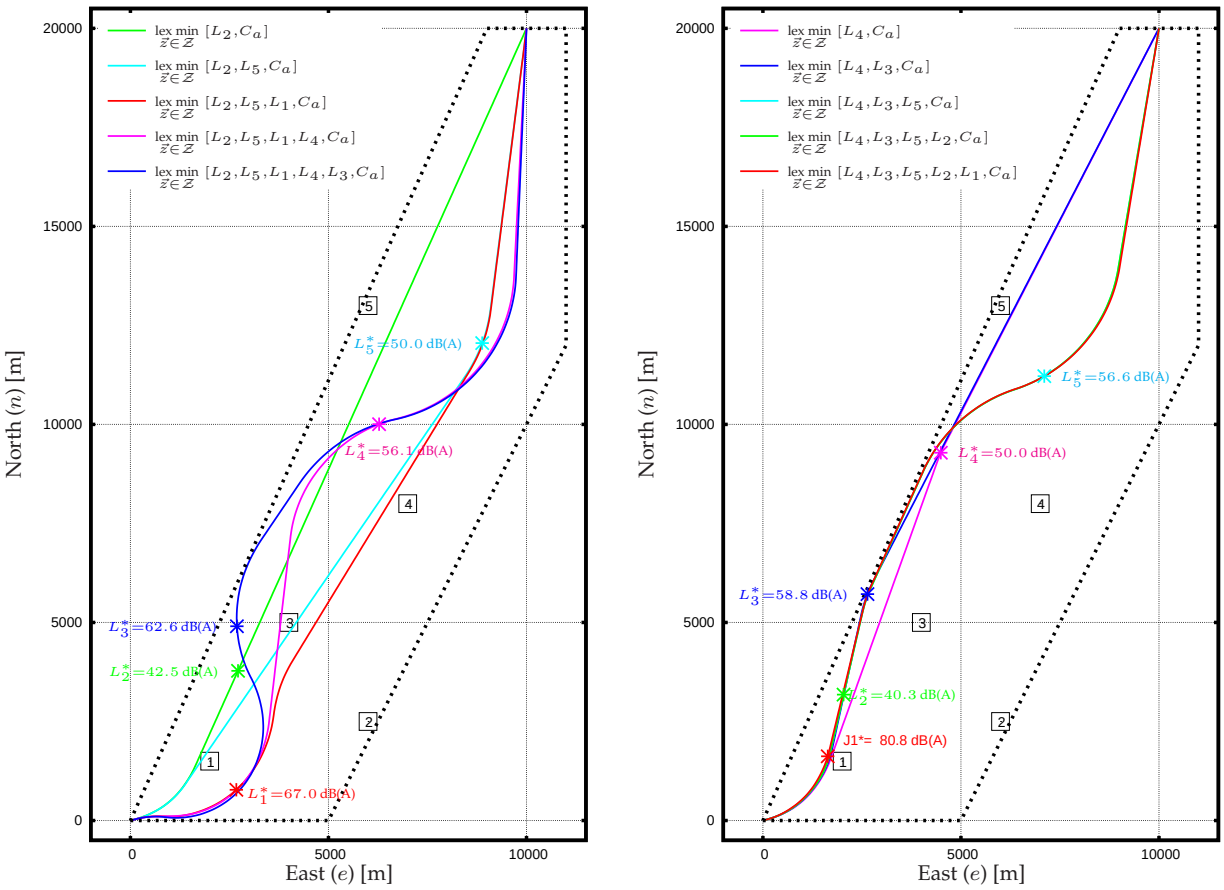

(a) Prioritisation *2-5-1-4-3* (b) Prioritisation *4-3-5-2-1*

Figure V-2: *Horizontal track for all lexicographic steps considering ambient noise*

of the flight time, corresponding to the final optimal trajectory. As it can be seen, when the optimisation starts, the aircraft is climbing from $h = 122\,\text{m}$ with a constant speed of $v = V_2 = 94.1\,\text{ms}^{-1}$. When the aircraft height is about $h = 250\,\text{m}$, maximum thrust is cut to *Climb* thrust setting and speed is increased in order to perform the first flap retraction. During this short acceleration, the altitude is almost constant and when CONF2 flap setting is achieved, the aircraft climbs again for a short period of time. This initial climb maximises the altitude while flying near locations #1 and #3. At $t \simeq 45\,\text{s}$ maximum noise at location #3 is achieved and then the aircraft initiates a flat segment while accelerating to $v = 128.6\,\text{ms}^{-1}$, passing progressively to flaps CONF1+F and CONF1. When this speed is achieved (being the maximum speed allowed below $3\,000\,\text{m}$) the climb resumes reaching a final height of $h_f = 1\,727\,\text{m} \simeq 5\,663\text{ft}$ at the end of the trajectory. The flat acceleration segment allows the aircraft to clean the flap/slats settings and, by doing so, climb performances of the following segment are significantly improved. Then, locations #4 and #5 are over-flown at a higher altitude producing less noise.

Giving another example, this time corresponding to prioritisation *4-3-5-2-1*, all lexicographic partial optimal trajectories are shown in Figure V-2(b). In this case, the first optimisation leads to a value of $L_4^* = 50.0\,\text{dB(A)}$ at location #4. The second optimisation can only slightly improve the noise impact at location #3, with $L_3^* = 58.8\,\text{dB(A)}$. The third optimisation, in turn, has more degrees of freedom, enabling the reduction of noise at location #5 up to $L_5^* = 56.6\,\text{dB(A)}$, performing a right turn just after the point where the maximum noise at location #4 reaches its maximum. Then, noise bound at location #2 is set to the ambient noise and finally noise optimisation at location #1 encounters almost no degrees of freedom. Thus, the computed trajectory does not differ

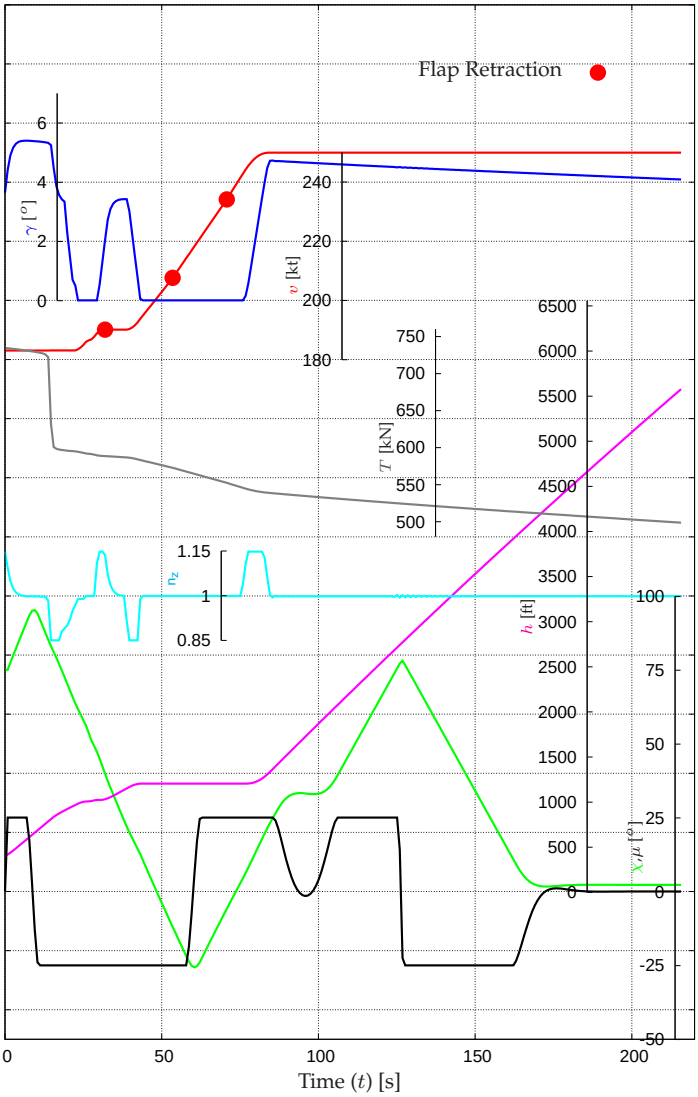

Figure V-3: *TAS, FPA aerodynamic heading and control variables for the optimal trajectory corresponding to the* 2-5-1-4-3 *prioritisation*

from the previous one, resulting in no improvement at all at location #1.

Finally, Figures V-4 (a) and (b) show respectively, the final horizontal and vertical trajectories for three different optimisation prioritisations:

$$\begin{aligned} &\underset{\vec{z}\in\mathcal{Z}}{\text{lex min}}\ [L_2, L_5, L_1, L_4, L_3, C_a] \\ &\underset{\vec{z}\in\mathcal{Z}}{\text{lex min}}\ [L_4, L_1, L_3, L_5, L_1, C_a] \\ &\underset{\vec{z}\in\mathcal{Z}}{\text{lex min}}\ [L_1, L_2, L_3, L_4, L_5, C_a] \end{aligned} \tag{V.6}$$

Each optimisation leads to a different horizontal/vertical trajectory and therefore optimal values obtained at each sensitive location are different according to the *a priori* established priority.

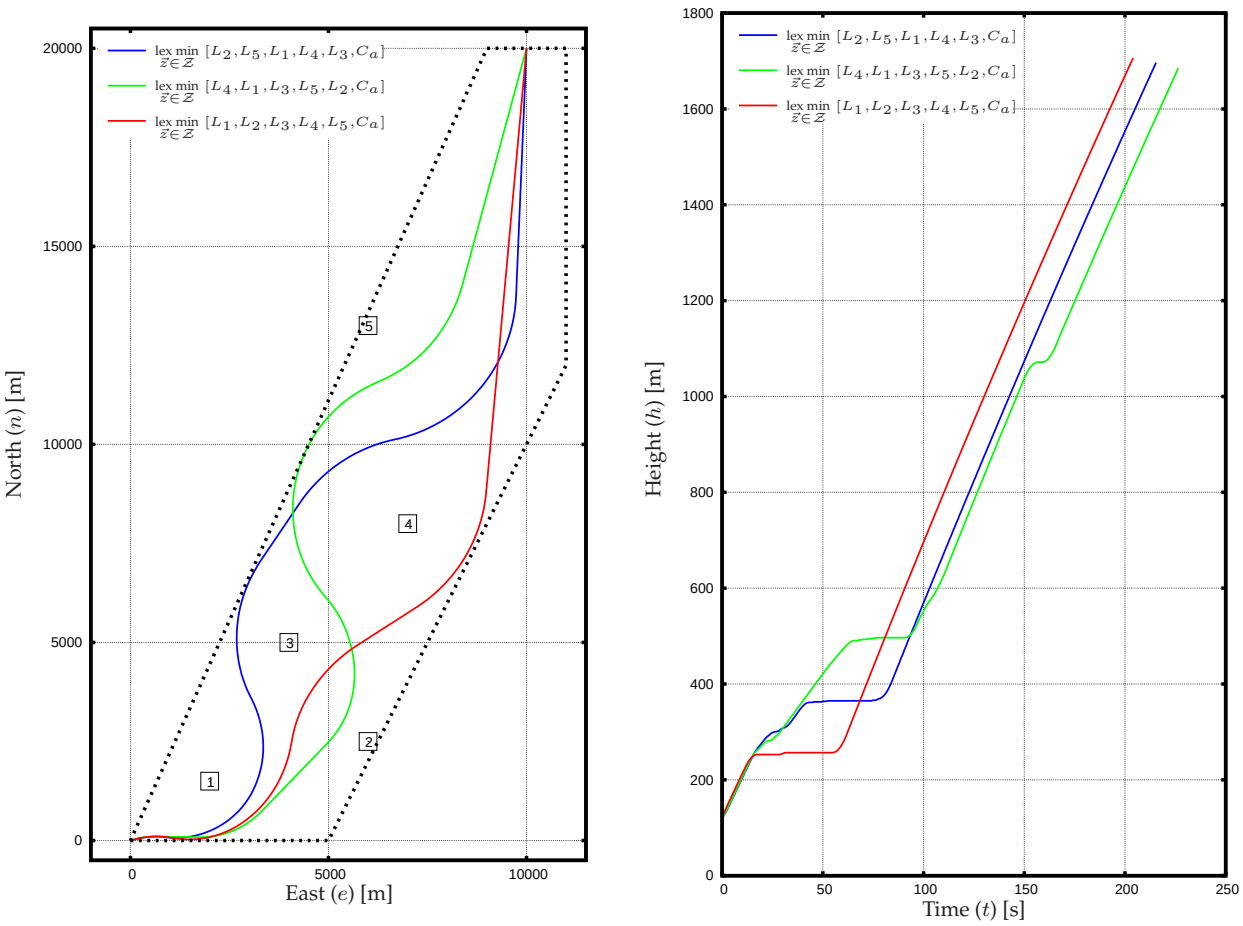

(a) Horizontal track (b) Vertical profile

Figure V-4: *Optimal trajectories for* 2-5-1-4-3, 4-1-3-5-2 *and* 1-2-3-4-5 *prioritisations*

V.2 Priority analysis

We can assume that the procedure designer in charge of publishing such a departure trajectory (*i.e.* the decision maker of this optimisation process) has a clear idea of which prioritisations should be given to each location (for example, hospitals are more important than residential zones, which in turn are more important than industrial zones, etc.). Moreover, even *political reasons* could lead to establish a given priority ranking among the different optimisation criteria. Consequently, Algorithm IV.1 leads to the best trajectory according to the desired hierarchy. However, in the case where this prioritisation is not clear, or when a more accurate scenario study is necessary, it is conceivable to run all optimisations by using all possibilities in the prioritisation order. The number of different prioritisations is $n_P = n_L!$, where n_L is the total number of noise sensitive locations.

In the previous example we have $n_P = 5! = 120$ and Figure V-5 shows all the optimal trajectories resulting from these 120 different lexicographic optimisations. From this study an important conclusion arises: some *flight segments* can be identified as common segments in different optimal trajectories. Further more, two or more different prioritisations can lead exactly to the same final optimal trajectory.

For this example, 12 different optimal trajectories are obtained: namely, trajectory A to trajectory L. Table V-4 lists all priority orders leading to each of the 12 different solutions and Figure V-6 shows all these trajectories separately.

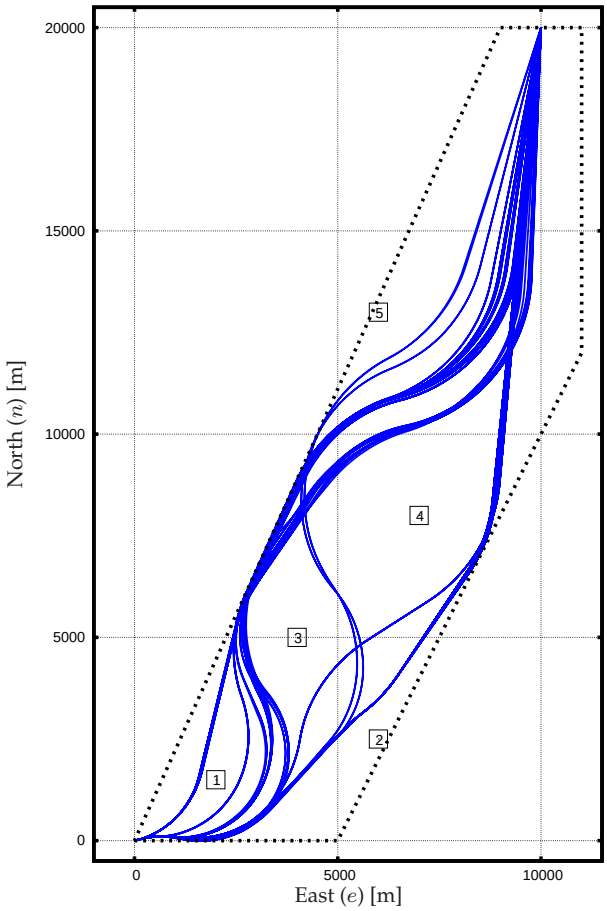

Figure V-5: *Optimal trajectories for all different prioritisations*

Table V-5: *Noise optimal values for the final trajectories and values for the four different performance indexes*

	L_1^P	L_2^P	L_3^P	L_4^P	L_5^P	Δ_{MA}^P	Δ_{AA}^P	Δ_{MR}^P	Δ_{AR}^P
Trajectory A:	79.88	40.92	59.97	55.10	50.00	18.23	6.66	29.57	11.94
Trajectory B:	61.71	54.30	64.11	50.00	56.00	14.11	4.89	28.22	9.78
Trajectory C:	61.65	68.70	62.38	50.00	64.65	18.70	9.15	37.40	18.30
Trajectory D:	**62.23**	**53.75**	**63.81**	**55.10**	**50.00**	13.81	**4.65**	27.62	9.25
Trajectory E:	79.66	41.51	60.49	50.00	55.15	18.01	6.73	29.21	12.10
Trajectory F:	77.21	45.18	58.82	56.86	50.00	15.56	6.25	25.24	11.32
Trajectory G:	61.65	71.46	50.00	60.05	48.89	21.46	6.30	42.92	12.61
Trajectory H:	**76.19**	**45.12**	**58.82**	**50.00**	**57.27**	14.54	6.13	**23.58**	11.15
Trajectory I:	**68.02**	**49.81**	**62.22**	**55.10**	**50.00**	**12.22**	4.74	24.44	**8.99**
Trajectory J:	66.96	49.80	62.69	50.00	56.54	12.69	4.91	25.38	9.41
Trajectory K:	61.65	54.53	64.05	60.14	48.39	14.05	5.75	28.10	11.50
Trajectory L:	61.65	71.01	62.38	50.00	62.31	21.01	9.14	42.02	18.28

NOTE: L_i^P, Δ_{MA}^P and Δ_{AA}^P are expressed in dB(A), while Δ_{MR}^P and Δ_{AR}^P are expressed in %

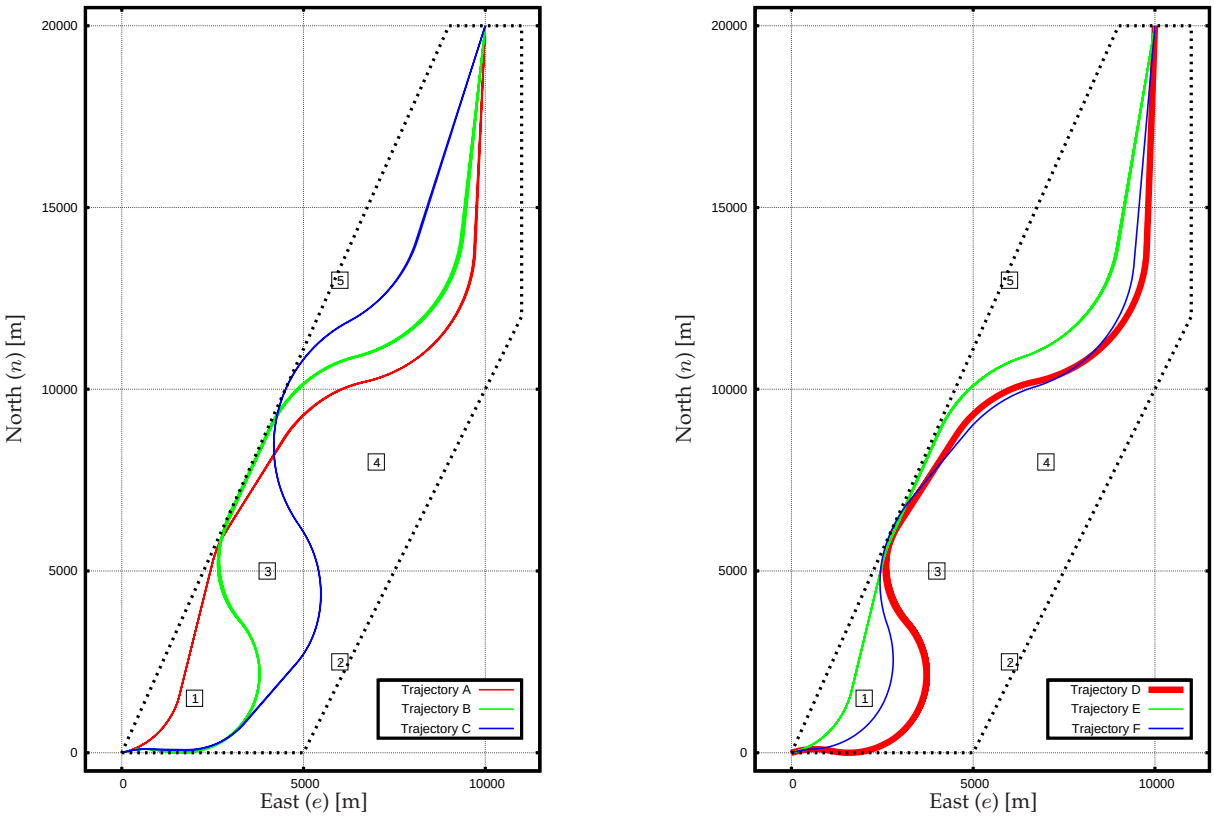

(a) A, B, and C optimal trajectories

(b) D, E, and F optimal trajectories

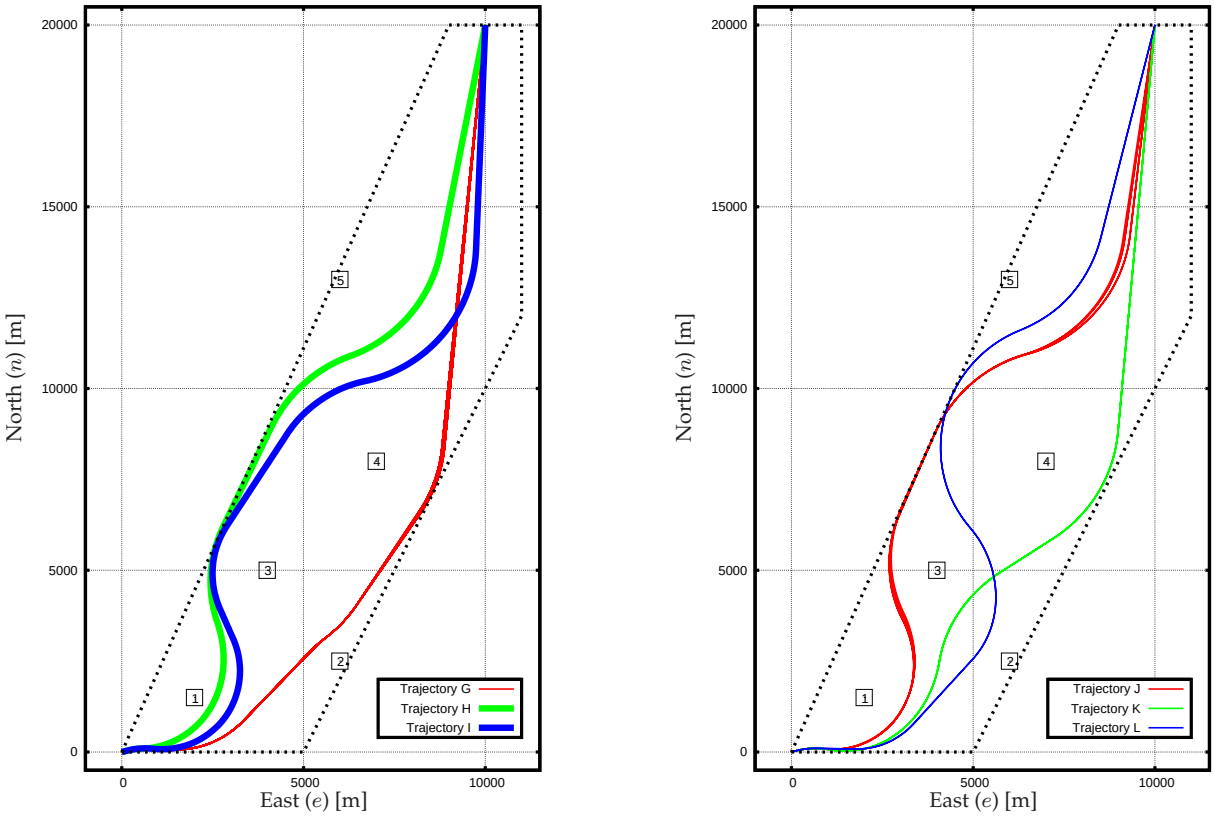

(c) G, H, and I optimal trajectories

(d) J, K, and L optimal trajectories

Figure V-6: *Optimal trajectories for all different prioritisations. Separate plots.*

V.2.1 From the optimisation to the decision problem

As seen previously, even if the total amount of possible priority orders is high, depending on the given scenario the optimal trajectories can be the same for several priorities. Therefore, the final number of Pareto-optimal trajectories is reduced and the decision task of selecting the final trajectory is easier. Nevertheless, if with the remaining solutions this decision can not be made directly, some down-selection support strategies can be considered. For instance, one or several performance indexes can be defined aiming at determining more objectively the final desired trajectory. Then, each optimal trajectory corresponding to a prioritisation P can be evaluated according to these performance indexes and ease the decision making process.

Let $L_i^\star$ be the ideal maximum noise level that can be achieved at sensitive location i (*i.e.* when location i is in the first priority). Let L_i^P be the maximum noise level reached at location i with the optimal trajectory corresponding to priority P. For each priority P we define four performance indexes like the Maximum Absolute deviation (MA) to the ideal value, the Maximum Relative deviation (MR), the average sum of Absolute deviations (AA) or the Average sum of Relative deviations (AR). Mathematically, these indices are defined as:

$$\begin{aligned} \Delta_{MA}^P &= \max_i \left(L_i^P - L_i^\star\right) & \Delta_{MR}^P &= \max_i \left(100\tfrac{L_i^P - L_i^\star}{L_i^\star}\right) \\ \Delta_{AA}^P &= \tfrac{1}{n_L}\sum_{i=1}^{n_j}\left(L_i^P - L_i^\star\right) & \Delta_{AR}^P &= \tfrac{1}{n_L}\sum_{i=1}^{n_j}\left(100\tfrac{L_i^P - L_i^\star}{L_i^\star}\right) \end{aligned} \tag{V.7}$$

According to these criteria, the *best* trajectory $\vec{z_k}^*$, for each performance index Δ_k^P, corresponds to the priority that minimises it:

$$\vec{z_k}^* = \arg(\min_P \ \Delta_k^P) \tag{V.8}$$

Considering the previous application example with five noise sensitive locations, the ideal noise values turnout to be:

$$L_1^\star = 61.65\,\text{dB(A)}\,; \quad L_2^\star = L_3^\star = L_4^\star = L_5^\star = 50.00\,\text{dB(A)} \tag{V.9}$$

where a background noise of $50.00\,$dB(A) has been considered as a lower bound for the different $L_i^\star$.

Table V-5 shows the maximum noise levels measured in all locations for each of the 12 different optimal trajectories found within this scenario, corresponding to all possible prioritisations. In addition, the same Table shows the value of each performance index, as defined in equations (V.7), for each of these 12 different trajectories. As it can be seen, trajectory D turnout to minimise Δ_{AA}^P, *i.e.* the average absolute distance from the ideal noise value at each location with an optimal mean deviation value of $4.65\,$dB(A). Moreover, trajectory H minimises the maximum relative distance (Δ_{MR}^P) with an optimal value of $23.58\,\%$, while trajectory I minimises both Δ_{MA}^P and Δ_{AR}^P, with optimal values of $12.22\,$dB(A) and $8.99\,\%$ respectively. See Figures V-6(b) and V-6(c), where the horizontal tracks of these optimal trajectories are shown in bold lines.

Conparatively, Figure V-7 shows a path value chart aimed at assisting the decision maker in charge to choose a final single trajecetory. In this diagram, each line displays a different alternative and the noise values at each noise sensitive location are represented. Along with this, the shaded area represents the ideal noise values at each location.

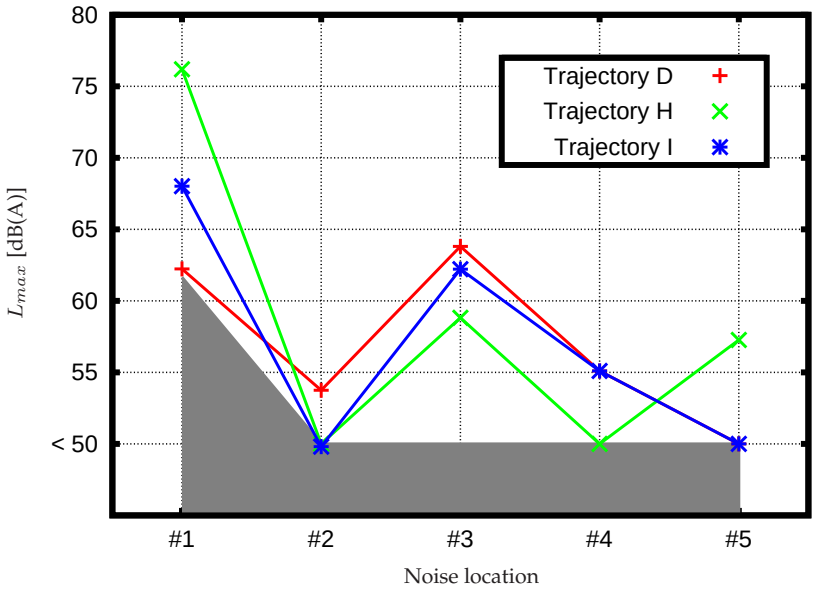

Figure V-7: *Value paths for the decision making process*

V.2.2 Computational cost

The previous scenario was solved using a common desktop PC, based on an Intel E6600 2.3 GHz processor. According to the output log file of the CONOPT solver, the problem had 9 801 variables and 13 305 constraints. In general, the first step in the lexicographic algorithm requires more time to converge than the ones following. This is because after the first step, the optimisation starts from an already feasible initial condition. Thus, the first step took an average of 3 minutes of CPU in the above mentioned machine while further steps required between 30 seconds to 1 minute. Therefore, a single prioritisation with 5 noise sensitive locations plus the airline cost minimisation as a last step, requires aproximately between 5 to 10 minutes. When solving all the possible prioritisations (*i.e.* the 120 of the previous example) a sequential tree structure can be used in order to reuse partial optimisations. For example, the partial optimal solution of the prioritisation 1-2 can be used to solve prioritisations 1-2-3, 1-2-4 or 1-2-5. In this case, the whole scenario presented above took about 5 hours and 30 minutes to be solved.

V.2.3 Introducing heuristics

As it was seen before, given a scenario with n_L different noise sensitive locations the total number of different prioritisations becomes $n_P = n_L!$. Then, in a real scenario with a high number of noise sensitive locations it is computationally impossible to check for all solutions if the decision maker is not able to fix the prioritisation among all the objectives beforehand. Alternatively, heuristic and iterative approaches can be used such that the lexicographic order is determined by fixing one by one the lexicographic priority orders of the objectives. For example in (Luss, 1999) the following rule is suggested that can be used to determine dynamically the lexicographic order in which the objectives should be minimised.

Let us establish beforehand a performance index, such as the maximum deviation from the ideal noise level, as defined in equation (V.7). Then, all objectives are minimised separately performing n_L mono objective optimisations. The first objective in the lexicographic order becomes the one that minimises the performance index. Once this first objective is determined, $n_L - 1$ lexicographic optimisations are run independently with the remaining criteria. Again, the optimisation that minimises the performance index is chosen and the second most important objective is fixed. This procedure is repeated iteratively until the lexicographic order of the whole set of crite-

Table V-6: *Different noise values obtained at each step of the lexicographic heuristic approach. Magnitudes are expressed in dB(A)*

	L_1^*	L_2^*	L_3^*	L_4^*	L_5^*	Δ_{MA}^P
$\min_{\vec{z}\in\mathcal{Z}} L_1$	61.65	56.04	**68.09**	68.00	60.70	**18.09**
$\min_{\vec{z}\in\mathcal{Z}} L_2$	83.22	42.54	**73.05**	55.06	67.27	23.05
$\min_{\vec{z}\in\mathcal{Z}} L_3$	79.81	71.42	50.00	**72.69**	54.15	22.69
$\min_{\vec{z}\in\mathcal{Z}} L_4$	**82.97**	41.56	66.86	50.00	69.62	21.32
$\min_{\vec{z}\in\mathcal{Z}} L_5$	88.98	46.52	**81.65**	71.45	50.00	31.65
$\text{lex}\min_{\vec{z}\in\mathcal{Z}} [L_1, L_2]$	61.65	54.53	**70.27**	66.94	61.22	**20.27**
$\text{lex}\min_{\vec{z}\in\mathcal{Z}} [L_1, L_3]$	61.65	**73.47**	50.00	72.50	54.30	23.47
$\text{lex}\min_{\vec{z}\in\mathcal{Z}} [L_1, L_4]$	61.65	54.26	**80.82**	50.00	68.70	30.82
$\text{lex}\min_{\vec{z}\in\mathcal{Z}} [L_1, L_5]$	61.65	58.31	62.17	**74.57**	50.00	24.57
$\text{lex}\min_{\vec{z}\in\mathcal{Z}} [L_1, L_2, L_3]$	61.65	54.53	64.05	**71.39**	59.09	**21.39**
$\text{lex}\min_{\vec{z}\in\mathcal{Z}} [L_1, L_2, L_4]$	61.65	54.53	**80.82**	50.00	68.70	30.82
$\text{lex}\min_{\vec{z}\in\mathcal{Z}} [L_1, L_2, L_5]$	61.65	54.53	66.57	**74.20**	50.00	24.20
$\text{lex}\min_{\vec{z}\in\mathcal{Z}} [L_1, L_2, L_3, L_4]$	61.65	54.53	64.05	**60.14**	48.39	**10.14**
$\text{lex}\min_{\vec{z}\in\mathcal{Z}} [L_1, L_2, L_3, L_5]$	61.65	54.53	64.05	**74.70**	50.00	24.70
$\text{lex}\min_{\vec{z}\in\mathcal{Z}} [L_1, L_2, L_3, L_4, L_5]$	**61.65**	**54.53**	**64.05**	**60.14**	**48.39**	

ria is established. If this heuristic approach is used, the total number of different optimisations is significantly reduced to $\frac{n_L}{2}(n_L+1)$. Nevertheless, this heuristic approach may not lead to the best solution (*i.e.* the one that minimises the performance index). In general, the solution obtained is not far from the optimal one (which can be exactly achieved with the exhaustive search when $n_L!$ optimisations are run) providing a good compromise with respect to the computational cost.

Table V-6 shows the different iterations that would be run if the previous example is solved by using this heuristic approach. With $n_L = 5$ noise sensitive locations, the number of iterations becomes $\frac{n_L}{2}(n_L + 1) = 15$. Here, the optimisation of location #1 leads to the trajectory with the minimum deviation from the ideal noise value. In this case, location #3 turnsout to be the worst location with a noise level of 68.09 dB(A). Therefore, location #1 becomes the first objective in the lexicographic ordering and 3 independent optimisations are run with the remaining criteria. In this second step the optimisation of L_2 leads to the best performance index and location #2 becomes the second most prioritised objective. As seen in the Table, this process goes on iteratively obtaining the final prioritisation ordering of P =*1-2-3-4-5*.

Table V-4 and Figure V-6(c) show that this prioritisation corresponds to trajectory K and the maximum deviation from the ideal noise values is 14.05 dB(A), corresponding to the noise measured at location #3.

However, as the problem we tackle is highly nonlinear, we can not prove that this (or any other) heuristic approach may lead always to an acceptable result close to the actual optimal one, independently of the studied scenario.

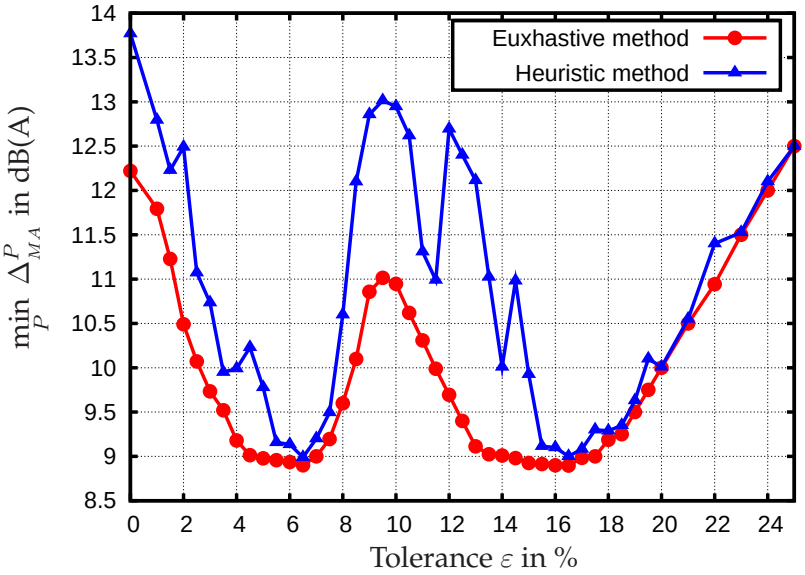

Figure V-8: *Best worst-case performance index ($\min_P (\Delta^P_{MA})$) for the exhaustive and heuristic hierarchical optimisation optimal solutions in function of the tolerance value (ε)*

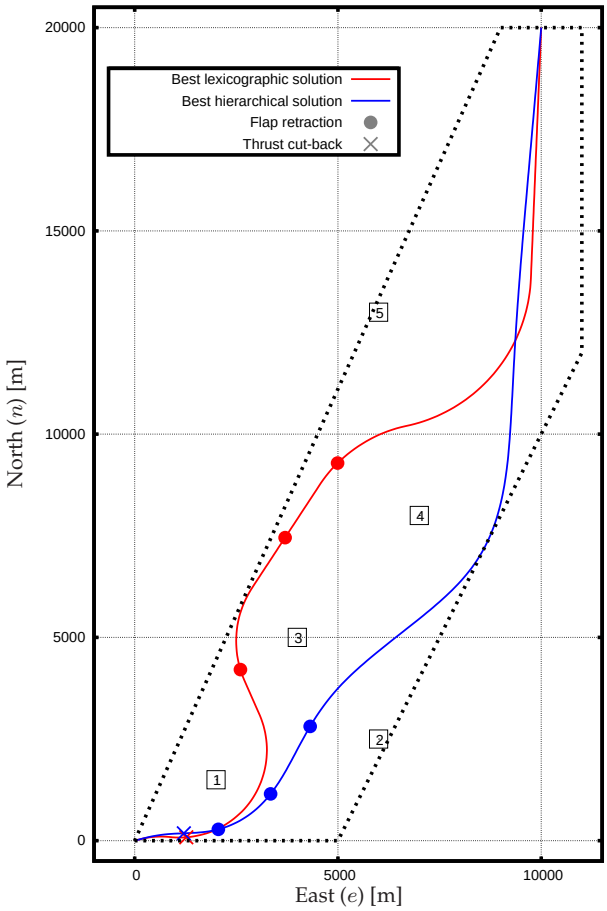

Figure V-9: *Best lexicographic and hierarchical trajectories. Horizontal track*

V.3 Hierarchical optimisation

The previous lexicographic approach with priority discovering, by either using the exhaustive lexicographic search approach or the heuristic method proposed in the previous section, can be

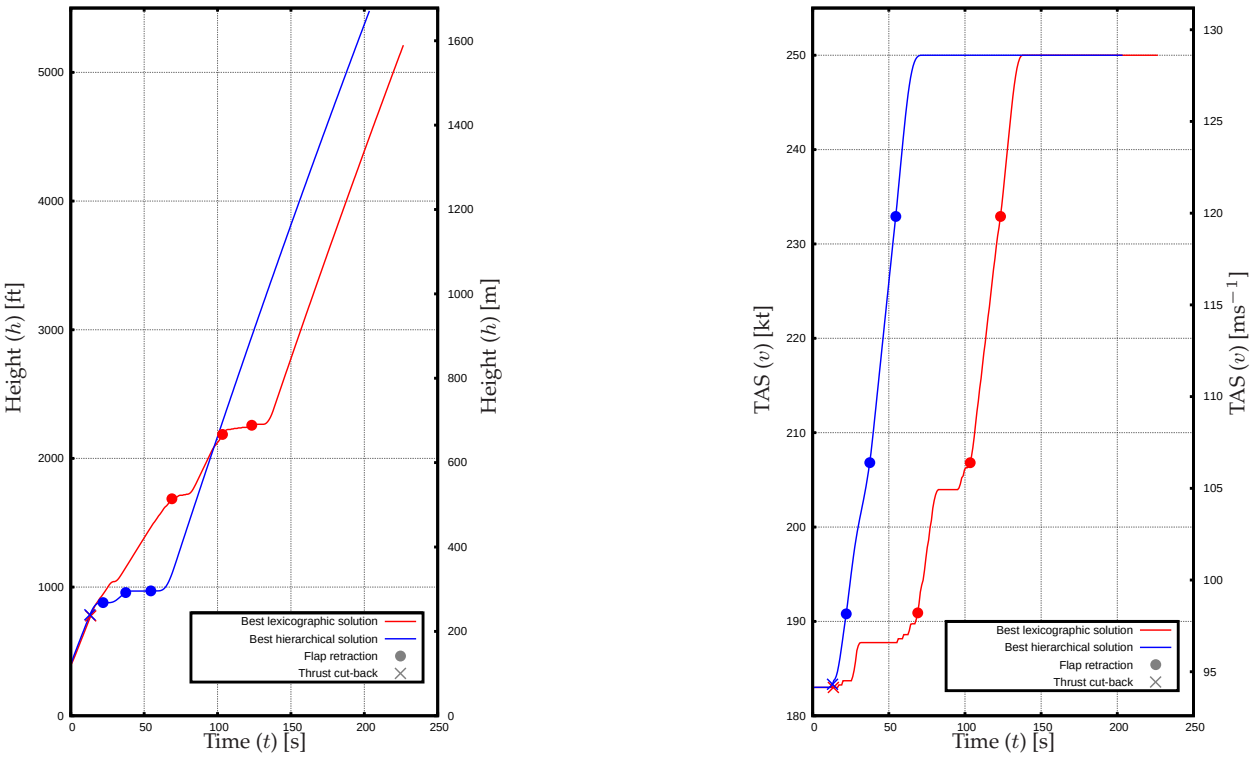

(a) Vertical profile (b) Speed profile

Figure V-10: *Best lexicographic and hierarchical trajectories. Vertical and speed profiles*

further elaborated if the sensitivity of the criteria is assessed. As explained in section IV.2.3, with lexicographic optimisation only a subset of solutions of the Pareto optimal frontier is actually explored. Mathematically, all solutions in the Pareto optimal frontier should be considered equally and then, according to a performance index or an expert judgement, the decision maker should choose one solution from the Pareto set. If we consider the minimisation of the maximum deviation from the ideal noise values (worst-case minimisation) as stated in equation (V.7), several hierarchical optimisations with different relaxations can be run, coupled with an exhaustive or heuristic priority discovering as explained in the previous section.

As presented in section IV.2.4, hierarchical optimisation accepts a certain degree of relaxation (ε) in the optimal objectives fixed as constraints in the lexicographic optimisation process. Varying the values of ε, the exploration of the Pareto optimal frontier can be achieved and the best solution based on on the minimisation of a given performance index can be found (see Figure IV-3). The same hypothetical scenario used in previous sections is solved now by using the hierarchical optimisation method. In this example, the exhaustive and heuristic methods have been tested for different values of ε ranging from 0% (pure lexicographic, as presented in previous section) to 25% increasing by regular intervals of 0.5%.

The maximum absolute deviation from the ideal value, Δ^P_{MA} in equation (V.7), is used as a performance index allowing the choice of the *best* optimal trajectory among all Pareto solutions. Figure V-8 shows the minimum performance index (*i.e.* the minimum deviation from the ideal noise value for the worst-case location) in function of the tolerance value ε. In red, the exhaustive hierarchical method is applied so the best prioritisation that minimises the performance index has been chosen among all 120 different prioritisations for this scenario. In blue the heuristic approach with adaptative priority discovering, presented in the last section, has been used performing only 15 optimisations for each different tolerance value.

It turns that almost two identical minima are obtained with $\varepsilon = 6.5\%$ and $\varepsilon = 16.5\%$ with an

Table V-7: *Noise levels at all locations for the ideal, lexicographic and hierarchical trajectories. Magnitudes are expressed in dB(A)*

	L_1^*	L_2^*	L_3^*	L_4^*	L_5^*	$\min_P \Delta_{MA}^P$
Ideal (utopian) trajectory	61.65	50.00	50.00	50.00	50.00	–
Best lexicographic trajectory	68.02	49.81	**62.22**	55.09	50.00	12.22
Best hierarchical trajectory	68.02	57.30	58.25	**58.86**	44.84	8.86

optimal worst-case noise deviation of 8.86 dB(A). In the first case the best hierarchical prioritisation corresponds to the ordering P =*5-2-4-1-3*. In the second case, the ordering is P =*1-2-3-5-4*. However, when both prioritisations are relaxed with the respective optimal tolerance values, the final resulting trajectory is the same for both cases, *i.e.* the obtained Pareto solution is the same. Recalling the simple graphical example of Figure IV-3, it can be seen that a same point in the Pareto frontier can be reached by relaxing properly either prioritisation P =*1-2* or prioritisation P =*2-1*.

This behaviour is particularly advantageous when using the hierarchical heuristic method. This method, as explained earlier, has the advantage of being much more computationally friendly but it is not guaranteed that the most equitable solution is obtained by using it. When using the ε relaxations, the convergence of the optimal trajectories to a single one, allows the solution obtained with the heuristic method to be closer to the solution obtained with the exhaustive method.

Figure V-9 shows the horizontal track of the *best* lexicographic trajectory obtained in the previous section, (trajectory I in Figure V-6(c)) and the *best* hierarchical trajectory. Where as, Figure V-10 shows the vertical and speeds profiles for both trajectories.

Evidently, both trajectories are significantly different. Table V-7 contains the noise values at all locations for the ideal outcome, *best* lexicographic and *best* hierarchical optimal trajectories. In the lexicographic case, location #3 resulted in the furthest noise deviation value from the ideal one with a deviation of 12.22 dB(A). However this value was the best one among all different lexicographic prioritisations. When the hierarchical case is run, different criteria are traded off resulting with a trajectory of a better worst noise deviation value. In this case, noise at location #3 can be reduced at the expense of increasing noise at locations #2 and #4. Therefore, the best worst-case noise deviation is obtained in location #4 with a value of 8.86 dB(A).

V.4 Dealing with local minima

As commented in Chapters II and IV, one of the most important issues of the implemented optimisation thechnique is the impossibility to gurantee a global optimum as a final solution. In a non-convex problem the obtained solution may be sensitive to the values of the different decision variables at the begining of the optimisation algorithm. The majority of the optimisation packages (such as the CONOPT solver being used in this work) allow the user to specify these *initial* or *guess* values.

In all the examples shown above, the initial *guess trajectory* for the first lexicographic (or hierarchical) step was a direct trajectory joining the initial and final points. Then, for the lexicographic (or hierarchical) step k, the trajectory obtained in the previous step $k-1$ was used as the guess trajectory. This strategy allowed a fast convergence in the optimisation algorithm. However, a deeper analysis was required in order to overcome local optima in some cases.

As an example, let us consider the lexicographic optimisation of the prioritisation *1-2-3-5-*

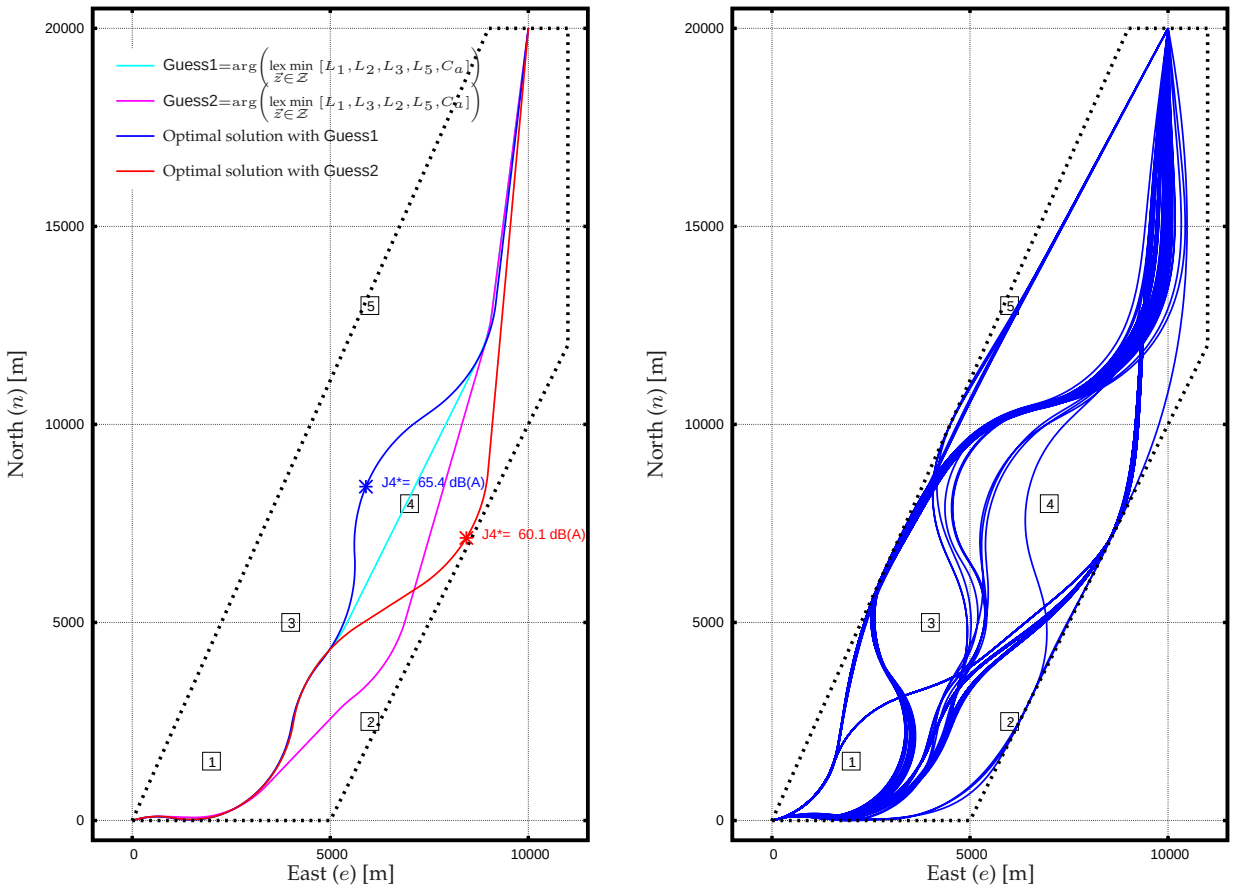

(a) Local minimum in a lexicographic step (b) Local minima when using a scalarisation approach

Figure V-11: *Examples of local minima*

4. Figure V-11(a) focuses on the step of the algorithm where the noise at location #4 is to be minimised. The blue trajectory is the result of this optimisation when the normal procedure is applied (*i.e.* we have used as initial guess the optimal trajectory of the previous lexicographic step). In this case, the optimal maximum noise level attained at location #4 with this optimisation is 65.4 dB(A). On the other hand, the red trajectory shows the result of the same optimisation problem but when a different initial guess is used (in this case taking the result of prioritisation *1-3-2-5*), obtaining a value of 60.1 dB(A). As seen in the figure, the Guess1 trajectory sigthly over-flies the West of location #4 while the Guess2 trajectory flies East of this location. Since the optimisation technique being used is a gradient search, the objective function decreases when moving to the West in the first case and to the East in the second case explaining, in this way, the substancial differences of both final trajectories.

In this context, the step by step nature of the lexicographic (or hierarchical) strategy is an advantageous feature when identifying possible local minima. After an optimisation step, the user can examine the resulting trajectory and easily identify if the algorithm has been stuck in a local minimum. In the previous example, the user may ask himself whether the optimal trajectory should fly East or West of location #4 and try another optimisation by changing the initial guess. On the other hand, if a single step optimisation technique is used (such as the scalarisation or egalitarian methods presented in previous Chapter) this task becomes more difficult. As an example, Figure V-11(b) shows the optimal trajectories obtained with different initial guesses when the scalarisation problem is solved (see equation (IV.24)). In this case, the same weight was given at each noise sensitive location (according to the equation (IV.25)). Moreover, the trajectories coming

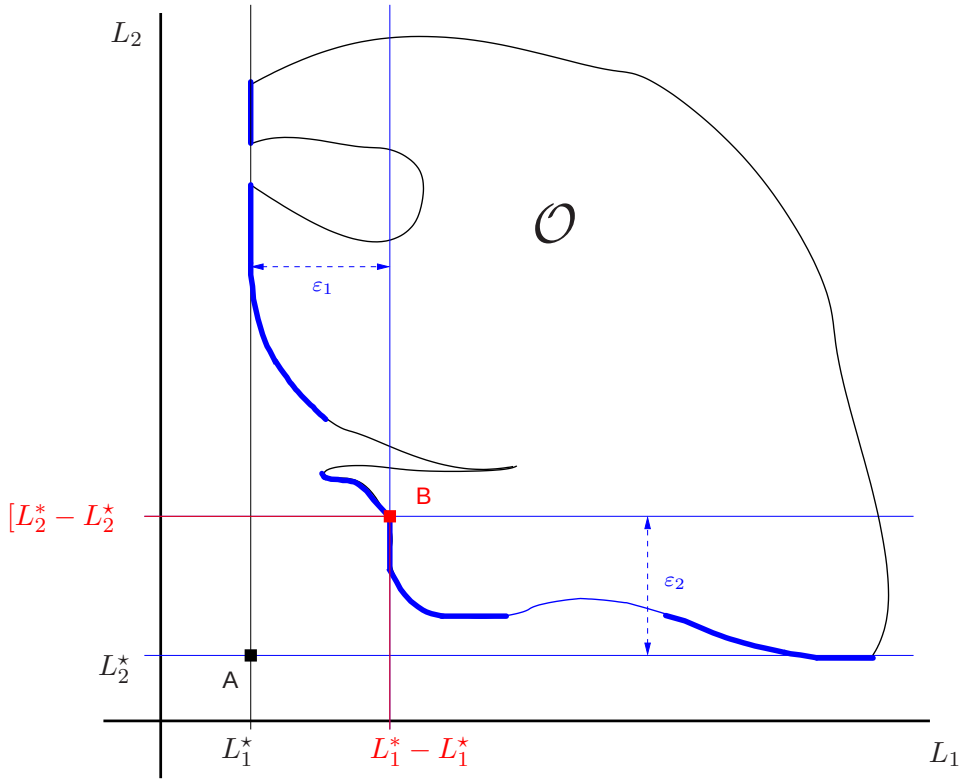

Figure V-12: *Example of Tchebycheff optimisation strategy for a two criteria multi-objective minimisation problem*

from all the different lexicographic prioritisations (see Figure V-5 and Table V-4) were taken as initial guess trajectories. As seen in the figure, the optimiser is clearly sensitive to the initial guess trajectory. Even if we take the trajectory which gives the lowest criterion, it is difficult to assess if this trajectory is globally optimal or if we should keep trying other initial guesses.

V.5 Discussion of the results

So far, lexicographic and hierarchical optimisation techniques have been presented and applied in the resolution of a basic trajectory optimisation problem. It has been shown that the lexicographic optimisation is a simple and suitable technique when the prioritisation among the different objective functions is clear and can be established beforehand. In the case that all the criteria share the same importance, it is proposed an exhaustive approach where all the possible prioritisations are analysed. In this case, the decision maker shall define an extra metric (or set of metrics) aimed at choosing a solution among all the possible ones that are obtained from the different priotisations.

Otherwise, hierarchical optimisation allows relaxing the higher prioritisated objectives and permits the trade-off among them. In this way a wider range of Pareto solutions can be explored and the obtained solution may be better according to the metrics (or performance indexes) established by the decision maker. Then, another exhaustive search technique is presented where besides all possible prioritisations, different relaxation values (ε) are also tested. By doing this, it was found that there exists a prioritisation plus a relaxation value that minimise a given decision metric. The metric that was used in this last example was the maximum absolute deviation from the ideal value, taking into account all objectives: Δ_{MA}^{P} in equation (V.7).

Then, if the relaxation parameter (ε) is big enough, the hierarchical optimisation described above leads to the same solution as if the optimisation problem was formulated directly as:

$$\min_{\vec{z}\in\mathcal{Z}} \{L_1(\vec{z}), L_2(\vec{z}), \cdots, L_{n_L}(\vec{z})\} = \min_{\vec{z}\in\mathcal{Z}} \left[\max_{i\in\mathcal{L}} (L_i(\vec{z}) - L_i^\star)\right] \tag{V.10}$$

where n_L is the total number of noise sensitive locations (*i.e.* objective functions), $\mathcal{L}$ the set of these locations and $L_i^\star$ the ideal value for objective #i.

That is, an egalitarian formulation where the objective function turns to be the absolute distance between the ideal value and the feasible objective region, considering that all these distances are thought to be equally important. This egalitarian problem was presented in section IV.2.5 and it is also called a min-max or a *Tchebycheff* problem. Moreover it can be expressed as the following limit of a more general p-metric multi-objective minimisation problem (Miettinen, 1999):

$$\min_{\vec{z}\in\mathcal{Z}} \left[\max_{i\in\mathcal{L}} (L_i(\vec{z}) - L_i^\star)\right] = \min_{\vec{z}\in\mathcal{Z}} \left[\lim_{p\to\infty} \left(\sum_{i=1}^{n_L} (L_i(\vec{z}) - L_i^\star)^p\right)^{\frac{1}{p}}\right] \tag{V.11}$$

Recalling the graphical representation that we used in the previous Chapter for showing a two-dimensional Pareto frontier, the previous equivalence is shown in Figure V-12. Thus, if the allowed relaxation ε were big enough, it would be possible to achieve point B in the Pareto front, where the distance $L_i^*(\vec{z}) - L_i^\star$ is equally minimised for $i = 1, 2$. That is:

$$L_1^* - L_1^\star = L_2^* - L_2^\star \tag{V.12}$$

where $[L_1^*, L_2^*]$ is the solution of equation (V.10) problem.

Then, when the maximum absolute deviation from the ideal value of the criteria is chosen as decision performance index, equation (V.10) would be regarded as an equivalent method to the hierarchical optimisation presented above. Moreover, equation (V.10) only occurs in one optimisation problem and does not suffer from the limitations on the number of objectives, as does the hierarchical approach, where a high computationally burden was required. Therefore, this more computational friendly solution will allow us to explore more complex scenarios with a large number of noise sensitive locations to take into account.

In theory there is no difference between theory and practice. In practice there is.

— Berra Yogi

The value of an idea lies in the using of it.

— Thomas A. Edison

VI

Optimisation of NADP for complex scenarios

In Chapter IV, the basic concepts of multi-criteria optimisation were presented and lexicographic, hierarchical, egalitarian and goal optimisation were introduced at theoretical level. Then, in Chapter V, the lexicographic and hierarchical approaches were tested in a hypothetical scenario with only a few noise sensitive locations. There, we concluded that a hierarchical optimisation is equivalent to an egalitarian (also called min-max or Tchebycheff) optimisation if the objective function at the worst-case criterion is minimised. Moreover, as it was seen in Chapter III, in this work we propose to deal with noise annoyance instead of just the acoustical magnitudes of noise. In the same Chapter, it was shown how the annoyance criterion can easily be built from nonlinear functions which in turn, can be derived from more complex fuzzy logic models. Also, a simple model was proposed where the noise annoyance was modelled as a function of the maximum A-weighted noise level, the period of the day and the type of over-flown zone (considering *hospitals, schools, residential* and *industrial* zones).

In this Chapter, egalitarian optimisation is explored further, assessing *fairness* and *Pareto efficiency* of the solutions. Furthermore, a final optimisation strategy is presented where different approaches are mixed, such as hierarchical, lexicographic and goal optimisation. In addition, we will tackle the problem of complex scenarios where a significant number of different noise sensitive locations exist. Therefore, problems where noise abatement procedures may be designed over a wide area with several populated zones will be considered in this Chapter.

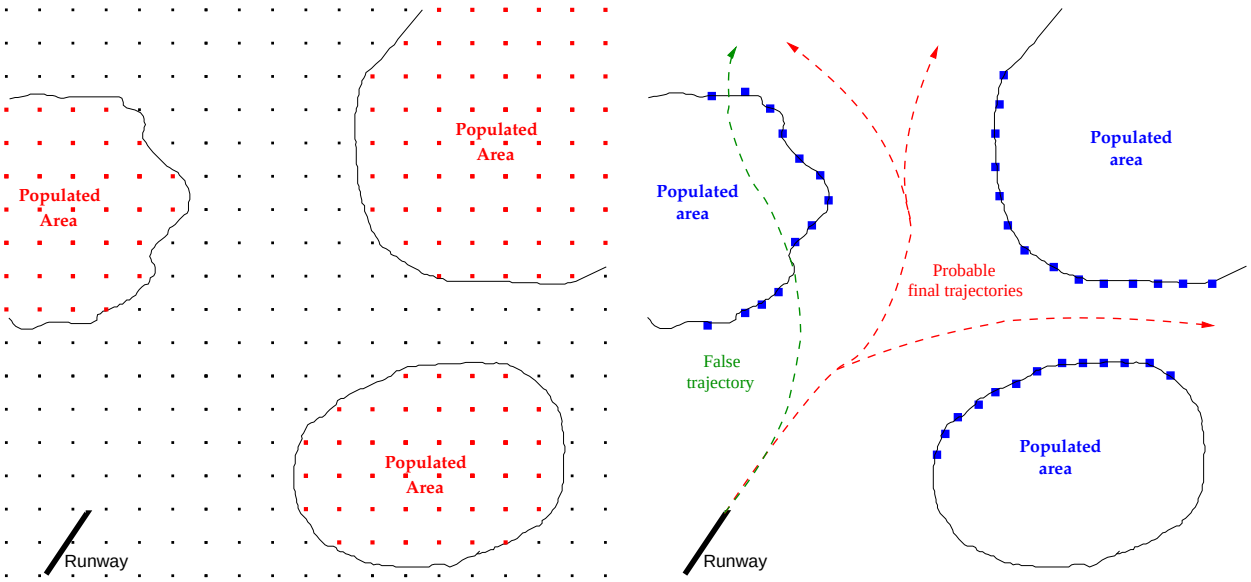

(a) Regular grid (b) Ad hoc irregular grid

Figure VI-1: *Example of different grid solutions for the placement of the measurement points*

VI.1 Definition of the measurement grid

In real scenarios *areas* of population exist, instead of a limited set of *singular points* as used in the previous Chapter. A usual way to take populated areas into account is by defining a set of observer locations arranged in the form of a geometric grid of points (see Figure VI-1(a)). However, compromises occur between the desired accuracy and the computational burden when solving the optimisation problem. Obviously, the larger the size and/or mesh of the grid the more accurate the solution would be. Yet, it would be more computationally expensive too. A possible solution to improve the computational load would be to *manually erase* all those points that are not inside a populated area, *i.e.* only consider the red points in Figure VI-1(a). However, with large scenarios even this approach would be prohibitive if a fine mesh is used.

As commented on in Chapter IV, a classic approach to solving a multi-criteria optimisation problem is by using a scalarisation function. In this case where all the objectives have the same importance regarding the optimisation the same weight is given to all of them (see equations (IV.24) and (IV.25)). Therefore, the *average* noise (or annoyance) is minimised as a single objective optimisation problem. If this technique is used, a grid like the one shown in Figure VI-1(a) must be used in order to take into account all observation points to be averaged.

In this Chapter, a different solution for modelling populated areas is proposed aiming at simplifying considerably the number of points on the measurement grid. Taking advantage of the Tchebycheff optimisation formulation, we propose considering only those *relevant* points that produce a significant influence in the optimisation process. This task is not straightforward and can not be formulated objectively. Therefore, we appeal to the *common sense* or *experience* of the operator in charge of using the optimisation tool.

For example, Figure VI-1(b) shows a possible solution for the previous example scenario. If the initial and final points of the trajectory are known before-hand, the operator may guess how the optimal trajectory could be. Depending on the scenario, several equally likely solutions may exist, as it is shown in Figure VI-1(b). It is obvious that the optimal trajectory may try to avoid populated areas, while respecting the flight dynamics constraints of the aircraft. Then, a distribution of observation points following certain borders of the populated areas closer to the final trajectory would be enough. Since the *average* noise annoyance is not minimised in this case

(as done with classical scalarisation techniques) it is not necessary to measure the noise annoyance in the inner parts of the populated areas. There, the acoustical conditions will be better than or equal to those measured in the borders of the area.

Depending on the scenario complexity, this process may not be easy at the beginning, and perhaps some initial trials will be needed in order to adjust the final distribution of measurement points. It is clear that the greater the number of points, the greater the computational burden would be. However, if the distance between two points is too large the obtained optimal trajectory may fly in between them. This would lead to a virtual optimal solution that would be false because the noise annoyance in the inner part of the inhabited area has not been considered (see green trajectory of Figure VI-1(b)). Therefore, the user of this optimisation tool should be aware of these possible false solutions and choose accordingly the most convenient distribution of measurement points, check the obtained solution and repeat the optimisation if necessary.

VI.2 Multi-objective optimisation

As discussed before, the noise annoyance at all measurement points of the grid will define the different optimisation criteria to be minimised. Moreover, the cost for the operator, such as fuel burnt or time spent in the whole trajectory, should also be taken into account. This airliner cost (C_a), as defined in equation (IV.8), is also considered as an optimisation objective.

However, instead of using the annoyance values directly, we propose to use the *annoyance deviation* at each noise measurement point as objective function. This deviation is simply defined as:

$$\Delta_i^{\mathfrak{h}}(\vec{z}(t)) = A(L_i(\vec{z}(t)), \mathfrak{h}) - A_i^{\star}(\mathfrak{h}) \tag{VI.1}$$

where $A(L_i(\vec{z}(t)), \mathfrak{h})$ is the perceived noise annoyance at measurement point i, at hour of the day $\mathfrak{h}$ and for a given trajectory $\vec{z}(t)$. On the other hand, $A_i^{\star}(\mathfrak{h})$ is the *ideal* noise annoyance value at the same location and time period (*i.e.* the result of the single objective optimisation problem where only $A(L_i(\vec{z}(t)), \mathfrak{h})$ is minimised). For the sake of clarity, let us drop the trajectory dependency $\vec{z}(t)$ for the forthcoming notation. Furthermore, the hour of the day $\mathfrak{h}$ dependency will be also dropped from the notation in the cases where confusion is not possible.

If absolute annoyance values A_i were used as optimisation criteria, the solution would be too sensitive vis-à-vis those locations which are too close to the airport. Let us suppose, for example, that the ideal annoyance value at location #1 is already $A_1^{\star} = 0.5$ and the ideal value at location #2 is zero. We consider that it is not *fair* to try to equally minimise A_1 and A_2 because the optimisation process would give more priority to the minimisation of the noise annoyance at location #1 rather than the noise annoyance at location #2. For that reason, if the noise annoyance deviations were to be used as objectives, the optimisation process would consider just the deviations to be minimised and a *fairer* solution among the objectives would be obtained.

VI.2.1 Optimisation strategy

The optimisation strategy proposed for solving a complex and realistic scenario takes the best features of the different strategies presented in previous Chapters, such as egalitarian, lexicographic, hierarchical and goal optimisation. The expert user, or users, of this tool will have a significant role in how the optimisation process is carried out.

After defining a convenient measurement grid, as discussed previously, the user may want to select some *special* locations where instead of minimising the noise annoyance, he/she would

prefer to set a maximum aspiration noise annoyance level. For this work, we propose that hospital and school locations may be treated as this kind of special locations.

Let $\mathcal{G} = \{1, ..., n_G\}$ be the set of hospital and school locations, n_G the total number of these *special* locations and $\bar{A}_j(\mathfrak{h})$ be the aspiration level at the j-th location $\forall j \in \mathcal{G}$ at the hour of the day $\mathfrak{h}$. Then, these maximum (or *goal*) values are simply modelled as additional constraints in the optimisation process:

$$A_j(\mathfrak{h}) \leq \bar{A}_j(\mathfrak{h}) \quad \forall j \in \mathcal{G} \tag{VI.2}$$

Alternatively, the noise annoyance deviations at residential and industrial zones are taken into account as optimisation objectives, as well as the airliner cost. In a first phase, a hierarchical optimisation approach is proposed for dealing with these two conflicting objectives. First, noise annoyance deviation is minimised in all measurement points. Let n_L be the total number of noise sensitive locations (*i.e.* the total number of points in the measurement grid) and $\mathcal{L} = \{1, ..., n_L\}$ the set of these locations. Therefore, for a given hour of the day $\mathfrak{h}$, this multi-criteria optimisation problem is written as:

$$\min_{\vec{z} \in \mathcal{Z}} \{\Delta_1, \Delta_2, \cdots, \Delta_{n_L}\} \tag{VI.3}$$

where the vector $\vec{\Delta}^* = [\Delta_1^*, \Delta_2^*, \cdots, \Delta_{n_L}^*]^T$ is the solution of this minimisation problem.

As a second step, the airliner cost will be minimised without wasting the optimal noise annoyance values obtained in the previous solution. Yet, some relaxation in these values will be permitted below a certain threshold value. Therefore, airliner cost minimisation is performed as follows:

$$\begin{aligned} & C_a^* = \min\ C_a \\ & \text{Subject to: } \begin{array}{l} A_i \leq \max\left(\bar{A}, A_i^*\right) \quad \forall i \in \mathcal{L} \\ \vec{z} \in \mathcal{Z} \end{array} \end{aligned} \tag{VI.4}$$

where C_a is the airliner cost and $\bar{A}$ is a configurable threshold value. Note that in previous formulation, the $\max(\cdot)$ function does not suppose an issue regarding its non-differentiability since this operation is performed before running the optimisation problem (both, $\bar{A}$ and A_i^* values, are known beforehand).

With this strategy, the noise annoyance is considered infinitely more important than the airliner cost in those noise sensitive locations where the optimal noise values are greater than the threshold values. However, in those places where the optimal annoyance values are below this threshold, the airliner cost becomes the objective function with the highest priority, providing that noise annoyance in those locations will never exceed the above mentioned threshold.

Figure VI-2 summarises this optimisation strategy, for a given hour of the day $\mathfrak{h}$. Firstly, the user defines the ad hoc grid of measurement points for the industrial and residential zones. The hospital and school locations are also defined along with the optimisation constraints (such as airspace constraints, aircraft performance etc.). Then, n_L single objective optimisations are carried out in order to compute the ideal values at each industrial and residential location ($A_i^\star,\ \forall i \in \mathcal{L}$). In addition, the aspiration levels for the noise annoyance at hospitals and schools locations are also defined and the annoyance optimisation is performed. An egalitarian iterative optimisation approach is proposed for solving this particular multi-criteria problem and will be explained in detail in the following section.

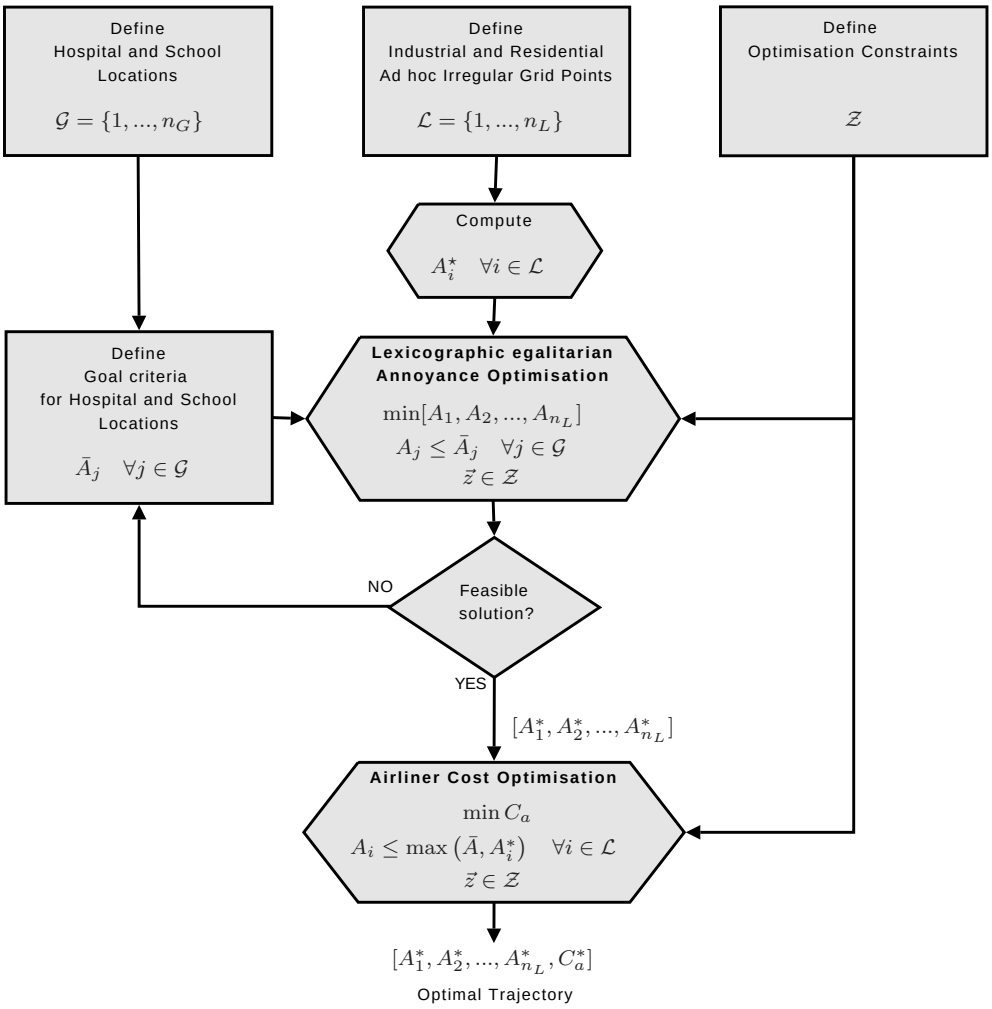

Figure VI-2: *Flow chart of the optimisation strategy for a given hour of the day* $\mathfrak{h}$

After this first optimisation step, the user may encounter that there is no feasible solution satisfying all the constraints. In this case, he/she may consider to relax one or more of the optimisation goals for the hospitals or schools and the optimisation can be performed again. This process can go iteratively until a feasible solution is found and the user is satisfied with the aspiration levels established at the special locations and with the optimal noise annoyance results in residential and industrial areas.

Finally, the last optimisation takes place where the airliner cost is minimised while taking into account the optimal noise annoyance values of the previous step. As commented on previously, some tolerance is given at the noise sensitive locations, where the noise annoyance can be increased up to a maximum threshold level ($\bar{A}$) in order to allow more flexibility in this last optimisation. At this stage, the user may perform, eventually, some iterations with different values of $\bar{A}$ until an acceptable trade-off trajectory is found, according to his/her purposes and experience.

VI.2.2 Lexicographic egalitarian optimisation

In section IV.2.5 the egalitarian (or min-max) optimisation was introduced. This approach is useful if we want to guarantee some *fairness* among the optimisation criteria. In our application, this technique will be used for the minimisation of the noise annoyance deviation at the worst-off noise-sensitive location (at a given hour of the day). Therefore, the multi-objective optimisation problem stated in equation (VI.3) is transformed into the following egalitarian optimisation prob-

lem:

$$\min_{\vec{z}\in\mathcal{Z}} \{\Delta_1, \Delta_2, \cdots, \Delta_{n_L}\} = \min_{\vec{z}\in\mathcal{Z}} \left[\max_{i\in\mathcal{L}} \Delta_i\right] \tag{VI.5}$$

where $\mathcal{L} = \{1, ..., n_L\}$ is the set of the noise sensitive locations being considered in the irregular measurement grid.

The main problem of this formulation is the non-smoothness of function $\max(\cdot)$. Yet, an equivalent formulation into a differentiable form, if the objective and constraint functions are differentiable, is still possible (Miettinen, 1999). Instead of the previous Tchebycheff formulation, a new variable ζ is introduced and the problem to solve is rewritten as:

$$\begin{aligned} &\min\ \zeta \\ &\text{Subject to:}\quad \zeta \geq \Delta_i \quad \forall i \in \mathcal{L} \\ &\qquad\qquad\ \ \vec{z} \in \mathcal{Z} \end{aligned} \tag{VI.6}$$

As examined in section IV.2.5, the solution of this problem guarantees fairness, according to the Rawls' egalitarian principle, but the obtained solution is weakly Pareto optimal. However, the lexicographic extension of this Rawlsian criterion is indeed Pareto optimal (Chen, 2000; Miettinen, 1999). This extension has already been applied in engineering problems like, for example, in (Salles & Barria, 2008) where the problem of bandwidth allocation is assessed.

This lexicographic egalitarian (or lexicographic max-min) approach is adapted in this work as a multi-criteria optimisation strategy for the noise annoyance deviation objectives. Hence, an egalitarian problem, as described in equation (VI.5), is solved at each stage of the optimisation without wasting the solution of the previous stage, until a Pareto solution is found. In this way, the solution of this multi-criteria optimisation technique enjoys both fairness and efficiency properties.

Let $\daleth_1$ be the optimal noise annoyance deviation value obtained from the equation (VI.5), or its equivalent form as shown in equation (VI.6):

$$\daleth_1 = \min_{\vec{z}\in\mathcal{Z}} \left[\max_{i\in\mathcal{L}} \Delta_i\right] \tag{VI.7}$$

If after this optimisation there is no feasible way to decrease the noise annoyance in any location without increasing the $\daleth_1$ optimal value, the lexicographic egalitarian solution is already found and $\daleth_1$ is the Pareto optimal value of problem (VI.5).

On the other hand, in the case that an improvement can still be made in one or more noise sensitive locations, without increasing the value of $\daleth_1$ at some binding locations of the solution of equation (VI.7), the problem must continue. Therefore, the next step is to check which noise sensitive locations can be improved allowing noise annoyance deviations below $\daleth_1$. Mathematically, location $i \in \mathcal{L}$ is *blocked* iff:

$$\min_{\vec{z}\in\mathcal{Z}} \left[\Delta_i \mid \Delta_j \leq \daleth_1\,, \quad \forall j \in \mathcal{L}\backslash\{i\}\right] = \daleth_1 \tag{VI.8}$$

Let $\mathcal{B}_1 \subseteq \mathcal{L}$ represent the set of blocked noise sensitive locations that satisfy equation (VI.8) and $\mathcal{F}_1 = \mathcal{L}\backslash\mathcal{B}_1$ be the set of the remaining non-blocked, or *free* locations. As stated above, if $\mathcal{B}_1 = \mathcal{L}$ the algorithm is stopped due to the fact that all locations are already blocked. Otherwise, the new problem to be solved, as a second stage without wasting the previous solution, is:

Algorithm VI.1: *Lexicographic egalitarian optimisation of* $\min_{\vec{z}\in\mathcal{Z}} [\Delta_1, \Delta_2, \cdots, \Delta_{n_L}]$

1: Initialisation:
$k \leftarrow 0\,; \quad \mathcal{F}_0 \leftarrow \mathcal{L}\,; \quad \mathcal{B}_0 \leftarrow \emptyset$
2: **repeat**
3: Perform a constrained egalitarian optimisation:
$\daleth_{k+1} \leftarrow \min_{\vec{z}\in\mathcal{Z}} \left[\max_{i\in\mathcal{F}_k} \Delta_i \,|\, \Delta_{j_1} \leq \daleth_1, ..., \Delta_{j_k} \leq \daleth_k\,, \quad \forall j_1 \in \mathcal{B}_1, ..., \forall j_k \in \mathcal{B}_k\right]$
4: Determine the set of locations with an optimal value of $\daleth_{k+1}$:
$\mathcal{D} \leftarrow \{i \,|\, \Delta_i^* = \daleth_{k+1}\,, \quad \forall i \in \mathcal{F}_k\}$
5: Determine the new set of blocked locations $\mathcal{B}_{k+1}$:
$\mathcal{B}_{k+1} \leftarrow \{i \,|\, \daleth_{k+1} = \min_{\vec{z}\in\mathcal{Z},\, i\in\mathcal{D}} [\Delta_i \,|\, \Delta_j \leq \daleth_{k+1}\,, \quad \forall j \in \mathcal{F}_k \backslash \{i\}]\}$
6: Update the new set of non-blocked locations:
$\mathcal{F}_{k+1} = \mathcal{L} \backslash \{\bigcup_{m=1}^{m=k+1} \mathcal{B}_m\}$
7: Update step:
$k \leftarrow k+1$
8: **until** $(\mathcal{B}_k = \mathcal{L})$ **or** $(A_i \leq \bar{A}\,, \quad \forall i \in \mathcal{F}_k)$
9: **return** Egalitarian solution as : $[A_1^*, A_2^*, \cdots, A_{n_L}^*]$

$$\daleth_2 = \min_{\vec{z}\in\mathcal{Z}} \left[\max_{i\in\mathcal{F}_1} \Delta_i \,|\, \Delta_{j_1} \leq \daleth_1\,, \quad \forall j_1 \in \mathcal{B}_1\right] \tag{VI.9}$$

This procedure is repeated until all noise sensitive locations become blocked. Then generally, at step $k+1$ of this process we have:

$$\daleth_{k+1} = \min_{\vec{z}\in\mathcal{Z}} \left[\max_{i\in\mathcal{F}_k} \Delta_i \,|\, \Delta_{j_1} \leq \daleth_1, ..., \Delta_{j_k} \leq \daleth_k\,, \quad \forall j_1 \in \mathcal{B}_1, ..., \forall j_k \in \mathcal{B}_k\right] \tag{VI.10}$$

where $\mathcal{F}_k = \mathcal{L}\backslash\mathcal{B}_k$ and $\mathcal{B}_k = \bigcup_{m=1}^{m=k} \mathcal{B}_m$.

This iterative process is summarised in Algorithm VI.1 where a slight modification has been introduced in the loop stop condition. As explained before, the iterative process may end up when all optimisation criteria become blocked to their best egalitarian value. Furthermore, this iterative process may end up as well if the noise annoyance of the free remaining locations at stage k is below the minimum threshold value of $\bar{A}$. This means that there is no worth in further noise annoyance reduction below this threshold and some freedom is left for the minimisation of the airliner cost. Finally, values $[A_1^*, A_2^*, \cdots, A_{n_L}^*]$ correspond to the noise annoyances produced by the optimal trajectory obtained in the last step k:

$$A_i^* = A(L_i(\vec{z}^*(t))) \quad \forall i \in \mathcal{L} \tag{VI.11}$$

with $\vec{z}^*(t) = \arg(\daleth_k)$.

On the other hand, Figure VI-3 shows graphically the feasible objective region $\mathcal{O} \subseteq \mathbb{R}^2$ of a hypothetical two criteria minimisation problem with objectives A_1 and A_2. The egalitarian optimisation leads to a set of weakly Pareto solutions (blue thick line B) with an optimal value of $\daleth_1$. However, only objective A_1 becomes blocked according to equation (VI.8). This means that A_2 can still be improved in a second optimisation. This new step leads to an optimal value of $\daleth_2$ for location #2 and the final optimal solution turns to be point C.

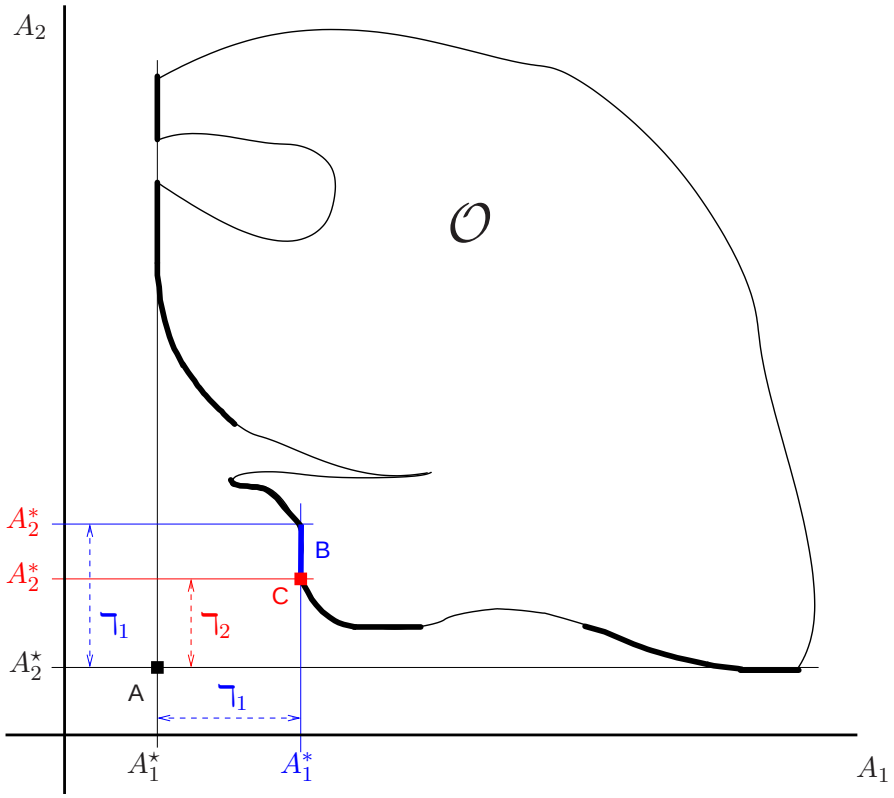

Figure VI-3: *Example of the lexicographic egalitarian optimisation strategy for a two criteria multi-objective minimisation problem*

VI.3 Application Example

This section presents some numerical examples based on a departure performed by two different aircraft: an Airbus A340-600 and an Airbus A321-200. Table VI-1 summarises, for each aircraft, the relevant data considered for this example.

Table VI-1: *Aircraft data for the application example*

	Airbus A340-600	**Airbus A321-200**
Take-off mass	368 000 kg	77 000 kg
Power-plant	Rolls-Royce Trent 556	IAE V2533-A5
Flaps/slats configuration	CONF 3	CONF 1+F
V_2 speed	183 kt	152 kt
Take-off Distance (TOD)†	2 440 m	1 200 m

† At International Standard Atmosphere (ISA) conditions

As it was explained in Chapter V, the initial take-off phase going from the brake release to the point where the aircraft reaches a height of 122 m (400 ft) is not considered in the optimisation process. In this initial phase the aircraft follows a straight trajectory, along the departing runway heading at a constant speed, which is set to the the operational V_2 speed.

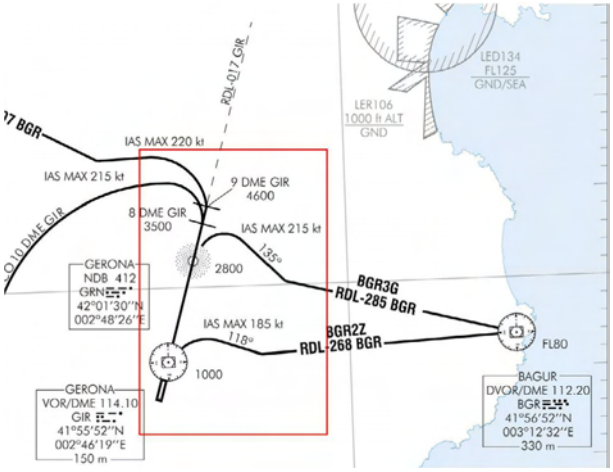

(a) Current SIDs towards the East.
Source: (AENA, 2009a)

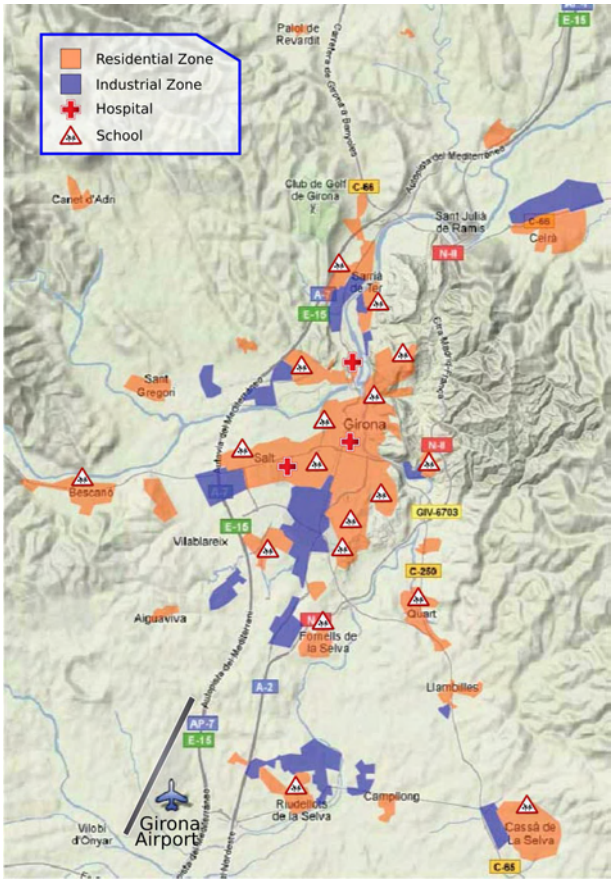

(b) Distribution of hospitals, schools, residential and industrial zones in the considered scenario.
Powered by Google Maps (©2009 Google. Map Data ©2009 Tele Atlas).

Figure VI-4: *Scenario for RWY 02 East departures at Girona airport*

VI.3.1 Considered scenario

For this example, we consider the East departures from runway 02 of Girona airport, in Catalonia (Spain). As it is shown in Figure VI-4(a), two different Standard Instrumental Departures (SID) ending up at Begur VOR/DME (BGR) are currently published: BGR3G and BGR2Z. Both departures consist of an initial straight segment followed by a right turn that ends with the interception of a VOR radial towards the facility. For the BGR2Z departure, this turn is performed when the aircraft reaches an altitude of 1 000 ft with a speed restriction during the turn of 185 kt of Indicated Airspeed. Whereas an aircraft flying the BGR3G departure follows a longer initial straight segment until Girona NDB (GRN) is over-flown (see Appendix A for some background in radionavigation systems). Then, the right turn is performed and the maximum speed restriction in this case is 215 kt. In general, a mid-range passenger jet aircraft, such as a Boeing B737 or an Airbus A320, will be able to execute the BGR1Z departure. On the other hand, heavier aircraft not able to meet this turning speed restriction will execute the BGR3G departure.

The origin of coordinates for this problem is placed at the threshold of runway 02. Table VI-2 contains the relevant information of this runway while Table VI-3 shows some additional data considered for this scenario. Moreover, Figure VI-4(b) shows a picture of the area North-East of the airport. The runway is depicted with a grey strip and is located at the lower left part of the Figure. In addition, all the residential zones are highlighted in orange, while industrial zones are in blue. The area covered by this Figure corresponds approximately to the red rectangle shown in Figure VI-4(a). This area will be considered for the study of the aircraft operations regarding the

Table VI-2: *Relevant data of the take-off runway for the application example. Source: (AENA, 2009a)*

Girona (LEGE) – Runway Threshold 02		
Threshold coordinates (WGS84)	$41^o\,53'\,41.7''$ N	$2^o\,45'\,29.7''$ E
Runway orientation	Geographic: 15.78^o	Magnetic†: 17^o
Available distances	TORA‡: 2 400 m	TODA♣: 2 460 m
Threshold elevation (Mean Sea Level)	122.86 m	

† At May 2009 ‡ Take-off Run Available ♣ Take-off Distance Available

population exposure to noise. Populated areas outside of this zone are sparse and also, out of this area the altitude of the aircraft will be high enough that the noise annoyance will be negligible. The exact locations of the measurement grid points chosen for this example are given in Appendix E. A total number of 140 residential points are placed irregularly as explained in section VI.1. Among them, 87 points are in residential areas while 32 are in industrial areas. Finally, 3 hospitals and 18 school locations have also been considered as special locations as shown in Figure VI-4(b).

Table VI-3: *Additional data defining the scenario*

$\chi_{RWY} = 15.78^{o\dagger}$	$s = 5.5\%^{\dagger}$	$V_{\max} = 128.6\,\mathrm{ms}^{-1}$ $(250\,\mathrm{kt})^{\ddagger}$
$CI = 70$	$HI = 0$	$\bar{A} = 0.25$ (*Small* Annoyance)
$W_n = 0\,\mathrm{km}^{-1}$	$W_e = 0\,\mathrm{km}^{-1}$	$W_h = 0\,\mathrm{km}^{-1}$

† Source: (AENA, 2009a)

‡ As in previous Chapter, the actual operational speed limitation is given in IAS. However, for this example and as a first approximation a TAS value is taken

VI.3.2 Baseline trajectories

Before showing the results obtained with the optimisation algorithm, a baseline case is presented where the current published trajectories are analysed (see Figure VI-4(a)). Figure VI-5 shows the noise annoyance maps for these baseline trajectories if they were flown at 04h. The Airbus A340-600 is executing the BGR3G departure while the Airbus A321-200 is considered able to depart via the BGR1Z departure. In the same way, Figures VI-6 and VI-7 show the noise annoyance maps for these trajectories if flown at 10h and 17h respectively.

Once a trajectory $\vec{z}(t)$ is known, the computation of these maps is not a problem from a computational point of view. Therefore, a regular (equally-spaced, rectangular) and more accurate grid has been used with a mesh of $100 \times 100\,\mathrm{m}$ of cell dimension. Let us define $\mathcal{M} = \{1, ..., n_M\}$ as the set of points that form this fine mesh. In addition, when drawing these maps the size of the pixels has been chosen in order to correctly tessellate the different areas.

As expected, the annoyance produced by the Airbus A340 when flying the BGR3G departure is quite significant. This is due to the fact that the trajectory is directly over-flying some residential zones at a relatively low altitude and with high thrust settings. During the night period (trajectory at 04h) several locations are exposed to the maximum value of noise annoyance, $\max_{i\in\mathcal{M}} A_i = 1.00$, while the maximum noise annoyance deviation in all the mesh area is $\max_{i\in\mathcal{M}} \Delta_i = 0.90$. Being residential and industrial zones less sensitive to noise during the morning periods, the corresponding results are obviously better from an annoyance point of view. The maximum value, at this time

period is 0.72, while the maximum noise annoyance deviation has been reduced to 0.64. For the afternoon period, the Normalised Annoyance Index rises again and the maximum annoyance in-

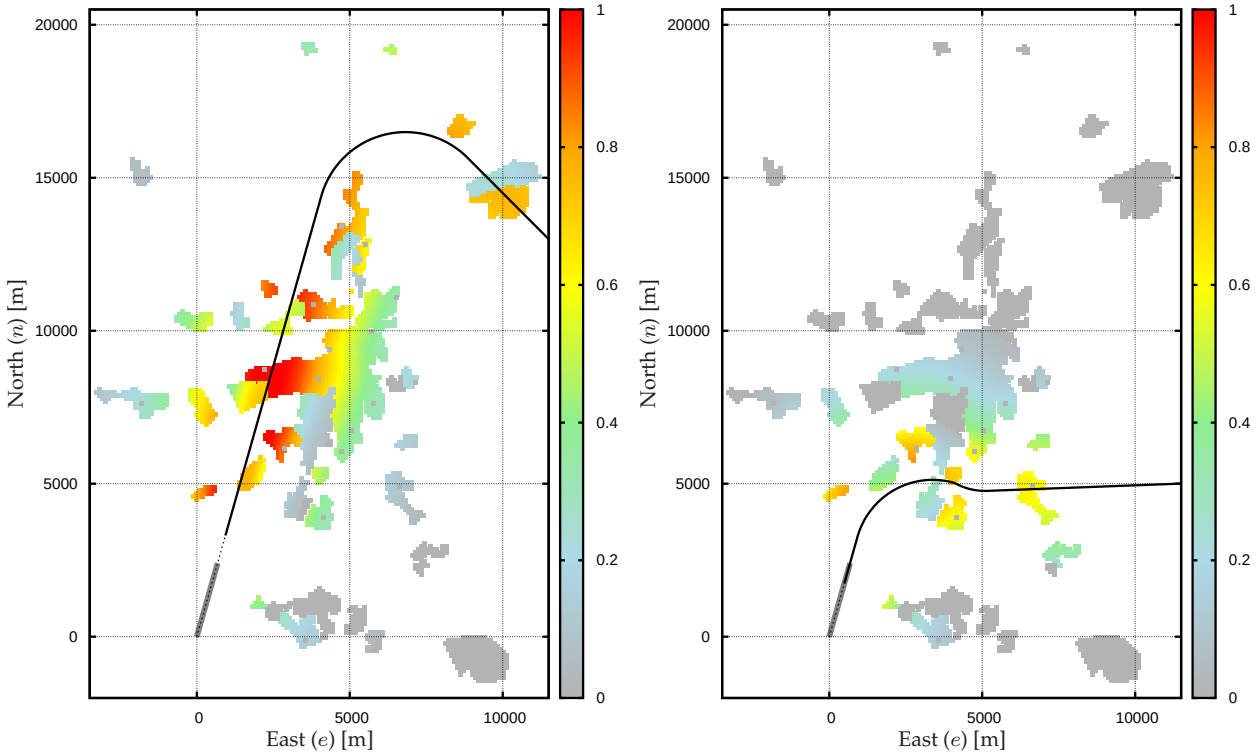

(a) Airbus A340 (via BGR3G) (b) Airbus A321 (via BGR1Z)

Figure VI-5: *Noise annoyance maps for the baseline trajectories at 04h*

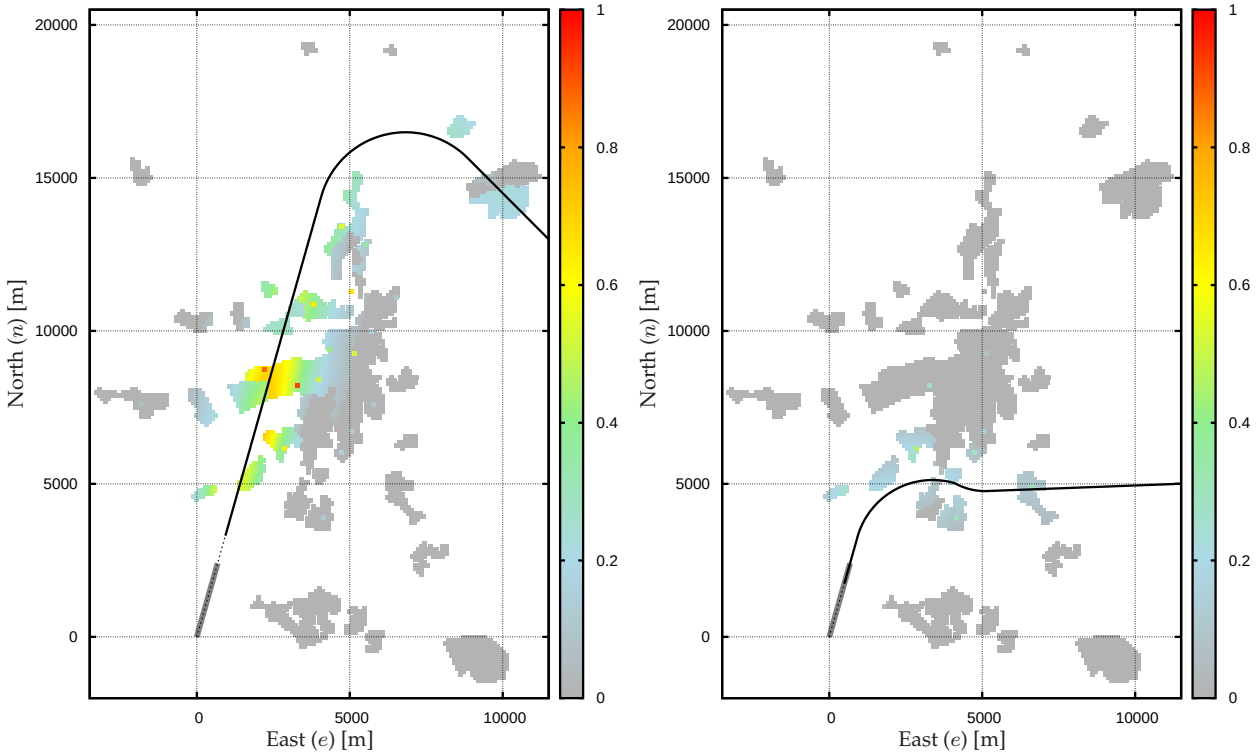

(a) Airbus A340 (via BGR3G) (b) Airbus A321 (via BGR1Z)

Figure VI-6: *Noise annoyance maps for the baseline trajectories at 10h*

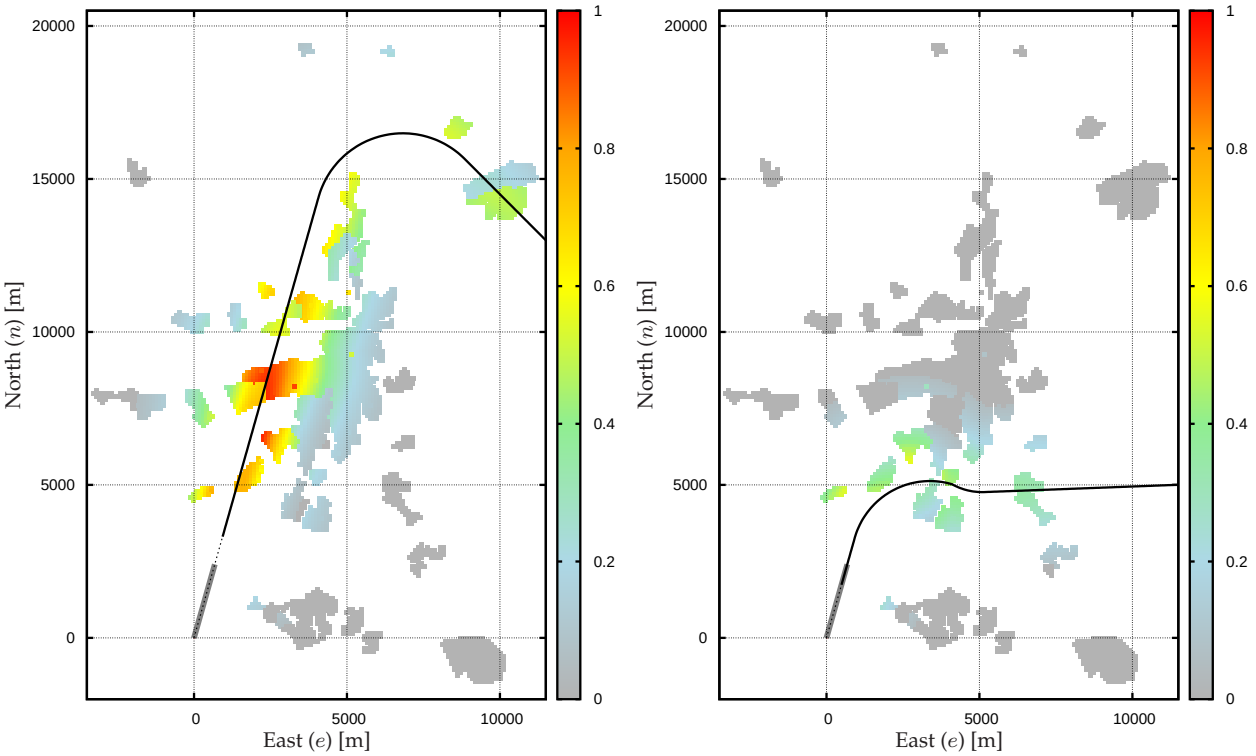

(a) Airbus A340 (via BGR3G) (b) Airbus A321 (via BGR1Z)

Figure VI-7: *Noise annoyance maps for the baseline trajectories at 17h*

Table VI-4: *Absolute Normalised Annoyance Index and annoyance deviation values, at residential and industrial areas, corresponding to the baseline trajectories*

	Airbus A340		**Airbus A321**	
	$\max_{i\in\mathcal{M}} A_i$	$\max_{i\in\mathcal{M}} \Delta_i$	$\max_{i\in\mathcal{M}} A_i$	$\max_{i\in\mathcal{M}} \Delta_i$
04h	1.00	0.90	0.82	0.70
10h	0.72	0.64	0.29	0.20
17h	0.96	0.88	0.55	0.43

dex is 0.97, while the maximum annoyance deviation is 0.88. On the contrary, the trajectory flown by the A321 via the BGR1Z departure produces much less noise annoyance, as seen in Table VI-4 where are summarised the absolute noise annoyance and the deviation noise annoyance values for both aircraft and at each day period. Finally, Table VI-5 shows the special locations (Hospitals or Schools) where the annoyance value exceeds the aspiration level of $\bar{A} = 0.25$ giving, as well, the perceived annoyance value. These locations are also observed in Figures VI-5, VI-6 and VI-7 and their exact location and identification number are given in Appendix E.

VI.3.3 Optimised trajectories

As shown in Figure VI-4, the final departure point (BGR VOR/DME) falls well outside of the noise sensitive area considered for this study. Therefore, aiming at reducing the computational load of the problem, only the trajectory inside this area will be considered. It is assumed that the remaining segment is flown directly to the VOR/DME facility and, instead of fixing a final point in the trajectory to be optimised, a more general restriction is imposed:

Table VI-5: *Hospital or School locations where the aspiration level ($\bar{A} = 0.25$) has been infringed for the baseline trajectories*

	Airbus A340		Airbus A321	
	Location Id.	Annoyance	Location Id.	Annoyance
Hospitals (at 04h,10h,17h)	#120	$A_{120} = 0.66$	#121	$A_{121} = 0.29$
	#121	$A_{121} = 0.92$		
	#122	$A_{122} = 0.52$		
Schools (at 10h,17h)	#128	$A_{128} = 0.64$	#125	$A_{125} = 0.30$
	#133	$A_{133} = 0.42$	#126	$A_{126} = 0.32$
	#134	$A_{134} = 0.51$	#127	$A_{127} = 0.28$
	#135	$A_{135} = 0.88$	#128	$A_{128} = 0.46$
	#137	$A_{137} = 0.65$		
	#138	$A_{138} = 0.36$		
	#139	$A_{139} = 0.55$		

$$e(t_f) \geq 11\,000\,\text{m} \tag{VI.12}$$

leaving free the final condition for the north coordinate, $n(t_f)$. Otherwise, an additional constraint must be added in order to guarantee that the aircraft flies directly from the final point of the optimisation to the actual final point of the departure:

$$\chi(t_f) = \begin{cases} \pi - \arctan\left(\frac{e_{VOR} - e(t_f)}{n(t_f) - n_{VOR}}\right) & \text{if} \quad n(t_f) > n_{VOR} \\ \arctan\left(\frac{e_{VOR} - e(t_f)}{n_{VOR} - n(t_f)}\right) & \text{if} \quad n(t_f) < n_{VOR} \\ \frac{\pi}{2} & \text{if} \quad n(t_f) = n_{VOR} \end{cases} \tag{VI.13}$$

where e_{VOR} and n_{VOR} are, respectively, the East and North coordinates of the BGR VOR/DME.

On the other hand, the complexity of this scenario requires to try more than one guess (or initial) trajectory in order to minimise the probability to end up into a locally optimal solution. Figure VI-8 shows some examples of guess trajectories that have been used for the optimisation of the A340 procedures. The solution, or solutions, giving the lowest objective value ($\urcorner_1$) are kept. Then, the successive steps in the lexicographic egalitarian optimisation start from the optimal trajectory obtained in the previous step. As commented in Section V.4, after each step an assessment should be done in order to detect possible local optima. This requires, in some cases, to repeat the optimisation with different guesses. Despite being a tedious task, the step by step nature of this technique allows the user to check regularly for possible local optima and maximise the probability to end up with a globally optimal solution in the last step.

VI.3.3.1 Step by step optimisation

In order to better illustrate how the proposed multi-objective methodology works, the algorithm that derives from equations (VI.5–VI.10) is presented step by step in the following example, where the optimisation of the Airbus A340 departure at 04h is considered. As explained in section VI.2.2, the first step of the optimisation consists of minimising the maximum noise annoyance deviation regarding all locations (see equation (VI.5)). After performing this optimisation, an optimal value of $\urcorner_1 = 0.97$ is obtained and the resulting trajectory is shown in black, in Figure VI-9. As seen,

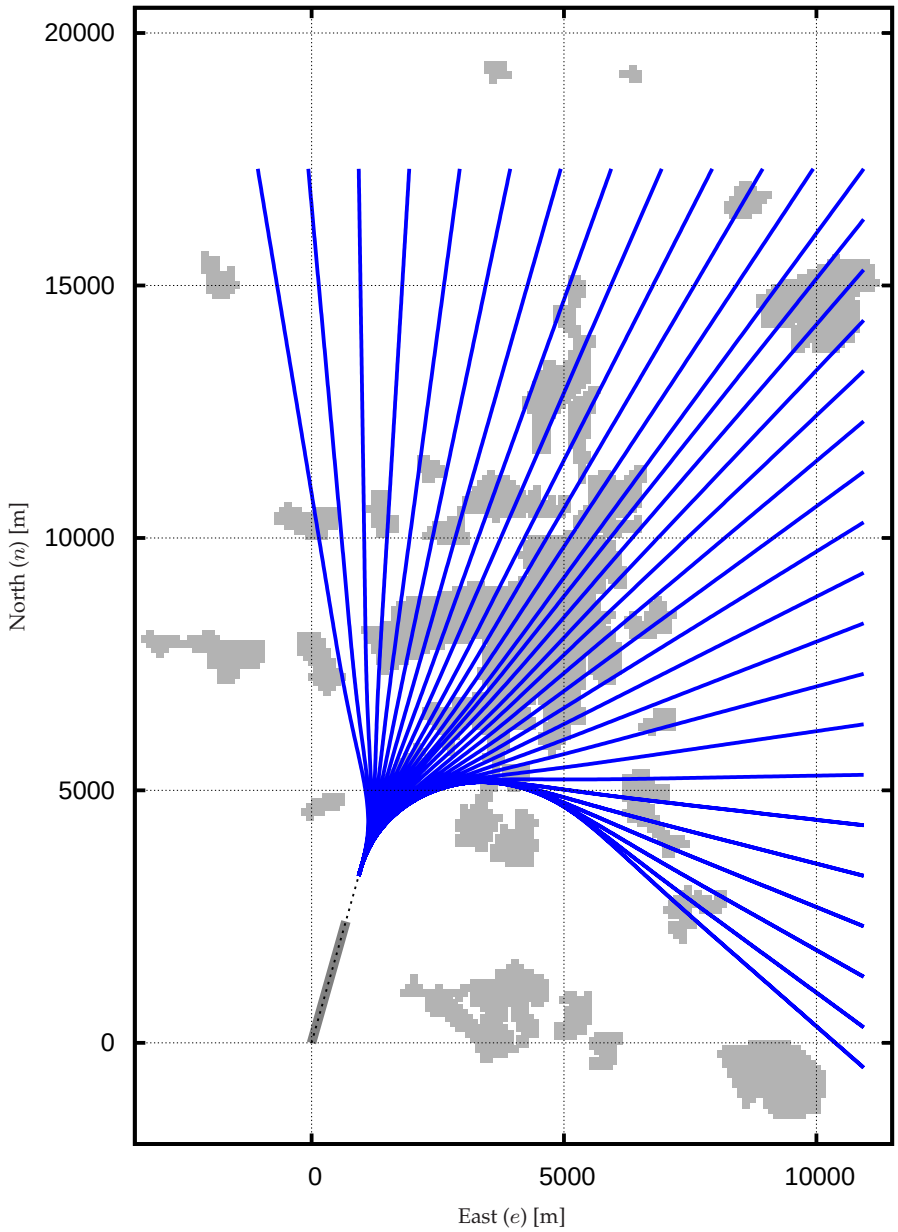

Figure VI-8: *Example of different initial trajectory guesses used in this scenario for the Airbus A340 procedures*

the optimal trajectory flies further West than the baseline published trajectory. In this case, residential zones "A" become the binding locations according to the egalitarian principle explained previously (see equation (VI.8)). Then, after flying in between the two "A" zones, the trajectory turns right and flies almost directly to the final point. The shape of this optimal trajectory, once the "A" areas have been passed, is only affected by the restrictions in noise annoyance imposed at the hospitals. Due to these special locations, the trajectory maintains an *annoyance-constant* distance from them while flying to the East.

More precisely, only a few points located at the outer edges of zones "A" actually bind the restrictions for the next step in the optimisation process. Yet, other measurement points located close to these initial binding locations become blocked immediately during the subsequent steps. Therefore, for these successive steps the obtained trajectory has no appreciable changes if compared with the first step solution and the successive optimal annoyance deviations take almost the same $\urcorner_1$ value. However, when all the measurement locations that are located in residential zones "A" are taken into account as constraints (*i.e.* all of them become blocked) a significant

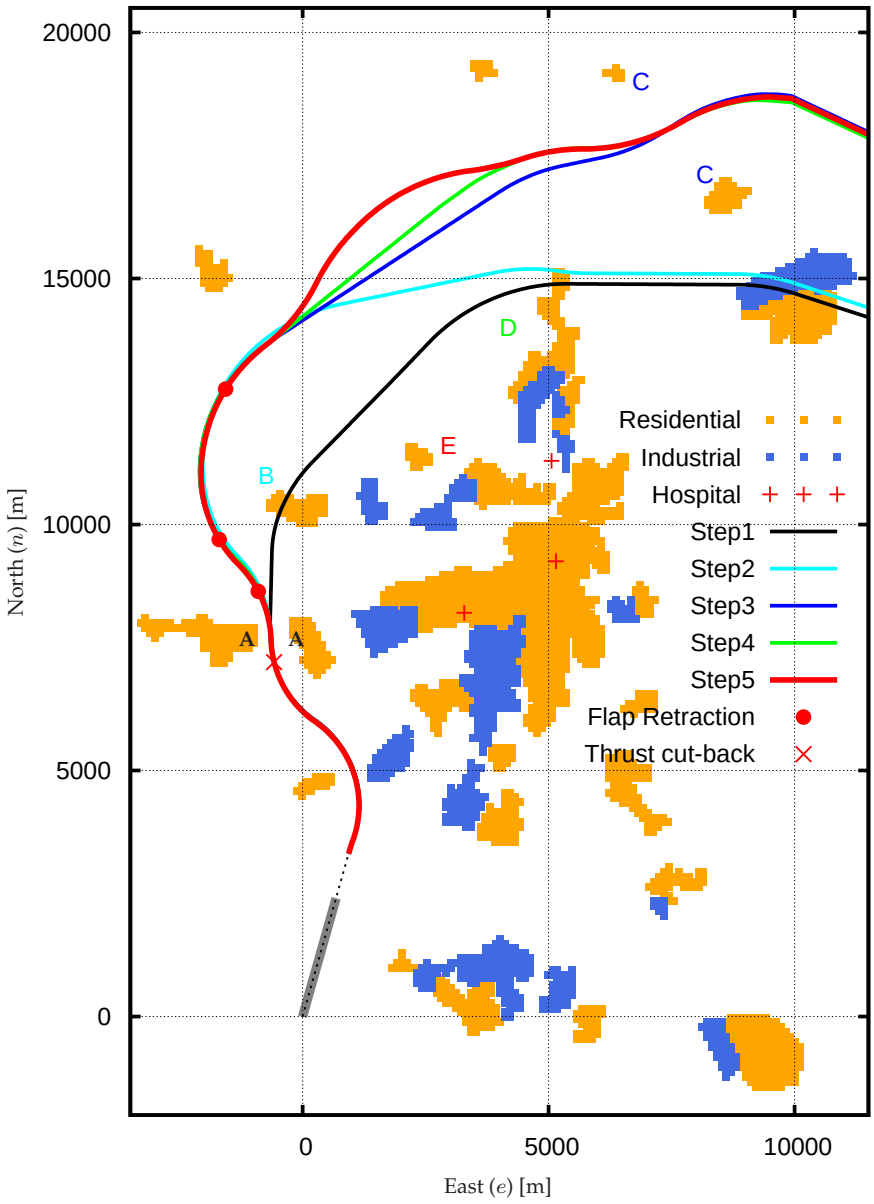

Figure VI-9: *Significant intermediate steps in the optimisation process for the Airbus A340 during night periods (04h)*

change is observed in the following step of the algorithm. The trajectory obtained at this *second significant step* is shown in cyan in Figure VI-9. Evidently, after over-flying locations "A", the trajectory continues Westwards and avoids the residential zone "B". The new optimal noise annoyance deviation becomes $\urcorner_2 = 0.81$.

Then, the third *significant step* produces a trajectory with an optimal annoyance deviation of $\urcorner_3 = 0.62$, corresponding to binding locations at zones "C", as seen in blue in Figure VI-9. The next *significant step* binds locations "D" with $\urcorner_4 = 0.34$ (green trajectory) and finally the last *significant step* achieves a $\urcorner_5 = 0.30$ binding locations "E" (red trajectory). At this stage, all the noise sensitive locations become blocked and therefore, the obtained solution is Pareto efficient.

As commented in section VI.2.1, once the egalitarian optimisation is over a final minimisation of the airliner cost is done. In this particular case, the optimisation is so constrained by the annoyance at all the locations that almost no freedom is left for the airliner cost minimisation. In fact, the fuel consumption is reduced only by a 1.3% after this last minimisation, which is almost a negligible improvement. In this final trajectory, the horizontal track is not changed, if compared

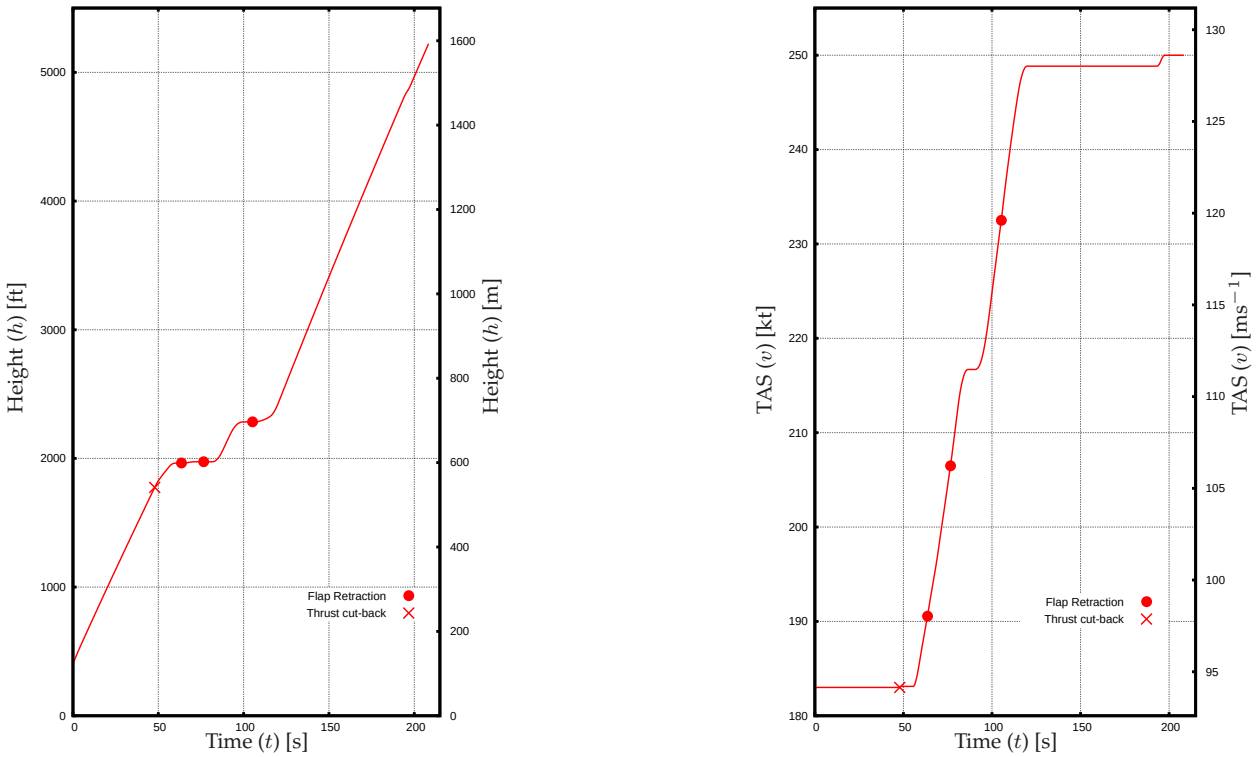

(a) Vertical profile

(b) Speed profile

Figure VI-10: *Vertical and speed profiles for the optimal trajectory computed at 04h for the Airbus A340*

with the egalitarian trajectory, and only slight variations in the speed and altitude profiles are observed. Figure VI-10 shows these final vertical and speed optimal profiles.

As seen in both Figures, an initial climb is performed at the initial V_2 speed. Then, the thrust cut-back is performed passing from *Take-off–Go Around* configuration to *Climb* configuration. This thrust reduction is performed just before over-flying in between locations "A", as seen in Figure VI-9. In this initial phase, the high thrust setting, in combination with the low speed of the aircraft allows the best climb performance. In this way, the altitude is maximised when approaching locations "A" and, in turn, the annoyance is reduced. Besides the altitude, the reduction in thrust just before over-flying the inhabited areas decreases the perceived noise at these locations as well.

A few seconds after the thrust cut-back, the aircraft is levelled off at almost 2 000 ft. This flat segment is used to accelerate the aircraft and to transition successively from CONF3 to CONF1+F flaps/slats configuration. Another short climb follows, improving the annoyance at locations "B". When these locations are far enough, a second flat segment at about 2 300 ft is used again to accelerate to the final climbing speed and adopt the CONF1 flaps/slats configuration.

VI.3.3.2 Final optimal trajectories

The same kind of optimisation explained before has been performed at different day periods and for both considered aircraft. Figure VI-11(a) shows the annoyance map corresponding to the previous optimal trajectory for the Airbus A340 at 04h.

When the departure for the same aircraft at 10h is considered, the egalitarian optimisation returns no feasible solution. This means that with this aircraft it is not possible to fulfil all the goal constraints at schools and hospitals. When the night trajectory was considered the annoyance at

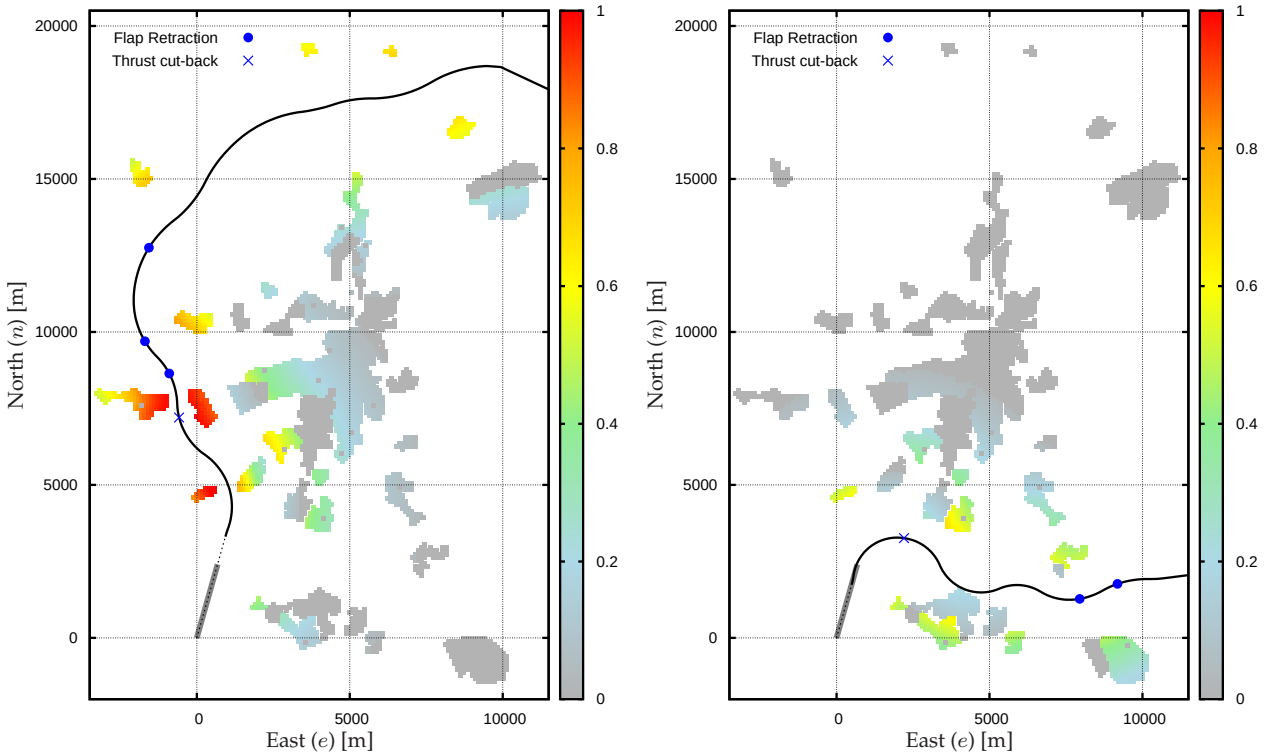

(a) Airbus A340 (b) Airbus A321

Figure VI-11: *Noise annoyance maps for the optimal trajectories at 04h*

all schools was null and a feasible trajectory was found (actually it is possible to see the school locations by the *blank* pixels in Figure VI-11(a)).

However, near locations "A" of Figure VI-9, there exists a school location that forces the aircraft to fly much more eastwards if compared with the optimal trajectory at 04h. This school location is depicted by an "1" label in Figure VI-12(a). However, flying eastwards is also restricted by the hospital, labelled as "2", and also by some nearby schools (locations "3" and "4" in the same Figure). Performing an initial tight right turn is neither feasible due to the influence of the mentioned hospital.

In this situation, the decision maker must relax one or several goal constraints in order to obtain a feasible solution. We suppose that the decision of which goal(s) is(are) relaxed is taken by the operator according to his/her priorities and experience. In this example, we have supposed that the maximum annoyance permitted in the hospital and the schools "3" and "4" can rise up to *Moderate* annoyance. Therefore, the aspiration levels for only these three locations are overridden and set to $\bar{A} = 0.50$, leaving all the other hospital and school locations at the original value of $\bar{A} = 0.25$.

Figure VI-12(a) shows the horizontal track (and the associated annoyance map) for the optimal trajectory obtained according to these new constraints. As it can be seen, the optimal trajectory is formed by a sequence of smooth turns that avoid populated areas. Because industrial zones are less sensitive to noise than residential zones, the trajectory remains closer to the industrial ones, maintaining somehow a *constant* level of annoyance. Vertical and speed profiles for this trajectory are shown in Figure VI-14. Instead of using level segments at a certain altitude to accelerate the aircraft, as it was done at 04h, at 10h we observe an *energy sharing* profile where the aircraft both climbs and accelerates. This energy trade-off gives less climbing performance during the initial segment but a higher climb is achieved in the intermediate an final segments of the trajectory. Moreover, the thrust reduction is performed just before over-flying next to the major residential

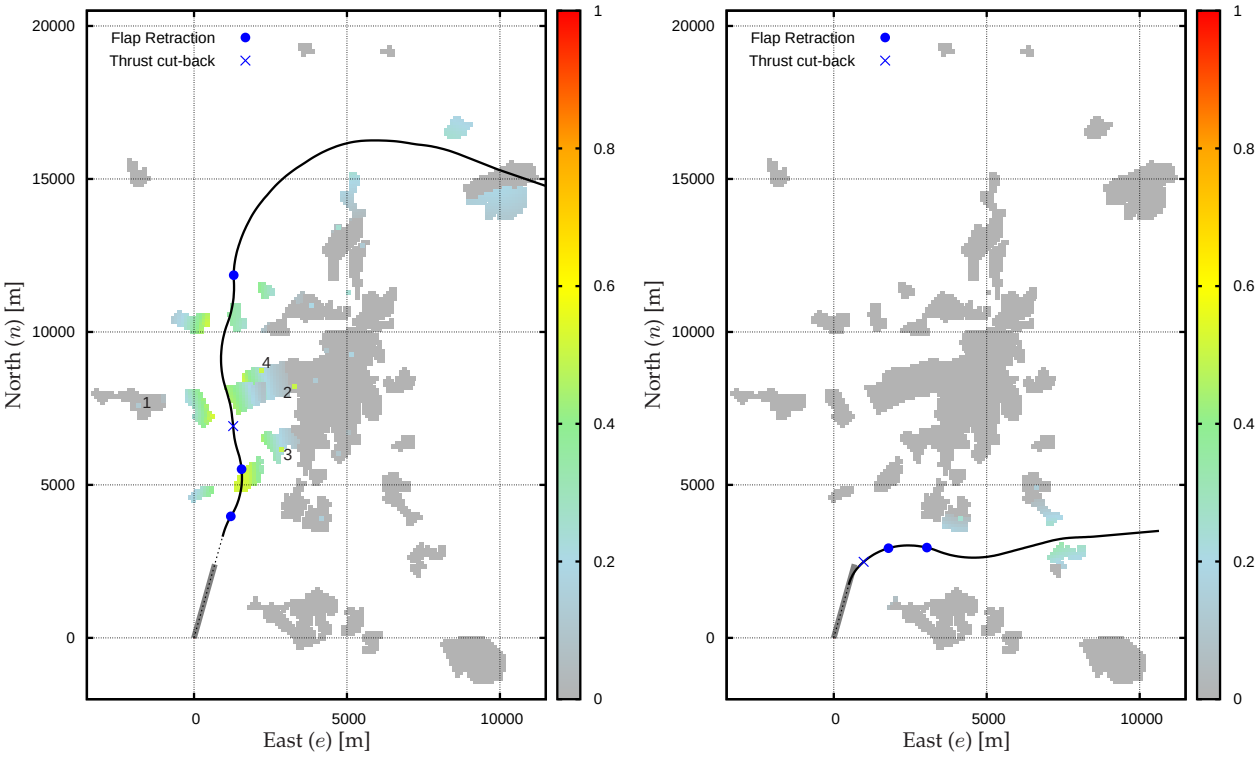

(a) Airbus A340 (b) Airbus A321

Figure VI-12: *Noise annoyance maps for the optimal trajectories at 10h*

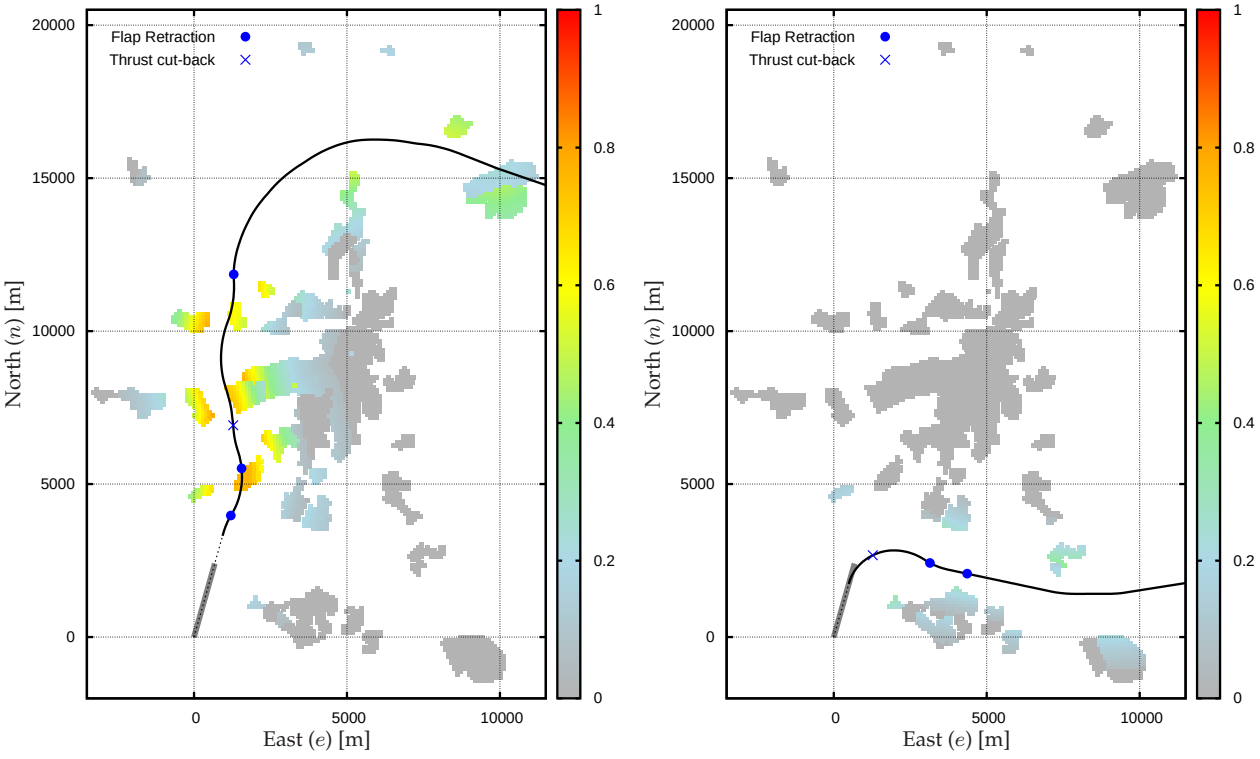

(a) Airbus A340 (b) Airbus A321

Figure VI-13: *Noise annoyance maps for the optimal trajectories at 17h*

areas.

At 17h, the same infeasibilities that were found at 10h appear and the same relaxation policy

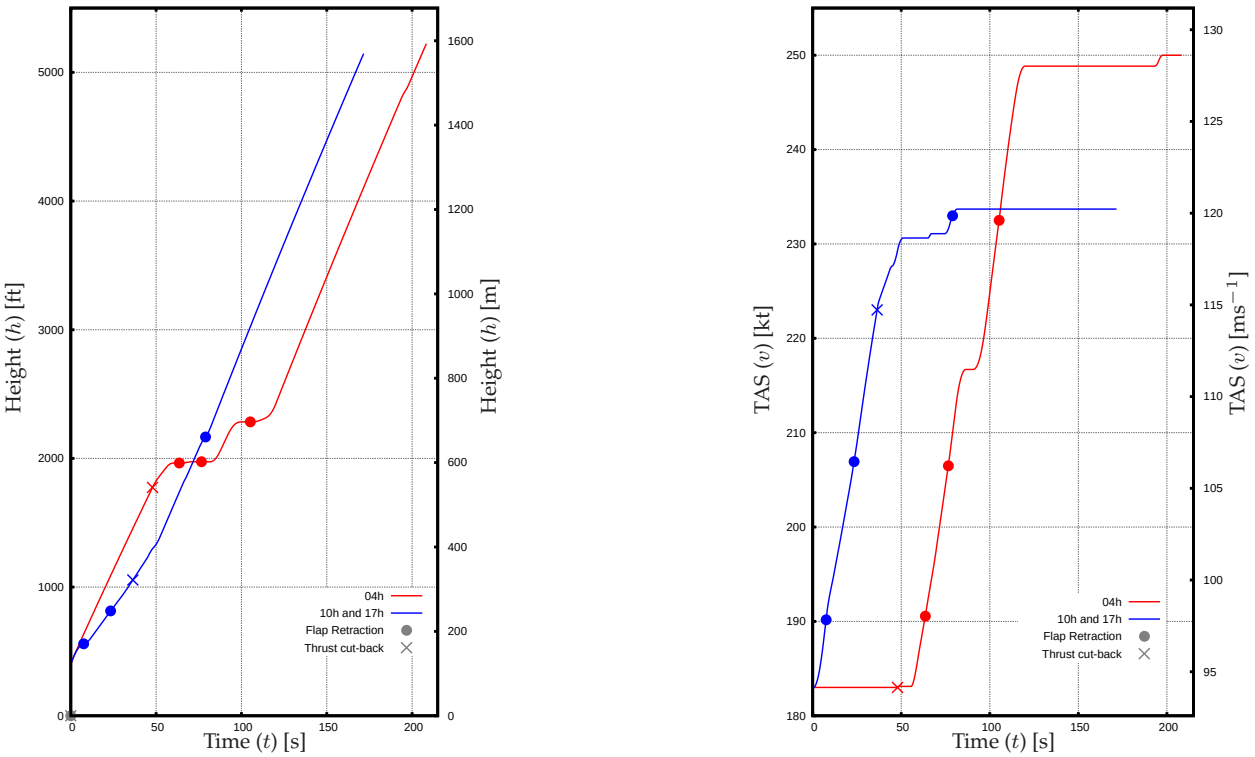

(a) Vertical profile (b) Speed profile

Figure VI-14: *Optimal vertical and speed profiles for the different trajectories flown by the Airbus A340*

has also been applied. Obviously, the optimal trajectory turns to be the same as obtained at 10h. Figure VI-13(a) shows the new annoyance map for this trajectory where, as expected, we observe higher annoyance values if compared to the 10h case.

Finally, Figures VI-11(b), VI-12(b) and VI-13(b) show the horizontal optimal track for the Airbus A321 departures flown at 04h, 10h and 17h respectively. Moreover, Figure VI-15 shows the vertical and speed profiles for these optimal departures. For night trajectories, the aircraft executes several tight turns in order to avoid as much as possible the populated areas. Compared with the A340, the flight performances of the A321 allows an initial sharp turn on the right to be performed and fly south from the major populated areas. Thrust cut-back is performed at 2 150 ft, just before flying next to the closest residential area. Also, the trajectory maximises the initial climb and a relative low airspeed is scheduled. The acceleration segment does not come until all significant populated areas are over-flown. Then, a flat segment is used to accelerate and clean the flaps/slats configuration.

The egalitarian optimisation for 10h departures converges to almost the same trajectory described above (at 04h). However, at 10h all annoyance values are below the chosen threshold of $\bar{A} = 0.25$. Then, the airliner cost minimisation that comes as the last step of the presented strategy (see Figure VI-2) changes significantly the final trajectory. As expected, a much more smooth trajectory is found which flies almost directly to the final departure point. Moreover, the thrust reduction is performed at the lowest possible altitude, minimising the noise impact. The speed and vertical profiles also completely change, if compared with the optimal profiles at 04h. Shortly after the thrust cut-back a short level flight is performed and the aircraft transitions to clean configuration. This improves climb performance but also minimises fuel and time consumption.

For afternoon trajectories (at 17h) a similar behaviour is observed. After the egalitarian optimisation is concluded, and all binding locations have been taken into account as restrictions, the

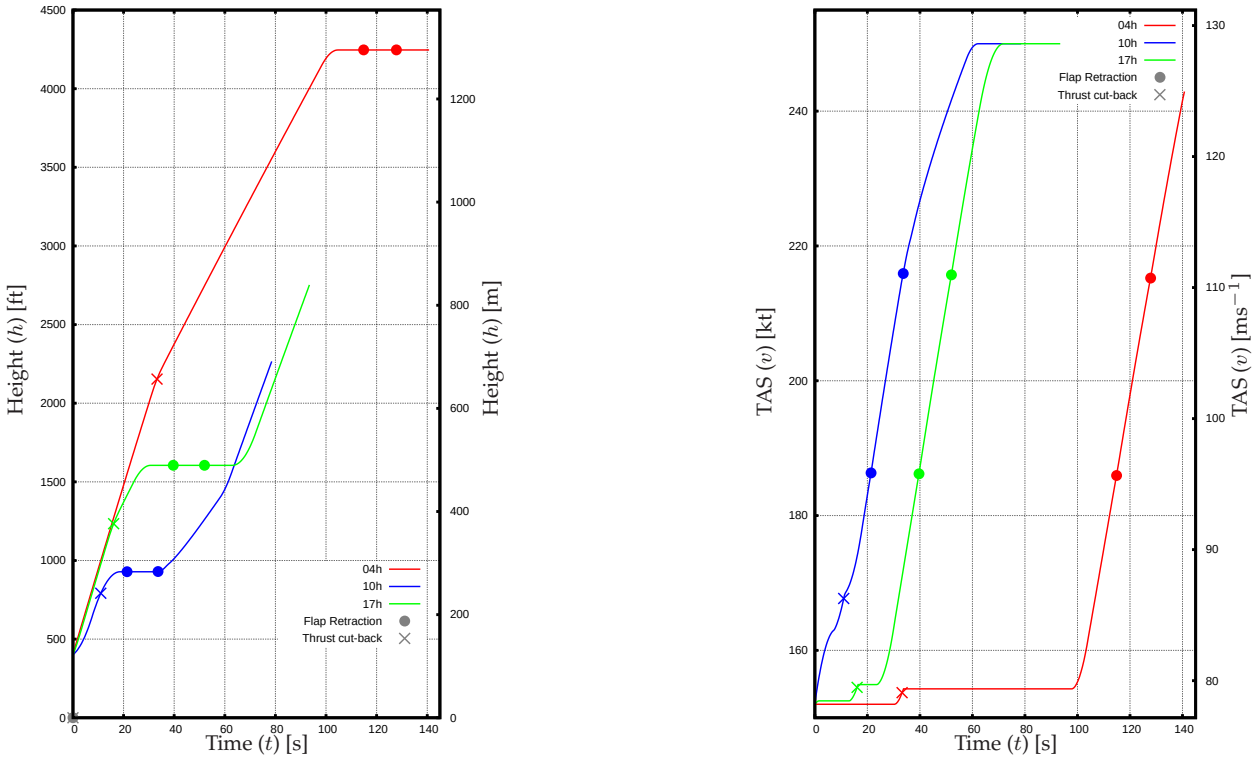

(a) Vertical profile

(b) Speed profile

Figure VI-15: *Optimal vertical and speed profiles for the different trajectories flown by the Airbus A321*

airliner cost minimisation smoothes again the trajectory. Compared with the optimal trajectory at 10h, this trajectory starts with an initial climb at a low speed, followed by a flat segment at about 1 600 ft where the acceleration is carried out. In addition, thrust reduction is performed at a higher altitude and the ground track is slightly different, especially at the final segment of the trajectory.

Table VI-6 wraps up the optimal noise annoyance values obtained for both aircraft and at the three considered hours of the day. The cost for the operator C_a corresponding to the final trajectory is also given in this table. There, we can observe significant differences in fuel (and time) consumption for the three trajectories of the A321 thanks to the airliner cost minimisation that comes after the egalitarian process. Finally, Figure VI-18 (at the end of this Chapter) shows a couple of three dimensional views of the final optimal trajectories for both of the aircraft.

Table VI-6: *Operator's cost, absolute annoyance and annoyance deviation values, at residential and industrial areas, corresponding to the optimal trajectories*

	Airbus A340			**Airbus A321**		
	$\max_{i\in\mathcal{M}} A_i$	$\max_{i\in\mathcal{M}} \Delta_i$	C_a	$\max_{i\in\mathcal{M}} A_i$	$\max_{i\in\mathcal{M}} \Delta_i$	C_a
04h	1.00	0.79	1 716 kg	0.63	0.47	481 kg
10h	0.52	0.41	1 416 kg	0.25	0.25	266 kg
17h	0.78	0.68	1 416 kg	0.30	0.25	318 kg

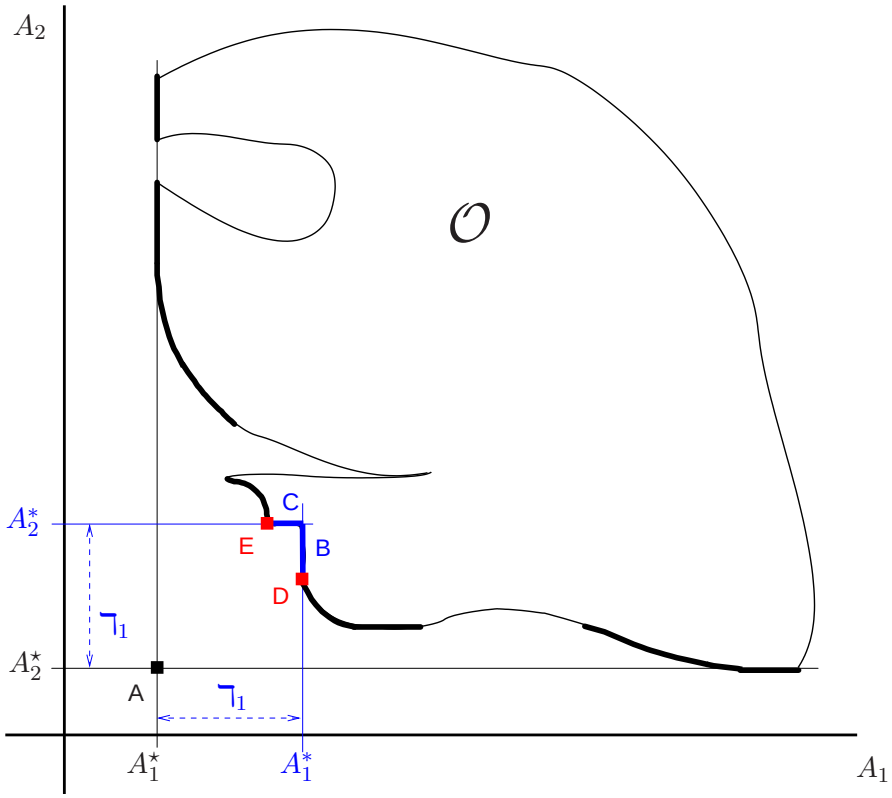

Figure VI-16: *Example of a multiple solution case using the lexicographic egalitarian optimisation strategy for a two criteria multi-objective minimisation problem*

VI.3.3.3 Computational cost

The previous scenario was solved using a common desktop PC, based on an Intel E6600 2.3 GHz processor. According to the output log file of the CONOPT solver, the problem had 179 752 variables and 271 279 constraints. As explained in previous Chapter, the first step in the lexicographic algorithm required more time to converge than the ones following. In this case, the first optimisation steps took an average of 2 hours of CPU to converge. Further egalitarian steps required from few seconds to 30 minutes, depending on the flexibility left in the optimisation. Finally, the airliner cost optimisation took an average of 1 hour of CPU.

VI.3.4 Discussion of the results

In the previous example, we have shown how the proposed optimisation methodology permits us to obtain a *fair* and also Pareto efficient solution for a complex scenario. *Fairness* is a concept that is not straightforward to define. So far, the definition of fairness we have adopted is that the maximum annoyance deviation at any location should be minimised up to a certain threshold level. Next, we discuss two issues that could arise when using this kind of strategy, but that will not be deeply studied in this dissertation and are left for a future research on this domain.

VI.3.4.1 Lack of blocking locations

It is possible that after a given optimisation step in the lexicographic egalitarian process (see algorithm VI.1), the new set of blocked locations would not change. This would mean that the optimisation step has not blocked any location, according to equation (VI.8). In this case the presented algorithm can not continue unless an external decision is made by blocking artificially at least one location. Using again a simple graphical example, Figure VI-16 shows this situation for

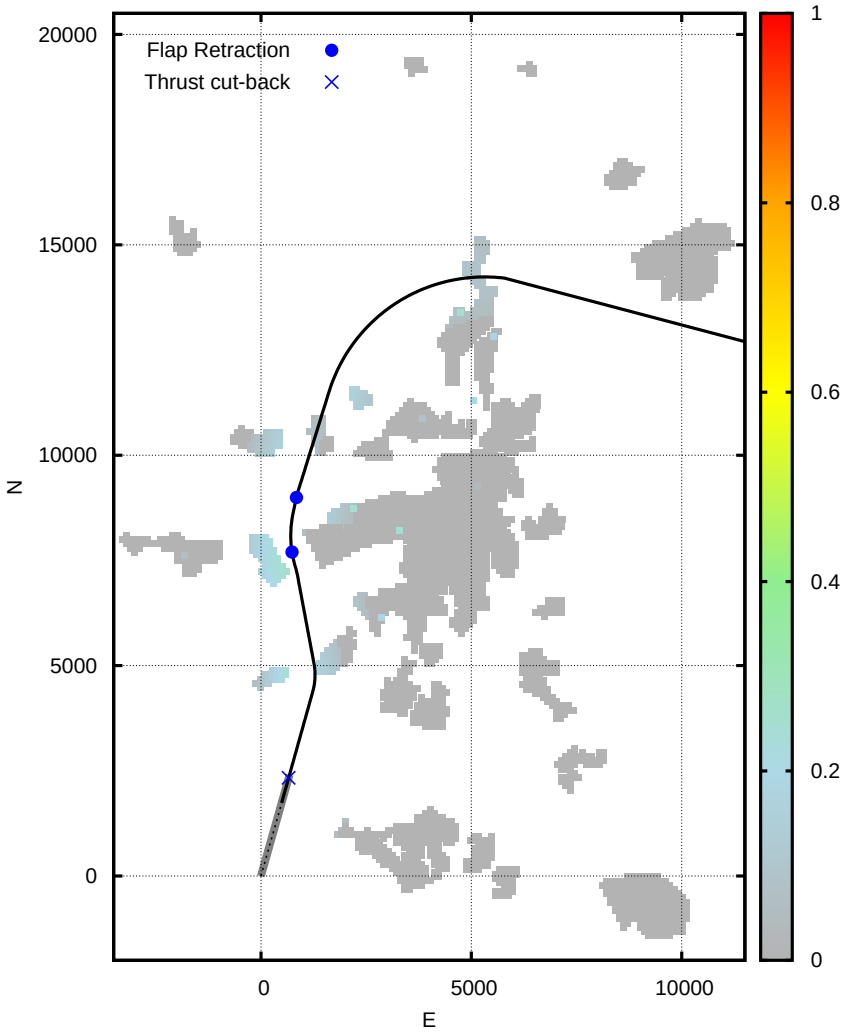

Figure VI-17: *Example of a sub-optimal trajectory for the Airbus A321 producing the same annoyance impact than the optimal one flown at 10h*

an hypothetical optimisation problem with only 2 objectives. As seen in the Figure, the egalitarian optimisation leads to a set of weakly Pareto solutions formed by the blue thick lines B and C with an optimal value of $\urcorner_1$. In this case, neither of the two objectives become blocked meaning that the optimisation could follow by minimising either objective A_1 or objective A_2. Thus, the decision maker should manually intervene and chose between solutions D or E.

Even although this issue is rarely to be observed, it is worth mentioning that it can potentially appear at any stage of the optimisation algorithm. This means that once a decision is made, the following steps can lead to a quite different solution when compared with that solution that would result from another decision. Therefore, the decision maker should be aware of this behaviour and perhaps perform different trials or even use additional metrics in order to compare two *equally fair* solutions.

VI.3.4.2 Potential use of sub-optimal trajectories

Recalling the optimisation strategy shown in Figure VI-2, the egalitarian optimisation proposed in this work is considered up to a certain threshold level $\bar{A}$. If this threshold is considered in the loop stop condition of Algorithm VI.1 , in certain cases we would obtain more than one egalitarian optimal solution. However, when airliner cost is considered as the following step, a unique final solution minimising this cost will be chosen among all these possibilities.

Figure VI-17 shows a *sub-optimal* trajectory for the Airbus A321 at 10h. We call it sub-optimal because the optimal trajectory shown previously in Figure VI-12(b) has a smaller value of the airliner cost if compared with this new trajectory. However, from an annoyance point of view both trajectories are equivalent because in both cases the noise annoyance in all locations is below the threshold level: $A_i \leq \bar{A} \quad \forall i \in \mathcal{L}$. Therefore, this sub-optimal trajectory could be used to better spread the noise annoyance in the populated areas. In this way, we could tackle the problem of having successive over-flights and consider this variable in the annoyance model. Then, for a given departure, instead of flying the *best* procedure for a single over-flight, more than one noise abatement procedures could be used. In addition, even an increase in noise annoyance when flying sub-optimal procedures could be traded-off with the allocation of noise in a wider area. These sub-optimal procedures could be easily generated by the egalitarian algorithm presented above and by setting different values of the threshold level $\bar{A}$. However, this problem is out of the scope of this work and it is considered as further research.

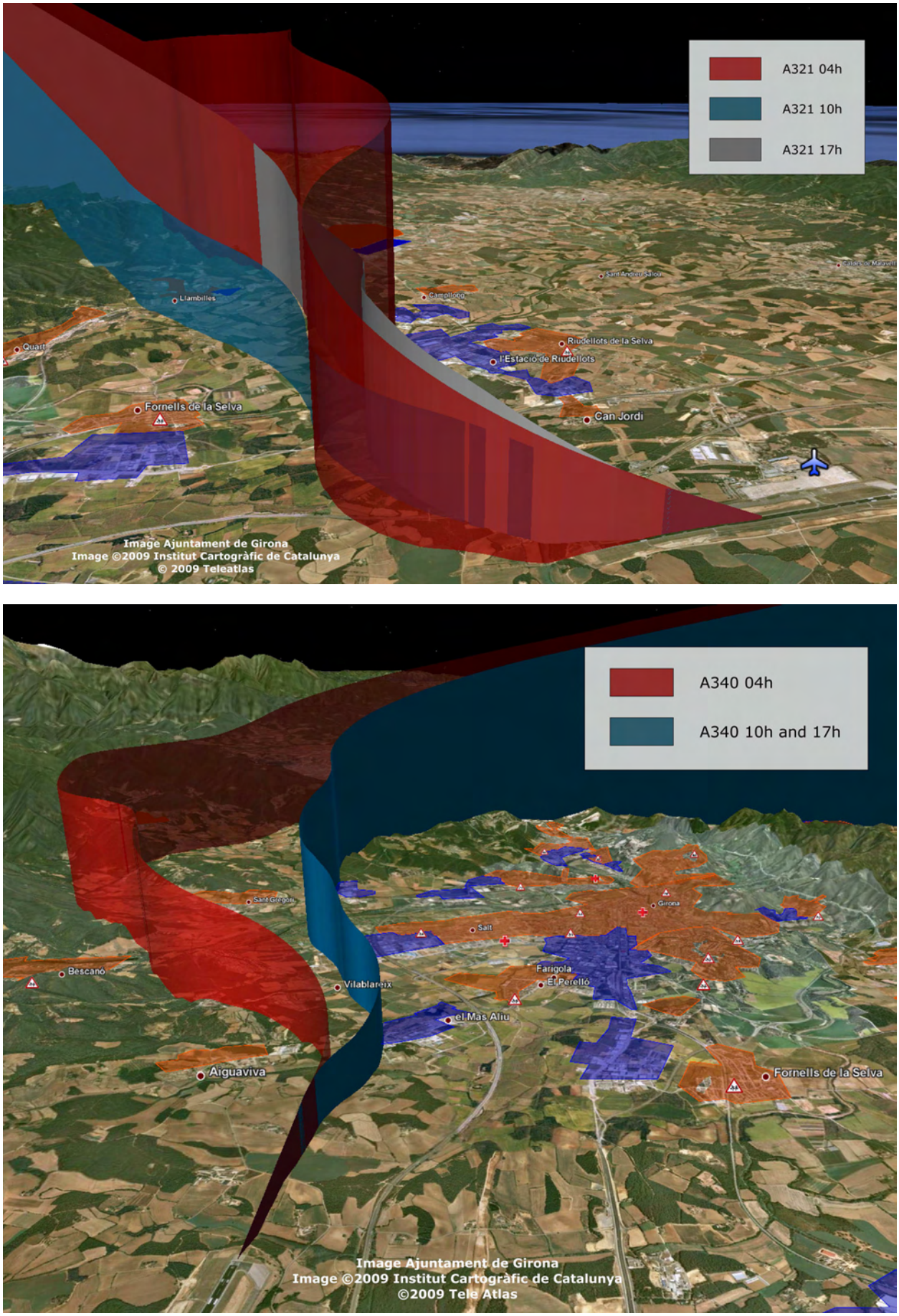

Figure VI-18: *Three dimensional views of the final optimal trajectories Powered by Google Earth (©2008 Google).*

Applaud, my friends, the comedy is finished.

— Ludwig van Beethoven

One generation plants the trees; another gets the shade.

— Chinese proverb

VII

Concluding Remarks

Aircraft operations around airports generate high levels of noise that occur as quickly as they fade. Containing the sound generated by these operations, while meeting the increasing demand for air travel, is one of the major challenges for the air transportation stake-holders. Thus, the main objective of this doctoral thesis was the development of an optimisation framework aimed at computing optimal noise annoyance abatement procedures for aircraft. During this work some questions arose that were assessed and some of them are still open and could be topics of further research. A brief summary and conclusions of the achieved results, as well as hints on the possible directions for future work, are presented in what follows.

VII.1 Summary of contributions

The main contributions of this PhD thesis are summarised as follows:

- An extensive study of the state of the art in the design of noise abatement procedures was presented firstly in Chapter II. We identified that there exist several strategies that permit the design of more noise friendly trajectories. The majority of operational strategies used nowadays are specific *recipes* that have been proved to improve noise footprints in some conditions or in particular segments of the trajectory. However, an assessment of the whole trajectory and therefore the *optimisation* of the noise impact is still an on-going topic of research. Several optimisation approaches appear to be useful for the design of such optimised procedures. We have identified the calculus of variations, the brute force (or exhaustive) method, the nonlinear and dynamic programing techniques, and finally, the stochastic algo-

rithms. Regardless of the chosen method, the main difficulties encountered for the problem we tackle are the required computational burden for realistic scenarios, the possibility and easiness to model all kind of constraints, the sensitivity to local minima due to the non-convexity of the problem and the implication of the user at *low level* issues related with the optimisation process. At operational level, the main difficulties of this problem is the assessment of multiple conflicting objectives, taking into account not only noise criteria but also airport capacity, airspace and traffic separation constraints.

- A survey on noise annoyance models was also included. We saw that there exist multiple ways of measuring noise by using several metrics and spectral ponderation strategies. Moreover, several studies were pointed out showing that noise annoyance not only depends on the acoustical magnitudes but also on a diversity of factors such as the hour of the day, the type of affected zone, subjective and personal elements of the affected people etc. Thus, building a noise annoyance model is not an easy and straightforward task. Furthermore, it is not clear how a hypothetical detailed and complex model could be considered in an optimisation framework for optimal flight procedures. In this context, fuzzy logic approaches were identified as a possible way to model the complexity of noise annoyance by using knowledge based reasoning.

- A modelling methodology was developed in Chapter III in order to build the required models for solving the optimisation problem. We developed a state representation of the dynamic equations describing the aircraft movements. This model turned out to be a hybrid model where different dynamics appeared in function of certain flight phases (when flap/slats and possible thrust configurations were considered). Knowing this, a methodology was proposed to deal with these switching behaviours by using smooth transitional functions that proved to be more suitable in the optimisation algorithm. On the other hand, a basic fuzzy logic model was developed in order to show how complex and knowledge based models could be treated in the optimisation. In this way, we showed that after a defuzzification process, the noise annoyance could be expressed also as a set of nonlinear functions.

- The optimisation of noise abatement procedures was formally written as a nonlinear optimal control problem in Chapter IV. A direct transcription into a Non Linear Programming (NLP) problem was implemented and a commercial NLP solver was used. The computational burden in all the examples that followed remained acceptable. The major drawback of this technique is the high sensitivity to locally optimal solutions. Indeed, the problem is highly non-convex and the NLP solver has no means to avoid local minima. Global optimisation packages were tested unsuccessfully due to the high computational burden required. At this point, we conclude that with this technique the optimisation of this kind of trajectories, in a *fully automated* way, is not possible with nowadays technology. This leads to another paradigm where more interaction is required from the user of the optimisation framework. Thus, convenient *guesses* or initial trajectories should be given to the NLP solver based on the user's experience and common sense. Then, a thorough post analysis of the results would also be required in order to identify possible locally optimal solutions requiring new optimisation runs if necessary.

- One of the most important contributions of this PhD thesis is the assessment of different multi-objective optimisation techniques. Scalarisation methods were identified as the most widely used methodologies for solving these kinds of problems. They have the enormous advantage that a multi-criteria optimisation problem is transformed into a single-objective optimisation problem where a *weighted average criterion* is optimised. However, they present some drawbacks as we identified in Chapter IV. Lexicographic, hierarchical, egalitarian and goal optimisation strategies were presented and tested.

- Lexicographic optimisation was used in Chapter V with a hypothetical scenario where an aircraft departure was optimised. We concluded that this kind of strategy is very convenient when the decision maker has a clear idea of the priorities among the optimisation objectives. In a scenario where different locations can be arranged according to these priorities, a Pareto optimal solution can be obtained by means of an easy iterative and intuitive algorithm. Moreover, this staged optimisation helps when considering non-commensurable criteria such as noise and fuel or time consumption.

- An additional advantage of lexicographic or hierarchical optimisation is that the user has more control on the local minima problem. Since these optimisation techniques are executed with successive iterative steps, the user can perform an analysis at each intermediate result. This advantage is not possible, for instance, if the common scalarisation technique is used. In that case, only one optimisation is run and local minima can only be avoided by running the optimiser several times starting from different initial guess conditions.

- As expected, a serious drawback of lexicographic optimisation was in its application in the case where the priority ranking among the objectives is unknown. This could easily be the case in noise abatement procedures if several *equally important* populated locations have to be considered. A *naive* solution was firstly explored by computing all possible lexicographic prioritisations for a given scenario. Then, a new door opened where a global performance criterion (or a set of criteria) had to be defined in order to choose a final trajectory. By doing this, the decision maker would have some final trajectories minimising each performance criterion, and according to his/her experience, could select one among them. A first conclusion of this method was that several prioritisations may lead to the same final trajectory, depending on the scenario characteristics and the placement of the noise sensitive locations. This was due to the degrees of freedom that the lexicographic algorithm leaves to lower prioritised objectives once the higher prioritised ones no longer have influence in the optimisation. Obviously, the main drawback of this approach was a prohibitive computational burden for big scenarios. Heuristic methods aimed at reducing this computational load were tested, but then the problem of having a local optimal solution arose again.

- Chapter V also showed how it was possible to compromise among the noise sensitive locations by relaxing the lexicographic constraints. This method, called *hierarchical optimisation*, gave more sense to the global performance criterion defined previously and aimed at choosing a final solution. With this approach, heuristic methods performed better due to the fact that a relaxation value existed where all prioritisations led to the same final solution. Yet the main conclusion was, that by using different relaxation values the whole Pareto frontier could be completely explored. Therefore, the problem could be reformulated with the minimisation of the performance criterion as objective function itself.

- The maximum absolute deviation of all the objectives, from each respective ideal value, was then chosen as performance criterion to be minimised. This new formulation, named *min-max*, *egalitarian* or *Tchebycheff* was adopted in Chapter VI. In fact, the solution coming from this new optimisation problem was called *fair* because it minimised the final value of the worst objective. Moreover, this assessment on the fairness of the trajectory, drove us to choose the absolute annoyance deviation values as the final optimisation criteria.

- Egalitarian optimisation leads to weakly Pareto solutions. So, an egalitarian lexicographic algorithm was developed in order to obtain a fair but also Pareto efficient trajectory. This algorithm was successfully tested in Chapter VI. There, a final optimisation strategy, combining the best features of the egalitarian lexicographic, goal and hierarchical optimisation techniques was implemented.

- In the same Chapter, a complex real scenario was also considered. We presented a methodology to construct a grid of measurement points in order to consider a large amount of populated areas. Again, the user of this framework is called on to thoroughly choose the locations of these points. Taking advantage of the nature of the final optimisation strategy, the final number of measurement points could be considerably reduced consequently improving the computational burden.

- One of the main conclusions is the compromise existing between the automatisation of the process (*i.e.* a black box that computes a noise abatement procedure with a single mouse click) and the sensitivity to local minima. Although the presented methods can improve the task of avoiding these minima, a manual intervention by an expert user is still needed. However, we think that this tool can still improve the current situation where the automatisation is zero and much more trial and error is performed by the same group of expert users. With the presented methodology the problem is somehow divided in separated stages; by choosing first the aspiration levels at special locations (if any), selecting priorities among the objectives (if any), obtaining one or more noise annoyance optimal trajectories, considering other optimisation criteria such as fuel or time costs, and finally providing the decision maker with tools for selecting a final trajectory. Even if with this methodology some trial and error may be still recommended, we hope to have contributed to enhancing the efficiency, accuracy and scientific rigour in the design of optimal noise abatement procedures.

VII.2 Future Research

During this thesis new questions and research lines arose. Taking advantage of the optimisation framework that has been developed and for the sake of completeness, the following work items are proposed for the future:

- Albeit the developed equations for the dynamics of the aircraft took into account the wind vector, in the presented examples wind was always supposed to be zero. The main reason was the lack of knowledge on how wind conditions actually effect noise propagation equations. Therefore, if the noise model can be further improved by considering wind conditions, a sensitivity study of the optimal trajectories under these conditions would be worth carrying out.

- The noise annoyance models could be improved taking into account more non-acoustical factors and therefore, expanding the input variables and the set of rules in the inference process. In particular, the effect on the annoyance of multiple over-flights over the same populations should be considered. In addition, social surveys in the considered scenario could be a good starting point in order to enhance these models. Besides that, a more detailed modelling will also be needed, for example requiring empirical measurements (such as the background noise at the different locations) and the assessment of the problem for a multidisciplinary group of experts.

- Additional objectives could be added into the optimisation framework. With carbon emissions trading schemes on the horizon, we could improve the model taking into account these emissions. An interesting problem would arise because of the conflict in objectives among different emissions and the minimisation of noise.

- From an Air Traffic Management (ATM) point of view, we did not assess capacity issues in the case that such procedures may be flown in dense Terminal Manoeuvring Areas (TMA). Actually, if each aircraft is flying its own optimised trajectory, the regular traffic patterns

known today will no longer be useful. This leads to a more complex situation for ATM and the situational awareness of the pilots could be impacted as well, especially with respect to nearby traffic. The developed methodology has the possibility to impose time, altitude or speed constraints at given (way)points. Therefore, by using these features (and maybe other additional ones) it would be interesting to compute optimal trajectories with different traffic loads in the TMA and by enforcing other ATM restrictions.

- At operational level, some of the obtained trajectories may present some issues in their flyability (and would *scare* some pilots). It is clear that these trajectories are the *optimal* ones from a theoretical point of view. Then, a thorough operational assessment must follow. However, it would be convenient to define how this assessment should be done and if it would be possible to somehow automate it or even incorporate new features in the optimisation process.

- In this context, new operational paradigms should also be taken into account. For example, in the present work we have considered a manual thrust selection. Thus, during a departure only two thrust settings were possible, going from *Take-off–Go Around* to *Climb* thrust settings. Why not consider a future application in where the aircraft is flown automatically and thrust can be continuously adjusted?

- Considering the optimal problem resolution, we implemented the direct transcription into an NLP problem. Taking advantage of the already existing framework, different strategies such as stochastic algorithms or dynamical programming could be tested and a comparative study on their performances could be carried out too.

- In a similar way, we outlined what we thought they were the most appropriate multi-objective resolution techniques, such as lexicographic, hierarchical, egalitarian and goal optimisation. However, a collection of alternative methods exist that would be worth considering. In this way, more information could be provided to the decision maker and therefore his/her task could be easier.

And thus do we of wisdom and of reach, with windlasses and with assays of bias, by indirections find directions out.

—William Shakespeare
(Hamlet - Act II. Scene I)

A

Aircraft navigation

Air navigation is the process of directing an aircraft from a certain point to another by means of the own pilot ability or by using different kinds of navigation instruments. In civil aviation, there are two main ways to navigate and it is said that an aircraft is evolving accordingly to certain flight rules, which are:

- Visual Flight Rules (VFR); or
- Instrumental Flight Rules (IFR).

VFR navigation is based on visual references seen from the cockpit, such as: rivers, mountains, roads, etc. In this type of navigation almost no instruments are used and, if used, they are always a complementary means of navigation. Therefore, Visual Flight Rules are strictly bound to certain favourable meteorological conditions (measured in terms of visibility and minimum separation between the aircraft and the surrounding clouds) and, as a consequence, its use is almost restricted to private or leisure aviation.

On the other hand, an aircraft flying under IFR rules uses several navigation instruments which provide the pilot with the necessary information to follow its trajectory or navigation route with no need for external visual references. The route to be followed can not be any trajectory, but must be one being previously studied by the competent authorities in air traffic management, and being conveniently published. Particularly, these trajectories are called procedures (for airport departure, arrival or approach manoeuvres) or airways (for the en-route phase). The design of procedures and airways guarantees obstacle clearance by means of a minimum safe flight altitude, as well as the minimum separation between aircraft using different procedures or airways in the vicinity. Moreover, this kind of organisation helps on managing and controlling the air traffic.

A.1 Radionavigation systems

Most of the navigation instruments and equipment which support IFR flights use the radiofrequency technology and this is why they are called radionavigation instruments (or equipments). There are several types of these systems and the most used world-wide are the *Non Directional Beacon* (NDB), the *VHF Omnidirectional Range* (VOR), the *Distance Measurement Equipment* (DME) and the *Instrumental Landing System* (ILS). All of them consist of radio transmitters placed at known locations and, with the convenient receiver equipment on-board, valuable information can be derived for navigation purposes.

Roughly, a NDB on-board receiver (which is, actually, an Automatic Direction Finder or ADF) can determine the direction to the NDB station relative to the aircraft displaying it on a relative bearing indicator. A VOR equipment provides more information to the pilot, allowing the airborne receiving equipment to derive a magnetic bearing from the station to the aircraft (direction from the VOR station in relation to the Earth's magnetic North at the place of the ground facility). A DME provides a distance figure between the aircraft and the ground station based on a sequence of interrogations and responses between the on-board and the ground equipment. On the other hand, the main use of the ILS is to support the final approach phase for a given runway. This system is actually composed by two subsystems, the first one is the *Localizer* (LLZ) which gives lateral guidance with respect to the runway centreline and the second one is the *Glide Slope* (GS) giving vertical guidance with respect to a nominal glide path descending towards the runway threshold.

Summing up, all these systems can be treated as different radiobeacons which give to the user (the pilot) relevant information about his relative position to the beacon. Furthermore, the use of more than one system at the same time allows the pilot to compute the aircraft position in a map (by using for example a VOR radial and a DME arc, or two VOR radials, etc.). In this way, it is possible to define flight instrumental procedures to guide the aircraft that can be flown all time and with (almost) all weather conditions. It is out of the scope of this document to describe in detail these systems, which are often called as *conventional radionavigation systems*. For further details the reader can refer to (Sáez Nieto & Salamanca Bueno, 1995) or (Kayton & Fried, 1997).

A.1.1 Satellite navigation systems

A satellite navigation system uses a constellation of satellites, which transmit radio signals allowing the receivers to compute their current position. The most important global constellation of satellites is that of the Global Positioning System (GPS) developed by the United States of America. GLONASS[1], in turn, was developed by the former Soviet Union and uses another dedicated constellation. Finally, the European Union is developing nowadays their own navigation satellite system named GALILEO.

Despite that GPS has been available for civil use since mid 80's, in civil aviation these systems are still playing a secondary role. Civil air transport is considered as a safety of life application and all systems involved must verify very high and strict levels of performance. In this context GPS or GLONASS satellite navigation systems do not meet these requirements and can not be used in all phases of flight as primary means of navigation. One of the major drawbacks is the lack of *integrity*, which is defined as the ability of the system to provide timely and valid warnings to the user if it is not functioning properly. In addition, for some critical flight phases (such as the approaches) these systems may suffer from poor *accuracy* or *availability* too (ICAO, 1996). In this context, some solutions have been recently developed in order to overcome the problems of the stand alone use of GPS or GLONASS systems. With a generic name of *Augmentation Systems* these solutions provide GPS and GLONASS users with an extra set of information in order to enhance the whole system performances and achieve the strict requirements for using them in

[1] *GLObaluaya NAvigatsionnaya Sputnikovaya Sistema*

civil aviation.

There are three different types of augmentation systems, basically distinguished in function of the source which is providing this extra set of information: *Airborne Based Augmentation Systems (ABAS)*, *Ground Based Augmentation Systems (GBAS)* and *Satellite Based Augmentation Systems (SBAS)*. At present, SBAS systems are that ones being in a most advanced phase of development and certification. The first one being developed, and currently operational, is the American *Wide Area Augmentation System (WAAS)* followed by the *European Geostationary Navigation Overlay Service (EGNOS)* (expected to be fully operational at the end of 2009) and the Japanese *MTSAT Space Augmentation System (MSAS)* (still under development). Recently, the Indian government has announced the future development of its own SBAS system, GAGAN: the *Gps And Geo Augmented Navigation system* (Suryanarayana Rao & Pal, 2004).

The generic term Global Navigation Satellite System (GNSS) include all the systems which allow for the positioning of an aircraft by means of signals received from navigation satellites, including the global constellations but also all kinds of augmentation systems. For further reading, a description of the GPS system and its involved technology is deeply presented in (Parkinson & Spilker, 1996), while more information concerning European satellite navigation program can be found, for instance, in (Lucas *et al.* , 1996) or (Ventura-Travesset *et al.* , 2001) and in the European Space Agency navigation web page (ESA, 2009).

A.2 Flight Phases and navigation procedures

Flights under Instrumental Flight Rules (IFR) are often divided in different phases of flight which are summarised as follows.

A.2.1 Taxi and take-off

At present there are no specific radionavigation procedures for taxi and take-off and therefore, even with IFR flight these phases are always conducted under visual conditions. Should the visibility in the departing airport be seriously degraded, the capacity of the airport may be reduced (due to higher safety ground separation distances between aircraft) and eventually the airport may be temporally closed to traffic.

A.2.2 Departure

Just after take-off the departure procedure begins and it is aimed at guiding the aircraft from the departing runway to a given point to join the en-route airway structure. These procedures are called *Standard Instrumental Departure* (SID) and besides horizontal tracks, can also specify some restrictions in the altitude or speed profiles along the procedure. Generally, there exist a set of departure procedures covering all possible destinations of the departing aircraft. SIDs are usually enforced around these airports with a significant amount of traffic allowing, in this way, to better organise the departing traffic, minimising potential conflicts with arriving traffic and easing the tasks for both pilots and controllers which know beforehand the expected trajectory that the aircraft will follow. In addition, SIDs are designed in a way that the obstacle clearance margins are safely respected during the whole procedure. On the other hand, SIDs are not always the shortest routes departing an airport and therefore they are not the most economic ones from the airliner point of view. That is why in small airports with few traffic during the day, these kind of procedures may not be used.

A.2.3 En-route

After the departure the en-route phase follows. Here the aircraft navigates through a sequence of airways that covers more or less efficiently the airspace. Airways form a dense network of routes which have been designed to better manage the air traffic flow, assuring the separation between aircraft and making them compatible with restricted portions of the airspace.

A.2.4 Arrival

The arrival phase is defined in a similar way if compared with the departure. *Standard Terminal Arrival Routes* (STAR) are published in airports that require such procedures in order to better cope with high volumes of traffic. STAR procedures allow the aircraft to leave the airway en-route structure and direct it to a point where the approach to the landing runway can be safely initiated.

A.2.5 Approach and landing

The main purpose of an approach procedure is to properly align the aircraft with the runway centreline as well as to give a descend guidance to the runway threshold while maintaining the aircraft with a safe obstacle clearance margin during the whole procedure. The approach procedure is obviously runway dependent but also *system* dependent, *i.e.* there may exist different radionavigation systems used as primary means of navigation during the final approach segment. Thus, even if the initial approach point could be the same an aircraft may perform an approach procedure or another depending of the availability of radionavigation systems.

The most used type of approach in commercial aviation is the ILS approach, followed by the VOR-DME approach. However, it is expected that in a short-mid term GNSS based approaches will be more and more frequent. An approach procedure includes always a *missed approach procedure* which is the procedure to be followed if the approach is aborted, for instance, due to poor visibility conditions, potential traffic conflicts in the runway or wrong speed or altitude values prior to land.

In general, approaches are classified as either precision or non-precision. Precision approaches utilise both lateral and vertical guidance information while non-precision approaches provide lateral course information only.

A.3 Conventional and RNAV navigation

As it has been seen, the main role of the navigation instruments (and systems) is to assess the aircraft to follow certain flight procedures. During last decades, navigation in continental airspace has been based on the use of radionavigation aids spread widely in the territory but resulting sometimes in non-efficient and inflexible routes. This is the main cause of flight delays (due to bottle necks in some high over-flown radionavigation aids), environmental and noise issues and non-economically optimal routes for airline operators. This type of navigation, based on overflying a set of radionavigation aids and on following specific bearings to/from these aids is commonly known as *Conventional Navigation*.

With the introduction of computerised and digital avionics, jointly with an important onboard integration of different systems, new solutions have arisen to overcome the major drawbacks of conventional navigation. A first step into new navigation techniques was introduced with the *Area Navigation (RNAV)* concept. Aircraft equipped with suitable RNAV systems can fly routes that can be defined between arbitrary waypoints and, therefore, not necessarily placed over radionavigation aids, as required with conventional navigation. This concept is possible thanks to

the on-board Flight Management Systems (FMS) that continuously compute the position of the aircraft using data from one or several sensors. These new, and flexible, routes must be defined in an *Area* properly covered by one or more types of RNAV positioning aids (or sensors). This position computation can be done with VOR-DME positioning, DME-DME positioning, by using Inertial Reference Systems (IRS) or even with Global Navigation Satellite Systems (Eurocontrol, 1998). It should be noted that it is possible to define RNAV routes at any place in the world providing that aircraft will be equipped with an RNAV system with GNSS positioning capability.

RNAV was first introduced in Europe by April 1998 and is considered as a vitally important contribution to the development of an optimal en-route operating environment in European airspace. In addition, RNAV procedures are settled as an objective for all phases of flight in Europe[2]. In this context, EUROCONTROL (the European organisation for the safety of air navigation)[3] has defined RNAV concept GNSS as the key enablers for future improvements in terms of safety, efficiency and/or economy of flight, provided that their implementation is based on a fully co-ordinated, harmonised, evolutionary and flexible planning process (Eurocontrol, 2003).

The official and standardised methodology to design flight procedures is published by the International Civil Aviation Organisation in the Volume II of the document *8168. Procedures for Air Navigation Services - Aircraft Operations* (ICAO, 2006b). It provides basic guidelines to States or organisations in charge of designing instrumental flight procedures. The corresponding material specifically designated to flight operators (including flight crews), is found in Volume I of the same publication (ICAO, 2006a). Obstacle clearance is the primary safety consideration in developing such instrument procedures. However, other considerations, such as noise preferential routes and noise abatement procedures, are also taken into account when designing them.

A.3.1 RNAV path terminators

As explained before, an RNAV system receives data inputs from various sensors and (with a convenient database) computes aircraft position, interprets a flight plan, calculates what is required to achieve the desired flight path and then sends pitch or vertical speed/path and roll to the Flight Control Computers, which, in turn, will command the flight surfaces directing the aircraft on a particular path generated by the FMS.

The interpretation of a published procedure into a format that the FMS of the aircraft can interpret is a critical issue: in RNAV navigation the pilot is not longer flying "a chart" but it is the FMS which is flying "a database". To facilitate this interpretation there is a database standard published by Aeronautical Radio, Inc. (ARINC): the standard 424 (ARINC, 2000). This document details how navigation databases for FMSs are to be coded. One of the most important elements of this coding is that of Path Terminators, which provide the means to translate terminal area procedures, such as SIDs, STARs and approach procedures, into FMS readable code. Each Path Terminator is made up of a two letter code that defines a specific flight path and a specific type of termination for that flight path. It is important to note that there are 18 different published versions or supplements of the ARINC 424 standard and, therefore, not all existing FMSs have been implemented in the same way and in the same period. In practice, this leads to some track dispersion around the RNAV nominal path, especially during turns, but it means also that not all Path Terminators can be flown by all RNAV equipped aircraft.

One of the most relevant issue is how the turns are conducted when using RNAV navigation. There are two types of RNAV waypoints: *fly-over* waypoints and *fly-by* waypoints. In a fly-over waypoint (see Figure A-1(a)) the aircraft must over-fly it before directing to the next flight plan leg. On the other hand, in Figure A-1(b) a fly-by turn is shown. Here, the aircraft is allowed to

[2]Actually in the European Civil Aviation Conference Area (ECAC), which covers more countries that those just constituting the European Union

[3]http://www.eurocontrol.int

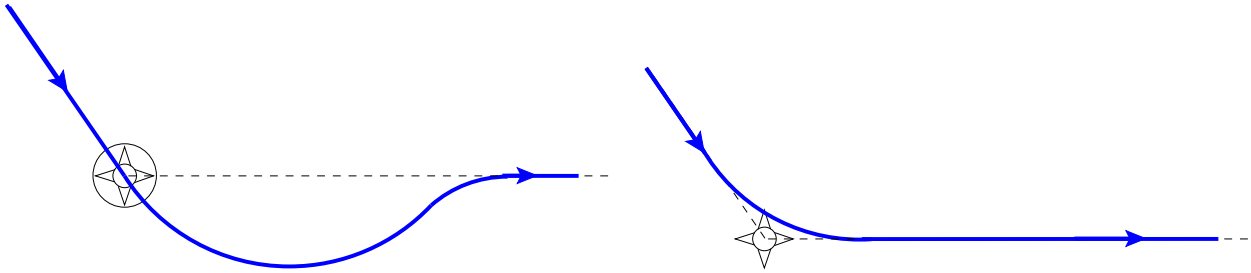

(a) Fly-over (b) Fly-by

Figure A-1: *RNAV waypoint types*

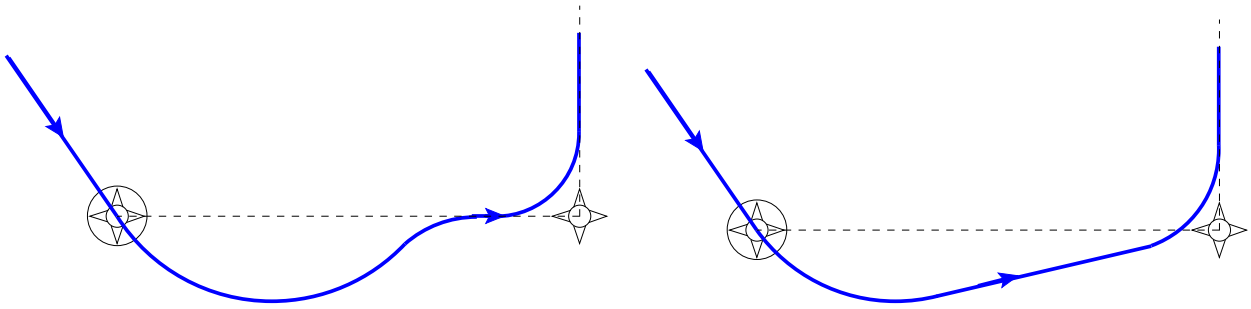

(a) Track between Fixes (TF) (b) Direct to a Fix (DF)

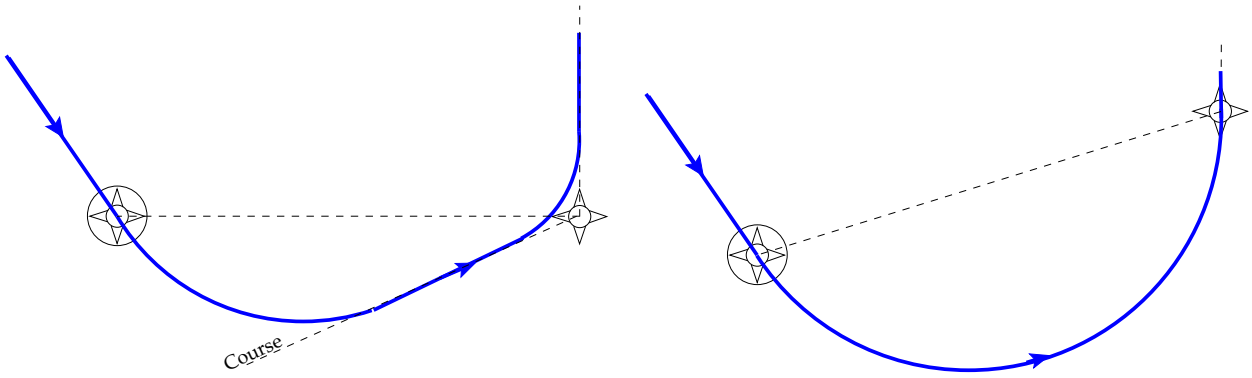

(c) Course to a Fix (CF) (d) Radius to a Fix (RF)

Figure A-2: *Example of some RNAV Path Terminators*

anticipate the turn in order to perform it smoothly an efficiently. The Distance Turn Anticipation (DTA) is the distance preceding a fly-by waypoint at which an aircraft is expected to start a turn to intercept the course of the next segment. DTA values are based on the true airspeed at which a turn is carried out, wind speed and direction, bank angle limitations and degrees of track change required for the turn.

The way the aircraft proceeds from one leg to another will depend on the coded Path Terminators. For example, after a fly-over waypoint one can proceed *Direct to* the next *Fix* (DF Path Terminator) or the aircraft may join the *Track between* the two *Fixes* (TF Path Terminator) or even join next fix by following a specific *Course to* the *Fix* (CF Path Terminator). Another important Path Terminator, which specifies a constant radius turn between two waypoints, is the *Radius to a Fix* (RF). Figure A-2 shows how the above mentioned path terminators would change the nominal aircraft trajectory for a same portion of the flight plan. The ARINC 424 standard specifies up to 23 different path terminators, even if most of the FMSs can usually execute an small set of them.

A.4 Airspace structure

In general, each state manages the airspace within the national boundaries. Airspace is divided in different Flight Information Regions (FIRs) and Upper Information Regions (UIRs) which are designed with the objective to better manage and control the en-route traffic flying over the State. The Air Navigation Service Provider (ANSP) is in charge of this airspace design and management providing alert (search and rescue) and information services to aircraft. In addition, in some portions of the airspace control services (*Air Traffic Control* or ATC) are also given, ensuring in this way, the separation between aircraft. Departing or arriving traffic is generally more difficult to handle because of the conflicting ascending and descending trajectories as well with the convergence of the routes to the airport areas. Then, around major airports (or group of nearby airports) there exist portions of airspace devoted to handle depart, arrival and approach procedures: the *Terminal Manoeuvre Area* or TMA. Therefore SIDs, STARs and approach procedures will be, in general, within the boundaries of a TMA.

Chance is a word void of sense; nothing can exist without a cause.

— François-Marie Arouet (Voltaire)

B

Background on aircraft noise

Aircraft noise is the perceived sound that is produced by any aircraft, or its components, during the different phases of a flight. This Appendix introduces some basic concepts in acoustics theory applied to aircraft noise. Different noise metrics and units are presented, all of them intended to measure the amount of noise or annoyance caused by one or several noisy events.

B.1 The Nature of Noise

A sound wave, in the direction of its propagation, carries with it a certain energy. The changes in air pressure which reach the human eardrum set it in vibration: the greater these changes, the louder is the sound. Due to the wide range of different sound pressures, this magnitude is often expressed by using a logarithmic scale:

$$N = 20 \log_{10} \left(\frac{P}{P_0} \right) \tag{B.1}$$

where N is the sound pressure level in decibels (dB), P is the sound pressure and P_0 is a reference noise pressure, which is usually taken as the international standardised human minimum audible threshold of $20\,\mu$Pa.

Human perception of loudness is highly nonlinear and the relationship between frequency, intensity, and loudness is quite complex. The human hearing system is more sensitive to some frequencies than others. Furthermore, its frequency response varies with the sound pressure level as has been demonstrated by the measurement of equal-loudness contours published by the In-

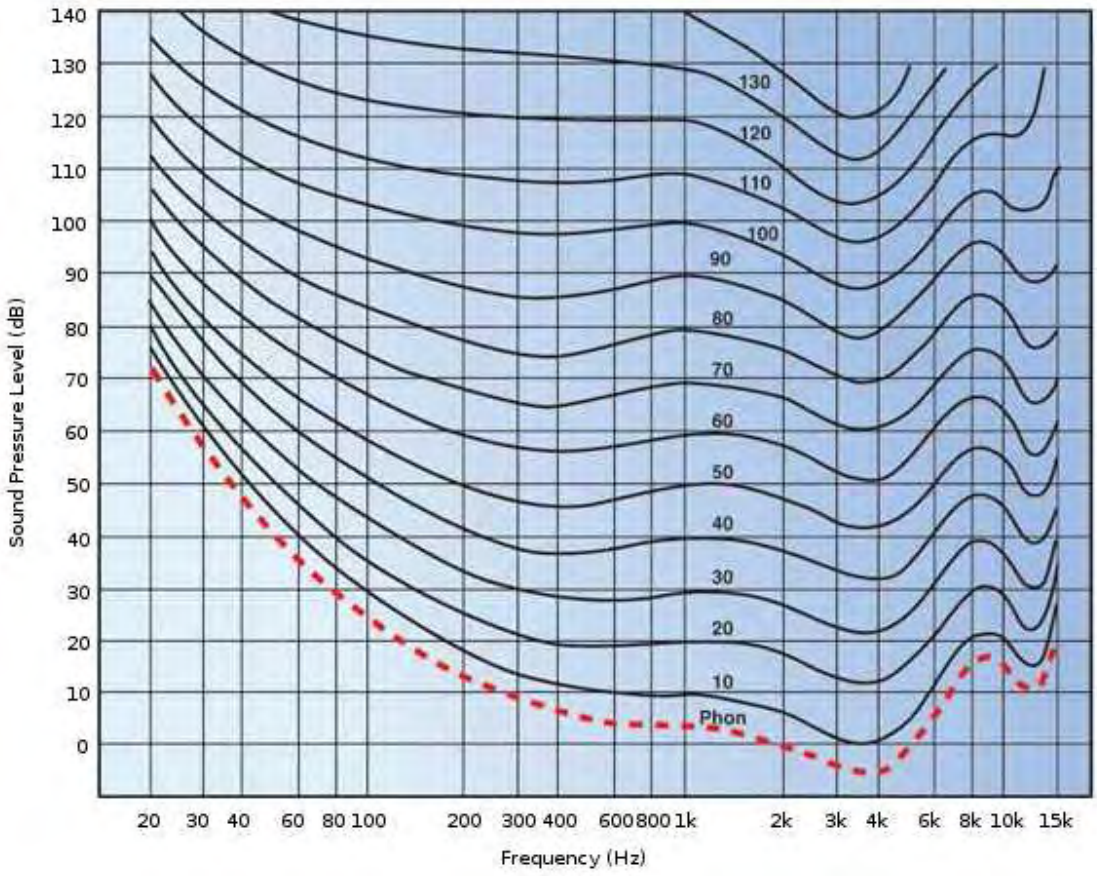

Figure B-1: *Equal-loudness contours as specified in (ISO, 2003)*

ternational Organisation for Standardisation (ISO, 2003). In Figure B-1, each solid line correspond to a equal-loudness contour, which is usually measured in *Phons*, the subjective unit for loudness. The dotted red line corresponds to the human minimum audible threshold. As it can be see in the Figure, in general, low frequency and high frequency sounds are perceived to be not as loud as mid-frequency sounds. This effect is more pronounced at low pressure levels, with a flattening of response at high levels.

This means that sound pressure levels are not well suited to express the loudness that humans are exposed to. Therefore, they might be corrected to correlate overall sound pressure with the frequency sensitivities of the human ear. This process, commonly referred as a *weighting* process, ponderates differently the noise pressure in function of the frequency of that noise component. There are several weighting techniques relating to the measurement of sound pressure level, as opposed to actual sound pressure. The A-weighted scale, defined in (IEC, 2003), emphasise sound components in the frequency range where most speech information resides, yielding higher levels in the mid-frequency range and lower levels in both low frequency and high frequency ranges (see Figure B-2). A-weighted noise level is used extensively world-wide for measuring community and transportation noise. When using this ponderation scale, noise levels are given in dB(A) units. Table B-1 shows some examples of A-weighted perceived noise levels for different kind of sources.

In addition, there exist other particular spectra corrections which are more suitable when modelling aircraft noise. The C-weighted decibel scale, which retains the low frequency portions of the spectrum, is intended to provide a means of simulating human perception of the loudness of sounds above 90 dB. Finally, the tone-corrected noise level scale is also used to estimate perceived noise from broadband sound sources, such as aircraft, which contain pure tones or other major irregularities in their frequency spectra. Noise levels in low and high frequency band are

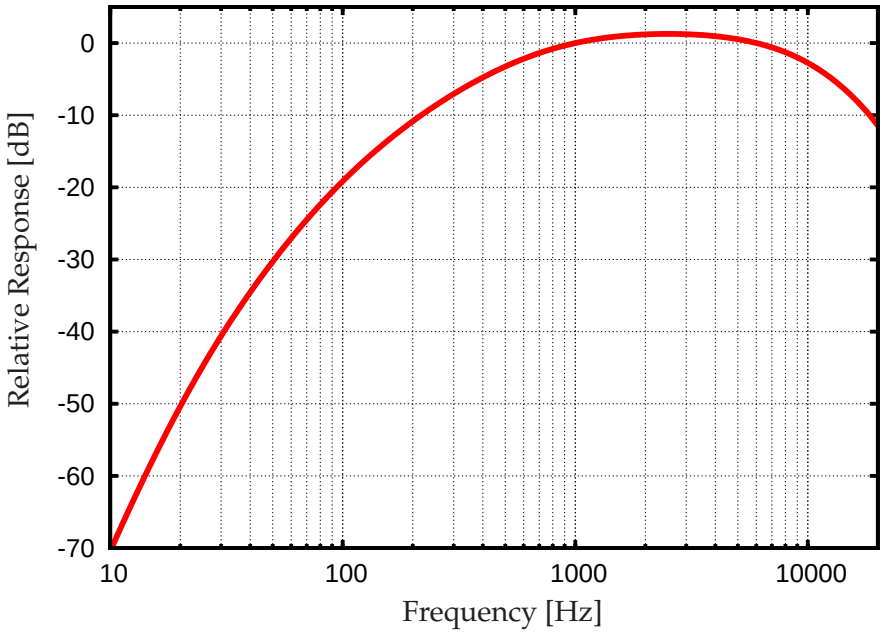

Figure B-2: *A-weighting scale*

Table B-1: *Typical A-weighted noise levels for different kind of emitting sources. Source: (Harris, 1997) and (Eurocontrol, 2009)*

Jet aircraft taking off at 25 m	140 dB(A)
Night club background noise	110 dB(A)
Printing workshop background noise	100 dB(A)
Heavy lorry at 15 m	90 dB(A)
Cement mixer at 15 m	80 dB(A)
Vacuum cleaner at 3 m	70 dB(A)
Car at 100 kmh^{-1} at 30 m	65 dB(A)
Normal conversation	60 dB(A)
Quiet urban daytime background noise	50 dB(A)
Country-side background noise	45 dB(A)
Whisper at 2 m	35 dB(A)
Recording studio background noise	25 dB(A)
Minimum audible threshold	0 dB(A)

depressed while metric levels are elevated if there exist pure tones in the spectra.

B.2 Aircraft noise

For a flying aircraft, two main sources of noise can be identified: airframe noise and engine noise. Airframe noise is the aerodynamic noise generated by all the non-propulsive components of an aircraft. As summarised by (Casalino *et al.* , 2008), five main mechanisms are recognised to contribute significantly to the airframe noise:

- the wing trailing-edge scattering of boundary-layer turbulent kinetic energy into acoustic energy;
- the vortex shedding from slat/main-body trailing-edges and the possible gap tone excitation

through nonlinear coupling in the slat/flap coves;

- the flow unsteadiness in the recirculation bubble behind the slat leading-edge;
- the roll-up vortex at the flap side edge; and
- the landing-gear multi-scale vortex dynamics and the consequent multi-frequency unsteady force applied to the gear components.

An accurate and complete review on this topic is done by (Crighton, 1991). In a first approximation, the acoustic intensity produced by airframe noise can be considered to be proportional to the cube of the relative air-to-aircraft speed (*True Airspeed*).

Concerning the power plant noise, for jet equipped aircraft, the noise is related to the four main components of the engines: compressors, turbines, combustion chamber and exhaust nozzle. Lighthill's *eighth power law* (Lighthill, 1954) states that the acoustic intensity radiated by a jet engine is proportional to the eighth power of the jet speed, presenting, as well, a clear directional distribution.

During a departure, high levels of thrust are used and, therefore, most of the emitted noise comes from the power-plant. On the other hand, for modern high-bypass engine powered commercial aircraft, the airframe noise represents the main contribution to the overall flyover noise levels during landing approach phases, when the high-lift devices and the landing-gear are deployed. For example, in (Guérin *et al.* , 2005) a set of measurements were conducted after several fly-overs of an Airbus A319. According to this study, during a departure the power-plant noise masks all noise contributions due to aerodynamic effects. Thus, different flap/slats configurations and climbing speeds have almost no influence in the perceived noise. As expected, this is not the situation when the measurements where conducted in approach and landing phases. In this case flap/slats settings and approach speeds have an important influence in the perceived noise with, for instance, an increment of 5 dB(A) for an increase of $15\,\mathrm{ms}^{-1}$ (30 kt) of the approach speed.

B.2.1 Noise metrics

There exist a wide variety of metrics aimed at representing and evaluating noise impact from aircraft operations. One possible acoustic measure to describe the magnitude of the noise produced by an over-flying aircraft is to measure the maximum sound level (L_{max}) that has been perceived (see Figure B-3).

However, the time duration of the event (*i.e.* the exposure to noise) is also an important component to be measured. In this context, there are several different exposure based metrics such as the Sound Exposure Level (SEL), which measures the sound level of a one-second event equivalent in acoustic energy to the original event. This metric allows comparing events that vary in duration. The Single Event Noise Exposure Level (SENEL) metric is a slight variant of SEL, in that it considers the noise level over a period during which the noise level exceeds a threshold level, rather than over its entire duration. In Figure B-3 SEL and SENEL values are represented for a same noise event, where A represents the total acoustic energy of the event while B is the acoustic energy computed only for the part of the event which has higher noise level than a specified threshold, which usually corresponds to the ambient noise level.

On the other hand, if multiple events are taken into account (such as aircraft flyovers during a day) a widely used metric is the L_{EQ} or Equivalent Sound Level. This metric is an accumulative measure of the perceived sound exposure level (SEL) during a 24-hour period. The Day-Night Average Sound Level metric (DNL) adds a 10 factor penalty multiplier to night noise events (occurring between 22h and 7h) taking into account their greater intrusiveness and eventual sleep disturbance. Similarly, the Day-Evening-Night-Level (DENL) has been defined with an extra 5 dB(A) penalty for the evening hours (from 19h to 23h) and again a 10 dB(A) penalty for the night hours

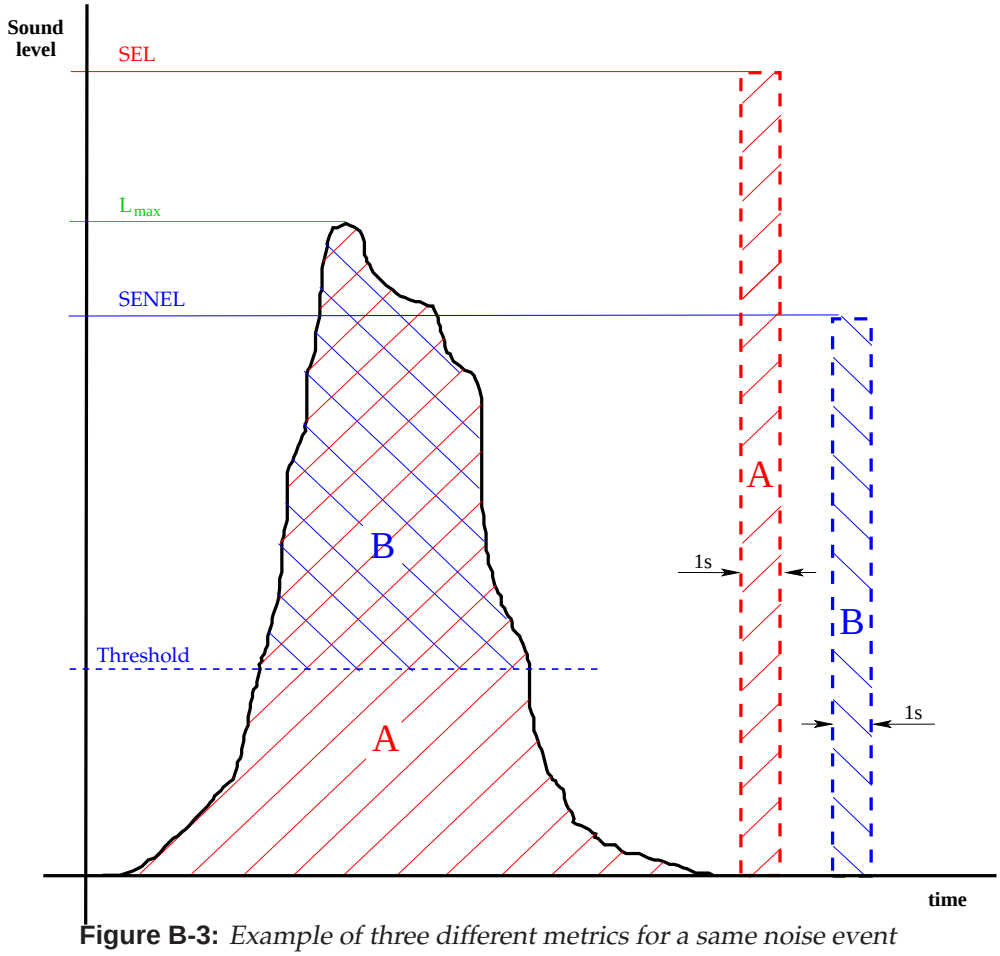

Figure B-3: *Example of three different metrics for a same noise event*

(from 23h to 7h). On the other hand, if the tone-corrected scale is used (instead of A,B or C weighting scales) the Perceived Noise (PN) and Effective Perceived Noise (EPN) metrics incorporate the different frequencies and duration of noise patterns, which result from various speeds and modes of operation of aircraft.

There are other metrics which deal with the time or percentage of time that the noise level is above a specified noise-level threshold, considering aircraft operations during a particular time period (usually 24h). Time Above (TA) metrics, are not often used but is very often requested by community members who believe it will represent their noise problem more convincingly than the others. Similarly, other metrics count for the number of events louder than a certain threshold value. An example for these kinds of metrics (notably used in Australia) is the N70 (or NA70) metric, where the threshold value is fixed to 70 dB(A). Its main advantage is that reports noise in a way that a person thinks and talks about aircraft noise (Southgate *et al.* , 2000). Summing up, we can distinguish among four different families of noise metrics:

- Maximum level based metrics (L_{max},PN,...)
- Exposure based metrics (SEL, SENEL, L_{EQ}, DNL, DENL, ...)
- Time above based metrics (TA,...)
- Event based metrics (N70,...)

For a detailed definition of these and more noise metrics and their exact computations the reader could refer to (Harris, 1997), (Burn *et al.* , 1995) or (Zaporozhets & Tokarev, 1998a).

Each metric differs significantly from the others both in the way it represents noise impact and in way the measure is best employed. For example, since DNL accounts for the loudness

of individual events and the number of operations, an equivalent DNL value can result from a few very loud over-flights or a large number of quieter ones. DNL is considered useful in predicting the average response of communities but not of individuals. There is no agreement, even amongst the experts, on which measurement is the most representative, or the most relevant in a particular situation. For example, the International Civil Aviation Organisation (ICAO) uses EPN for expressing its noise certification standards, see (ICAO, 1993a). On the other hand, A-weighted maximum sound level (LA_{max}) and equivalent sound level (LA_{EQ}) are often found as reference metrics in many state regulations: see for instance the Catalan law concerning the acoustical pollution (Generalitat de Catalunya, 2002). However, the European Commission proposes DENL as the common unit for measuring transport noise (European Parliament, 2002b; European Commission, 2003) even if nowadays there are also many *local* metrics around the world like for example the ANEF (Australian Noise Exposure Forecast) in Australia or the Kosten metric in The Netherlands, which is a exposure based metric that takes into account the way the airport is operated, and the position relative to the runway.

For most gulls, it is not flying that matters, but eating. For this gull, though, it was not eating that mattered, but flight.

— Richard Bach

C

Flight mechanics modelling

This Appendix provides sufficient background material to derive the equations of motion of an atmospheric flying rigid body aircraft and express them in a state-space form, in order to model the aircraft dynamics needed as constraints in the optimisation problem we study.

The state variables are defined as a set of variables such that knowledge of the state vector at a particular time, and the control vector after this time, completely defines the motion (state trajectory) from that time on. See (Kalman, 1963) for a formal definition of the state representation technique. In other words, the state variables shall be any set of variables that completely define the *state of the system* which, in turn, is an indication of the stored energy of the system (*i.e.* the potential and kinetic energies of the aircraft) and its distribution. It is desirable to choose a minimal set of independent state variables and, obviously, the reduction of the equations of motion to state-space form may include the derivatives of some state variables as state variables in their own right. As an alternative to the state equations, the aircraft mathematical model could be built from a set of simultaneous ordinary differential equations of various orders. However, the formalism and advantages that the state-space formulation provides are much more desirable for the problem we tackle.

Therefore, the equations of motion of a flying aircraft in the state-space form will be written as:

$$\frac{\mathrm{d}\vec{x}(t)}{\mathrm{d}t} = \dot{\vec{x}}(t) = \vec{f}(\vec{x}(t), \vec{u}(t)) \tag{C.1}$$

where $\vec{x}(t) \in \mathbb{R}^{n_x}$ is the *state vector*, $\vec{u}(t) \in \mathbb{R}^{n_u}$ is the *control vector* and $\vec{f}: \mathbb{R}^{n_x+n_u} \to \mathbb{R}^{n_x}$ is a vector-valued nonlinear function of the individual states and controls. For the sake of simplicity,

the time dependence (t) is dropped from the notation from now on.

The previous vector equation symbolises the n_x first-order, coupled ordinary differential equations

$$\begin{aligned} \dot{x}_1 &= f_1(x_1, \cdots, x_{n_x}, u_1, \cdots, u_{n_u}) \\ \vdots & \qquad\qquad \vdots \\ \dot{x}_{n_x} &= f_{n_x}(x_1, \cdots, x_{n_x}, u_1, \cdots, u_{n_u}) \end{aligned} \tag{C.2}$$

where the f_i represent different nonlinear functions of the n_x state variables (x_i) and n_u input variables (u_i).

Finally, it should be outlined that regarding vectors and reference frames, the following notation has been adopted in this Appendix: let $\vec{a}$ be a given vector, then $\vec{a}_X$ will be vector $\vec{a}$ expressed in X reference frame coordinates. On the other hand, if $\vec{b}$ is a velocity vector, we will note $\vec{b}_X^Y$ as the velocity $\vec{b}$ seen from reference frame Y, expressed in X reference frame coordinates. Finally, the operator $\frac{\mathrm{d}}{\mathrm{d}t_X}(.)$ stands for the time derivative as seen from reference frame X.

C.1 Definition of the reference frames

In general, three different reference frames are commonly used to describe the equations of motion for a rigid aircraft. There, the rotational motion of the aircraft (angular positions and rates) can be expressed. A *Ground* reference frame which will be used as inertial frame, an *Air* reference frame where the aerodynamic forces are easily expressed and therefore we will develop the dynamic equations and finally a *Body* reference frame used as an intermediate frame to convert Air magnitudes to Ground magnitudes. These three reference frames are defined as:

- **Ground reference frame**: $\mathbf{G} = [O_G; e, n, h]$. East, North, Height (or Up) conventional right handed frame on the surface of the Earth with a given origin O_G. The h axis points upwards following the local vertical direction (i.e with the same direction of the local gravity vector, $\vec{g}$ but in the opposite sense) and the n-e plane is tangent to the Earth's surface at O_G. The e axis points Eastwards and therefore the n axis points to the North.
- **Body reference frame**: $\mathbf{B} = [O_B; x_B, y_B, z_B]$. Conventional right handed set of body fixed axes with origin O_B at the centre of mass of the aeroplane. The x_B axis is forward aligned (usually with the principal inertia axis of the aeroplane), y_B axis starboard aligned and perpendicular to the symmetry plane of the aircraft and z_B axis downwards the symmetry plane of the aircraft and perpendicular to the x_B axis. The $x_B - z_B$ plane coincides with the symmetry plane of the aircraft.
- **Air reference frame**: $\mathbf{A} = [O_B; x_A, y_A, z_A]$. Conventional right handed frame with origin O_B, the centre of mass of the aeroplane. The x_A axis is always aligned with the relative velocity vector between the air and the aeroplane. y_A axis is perpendicular to x_A and starboard aligned while z_A axis goes down the aircraft and it is perpendicular to the x_A-y_A plane.

Three consecutively rotations are defined to describe the instantaneous attitude of the aircraft (Body reference frame) with respect to the Ground reference frame. Starting from $\mathbf{G}$ these rotations are (see Figure C-1):

- First rotation about the h axis, nose right (*yaw* angle ψ)

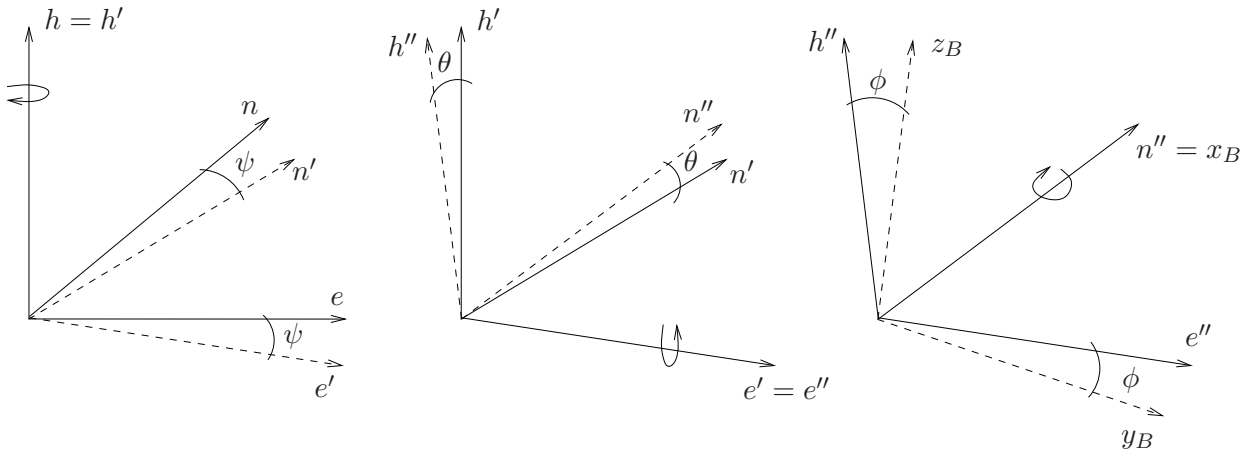

Figure C-1: *Euler angles for the* $\mathbf{G}$ *to* $\mathbf{B}$ *coordinate transformation*

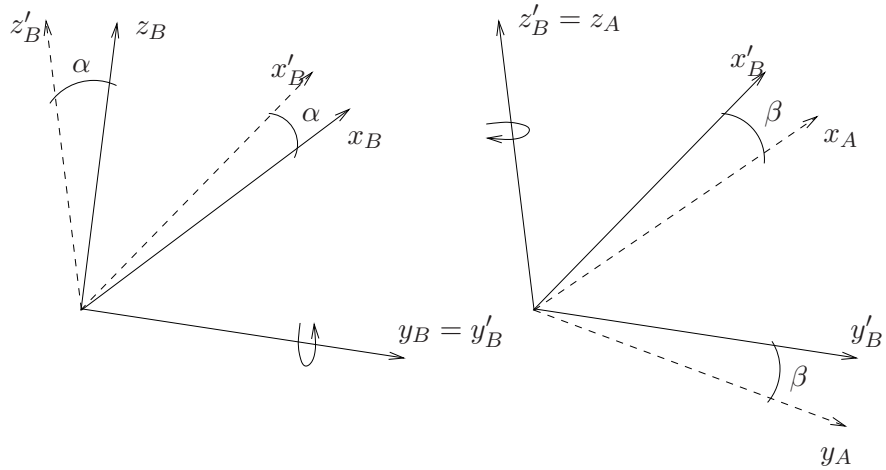

Figure C-2: *Euler angles for the* $\mathbf{B}$ *to* $\mathbf{A}$ *coordinate transformation*

- Second rotation about the new e' axis, nose up (*pitch* angle θ)
- Third rotation about the new n'' axis (x_B axis), right wing down (*roll* angle ϕ)

In the same way, two consecutively rotations allow to pass from the body frame $\mathbf{B}$ to the aerodynamic reference frame $\mathbf{A}$ (see Figure C-2):

- First rotation about the y_B axis, upwards (*angle of attack* angle, α)
- Second rotation about the new z'_B axis (z_A axis), rightwards (*sideslip* angle, β)

C.1.1 Transformation between Body and Ground frames

If $\vec{r}_G = [a_e\ a_n\ a_h]^T$ and $\vec{r}_B = [a_{x_B}\ a_{y_B}\ a_{z_B}]^T$ are the position vectors of a given point $\vec{r}$ in frames $\mathbf{G}$ and $\mathbf{B}$ respectively, in terms of coordinate transformations we have:

$$\vec{r}_G = \boldsymbol{\mathcal{R}}^{\psi}\boldsymbol{\mathcal{R}}^{\theta}\boldsymbol{\mathcal{R}}^{\phi}\vec{r}_B \tag{C.3}$$

where $\boldsymbol{\mathcal{R}}^i$ is the rotation matrix associated to the reference frame rotation caused by angle i. Expanding the three rotation matrices, equation (C.3) yields to:

$$\begin{bmatrix} a_n \\ a_e \\ a_d \end{bmatrix} = \begin{bmatrix} \cos\psi & -\sin\psi & 0 \\ \sin\psi & \cos\psi & 0 \\ 0 & 0 & 1 \end{bmatrix} \cdot \begin{bmatrix} \cos\theta & 0 & \sin\theta \\ 0 & 1 & 0 \\ -\sin\theta & 0 & \cos\theta \end{bmatrix} \cdot \begin{bmatrix} 1 & 0 & 0 \\ 0 & \cos\phi & -\sin\phi \\ 0 & \sin\phi & \cos\phi \end{bmatrix} \cdot \begin{bmatrix} a_{x_B} \\ a_{y_B} \\ a_{z_B} \end{bmatrix} \quad \text{(C.4)}$$

Thus, the transformation from the position expressed in the Body reference axes to Ground reference axes is:

$$\vec{r}_G = \boldsymbol{\mathcal{R}}_{GB}\vec{r}_B \quad \text{(C.5)}$$

being the transformation matrix:

$$\boldsymbol{\mathcal{R}}_{GB} = \begin{bmatrix} \cos\psi\cos\theta & -\sin\psi\cos\phi + \cos\psi\sin\theta\sin\phi & \sin\psi\sin\phi + \cos\psi\sin\theta\cos\phi \\ \sin\psi\cos\theta & \cos\psi\cos\phi + \sin\psi\sin\theta\sin\phi & -\cos\psi\sin\phi + \sin\psi\sin\theta\cos\phi \\ -\sin\theta & \cos\theta\sin\phi & \cos\theta\cos\phi \end{bmatrix} \quad \text{(C.6)}$$

Shall the coordinate transformation be from Ground reference frame to Body reference frame, we have:

$$\vec{r}_B = \boldsymbol{\mathcal{R}}_{BG}\vec{r}_G = (\boldsymbol{\mathcal{R}}_{GB})^{-1}\vec{r}_G \quad \text{(C.7)}$$

On the other hand, it can be easily proved that $(\boldsymbol{\mathcal{R}}_{GB})^{-1} = (\boldsymbol{\mathcal{R}}_{GB})^T$, then:

$$\boldsymbol{\mathcal{R}}_{BG} = \begin{bmatrix} \cos\psi\cos\theta & \sin\psi\cos\theta & -\sin\theta \\ -\sin\psi\cos\phi + \cos\psi\sin\theta\sin\phi & \cos\psi\cos\phi + \sin\psi\sin\theta\sin\phi & \cos\theta\sin\phi \\ \sin\psi\sin\phi + \cos\psi\sin\theta\cos\phi & -\cos\psi\sin\phi + \sin\psi\sin\theta\cos\phi & \cos\theta\cos\phi \end{bmatrix} \quad \text{(C.8)}$$

C.1.2 Transformation between Body and Air frames

If $\vec{r}_A = [a_{x_A}\ a_{y_A}\ a_{z_A}]^T$ is the position vector of a given point a in Air frame $\mathbf{A}$, the coordinate transformation from Body reference frame leads to:

$$\vec{r}_A = \boldsymbol{\mathcal{R}}^{\alpha}\boldsymbol{\mathcal{R}}^{\beta}\vec{r}_B \quad \text{(C.9)}$$

having, in this case, only two rotations from $\mathbf{B}$ to $\mathbf{A}$ with the following transformation matrices:

$$\begin{bmatrix} a_{x_A} \\ a_{y_A} \\ a_{z_A} \end{bmatrix} = \begin{bmatrix} \cos\alpha & 0 & -\sin\alpha \\ 0 & 1 & 0 \\ \sin\alpha & 0 & \cos\alpha \end{bmatrix} \cdot \begin{bmatrix} \cos\beta & -\sin\beta & 0 \\ \sin\beta & \cos\beta & 0 \\ 0 & 0 & 1 \end{bmatrix} \cdot \begin{bmatrix} a_{x_B} \\ a_{y_B} \\ a_{z_B} \end{bmatrix} \quad \text{(C.10)}$$

Then, we have

$$\vec{r}_A = \boldsymbol{\mathcal{R}}_{AB}\vec{r}_B \quad \text{(C.11)}$$

with:

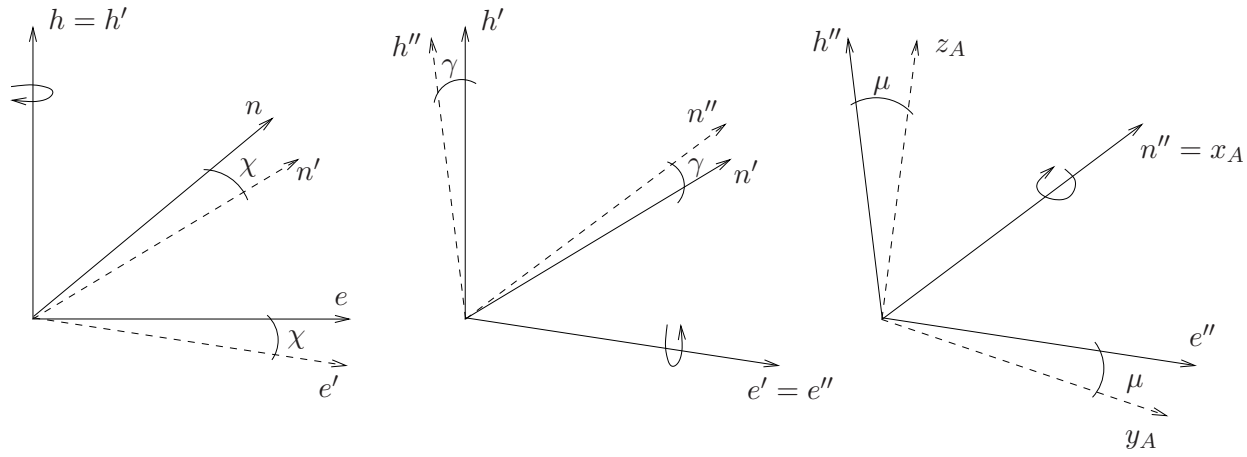

Figure C-3: *Euler angles for the* **G** *to* **A** *coordinate transformation*

$$\boldsymbol{\mathcal{R}}_{AB} = \begin{bmatrix} \cos\alpha\cos\beta & -\cos\alpha\sin\beta & -\sin\alpha \\ \sin\beta & \cos\beta & 0 \\ \sin\alpha\cos\beta & -\sin\alpha\sin\beta & \cos\alpha \end{bmatrix} \tag{C.12}$$

Shall the coordinate transformation be from Air reference frame to Body reference frame, we have:

$$\vec{r}_B = \boldsymbol{\mathcal{R}}_{BA}\vec{r}_A = (\boldsymbol{\mathcal{R}}_{AB})^{-1}\vec{r}_A \tag{C.13}$$

with:

$$\boldsymbol{\mathcal{R}}_{BA} = \begin{bmatrix} \cos\alpha\cos\beta & \sin\beta & \sin\alpha\cos\beta \\ -\cos\alpha\sin\beta & \cos\beta & -\sin\alpha\sin\beta \\ -\sin\alpha & 0 & \cos\alpha \end{bmatrix} \tag{C.14}$$

C.1.3 Transformation between Air and Ground frames

It is also possible to define three new angular rotations which led us to transform Ground referenced magnitudes directly to Air referenced ones. In this case, starting from reference frame **G**, these rotations are defined as (Figure C-3):

- First rotation about the h axis, nose right (aerodynamic *heading* angle χ)
- Second rotation about the new e' axis, nose up (aerodynamic *flight path* angle γ)
- Third rotation about the new n'' axis (x_A axis), right wing down (aerodynamic *bank* angle μ)

Again, in terms of coordinate transformations we have:

$$\vec{r}_G = \boldsymbol{\mathcal{R}}^{\chi}\boldsymbol{\mathcal{R}}^{\gamma}\boldsymbol{\mathcal{R}}^{\mu}\vec{r}_A \tag{C.15}$$

with the following transformation matrices:

$$\begin{bmatrix} a_n \\ a_e \\ a_d \end{bmatrix} = \begin{bmatrix} \cos\chi & -\sin\chi & 0 \\ \sin\chi & \cos\chi & 0 \\ 0 & 0 & 1 \end{bmatrix} \cdot \begin{bmatrix} \cos\gamma & 0 & \sin\gamma \\ 0 & 1 & 0 \\ -\sin\gamma & 0 & \cos\gamma \end{bmatrix} \cdot \begin{bmatrix} 1 & 0 & 0 \\ 0 & \cos\mu & -\sin\mu \\ 0 & \sin\mu & \cos\mu \end{bmatrix} \cdot \begin{bmatrix} a_{x_A} \\ a_{y_A} \\ a_{z_A} \end{bmatrix} \tag{C.16}$$

Then,

$$\vec{r}_G = \boldsymbol{\mathcal{R}}_{GA}\vec{r}_A \tag{C.17}$$

with:

$$\boldsymbol{\mathcal{R}}_{GA} = \begin{bmatrix} \cos\chi\cos\gamma & -\sin\chi\cos\mu + \cos\chi\sin\gamma\sin\mu & \sin\chi\sin\mu + \cos\chi\sin\gamma\cos\mu \\ \sin\chi\cos\gamma & \cos\chi\cos\mu + \sin\chi\sin\gamma\sin\mu & -\cos\chi\sin\mu + \sin\chi\sin\gamma\cos\mu \\ -\sin\gamma & \cos\gamma\sin\mu & \cos\gamma\cos\mu \end{bmatrix} \tag{C.18}$$

Finally, the coordinate transformation from Ground reference frame to Air reference frame, we have:

$$\vec{r}_A = \boldsymbol{\mathcal{R}}_{AG}\vec{r}_G = (\boldsymbol{\mathcal{R}}_{GA})^{-1}\vec{r}_G \tag{C.19}$$

with:

$$\boldsymbol{\mathcal{R}}_{AG} = \begin{bmatrix} \cos\chi\cos\gamma & \sin\chi\cos\gamma & -\sin\gamma \\ -\sin\chi\cos\mu + \cos\chi\sin\gamma\sin\mu & \cos\chi\cos\mu + \sin\chi\sin\gamma\sin\mu & \cos\gamma\sin\mu \\ \sin\chi\sin\mu + \cos\chi\sin\gamma\cos\mu & -\cos\chi\sin\mu + \sin\chi\sin\gamma\cos\mu & \cos\gamma\cos\mu \end{bmatrix} \tag{C.20}$$

C.2 Equations of motion

The equations of motion of a rigid body can be separated (decoupled) into rotational equations and translational equations if the coordinate origin is chosen to be at the centre of mass (Wells, 1967). The rotational motion of the aircraft will then be equivalent to yawing, pitching and rolling motions about the centre of mass as if it were a fixed point in space. However, this rotational motion will be neglected assuming that the aircraft is equipped with basic auto-pilots which deal efficiently with their fast dynamics and thus controls its body attitude (yawing, pitching and rolling motions).

At this point, Newton's Second Law will be applied to a given flying aeroplane. First of all, some basic hypotheses shall be considered.

C.2.1 Basic hypotheses

HYPOTHESIS 1 : The aircraft is supposed to be rigid
This hypothesis implies that all points in the aircraft structure maintain fixed relative positions in space at all time. It is common to have flexing of the wings of a large passenger aircraft during a flight. However, the interaction of flexibility effects with the aerodynamics greatly complicates

the model and this field is still subject of ongoing research. Nevertheless, the rigid model as a preliminary approximation is by far accurate enough to be considered in this study.

HYPOTHESIS 2 : The local wind flow field is known and steady
It is worth to assume that the wind velocity vector is constant over a region much larger than the size of the aircraft, so wind shearing effects and torques will be neglected for this study.

HYPOTHESIS 3 : The total mass of the aeroplane remains constant with time
In the problem we tackle we will consider the take-off or approach manoeuvres of a conventional commercial aeroplane. For example, a typical aeroplane of 180 passengers will consume around $1\,000\,kg$ *during a climb to cruise altitude, being its total mass of about* $70\,000\,kg$*. Therefore the mass change over the considered time period will be about 1.5% which is negligible for our problem.*

HYPOTHESIS 4 : The mass distribution is also constant with time
Passenger movements, fuel sloshing and shifting payloads effects are neglected and therefore the centre of gravity of the aeroplane will be supposed to stay in the same place during the time period of consideration.

HYPOTHESIS 5 : The reference frame G is supposed to be an *inertial* frame
In fact, Ground reference fame is both accelerating and rotating, however the accelerations associated with the Earth's motion can be neglected if compared to the accelerations that will experiment the manoeuvring aircraft. This is equivalent to consider a flat non-rotating Earth.

C.2.2 Dynamic analysis

Taking into account all above hypotheses, Newton's Second Law, applied to translational motion, can be written in the Ground (inertial) reference frame as:

$$\sum \vec{F}_G = m\left[\frac{d}{dt_G}\vec{v}_G^G\right] = m\left[\frac{d}{dt_G}\left(\vec{v}_G^A + \vec{w}_G^G\right)\right] = m\left[\frac{d}{dt_G}\vec{v}_G^A\right] \tag{C.21}$$

were $\sum \vec{F}_G$ is the sum of all external forces applied to the aircraft, m is the total mass of the aircraft, $\vec{v}$ is the velocity of the centre of mass of the aircraft and $\vec{W}$ is the local wind velocity.

As it will be seen later, aerodynamic forces are much simpler if represented in the Air reference frame. Therefore, it is interesting to rewrite equation (C.21) and express all magnitudes with respect to this frame. See, for instance, (Beer *et al.* , 2004) for the details in how to transform derivative magnitudes from one reference frame to another:

$$\sum \vec{F}_A = m\left[\frac{d}{dt_G}\vec{v}_A^A\right] = m\left[\frac{d}{dt_A}\vec{v}_A^A + \vec{\omega}_A^{GA}\times\vec{v}_A^A\right] = m\left[\dot{\vec{v}}_A^A + \vec{\omega}_A^{GB}\times\vec{v}_A^A + \vec{\omega}_A^{BA}\times\vec{v}_A^A\right] \tag{C.22}$$

where $\vec{\omega}^{XY}$, is the angular velocity vector of frame Y relative to frame X.

The sum of all external applied forces can be split as:

$$\sum \vec{F}_A = \vec{F}_A^a + \vec{F}_A^p + m\boldsymbol{\mathcal{R}}_{AB}\boldsymbol{\mathcal{R}}_{BG}\vec{g}_G \tag{C.23}$$

were $\vec{F}^a$ represents the sum of all aerodynamic forces, $\vec{F}^p$ the sum of all propulsive forces and $\vec{g}$ is the local gravity vector.

Finally, by using last force representation and substituting $\vec{\omega}_A^{GB}$ by $\boldsymbol{\mathcal{R}}_{AB}\vec{\omega}_B^{GB}$, Newton's Second Law expressed in Air reference frames is given by:

$$\vec{F}_A^a + \vec{F}_A^p + m\boldsymbol{\mathcal{R}}_{AB}\boldsymbol{\mathcal{R}}_{BG}\vec{g}_G = m\left[\dot{\vec{v}}_A^A + \boldsymbol{\mathcal{R}}_{AB}\vec{\omega}_B^{GB} \times \vec{v}_A^A + \vec{\omega}_A^{BA} \times \vec{v}_A^A\right] \tag{C.24}$$

And in the case we use the direct relation between $\mathbf{G}$ and $\mathbf{A}$ reference frames, last expression becomes:

$$\vec{F}_A^a + \vec{F}_A^p + m\boldsymbol{\mathcal{R}}_{AG}\vec{g}_G = m\left[\frac{d}{dt_G}\vec{v}_A^A\right] = m\left[\frac{d}{dt_A}\vec{v}_A^A + \vec{\omega}_A^{GA} \times \vec{v}_A^A\right] \tag{C.25}$$

Now, all vectors used in equations (C.24) and (C.25) will be expanded in their three components.

As commented before, in the Air reference frame aerodynamic forces can easily written as:

$$\vec{F}_A^a = \begin{bmatrix} -D \\ Y \\ -L \end{bmatrix} \tag{C.26}$$

Where D and L are the *Drag* and *Lift* aerodynamic forces and Y the aerodynamic sideforce component along the Air y_A axis.

Concerning the propulsive forces, we will assume the following hypothesis:

HYPOTHESIS 6 : The sum of all propulsive forces is a vector along $\mathbf{x_B}$ axis
In modern jet aircraft, with the engines under the main wings, there exist typically a small thrust component in the vertical z_B body axis that will be neglected in this study. In addition we will assume that in our study all aircraft's engines are always operative producing a symmetrical thrust force regarding the x_B-z_B plane.

Therefore, we have:

$$\vec{F}_A^p = \boldsymbol{\mathcal{R}}_{AB}\vec{F}_B^a = \begin{bmatrix} \cos\alpha\cos\beta & \sin\beta & \sin\alpha\cos\beta \\ -\cos\alpha\sin\beta & \cos\beta & -\sin\alpha\sin\beta \\ -\sin\alpha & 0 & \cos\alpha \end{bmatrix} \begin{bmatrix} T \\ 0 \\ 0 \end{bmatrix} = \begin{bmatrix} T\cos\alpha\cos\beta \\ -T\cos\alpha\sin\beta \\ -T\sin\alpha \end{bmatrix} \tag{C.27}$$

where T is the total net thrust force generated by all the engines of the aircraft.

The local gravity vector $\vec{g}$ in the Ground reference frame is simply:

$$\vec{g}_G = \begin{bmatrix} 0 \\ 0 \\ g \end{bmatrix} \quad \text{with } g \simeq 9.81\ ms^{-2} \tag{C.28}$$

On the other hand, and by definition, $\vec{v}^A$ in $\mathbf{A}$ reference frame is written as:

$$\vec{v}_A^A = \begin{bmatrix} v \\ 0 \\ 0 \end{bmatrix} \tag{C.29}$$

where v is module of the relative air to aircraft velocity, also known as the *True Airspeed* (TAS). The components of vectors $\vec{\omega}_G^{GB}$ and $\vec{\omega}_A^{GA}$ are defined as:

$$\vec{\omega}_G^{GB} = \begin{bmatrix} p_B \\ q_B \\ r_B \end{bmatrix} \quad \vec{\omega}_G^{GA} = \begin{bmatrix} p_A \\ q_A \\ r_A \end{bmatrix} \tag{C.30}$$

Finally, in (Stevens & Lewis, 1992) is shown that vector $\vec{\omega}_A^{BA}$ can be expressed as:

$$\vec{\omega}_A^{BA} = \begin{bmatrix} -\dot{\alpha}\sin\beta \\ -\dot{\alpha}\cos\beta \\ \dot{\beta} \end{bmatrix} \tag{C.31}$$

In our study it will be perfectly reasonable to assume the following hypothesis:

HYPOTHESIS 7 : The sideslip angle is considered to be zero
This hypothesis assumes that the flight is always symmetrical and turns are always coordinated, which is perfectly reasonable in civil transport aircraft when all engines are operative. Then we assume $\beta \simeq 0$.

Last hypothesis leads to $Y = 0$ and $\boldsymbol{\mathcal{R}}_{AB}$ becomes:

$$\boldsymbol{\mathcal{R}}_{AB} = \begin{bmatrix} \cos\alpha & 0 & \sin\alpha \\ 0 & 1 & 0 \\ -\sin\alpha & 0 & \cos\alpha \end{bmatrix} \tag{C.32}$$

Taking into account all above considerations, equation (C.24) can be finally expanded as:

$$\begin{aligned} \dot{v} &= \tfrac{1}{m}T\cos\alpha - \tfrac{1}{m}D + g(-\cos\alpha\sin\theta + \sin\alpha\cos\theta\cos\phi) \\ 0 &= vp\sin\alpha - vr\cos\alpha + g(\cos\theta\sin\phi) \\ \dot{\alpha}v &= -\tfrac{1}{m}T\sin\alpha + \tfrac{1}{m}L - vq + g(\sin\alpha\sin\theta + \cos\alpha\cos\theta\cos\phi) \end{aligned} \tag{C.33}$$

On the other hand, when the Air reference frame is considered, equation (C.25) is expanded as:

$$\begin{aligned} \dot{v} &= \tfrac{1}{m}T\cos\alpha - \tfrac{1}{m}D - g\sin\gamma \\ 0 &= vr_A - g(\cos\gamma\sin\mu) \\ 0 &= -vq_A + \tfrac{1}{m}L + \tfrac{1}{m}T\sin\alpha - g\cos\gamma\cos\mu \end{aligned} \tag{C.34}$$

C.2.3 Kinematic analysis

The determination of the flight path of the aeroplane relative to the Ground reference system will be done by numerical integration of the Ground coordinates of the aeroplane, which in turn, are expressed as functions of the velocity of centre of mass of the aircraft as:

$$\dot{\vec{r}}_G = \vec{v}_G^G = \boldsymbol{\mathcal{R}}_{GB}\boldsymbol{\mathcal{R}}_{BA}\vec{v}_A^A + \vec{W}_G^G \tag{C.35}$$

If we assume that the local wind has north, east and up velocity components as:

$$\vec{W}_G^G = \begin{bmatrix} W_n \\ W_e \\ W_h \end{bmatrix} \tag{C.36}$$

the expansion of equation (C.35) leads to:

$$\begin{bmatrix} \dot{n} \\ \dot{e} \\ \dot{h} \end{bmatrix} = v \begin{bmatrix} \cos\psi(\cos\alpha\cos\theta + \sin\alpha\sin\theta\cos\phi) + \sin\psi\sin\alpha\sin\phi \\ \sin\psi(\cos\alpha\cos\theta + \sin\alpha\sin\theta\cos\phi) - \cos\psi\sin\alpha\sin\phi \\ -(\cos\alpha\sin\theta - \sin\alpha\cos\theta\cos\phi) \end{bmatrix} + \begin{bmatrix} w_n \\ w_e \\ w_h \end{bmatrix} \tag{C.37}$$

And in the case we use the direct relation between Ground and Air reference frames, last expression becomes:

$$\dot{\vec{r}}_G = \vec{v}_G^G = \boldsymbol{\mathcal{R}}_{GA}\vec{v}_A^A + \vec{W}_G^G \tag{C.38}$$

$$\begin{bmatrix} \dot{n} \\ \dot{e} \\ \dot{h} \end{bmatrix} = v \begin{bmatrix} \cos\chi\cos\gamma \\ \sin\chi\cos\gamma \\ -\sin\gamma \end{bmatrix} + \begin{bmatrix} W_n \\ W_e \\ W_h \end{bmatrix} \tag{C.39}$$

In order to perform this integration, the set of Euler angles $[\psi\ \theta\ \phi]$, which are functions of time, should be known. In this context, the angle rates can be written as functions of the angular rates of the Body axes $\vec{\omega}_G^{GB} = [p\ q\ r]^T$. In order to do so, we should consider that each Euler angle rate is expressed, by definition, in a different reference frame. Then, we have:

$$\begin{bmatrix} p \\ q \\ r \end{bmatrix} = \begin{bmatrix} \dot{\phi} \\ 0 \\ 0 \end{bmatrix} + \boldsymbol{\mathcal{R}}^{\phi} \begin{bmatrix} 0 \\ \dot{\theta} \\ 0 \end{bmatrix} + \boldsymbol{\mathcal{R}}^{\phi}\boldsymbol{\mathcal{R}}^{\theta} \begin{bmatrix} 0 \\ 0 \\ \dot{\psi} \end{bmatrix} \tag{C.40}$$

and, therefore:

$$\begin{bmatrix} p \\ q \\ r \end{bmatrix} = \begin{bmatrix} \dot{\phi} - \dot{\psi}\sin\theta \\ \dot{\theta}\cos\phi + \dot{\psi}\cos\theta\sin\phi \\ \dot{\psi}\cos\theta\cos\phi - \dot{\theta}\sin\phi \end{bmatrix} \tag{C.41}$$

On the other hand, if Air to Ground angles $[\chi\ \gamma\ \mu]$ are used, we can relate their rates to the Air axes angular rates $\vec{\omega}_G^{GA} = [p_A\ q_A\ r_A]^T$ as:

$$\begin{bmatrix} p_A \\ q_A \\ r_A \end{bmatrix} = \begin{bmatrix} \dot{\mu} \\ 0 \\ 0 \end{bmatrix} + \boldsymbol{\mathcal{R}}^{\mu} \begin{bmatrix} 0 \\ \dot{\gamma} \\ 0 \end{bmatrix} + \boldsymbol{\mathcal{R}}^{\mu}\boldsymbol{\mathcal{R}}^{\gamma} \begin{bmatrix} 0 \\ 0 \\ \dot{\chi} \end{bmatrix} \tag{C.42}$$

and, therefore:

$$\begin{bmatrix} p_A \\ q_A \\ r_A \end{bmatrix} = \begin{bmatrix} \dot{\mu} - \dot{\chi}\sin\gamma \\ \dot{\gamma}\cos\mu + \dot{\chi}\cos\gamma\sin\mu \\ \dot{\chi}\cos\gamma\cos\mu - \dot{\gamma}\sin\mu \end{bmatrix} \tag{C.43}$$

C.2.4 Aerodynamic and propulsive forces

As it was seen in equation (C.23), an aeroplane flying through the atmosphere experiments gravitational, aerodynamic and propulsive forces. The reader should refer, for example, to (Anderson, 2008) or (Roskam, 2001) for a detailed view in the modelling of aircraft aerodynamics.

Summing up, aerodynamic components L and D (see equation (C.26)) can be modelled in function of the aerodynamic coefficients C_L and C_D as:

$$L = \frac{1}{2}\rho(h)Sv^2C_L \tag{C.44}$$

$$D = \frac{1}{2}\rho(h)Sv^2C_D \tag{C.45}$$

where $\rho(h)$ is the air density, which can be considered only altitude dependant and S is the total surface of the wings. On the other hand, aerodynamic coefficient C_D is in a first approximation usually modelled as a quadratic function of C_L:

$$C_D = C_{D_0} + \frac{1}{\pi AR\bar{e}}{C_L}^2 \tag{C.46}$$

where C_{D_0} is a known aerodynamic parameter, AR is the aspect ratio of the wing $AR = \frac{\bar{b}^2}{S}$ (with $\bar{b}$ the total wing span) and $\bar{e}$ the *Oswald factor* of the wing. On the other hand, lift coefficient is usually fitted to a linear function of the angle of attack:

$$C_L = C_{L_0} + C_{L_\alpha}\alpha \tag{C.47}$$

where C_{L_0} and C_{L_α} are two known aerodynamic parameters of the aircraft.

By using equations (C.44), (C.46), (C.47) and (C.45) we can express the aerodynamic drag force as a function of the airspeed and air density as:

$$D = \frac{SC_{D_0}}{2}\rho(h)v^2 + \frac{2}{\pi AR\bar{e}S}\frac{L^2}{\rho(h)v^2} \tag{C.48}$$

Finally, concerning the propulsive force, for a turbofan engine type, this force usually depends on the thrust setting σ (configured by the pilot) as well as the altitude and velocity of the aircraft:

$$T = T(\sigma, v, h) \tag{C.49}$$

C.2.4.1 Atmosphere model

The International Standard Atmosphere (ISA) is an atmospheric model of how the pressure, temperature, density, and viscosity of the Earth's atmosphere change over a wide range of altitudes. It consists of tables of values at various altitudes, plus some formulas by which those values were derived. The International Civil Aviation Organisation (ICAO) has adopted this standard with

Table C-1: *Basic parameters used in the International Standard Atmosphere (ISA)*

$\rho_0 = 1.225\ \frac{Kg}{m^3}$	standard sea level air density
$\mathcal{T}_0 = 288.15\ K$	standard sea level air temperature
$K_{\mathcal{T}} = -6.510^{-3}\ \frac{K}{m}$	ISA temperature gradient below tropopause
$R = 287.04\ \frac{m^2}{Ks^2}$	ideal gas constant for the atmosphere

some few modifications. In (ICAO, 1993b) is shown a model for the air density as a function of the altitude and is summarised as follows:

Below the tropopause, the air density is calculated as a function of temperature $\mathcal{T}$, assuming the following perfect gas equation:

$$\rho = \rho_0 \left[\frac{\mathcal{T}}{\mathcal{T}_0}\right]^{-\left(1+\frac{g}{K_{\mathcal{T}}R}\right)} \tag{C.50}$$

where each ISA parameter is defined in Table C-1.

On the other hand, the ISA vertical temperature profile is defined as:

$$\mathcal{T} = \mathcal{T}_0 + K_{\mathcal{T}} h \tag{C.51}$$

and finally, from equations (C.50) and (C.51) it follows:

$$\rho(h) = \rho_0 \left[1 + \frac{K_{\mathcal{T}}}{\mathcal{T}_0} h\right]^{-\left(1+\frac{g}{K_{\mathcal{T}}R}\right)}. \tag{C.52}$$

C.3 State-space representation

As explained in the introduction of this Appendix, the state variables are defined as a set of variables such that the knowledge of the state vector at a particular time and the control vector after this time, completely defines the motion from that time on.

The typical control variables used in common autopilots for attitude guidance are pitch and roll angles, $[\theta,\ \phi]$, being these three magnitudes easily measured by common gyroscopic systems installed in the majority of aircraft. However, the use of these three angles (plus the trust setting variable) as the control vector leads to a complex state-space representation when joining equations (C.33), (C.37) and (C.41). On the other hand, if we suppose that the autopilot system can deal with $[\gamma, \mu]$ or $[\alpha, \mu]$ angles there is the possibility of expressing all magnitudes into the Air reference frame, which simplifies considerably the state equations and playing an important role for easing further optimisation algorithms. This assumption is not a serious drawback because the main goal of this work is not to build an autopilot system but to compute an optimal trajectory. Therefore, once the optimal trajectory has been obtained the optimal values of angles $[\theta,\ \phi]$ or whatever the autopilot system needs can be easily computed by applying the proper transformation matrices. In addition, it should be noted that thanks to the wide use of high performance inertial reference systems and integrated auto-pilots architecture, it is worth to suppose that in a near future an autopilot may deal directly with $[\alpha, \mu]$ or even $[n_z, \mu]$ as control guidance inputs,

being $\mathsf{n_z}$ the vertical load factor as it will be introduced next. Similar works in the domain of trajectory optimisation already use the load factor as input variable, see for instance the optimisation software described in (Virtanen *et al.* , 1999).

Then, using the direct relation between **G** and **A** reference frames we substitute equations (C.43) into (C.34), obtaining:

$$\begin{aligned} \dot{v} &= \tfrac{1}{m}T\cos\alpha - \tfrac{1}{m}D - g\sin\gamma \\ \dot{\chi} &= \tfrac{1}{mv\cos\gamma}L\sin\mu + \tfrac{1}{mv\cos\gamma}T\sin\mu\sin\alpha \\ \dot{\gamma} &= \tfrac{1}{mv}L\cos\mu + \tfrac{1}{mv}T\cos\mu\sin\alpha - \tfrac{g}{v}\cos\gamma \end{aligned} \tag{C.53}$$

Let us define the state and control vectors as:

$$\begin{aligned} \vec{x} &= [v\ \chi\ \gamma\ n\ e\ h]^T \\ \vec{u} &= [\alpha\ \mu\ \sigma]^T \end{aligned} \tag{C.54}$$

And merging equations (C.53) and (C.39) in a one single expression we obtain a state-space representation as:

$$\begin{bmatrix} \dot{v} \\ \dot{\chi} \\ \dot{\gamma} \\ \dot{n} \\ \dot{e} \\ \dot{h} \end{bmatrix} = \begin{bmatrix} \frac{1}{m}\left[T(\sigma,v,h)\cos\alpha - D(\alpha,v,h) - mg\sin\gamma\right] \\ \frac{\sin\mu}{mv\cos\gamma}[L(\alpha,v,h) + T(\sigma,v,h)\sin\alpha] \\ \frac{1}{mv}\left[L(\alpha,v,h)\cos\mu + T(\sigma,v,h)\cos\mu\sin\alpha - mg\cos\gamma\right] \\ v\sin\chi\cos\gamma + W_e \\ v\cos\chi\cos\gamma + W_n \\ v\sin\gamma + W_h \end{bmatrix} \tag{C.55}$$

This state space representation can be further simplified if the vertical load factor is used as an input variable instead of α. The vertical load factor is defined by:

$$\mathsf{n_z} = \frac{L}{mg} \tag{C.56}$$

In recent fly-by-wire auto-flight systems, the vertical load factor has been used as an input control variable even in manual modes. See, for example (Favre, 1996), where the introduction of fly-by-wire technology by Airbus Industries is explained. In the Airbus A320 or A340 families the *pitch* input produced by moving forward and backwards the side-stick control yoke is directly proportional to the vertical load factor that the pilot desires. In addition, let us consider the following two hypotheses:

HYPOTHESIS 8 : The angle of attack is supposed small
If we consider normal *depart or approach flight operations for a jet transport aircraft, it is worth supposing that the angle of attack α is small. In general, it takes values of few degrees and can reach exceptionally values around 10^o. This assumption leads to the following approximations:* $\cos\alpha \simeq 1$ *and* $\sin\alpha \simeq \alpha$.

HYPOTHESIS 9 : The vertical component of the thrust vector can be neglected
For normal jet transport aircraft it holds that $\frac{T}{mg}\sin\alpha << \mathsf{n_z}$. *Actually,* $\mathsf{n_z}$ *takes values from* 0.85 *to*

1.15 *in normal operations. Moreover, for the case of the Airbus A340-600, the typical empty weight is* 177 000 *kg, while the maximum thrust at sea level and per engine is approximately* 184 000 *N. For 4 operative engines and a relatively high angle of attack of* 7^o *we have* $\frac{T}{mg}\sin\alpha \simeq 0.05$*, which can be neglected. It should be noted that this value is the limiting worst case value since the mass of the aircraft will be higher (the maximum take-off mass for this aircraft is* 368 000 *kg) and the thrust will notably decrease with the altitude.*

Then, taking all above considerations into account, the final state-space representation for the aircraft equations of motion becomes:

$$\begin{aligned}\vec{x} &= [v\ \chi\ \gamma\ n\ e\ h]^T \\ \vec{u} &= [\mathsf{n_z}\ \mu\ \sigma]^T\end{aligned} \tag{C.57}$$

$$\begin{bmatrix}\dot{v}\\ \dot{\chi}\\ \dot{\gamma}\\ \dot{n}\\ \dot{e}\\ \dot{h}\end{bmatrix} = \begin{bmatrix}\frac{1}{m}\left[T(\sigma,v,h) - D(\mathsf{n_z},v,h) - mg\sin\gamma\right]\\ \frac{g}{v}\frac{\sin\mu}{\cos\gamma}\mathsf{n_z}\\ \frac{g}{v}\left[\mathsf{n_z}\cos\mu - \cos\gamma\right]\\ v\sin\chi\cos\gamma + W_e\\ v\cos\chi\cos\gamma + W_n\\ v\sin\gamma + W_h\end{bmatrix} \tag{C.58}$$

If the vertical load factor is used as input variable, the drag equation (C.48) is rewritten as follows,

$$D(v,\rho(h),\mathsf{n_z}) = \frac{1}{2}\rho(h)SC_{D_0}v^2 + 2\frac{(mg)^2}{\pi A\bar{e}S}\frac{\mathsf{n_z}^2}{\rho(h)v^2} \tag{C.59}$$

or, in a more general way:

$$D(v,\rho(h),\mathsf{n_z}) = \frac{1}{2}\rho(h)Sav^2 + \frac{2b}{\rho(h)S}\left[\frac{\mathsf{n_z}mg}{v}\right]^2 \tag{C.60}$$

where the aerodynamic parameters a and b are Mach dependant and influenced by the flap/slat and landing gear configuration. These parameters are, in general, empirically obtained and published by the aircraft manufacturer in performance data manuals.

C.4 Summary of the hypotheses adopted in the model

All hypotheses that have been used in this Appendix for constructing the flight mechanics model of a flying aeroplane are summarised below.

HYPOTHESIS 1 : The aircraft is supposed to be rigid

HYPOTHESIS 2 : The local wind flow field is known and steady

HYPOTHESIS 3 : The total mass of the aeroplane remains constant with time

HYPOTHESIS 4 : The mass distribution is also constant with time

HYPOTHESIS 5 : The reference frame $\mathbf{G}$ is supposed to be an *inertial* frame

HYPOTHESIS 6 : The sum of all propulsive forces is a vector along $\mathbf{x_B}$ axis

HYPOTHESIS 7 : The sideslip angle is considered to be zero

HYPOTHESIS 8 : The angle of attack is supposed small

HYPOTHESIS 9 : The vertical component of the thrust vector can be neglected

A single grain of sand is certainly not a heap. Nor is the addition of a single grain of sand enough to transform a non-heap into a heap. When we have a collection of grains of sand that is not a heap, then adding but one single grain will not create a heap. And so by adding successive grains, moving from 1 to 2 to 3 and so on, we will never arrive at a heap. And yet we know full well that a collection of 1,000,000 grains of sand is a heap, even if not an enormous one.

— Ubulides of Miletus (Sorites Paradox)

D

Background on fuzzy rule-based systems

In 1920, the Polish logician and philosopher Jan Łukasiewicz introduced the notion of a multi-valued logic by proposing a third additional truth value. This value was *possibly true or false* and belonged somewhere between true and false. Later on, he also explored a four-valued and five-valued logic. But it was Lofti Zadeh who introduced the fuzzy sets theory (Zadeh, 1965) and further developed its mathematical framework (Zadeh, 1975a; Zadeh, 1975b; Zadeh, 1975c; Zadeh, 1978; Zadeh, 1983).

Conventional, or regular sets are often called *crisp sets* in fuzzy logic terminology. Let $\mathcal{X}$ be a universal set, which contains all the elements of interest for our application. Let $\mathcal{A}$ be a subset of $\mathcal{X}$. The conventional membership function of $\mathcal{A}$ is defined such as a function $\mu_{\mathcal{A}} : \mathcal{X} \rightarrow \{0, 1\}$ denoting that an element $x \in \mathcal{X}$ is either a member of $\mathcal{A}$ or it is not:

$$\mu_{\mathcal{A}}(x) = \begin{cases} 1 & \text{if} \quad x \in \mathcal{A} \\ 0 & \text{if} \quad x \notin \mathcal{A} \end{cases} \tag{D.1}$$

In contrast, the fuzzy membership function can accommodate various *degrees of membership* on the real continuous interval $[0, 1]$, where the endpoints of 0 and 1 confirm to no membership and full membership, respectively, like in crisp sets. However, the infinite number of values in between the endpoints can represent various degrees of membership of the element x in the *fuzzy* set $\mathcal{A}$. Therefore, the membership function of a fuzzy set $\mathcal{A}$ maps from the universe $\mathcal{X}$ to this continuous interval: $\mu_{\mathcal{A}} : \mathcal{X} \rightarrow [0, 1]$.

Fuzzy sets enjoy from some properties, like crisp sets do. In addition, we can define some operations on these sets. For a detailed list of operations and properties of fuzzy and crisp sets and membership functions, the reader is referred for example, to (Buckley & Eslami, 2002) or (Ross, 1995).

Here, we summarise the basic notions of complementation, intersection and union of fuzzy sets. Let $\mathcal{X}$ be the universe of discourse, $\mathcal{A} \subseteq \mathcal{X}$ and $\mathcal{B} \subseteq \mathcal{X}$ be two fuzzy sets and $\mu_{\mathcal{A}}$ and $\mu_{\mathcal{B}}$ be their respective membership functions. We denote the complementation (or negation) of set $\mathcal{A}$ as [NOT $\mathcal{A}$] or simply $\bar{\mathcal{A}}$. This negation is defined as $\mu_{\bar{\mathcal{A}}}(x) = 1 - \mu_{\mathcal{A}}(x), \forall x \in \mathcal{X}$. It is worth mentioning that the generalisation of boolean operations on fuzzy sets is not unique. This is the case, for example for the intersection ($\cap$) and union ($\cup$) operations. Therefore, several *t-norms* and *t-conorms* can be defined for the intersection and union operations respectively. Table D-1 summarises the principal norms used in fuzzy logic applications.

D.1 Fuzzy rule-based systems

Natural language is perhaps the most powerful form of conveying information that humans possess for any given problem or situation that requires solving or reasoning. In fact, there is a certain amount of vagueness and ambiguity in our language that can be modelled by using fuzzy sets and fuzzy logic.

A fuzzy rule-based system processes one or several inputs deriving one or several outputs. The way in how the output is obtained depends on a set of rules that can be formulated in natural language by a group of experts, based on their knowledge. These rules will deal with fuzzy numbers or fuzzy sets representing the different magnitudes of the analysed system. However the input(s) of the system will be, in general real numbers for example, coming from input sensors. Therefore a *fuzzification* process will be firstly needed in order to build some fuzzy sets from the system input(s). In the same way, the output must be, in general, a real number understandable by a machine or computer. Then, a *defuzzification* will allow to extract these system output(s) from the fuzzy sets obtained as a conclusion derived from the application of the rules.

D.1.1 Fuzzification

Fuzzification is the process of making a crisp quantity fuzzy. In other words, one can talk about *fuzzy numbers*. For example, a fuzzy number expressing *approximately seven* can have a membership function that takes 1 if $x = 7$ but decreases progressively to 0 as x increases or decreases from $x = 7$. Therefore, we could say that if $x = 6.9$, x is approximately 7 in some degree of membership $\mu(x) \in [0, 1]$. See Figure D-1(a). Similarly, we can also construct *fuzzy intervals* if, for example we say that x is *approximately seven to nine* (see Figure D-1(b)).

In Figure D-1 we have used *triangular* shaped functions to denote the membership degree of each fuzzy set in the continuous case. Triangular functions are the simplest ones and they are the

Table D-1: *Principal t-norms and t-conorms used in fuzzy logic*

t-norms		t-conorms	
	$= \min(\mu_{\mathcal{A}}(x), \mu_{\mathcal{B}}(x))$		$= \max(\mu_{\mathcal{A}}(x), \mu_{\mathcal{B}}(x))$
$\mu_{\mathcal{A}\cap\mathcal{B}}$	$= \mu_{\mathcal{A}}(x) \cdot \mu_{\mathcal{B}}(x)$	$\mu_{\mathcal{A}\cup\mathcal{B}}$	$= \mu_{\mathcal{A}}(x) + \mu_{\mathcal{B}}(x)$
	$= \max(\mu_{\mathcal{A}}(x) + \mu_{\mathcal{B}}(x) - 1, 0)$		$= \min(\mu_{\mathcal{A}}(x) + \mu_{\mathcal{B}}(x), 1)$

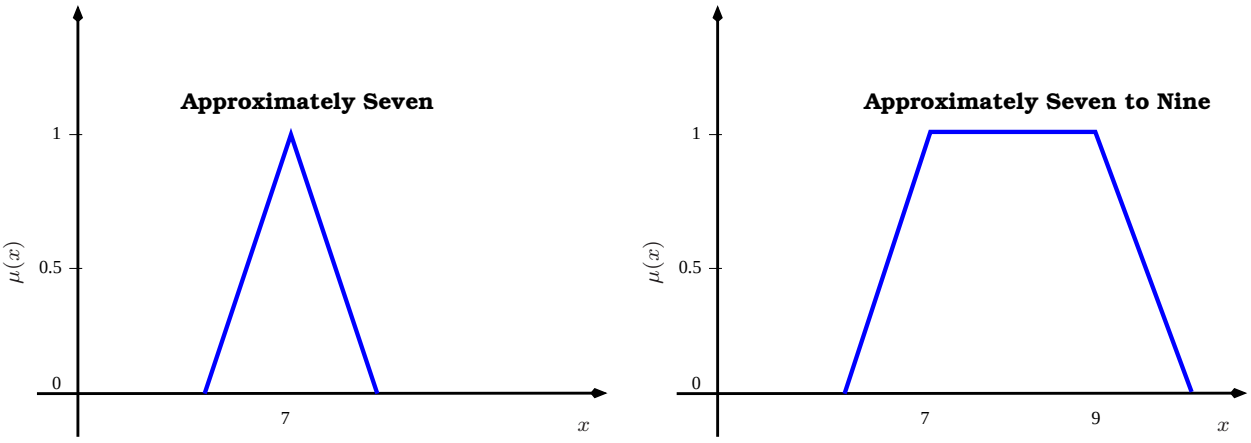

(a) Approximately seven (b) Approximately seven to nine

Figure D-1: *Simple examples for a fuzzy number and a fuzzy interval*

most used set-membership functions to describe fuzzy sets in fuzzy control. They are appropriate because the fuzzy reasoning and tuning process is simplified and they are more computational friendly too (Tanaka, 1997). Otherwise, if the universe of discourse $\mathcal{X}$ is discrete, a fuzzy set $\mathcal{A} \in \mathcal{X}$ is usually written by using the following notation:

$$\mathcal{A} = \left\{ \frac{\mu_{\mathcal{A}}(x_1)}{x_1}, \cdots, \frac{\mu_{\mathcal{A}}(x_n)}{x_n} \right\} \tag{D.2}$$

where n is the total amount of elements of discrete fuzzy set $\mathcal{A}$.

Finally, it is worth mentioning that in most applications it is convenient to define *convex* fuzzy sets forming a *fuzzy partition*. Let $\mathcal{X}$ be the universe of discourse. Then, the fuzzy set $\mathcal{A}$ is said to be *convex* if:

$$\mu_{\mathcal{A}}(\lambda x_1 + (1-\lambda)x_2) \leq \min(\mu_{\mathcal{A}}(x_1), \mu_{\mathcal{A}}(x_2)) \,; \quad \forall x_1, x_2 \in \mathcal{X}, \, \forall \lambda \in]0,1] \tag{D.3}$$

On the other hand n fuzzy sets $(\mathcal{A}_1, ..., \mathcal{A}_n)$ defined on the universe of discourse $\mathcal{X}$ form a *fuzzy partition* if:

$$\sum_{i=1}^{n} \mu_{\mathcal{A}}(x) = 1 \,; \quad \forall x \in \mathcal{X} \tag{D.4}$$

It can easily be proved that in the case of having a fuzzy partition composed by fuzzy convex sets, a maximum of two membership functions will take values for a same $x \in \mathcal{X}$.

D.1.2 Defuzzification

In contrast with the fuzzification method, the defuzzification assigns a real number to a fuzzy subset of the reals numbers. Several strategies exist to perform this operation. In general the output of a fuzzy process or system may be the the logical union of two or more fuzzy membership functions defined on the universe of discourse of the output variable, being this final output a fuzzy subset itself. But, if this final conclusion is to be communicated to a machine it must be defuzzified because a machine will not understand a complete fuzzy set.

There are several methods for defuzzifying fuzzy output functions (see (Hellendoorn & Thomas, 1993)). Let $\mathcal{A}$ be the fuzzy set to be defuzzified, $\mu_{\mathcal{A}}(x)$ the membership function of x into the set $\mathcal{A}$ and $\tilde{x}$ the defuzzified value of $\mathcal{A}$. Among the most popular

defuzzification methods, we cite the following:

- **The centroid**, centre of area, or centre of gravity method:

$$\tilde{x} = \frac{\int x\mu_{\mathcal{A}}(x)\,\mathrm{d}x}{\int \mu_{\mathcal{A}}(x)\,\mathrm{d}x} \tag{D.5}$$

  which, for the discrete case yields to:

$$\tilde{x} = \frac{\sum_{i=1}^{n} x_i\mu_{\mathcal{A}}(x_i)}{\sum_{i=1}^{n} \mu_{\mathcal{A}}(x_i)} \tag{D.6}$$

- **The centre of maxima**, height or max-membership method:

$$\tilde{x} = \{\tilde{x}\,|\,\mu_{\mathcal{A}}(\tilde{x}) \geq \mu_{\mathcal{A}}(x)\,,\quad \forall x \in \mathcal{A}\} \tag{D.7}$$

- **The mean of the maxima**, or middle of maxima or mean-max membership method:

$$\tilde{x} = \frac{\int_{\mathcal{B}} x\mu_{\mathcal{A}}(x)\,\mathrm{d}x}{\int_{\mathcal{B}} \mu_{\mathcal{A}}(x)\,\mathrm{d}x}\;; \qquad \mathcal{B} = \{y\,|\,\mu_{\mathcal{A}}(y) \geq \mu_{\mathcal{A}}(x)\,,\quad \forall x \in \mathcal{A}\} \tag{D.8}$$

  with an equivalent discrete form as in equation (D.6).

All these methods have advantages and disadvantages, regarding continuity, disambiguity, plausibility and computational simplicity and the chosen method should be assessed in terms of the goodness of the answer in the context of the data available. See (Ross, 1995) and the references therein.

D.1.3 Rule base

A method of processing information through fuzzy rules is called approximate reasoning. Perhaps, the most common way to represent human knowledge is to form it into natural language expressions of the type:

`IF` premise (antecedent), `THEN` conclusion (consequent)

This form is commonly referred to as the `IF-THEN` rule-based form, expressing an inference such that if we know a fact (antecedent), then we can infer another fact (conclusion). By using fuzzy logic terminology, if $\mathcal{A}$ and $\mathcal{B}$ are two fuzzy sets as defined above, we could easily transform the previous rule to a fuzzy rule like:

`IF` x `IS` $\mathcal{A}$, `THEN` y `IS` $\mathcal{B}$

Usually, a premise in a rule is formed from complicated propositions which, in turn, are formed by applying certain operations on atomic propositions. Such operations are, for example, the negation (`NOT`), the conjunction (`AND`) or the disjunction (`OR`). However, even a complex rule can be easily be written with the following general form:

`IF` [x_1 `IS` $\mathcal{A}_1$ `AND` $\cdots$ `AND` x_2 `IS` $\mathcal{A}_2$], `THEN` y `IS` $\mathcal{B}$

A powerful use of rule-based systems is when we use *linguistic variables* in the antecedents and consequents. As shown previously, these linguistic variables can be naturally represented by the fuzzy sets and logical connectives of these sets. Therefore, we call *linguistic values* to the different (fuzzy or crisp) sets that form a given linguistic variable.

D.1.3.1 Properties of the rule base

Most rule-based systems involve more than one rule at the same time. Then we talk about a *rule base*, which might satisfy certain properties, such as *continuity*, *consistency* and *completeness*. Next, we define briefly these properties, which can be further explored in (Kovacic & Bogdan, 2005):

- **Continuity:** A fuzzy rule base is said *continuous* if all the rules with *adjacent* premises have *adjacent* conclusions. The *adjacency* of fuzzy sets consists on placing them in a certain order in their universe of discourse, such as:

$$\mathcal{A}_1 < \mathcal{A}_2 < \cdots \mathcal{A}_i < \mathcal{A}_{i+1} < \cdots \tag{D.9}$$

  where $\mathcal{A}_i$ and $\mathcal{A}_{i+1}$ are adjacent in the same way that $\mathcal{A}_{i-1}$ and $\mathcal{A}_i$ are.

- **Consistency:** A fuzzy rule base is *consistent* if does not contain rules that have equal antecedent parts and different consequent parts:

$$\begin{array}{llll} \mathrm{R}_1\text{: } \texttt{IF} & \text{premise 1,} & \texttt{THEN} & \text{conclusion 1} \\ \mathrm{R}_2\text{: } \texttt{IF} & \text{premise 1,} & \texttt{THEN} & \text{conclusion 2} \end{array}$$

  In this case, rules R_1 and R_2 are not consistent or contradictory.

- **Completeness:** A fuzzy rule base is *complete* if for any combination in the input space there exist a rule that contains that particular combination of inputs in its antecedent part. In this case, it is said that a rule *fires* or *triggers* for a particular combination of inputs.

D.1.3.2 Inference and aggregation

Fuzzy inference is the process of formulating the mapping from a given input to an output using fuzzy logic. Therefore an implication operator ($\rightarrow$) must be also defined in order to evaluate the truthness degree for a given rule R such as `IF` $\mathcal{A}$, `THEN` $\mathcal{B}$ or, simply $\mathcal{A} \rightarrow \mathcal{B}$.

There exist several implication operators in function of the logic interpretation given to the $\mathcal{A} \rightarrow \mathcal{B}$ statement. For example, the classical interpretation of $\mathcal{A} \rightarrow \mathcal{B}$ is defined by $\bar{\mathcal{A}} \cup \mathcal{B}$. Otherwise, the so called *conjunctive implication* is defined by $\mathcal{A} \cap \mathcal{B}$. This last definition is the most commonly used in fuzzy logic applications. For example, the Mamdani implication is defined as:

$$\mu_{\mathrm{R}}(x, y) = \min(\mu_{\mathcal{A}}(x), \mu_{\mathcal{B}}(y)) \tag{D.10}$$

On the other hand, the Larsen implication is written by:

$$\mu_{\mathrm{R}}(x, y) = \mu_{\mathcal{A}}(x) \cdot \mu_{\mathcal{B}}(y) \tag{D.11}$$

For other forms of the implication operation, the reader should refer to (Ross, 1995) and the references therein.

Moreover, the *aggregation of rules* is the process of obtaining the overall consequent from the individual consequents contributed by separate rules. Depending on the selected operator for the implication (classic or conjunctive) the aggregation will be conjunctive or disjunctive respectively. Therefore, if we consider a conjunctive implication operator, the rule base is supposed to be formed by a set of m rules linked by the `OR` operator. Like in the inference mechanism, several aggregation operators may be defined such as *maximum*:

$$\mu_{\mathcal{B}}(y) = \max(\mu_{\mathcal{B}_i}(y), \cdots \mu_{\mathcal{B}_m}(y)) \tag{D.12}$$

or the *sum*:

$$\mu_{\mathcal{B}}(y) = \sum_{i=1}^{m} \mu_{\mathcal{B}_i}(y) \tag{D.13}$$

which, in general, can take values greater than 1. However in the case of working with convex fuzzy partition this sum will always be inside the $[0, 1]$ interval.

D.2 Example of application

In this section we illustrate the previous concepts by using the application presented in this dissertation and presented in section III.4. Let us suppose that we want to compute the Normalised Annoyance Index produced by a sound event with $L_{max} = 77$ dB(A), at $\mathfrak{h}$ =19h, over a *Residential Zone*. This computation is summarised graphically in Figure D-2 and explained as follows.

According to Figure III-5(c), a Noise level of $L_{max} = 77$ dB(A) is to some extent a *Medium (ME)* and a *High (HI)* noise. Being the membership functions triangular, we compute the degree of membership in both fuzzy sets as $\mu_{ME}(77) = 0.3$ and $\mu_{HI}(77) = 0.7$. In a similar way, from Figure III-5(a), the Period of Day of $\mathfrak{h}$ =19h is considered *Afternoon (A)* and *Night (N)* with degrees of membership: $\mu_A(19) = 0.75$ and $\mu_N(19) = 0.25$.

These linguistic variables *fire* four different rules in the rule base defined in Table III-3, which are:

R_1: IF [Type of Zone IS *Residential Zone (RZ)* AND Period of Day IS *Afternoon (A)* AND Noise Level IS *Medium (ME)*] THEN Annoyance IS *Moderate (MA)*

R_2: IF [Type of Zone IS *Residential Zone (RZ)* AND Period of Day IS *Afternoon (A)* AND Noise Level IS *High (HI)*] THEN Annoyance IS *High (HA)*

R_3: IF [Type of Zone IS *Residential Zone (RZ)* AND Period of Day IS *Night (N)* AND Noise Level IS *Medium (ME)*] THEN Annoyance IS *High (HA)*

R_4: IF [Type of Zone IS *Residential Zone (RZ)* AND Period of Day IS *Night (N)* AND Noise Level IS *High (HI)*] THEN Annoyance IS *Extreme (EA)*

For this work we have used the Larsen implication of equation (D.11) along with the sum method for the aggregation process given in equation (D.13). Finally, for the defuzzification process, the centroid method of equation (D.6) has been chosen. Therefore, for the four considered rules we have:

$$\begin{aligned}
\mu_{R_1}(19, 77) &= \mu_A(19) \cdot \mu_{ME}(77) = 0.75 \cdot 0.3 = 0.225 \\
\mu_{R_2}(19, 77) &= \mu_A(19) \cdot \mu_{HI}(77) = 0.75 \cdot 0.7 = 0.525 \\
\mu_{R_3}(19, 77) &= \mu_N(19) \cdot \mu_{ME}(77) = 0.25 \cdot 0.3 = 0.075 \\
\mu_{R_4}(19, 77) &= \mu_N(19) \cdot \mu_{HI}(77) = 0.25 \cdot 0.7 = 0.175
\end{aligned} \tag{D.14}$$

Being the Annoyance expressed by five crisp sets, as shown in Figure III-5(b), the overall Annoyance is to some extent *Moderate (MA)*, *High (HA)* and *Extreme (EA)* and corresponds to the following discrete fuzzy set:

$$\mathcal{B} = \left\{ \frac{0.225}{MA}, \frac{0.6}{HA}, \frac{0.175}{EA} \right\} \tag{D.15}$$

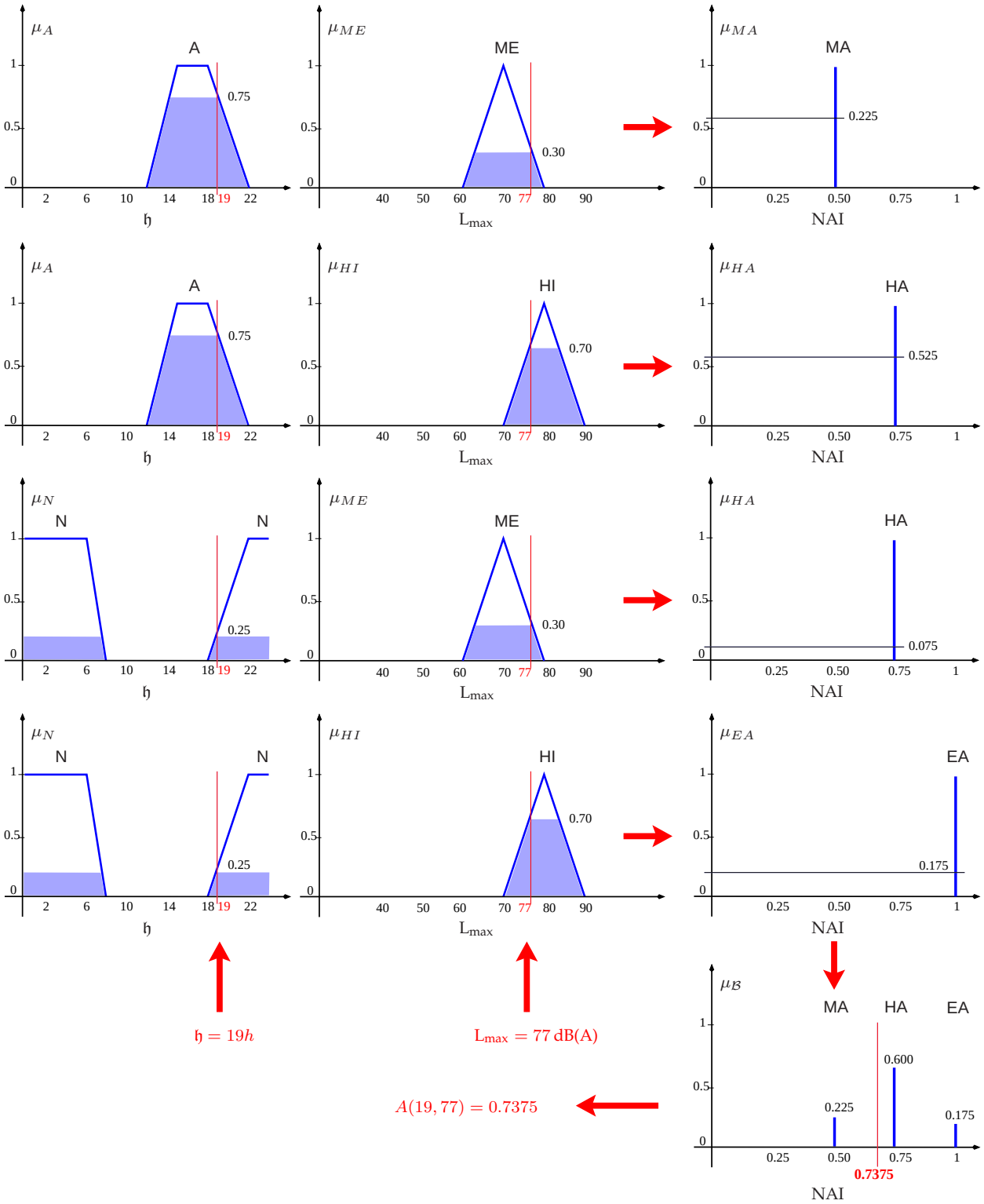

Figure D-2: *Graphical example for the computation of the Normalised Annoyance Index (NAI) corresponding to a sound event with L_{max} = 77 dB(A), at ħ =19h, over a Residential Zone. In this example we have used the Larsen implication method, the sum method for the aggregation process, and the centroid method for the defuzzification process.*

Finally, the defuzzification is rather simple and we obtain the final Normalised Annoyance Index for the residential zone as:

$$A(19, 77) = \frac{0.225 \cdot 0.5 + 0.6 \cdot 0.75 + 0.175 \cdot 1}{0.225 + 0.6 + 0.175} = 0.7375 \tag{D.16}$$

Keep it simple, as simple as possible, but no simpler.

— Albert Einstein

E

List of noise sensitive locations for the Girona scenario

This Appendix contains the exact locations of the measurement points chosen for the application example presented in Chapter VI. A total number of 140 residential points are placed, which 87 among them are in residential areas and 32 in industrial areas. Finally, 3 hospitals and 18 school locations are also considered as special locations. The origin of coordinates is placed at the runway 02 threshold of Girona's airport. This point is located at $41^o\,53'\,41.7''$ N $-2^o\,45'\,29.7''$ E (WGS84) and with an elevation of 122.86 m above the mean sea level (AENA, 2009a). The different locations are expressed by North, East and Height coordinates relatives to this origin. Figure E-1 shows the concerned area with all the measurement locations while their exact location is tabulated as follows.

MEASUREMENT LOCATIONS IN RESIDENTIAL AREAS

Id.	Location name	North (n)	East (e)	Height (h)
#1	Girona 1	6185 m	4685 m	−18 m
#2	Girona 2	5886 m	4893 m	−30 m
#3	Girona 3	6090 m	5132 m	−45 m
#4	Girona 4	6461 m	5390 m	−56 m
#5	Girona 5	7345 m	6053 m	−29 m
#6	Girona 6	11430 m	3637 m	−82 m
#7	Celrà	14509 m	9308 m	−123 m
#8	Medinyà	16858 m	8593 m	−143 m
#9	Ravós de Terri	19476 m	6567 m	−111 m
#10	Palol de Revardit	19493 m	3747 m	−82 m
#11	Fornells de la Selva 1	3894 m	3734 m	−25 m
#12	Fornells de la Selva 2	4283 m	3956 m	−29 m
#13	Fornells de la Selva 3	4544 m	4208 m	−36 m
#14	Fornells de la Selva 4	4622 m	4321 m	−40 m
#15	Fornells de la Selva 5	5078 m	4130 m	−21 m
#16	Fornells de la Selva 6	5208 m	4044 m	−20 m
#17	Fornells de la Selva 7	5354 m	3989 m	−30 m
#18	Fornells de la Selva 8	5488 m	3956 m	−36 m
#19	Fornells de la Selva 9	5543 m	4122 m	−29 m
#20	Fornells de la Selva 10	5549 m	4352 m	−20 m
#21	Fornells de la Selva 11	5380 m	4415 m	−19 m
#22	Fornells de la Selva 12	5227 m	4276 m	−18 m
#23	Fornells de la Selva 13	4443 m	4534 m	−46 m
#24	Fornells de la Selva 14	4013 m	4560 m	−42 m
#25	Fornells de la Selva 15	3648 m	4437 m	−51 m
#26	Fornells de la Selva 16	3618 m	4172 m	−47 m
#27	Fornells de la Selva 17	3656 m	3789 m	−35 m
#28	Salt 1	8737 m	1783 m	−68 m
#29	Salt 2	8048 m	2474 m	−67 m
#30	Perelló 1	6290 m	3419 m	−50 m
#31	Perelló 2	5885 m	2824 m	−49 m
#32	Perelló 3	5993 m	2675 m	−47 m
#33	Perelló 4	6650 m	2285 m	−49 m
#34	Montfullà 1	7281 m	584 m	−22 m
#35	Montfullà 2	7188 m	459 m	−5 m
#36	Montfullà 3	7094 m	290 m	1 m
#37	Montfullà 4	7217 m	148 m	16 m
#38	Montfullà 5	7374 m	20 m	30 m
#39	Montfullà 6	7519 m	124 m	27 m
#40	Montfullà 7	7882 m	−192 m	18 m
#41	Montfullà 8	8151 m	−219 m	−9 m
#42	Montfullà 9	8183 m	118 m	−33 m
#43	Montfullà 10	7899 m	291 m	−32 m
#44	Montfullà 11	7577 m	471 m	−26 m
#45	St. Gregori 1	10230 m	232 m	−67 m
#46	St. Gregori 2	10232 m	−53 m	−70 m

Id.	Location name	North (n)	East (e)	Height (h)
#47	St. Gregori 3	10353 m	−289 m	−70 m
#48	St. Gregori 4	10537 m	−691 m	−65 m
#49	St. Gregori 5	10805 m	−527 m	−62 m
#50	St. Gregori 6	10697 m	−210 m	−60 m
#51	St. Gregori 7	10705 m	335 m	−60 m
#52	St. Gregori 8	10542 m	416 m	−61 m
#53	St. Gregori 9	10381 m	321 m	−70 m
#54	Canet d'Adri	15182 m	−1752 m	34 m
#55	Aiguaviva 1	4798 m	620 m	2 m
#56	Aiguaviva 2	4683 m	310 m	9 m
#57	Aiguaviva 3	4525 m	−34 m	20 m
#58	Taialà 1	11480 m	2613 m	−68 m
#59	Taialà 2	11436 m	2359 m	−66 m
#60	Taialà 3	11753 m	2187 m	−32 m
#61	Palol d'Onyar	6454 m	6884 m	−68 m
#62	Quart 1	5340 m	6624 m	−58 m
#63	Quart 2	4599 m	6553 m	−40 m
#64	Quart 3	3928 m	7524 m	−17 m
#65	Llambilles	2766 m	7594 m	−19 m
#66	Cassà de la Selva 1	−108 m	9015 m	3 m
#67	Cassà de la Selva 2	−301 m	9945 m	26 m
#68	Campllong	107 m	6000 m	−19 m
#69	Riudellots	459 m	3769 m	−14 m
#70	Can Jordi	1036 m	2160 m	0 m
#71	Sarrià de Ter 1	12720 m	4502 m	−100 m
#72	Sarrià de Ter 2	13021 m	4367 m	−91 m
#73	Sarrià de Ter 3	13683 m	4759 m	−112 m
#74	Sarrià de Ter 4	13837 m	5352 m	−115 m
#75	Sarrià de Ter 5	13357 m	5540 m	−120 m
#76	St. Julià de Ramis 1	14186 m	5673 m	−124 m
#77	St. Julià de Ramis 2	14758 m	4922 m	−91 m
#78	St. Julià de Ramis 3	15412 m	5375 m	−98 m
#79	VilaRoja 1	8236 m	7061 m	−83 m
#80	VilaRoja 2	8655 m	7385 m	−22 m
#81	Bescanó 1	8020 m	−999 m	−57 m
#82	Bescanó 2	7814 m	−1022 m	−54 m
#83	Bescanó 3	7588 m	−1082 m	−48 m
#84	Bescanó 4	7566 m	−1281 m	−50 m
#85	Bescanó 5	7549 m	−1479 m	−44 m
#86	Bescanó 6	7295 m	−1611 m	−24 m
#87	Bescanó 7	7315 m	−1844 m	−44 m

MEASUREMENT LOCATIONS IN INDUSTRIAL AREAS

Id.	Location name	North (n)	East (e)	Height (h)
#88	Llambilles	2268 m	7436 m	−25 m
#89	Fornells de la Selva 1	4576 m	3112 m	−24 m
#90	Fornells de la Selva 2	4768 m	3489 m	−28 m

Id.	Location name	North (n)	East (e)	Height (h)
#91	Fornells de la Selva 3	5083 m	3604 m	−31 m
#92	Fornells de la Selva 4	4447 m	3815 m	−23 m
#93	Fornells de la Selva 5	3948 m	3491 m	−20 m
#94	Fornells de la Selva 6	4077 m	3035 m	−18 m
#95	Sarrià de Ter 1	11990 m	4595 m	−92 m
#96	Sarrià de Ter 2	12539 m	4513 m	−109 m
#97	Cassà	−187 m	8629 m	−7 m
#98	St.Gregori 1	10266 m	1382 m	−74 m
#99	St.Gregori 2	10742 m	1170 m	−66 m
#100	St.Gregori 3	11032 m	1349 m	−62 m
#101	St.Gregori 4	10529 m	1672 m	−69 m
#102	Girona 1	11150 m	3318 m	−75 m
#103	Girona 2	10656 m	3035 m	−83 m
#104	Girona 3	10235 m	2342 m	−82 m
#105	Girona 4	5636 m	3803 m	−41 m
#106	Girona 5	6212 m	3677 m	−53 m
#107	Campllnog	778 m	5420 m	−36 m
#108	Riudellots 1	1110 m	4756 m	−37 m
#109	Riudellots 2	1462 m	4145 m	−36 m
#110	Riudellots 3	1044 m	3337 m	−7 m
#111	Riudellots 4	961 m	2619 m	−16 m
#112	Perelló 1	5718 m	2218 m	−31 m
#113	Perelló 2	5224 m	2064 m	−23 m
#114	Perelló 3	5068 m	1922 m	−15 m
#115	Perelló 4	5002 m	1705 m	1 m
#116	Perelló 5	4950 m	1584 m	−4 m
#117	Salt 1	7535 m	1489 m	−57 m
#118	Salt 2	7891 m	1265 m	−58 m
#119	Salt 3	8270 m	1085 m	−61 m

HOSPITAL MEASUREMENT LOCATIONS

Id.	Location name	North (n)	East (e)	Height (h)
#120	Hospital Josep Trueta	11294 m	5060 m	−89 m
#121	Hospital Sta. Caterina	8207 m	3285 m	−68 m
#122	Clínica Girona	9255 m	5149 m	−81 m

SCHOOL MEASUREMENT LOCATIONS

Id.	Location name	North (n)	East (e)	Height (h)
#123	CEIP Riudellots de la Selva	−137 m	3563 m	−23 m
#124	IES Cassà de la Selva	−241 m	9511 m	20 m
#125	CEIP Forn d'Anells (Fornells)	3902 m	4154 m	−32 m
#126	EB Baldufa (Quart)	4903 m	6630 m	−54 m
#127	CEIP Madrenc (Vilabrareix)	6149 m	2861 m	−46 m
#128	Montessori Palau (Girona)	6039 m	4733 m	−22 m
#129	Les Alzines (Girona)	6728 m	5052 m	−15 m
#130	IES Montilivi (Girona)	7611 m	5770 m	−60 m

Id.	Location name	North (n)	East (e)	Height (h)
#131	CEIP Vilaroja (Girona)	8305 m	7143 m	−47 m
#132	Universitat de Girona	9977 m	5716 m	−68 m
#133	Maristes (Girona)	9386 m	4333 m	−88 m
#134	CEIP J. Dalmau Carles (Girona)	8427 m	3971 m	−78 m
#135	Dominiques de Salt	8744 m	2201 m	−71 m
#136	EB Casa del Bambini (Girona)	11100 m	6543 m	45 m
#137	IES Carles Rahola (Girona)	10875 m	3828 m	−82 m
#138	CEIP Sagrat Cor (Sarrià de Ter)	12821 m	5519 m	−115 m
#139	EB Confeti (Sarrià de Ter)	13399 m	4730 m	−108 m
#140	CEIP Sobrequés (Bescanó)	7612 m	−1811 m	−48 m

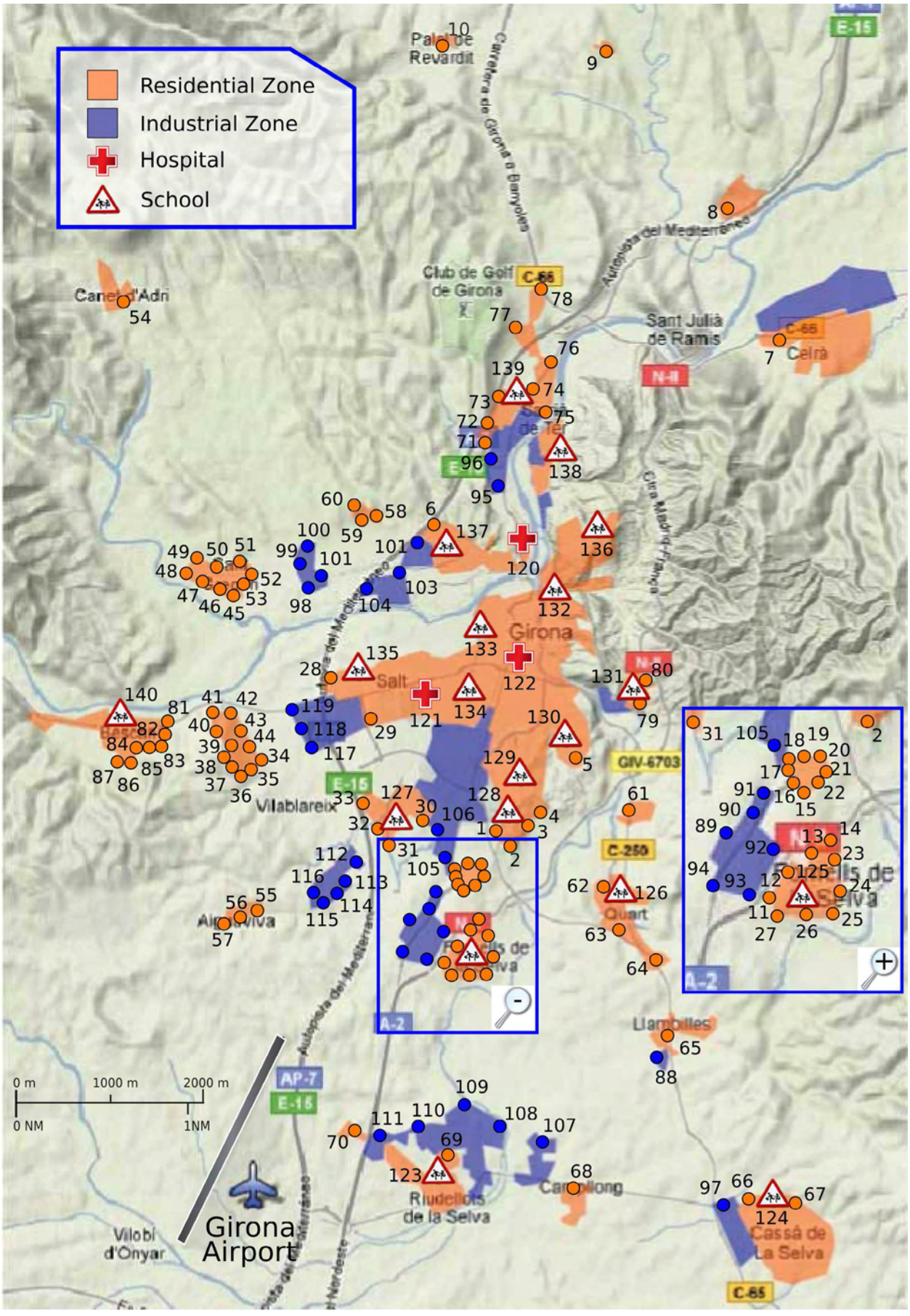

Figure E-1: *Noise measurment locations for the Girona scenario*

References

AENA. 2009a (Oct). *Girona (LEGE) aerodrome data*. Aeronautical Information Publications (AIP) – Part AD-LEGE. Available at: http://www.aena.es. 86, 145

AENA. 2009b (Oct). *Madrid Barajas Standard Instrumental Departures (SID)*. Aeronautical Information Publications (AIP) – Part AD-LEMD. Available at: http://www.aena.es. 4

AGGELOGIANNAKI, E., & SARIMVEIS, A. 2006. Multiobjective constrained MPC with simultaneous closed-loop identification. *International journal of adaptive control and signal processing*, **20**(4), 145–173. 53

AIR TRAFFIC CONTROL THE NETHERLANDS. 2009a (Oct). *Noise Abatement Procedures (NAP) at Schiphol airport. Amsterdam, The Netherlands*. Aeronautical Information Publications (AIP) – Part AD-EHAM 2.21. Available at: http://www.ais-netherlands.nl/aim/index.html. 4

AIR TRAFFIC CONTROL THE NETHERLANDS. 2009b (Feb). *Standard Instrument Departure (SID) chart RWY 24 at Schiphol airport. Amsterdam, The Netherlands*. Aeronautical Information Publications (AIP) – Part AD-EHAM. Available at: http://www.ais-netherlands.nl/aim/index.html. 14

AIRBUS. 2007. *Flying by nature. Global market forecast 2007-2026*. Airbus S.A.S., Toulouse (France). Availabe at http://www.airbus.com/en/airbusfor/analysts/. 2

AMOROSO, LUIGI. 1938. Vilfredo Pareto. *Econometrica*, **6**(1), 1–21. 50

ANDERSON, JOHN D. 2008. *Introduction to flight*. International edn. New York - London: McGraw-Hill. 131

ARINC. 2000 (Feb). *Navigation system database. ARINC specification 424*. 15 edn. Aeronautical Radio Inc., Annapolis, Maryland (USA). 13, 111

ATKINS, ELLA M., & XUE, MIN. 2004. Noise-sensitive final approach trajectory optimization for runway-independent aircraft. *Journal of aerospace computing, information and communication*, **1**(7), 269–287. 20

BAUMGARTNER, MARC. 2007. The organisation and operation of european airspace. *Chap. 1, pages 1–34 of:* COOK, ANDREW (ed), *European air traffic management. principles, practice and research.* Aldershot, England: Ashgate Publishing Limited. 11

BEER, FERDINAND, JOHNSTON, RUSSELL E., CLAUSEN, WILLIAM, EISENBERG, ELLIOT, & CORNWELL, PHILLIP. 2004. *Vector mechanics for engineers: Dynamics*. Seventh edn. New York - London: McGraw-Hill Science/Engineering/Math. 127

BELLMAN, R.E. 2003. *Dynamic programming*. Courier Dover Publications. 20

BENÍTEZ, J. M., CASTRO, J. L., & REQUENA, I. 1997. Are Artificial Neural Networks Black Boxes? *IEEE transactions on neural networks*, **8**(5), 1156–1164. 34

BERGLUND, BIRGITTA, & LINDVALL, THOMAS. (Eds.) 1995. Community noise. *Archives of the center for sensory research*, **2**(1), 1–195. Document prepared for the World Health Organization (WHO). Available at http://www.nonoise.org/library/whonoise/whonoise.htm. 22

BERTON, JEFFREY J. 2003. *Optimum climb to cruise noise trajectories for the high speed civil transport*. Tech. rept. NASA - Glenn Research Center, Cleveland, Ohio (USA). Document No: NASA-TM-2003-212704. 26

BESTLE, DIETER, & EBERHARD, PETER. 1997. Dynamic system design via multicriteria optimization. *Pages 467–478 of:* FANDEL, GÜNTER, & GAL, TOMAS (eds), *Multiple criteria decision making*. Proceedings of the twelfth international conference. Hagen (Germany), vol. Lecture Notes in Economics and Mathematical Systems, no. 448. Springer-Verlag. 55

BETTS, JOHN T. 1998. Survey of numerical methods for trajectory optimization. *Journal of guidance, control and dynamics*, **21**(2), 193–207. 193-226207. 19, 47

BETTS, JOHN T. 2001. Practical methods for optimal control using nonlinear programming. *In: Advances in design and control*. Society for Industrial Mathematics. 46, 47

BOEING. 2008. *Current market outlook 2008-2027*. Boeing Comertial Airplanes - Market Analysis, Seattle, Washington (USA). Availabe at http://www.boeing.com/commercial/cmo/index.html. 2

BOTTELDOOREN, DICK, & VERKEYN, ANDY. 2002. Fuzzy models for accumulation of reported community noise annoyance from combined sources. *Journal of acoustical society of America*, **112**(4), 1496–1508. 22

BOTTELDOOREN, DICK, VERKEYN, ANDY, & LERCHER, PETER. 2003. A fuzzy rule based framework for noise annoyance modeling. *Journal of acoustical society of America*, **114**(3), 1487–1498. 22

BOWER, GEOFFREY C., & KROO, ILAN M. 2008 (Sep). Multi-objective aircraft optimization for minimum cost and emissions over specific route networks. *In: Proceedings of the 26th international congres of the aeronautical sciences (ICAS)*. AIAA/ICAS, Anchorage, Alaska (USA). 55

BRYSON, ARTHUR E., & HO, YU-CHI. 1975. *Applied optimal control*. (USA): Hemisphere Publishing corporation. 18, 46

BUCKLEY, JAMES J., & ESLAMI, ESFANDIAR. 2002. *An introduction to fuzzy logic and fuzzy sets*. Advances in soft Computing Series. Heidelberg – New York: Physica-Verlag. 138

BULIRSCH, R., NERZ, E., PESCH, H. J., & VON STRYK, O. 1993. Combining direct and indirect methods in optimal control: Range maximization of a hang glider. *Pages 273–288 of:* HOFFMANN, K.H. (ed), *Optimal control (calculus of variations, optimal control theory and numerical methods)*. International Series of Numerical Mathematics, vol. 111. Birkhauser Verlag. 46

BURN, MELISSA, STUSNICK, ERIC, & EHRLICH, GARY. 1995. A comparison of different aircraft noise metrics for large, medium, and small airports. *The journal of the acoustical society of America*, **97**(5), 3304–3304. 119

CAPOZZI, BRIAN, AUGUSTINE, STEPHEN, & THOMPSON, TERENCE R. 2002 (Oct). An initial assessment of benefits for noise-aware decision-support tools. *In: Proceedings of the 2nd aircraft technology, integration and operations (ATIO) conference*. AIAA, Los Angeles, California (USA). 19

CASALINO, D., DIOZZI, F., SANNINO, R., & PAONESSA, A. 2008. Aircraft noise reduction technologies: A bibliographic review. *Aerospace science and technology*, **12**(1), 1–17. Aircraft noise reduction. 117

CHEN, M., 2000. 2000. Individual monotonicity and the leximin solution. *Economic theory*, **15**, 353–365. 82

CLARKE, JOHN-PAUL. 2000. A systems analysis of noise abatement procedures enabled by advance flight guidance technology. *Journal of aircraft*, **37**(2), 266–273. 19

CLARKE, JOHN-PAUL, & HANSMAN, R. JOHN. 1997. *A system analysis methodology for developing single event noise abatement procedures*. Tech. rept. Massachussets Institute of Technology - Aeronautical Systems Laboratory, Cambridge, Massachusetts (USA). Report No ASL-97-1. 18, 19

CLARKE, JOHN-PAUL, BENNETT, DANNIE, ELMER, KEVIN, FIRTH, JEFFERY, HILB, ROBERT, HO, NHUT, JOHNSON, SARAH, LAU, STUART, REN, LILING, SENECHAL, DAVID, SIZOV, NATALIA, SLATTERY, ROBERT, TONG, KWOK-ON, WALTON, JAMES, WILLGRUBER, ANDREW, & WILLIAMS, DAVID. 2006 (Jan). *Development, design, and flight test evaluation of a continuous descent approach procedure for nighttime operation at Louisville international airport*. Tech. rept. FAA PARTNER CDA Development Team. Report No. PARTNER-COE-2006-02. 17

CRIGHTON, DAVID G. 1991. Airframe noise. *Chap. 7, pages 391–447 of:* HUBBARD, HARVEY H. (ed), *Aeroacoustics of flight vehicles: Theory and practice, vol.1: Noise sources.* Hampton, Virginia (USA): NASA Langley Research Center. Document No: RP-1258-VOL-1. 118

DAS, INDRANEEL, & DENNIS, JOHN. 1997. A closer look at drawbacks of minimizing weighted sums of objectives for Pareto set generation in multicriteria optimization problems. *Structural optimization*, **14**(1), 63–69. 53

DE BEER, BART A.F., MULDER, MAX, VAN PAASSEN, M. M., & IN'T VELD, ALEXANDER C. 2008 (Aug). Development of an ecological interface for the three degree decelerating approach. *In: Proceedings of the AIAA guidance, navigation and control conference and exhibit*. AIAA, Honolulu, Hawaii (USA). Paper No: AIAA 2008-7158. 18

DE JONGE, H.W.G. 2002 (Mar). *Refined flow management. An operational concept for Gate-to-Gate 4D flight planning*. Tech. rept. Nationaal Lucht- en Ruimtevaartlaboratorium (NLR). Document No: NLR-TP-2002-057. 6

DE LÉPINAY, IVAN. 2002 (Jul). *EGNOS flight trials at nice airport*. Tech. rept. Environmental Studies Business Area, EUROCONTROL Experimental Centre, Bretigny sur Orge (France). Reference document No: EEC/ENV/2002/007. 13

DFT. 2003 (Feb). *Night noise quotas at Heathrow, Gatwick and Stansted airports*. Department for Transport – United Kingdom Government, London (UK). 4

DRUD, A. 1985. A GRG code for large sparse dynamic nonlinear optimization problems. *Mathematical programming*, **31**(2), 153–191. 48

DRUD, A. 1994. CONOPT : A large-scale GRG code. *ORSA journal on computing*, **6**(2), 207–216. 48

DRUD, ARNE. 2000. *CONOPT user's manual*. ARKI Consulting and Development A/S, Bagsvaerd, Denmark. 42

ELMER, KEVIN R. 2008 (Sep). Tailored arrivals operations at SFO and expected environmental benefits. *In: Proceedings of the 8th AIAA aviation technology, integration, and operations (ATIO) conference*. AIAA, Anchorage, Alaska (USA). Paper No: AIAA 2008-8868. 17

ERKELENS, L.J.J. 1999 (Nov). *Development of noise abatement procedures in the Netherlands*. Tech. rept. Nationaal Lucht- en Ruimtevaartlaboratorium (NLR). Document No: NLR-TP-99386. 17

ESA. 2009. *http://www.esa.int/esaNA/index.html*. European Space Agency. Last visited: October 2009. 109

EUROCONTROL. 1998 (Dec). *Eurocontrol standard document for area navigation equipment. Operational requirements and functional requirements*. 2.2 edn. Eurocontrol. Doc No: 003-93. Available at http://www.ecacnav.com/Document_Library. 111

EUROCONTROL. 2003. *The air traffic management strategy for the years 2000+. Volume II*. Eurocontrol, Brussels (Belgium). Availabe at http://www.eurocontrol.int/corporate/public/standard_page/cb_atm_strategy.html. 111

EUROCONTROL. 2008 (nov). *Eurocontrol Long-Term Forecast: IFR Flight Movements 2008-2030*. Eurocontrol, Brussels (Belgium). Doc No DAS/DIA/STATFOR 302. 2

EUROCONTROL. 2009. *http://www.eurocontrol.int/environment/public/standard_page/noise.html*. Last visited: February 2009. 117

EUROPEAN COMMISSION. 2003. Commission recommendation of 6 august 2003 concerning the guidelines on the revised interim computation methods for industrial noise, aircraft noise, road traffic noise and railway noise, and related emission data. *Pages 49–64 of: Official journal of the European Union. Number 212*. Brussels (Belgium): European Commission. 2003/613/EC. 120

EUROPEAN PARLIAMENT. 2002a. *Directive 2002/30/EC of the european parliament and of the council of 26 march 2002 on the establishment of rules and procedures with regard to the introduction of noise-related operating restrictions at community airports (text with eea relevance)*. Official Journal L 085, 28/03/2002. Pages 0040 – 0046. 4

EUROPEAN PARLIAMENT. 2002b. *Directive 2002/49/EC of the european parliament and of the council of 25 june 2002 relating to the assessment and management of environmental noise - declaration by the commission in the conciliation committee on the directive relating to the assessment and management of environmental noise*. Official Journal L 189, 18/07/2002. Pages 0012 – 0026. 4, 120

FAA. 2006 (May). *INM Version 6.2 Software Update*. Federal Aviation Administration. Office of Environment and Energy., Washington, DC. USA. 33

FAA. 2009a. *FAA Aerospace Forecast: Fiscal Years 2009-2025*. Federal Aviation Administration. 2

FAA. 2009b (Feb). *Instrumental Approach Procedure (IAP): RNAV (RNP) RWY 19 at Ronald Reagan Washington National airport. Washington D.C.* digital – Terminal Procedures Publication. Aeronautical Information Publications (AIP). Federal Aviation Administration (FAA). Available at: http://www.avn.faa.gov/digital_tpp.asp?ver=0813&eff=12-18-2008&end=01-15-2009. 15

FAHROO, FARIBA, & ROSS, I. MICHAEL. 2000 (Jun). Direct trajectory optimization by a Chebyshev pseudospectral method. *In: Proceedings of the American control conference*. 46, 47

FAVRE, C. 1996. Fly-by-wire for commercial aircraft: the Airbus experience. *Chap. 8, pages 221–229 of:* TISCHLER, MARK B. (ed), *Advances in aircraft flight control*. CRC Press. 133

FICAN. 1997 (Jun). *Effects of aviation noise on awakenings from sleep*. Tech. rept. Federal Interagency Committee on Aviation Noise (FICAN). 21, 22

FIDELL, SANDFORD, MILLS, JOHN, TEFFETELLER, SHERRI, & PEARSONS, KARL. 1982 (Jun). *Community response to three noise abatement departure procedures at John Wayne airport*. Tech. rept. NASA - Langley Research Center. BBN report No. 4743. 21

FIELDS, J. M., JONG, R. G. DE, GJESTLAND, T., FLINDELL, I. H., JOB, R. F. S., KURRA, S., LERCHER, P., VALLET, M., YANO, T., GUSKI, R., FELSCHER-SUHR, U., & SCHUMER, R. 2001. Standardized general-purpose noise reaction questions for community noise surveys: research and a recommendation. *Journal of sound and vibration*, **4**(242), 641–679. 22

FRANKLIN, GENE F., POWELL, J. DAVID, & EMAMI-NAEINI, ABBAS. 2006. *Feedback control of dynamic systems*. Upper Saddle River, NJ, USA: Prentice Hall PTR. 48

FRAPORT. 2009. *http://www.fraport.com/cms/company/dok/81/81482.halsdtop.htm*. Last visited: February 2009. 17

GAO. 2000 (Aug). *Report to the ranking democratic member, committee on transportation and infrastructure, house of representatives. aviation and the environment: Airport operations and future growth present environmental challenges.* Tech. rept. Committee on Transportation and Infrastructure, House of Representatives-General Accounting Office. Document No: GAO/RCED-00-153. Available from: http://www.gao.gov/archive/2000/rc00153.pdf. 2

GATH, PETER FRIEDRICH. 2002 (Nov). *CAMTOS - a software suite combining direct and indirect trajectory optimisation methods*. Ph.D. thesis, Insitut für Flugmechanik und Flugregelung. Universität Stuttgart, Stuttgart (Germany). 46, 47

GEN, M., & CHENG, R. 1997. *Genetic algorithms & engineering design*. New York (USA): Wiley-Interscience. 20

GENERALITAT DE CATALUNYA. 2002. Llei 16/2002, de 28 de juny, de protecció contra la contaminació acústica. *Pages 12639–12649 of: Diari Oficial de la Generalitat de Catalunya (DOGC). Numero 3675*. Barcelona, Catalunya (Spain): Generalitat de Catalunya - Departament de la Presidència. (in Catalan). 120

GIRVIN, RAQUEL. 2009. Aircraft noise-abatement and mitigation strategies. *Journal of air transport management*, **15**(1), 14–22. 4

GOMEZ COMENDADOR, VICTOR FERNANDO. 2004 (Feb). *Determinación de condiciones de compatibilidad en un TMA de tamaño medio de procedimientos ACDA de empuje mínimo, y perfil vertical variable o perfil de velocidad veriable, con procedimientos convencionales, minimizando su impacto sobre la capacidad*. Ph.D. thesis, Escuela Técnica Superior de Ingenieros Aeronáuticos (ETSIA). Universidad Politécica de Madrid (UPM), Madrid (Spain). (In Spanish). 17

GREENER BY DESIGN. 2005 (Jul). *Air travel – Greener by Design. Mitigating the environmental impact of aviation: Opportunities and priorities*. Tech. rept. Greener by Design – Science & Technology Sub-Group. Published by the Royal Aeronautical Society. Availabe at http://www.greenerdesign.com. 4

GUO, YI'NAN, CHENG, JIAN, & MA, XIAOPING. 2006. Coking optimization control model based on hierarchical multi-objective evolutionary algorithm. *Pages 6544–6548 of: Proceedings of the 6th world congress on intelligent control and automation*. 55

GUÉRIN, S., MICHEL, U., SILLER, H., FINKE, U., & SAUERESSIG, G. 2005 (May). Airbus A319 database from dedicated flyover measurements to investigate noise abatement procedures. *In: Proceedings of the 11th AIAA/CEAS aeroacoustics conference (26th AIAA aeroacoustics conference)*. AIAA/CEAS, Monterey, California (USA). 118

HAGELAUER, P., & MORA-CAMINO, F. 1998. A soft dynamic programming approach for on-line aircraft 4D-trajectory optimization. *European journal of operational research*, **107**(1), 87–95. 20

HARGRAVES, C.R., & PARIS, S.W. 1987. Direct trajectory optimization using nonlinear programming and collocation. *AIAA journal of guidance and control*, **10**(4), 338–342. 46

HARRIS, CYRIL M. (ed). 1997. *Handbook of acoustical measurements and noise control*. Third edn. London, UK: McGraw-Hill. 117, 119

HE, BILL, COINTIN, REBECCA, BOEKER, ERIC, DINGES, ERIC, & ROOF, CHRIS. 2007 (Oct). *Integrated Noise Model (INM) Noise Contour Comparison: Version 7.0 vs. 6.2a*. Federal Aviation Administration. Office of Environment and Energy., Washington, DC. USA. FAA-AEE-07-01. 33

HEBLIJ, SANDER J., & VISSER, HENDRIKUS G. 2008 (Aug). Advanced noise abatement departure procedures: custom-optimized departure profiles. *In: Proceedings of the AIAA guidance, navigation and control conference.* AIAA, Honolulu, Hawaii (USA). Paper number: 2008-7405. 20

HEBLIJ, SANDER J., HANENBURG, VICTOR A., WIJNEN, RONALD A.A., & VISSER, HENDRIKUS G. 2007. Development of a noise allocation planning tool. *In: Proceedings of the 45th AIAA aerospace sciences meeting and exhibit*. AIAA, Reno, Nevada (USA). Paper No: AIAA-2007-1335. 18

HELLENDOORN, H., & THOMAS, C. 1993. Defuzzification in fuzzy controllers. *Intelligent and fuzzy systems*, **1**, 109–123. 139

HERNDON, A.A., MAYER, R.H., OTTOBRE, R.C., & G.F., TENNILLE. 2006. *Analysis of advanced flight management systems (FMSs). FMC field observations trials.* Tech. rept. Mitre Corporation. Project 0206FB03-05. 13

HERNDON, A.A., CRAMER, M., SPRONG, K., & MAYER, R.H. 2007 (Sep). Analysis of advanced flight management systems (FMS), flight management computer (FMC) field observations trials, vertical path. *In: The 26th digital avionics systems conference (DASC)*. AIAA/IEEE, Columbia, Maryland (USA). 13

HERNDON, A.A., CRAMER, M., & SPRONG, K. 2008 (Oct). Analysis of advanced flight management systems (FMS), flight management computer (FMC) field observations trials, radius-to-fix path terminators. *In: The 27th digital avionics systems conference (DASC)*. AIAA, St. Paul, Minessota (USA). 13

HIRAMATSU, K., YAMAMOTO, T., TAIRA, K., ITO, A., & NAKASONE, T. 1997. A survey on health effects due to aircraft noise on residents living around Kadena air base in the Ryukyus. *Journal of sound and vibration*, **205**(4), 451–460. 22

HIRAMATSU, K., MATSUI, T., ITO, A., MIYAKITA, T., OSADA, Y., & YAMAMOTO, T. 2004. The Okinawa study: an estimation of noise-induced hearing loss on the basis of the records of aircraft noise exposure around Kadena air base. *Journal of sound and vibration*, **277**(3), 617–625. 22

HOGENHUIS, R. H., HEBLIJ, SANDER J., & VISSER, HENDRIKUS G. 2008 (Sep). Optimization of RNAV noise abatement arrival trajectories. *In: Proceedings of the 26th international congres of the aeronautical scences (ICAS)*. AIAA/ICAS, Anchorage, Alaska (USA). 20, 42

HUME, KEN, GREGG, MARTIN, THOMAS, CALLUM, & TERRANOVA, DANIELA. 2003. Complaints caused by aircraft operations: an assessment of annoyance by noise level and time of day. *Journal of air transport management*, **9**(3), 153–160. 34

HWANG, C.L., & MASSUD, A. S. M. 1979. *Multiple objective decision making - methods and applications: A state-of-the-art survey*. Vol. 164. Berlin - New York: Springer-Verlag. 50

IATA. 2000. *Aviation and the environment*. International Air Transport Association – Environmental Department, Geneva (Switzerland). 3

ICAO. 1993a (Jul). *Annex 16 to the convention on international civil aviation - Environmental protection - volume I, aircraft noise*. 3 edn. International Civil Aviation Organisation, Montreal (Canada). 3, 120

ICAO. 1993b. *Manual of the ICAO standard atmosphere: extended to 80 kilometres (262 500 feet)*. Third edn. International Civil Aviation Organisation, Montreal (Canada). Doc. 7488. 132

ICAO. 1996 (Jul). *Annex 10 to the convention on international civil aviation - Aeronautical Telecommunications - volume I, radionavigation aids*. 5 edn. International Civil Aviation Organisation, Montreal (Canada). 108

ICAO. 2000. *Convention on international civil aviation*. 8 edn. International Civil Aviation Organisation, Montreal (Canada). Doc No 7300. 3

ICAO. 2006a. *Procedures for air navigation services - aircraft operations (PANS-OPS) - volume I, flight procedures*. Fifth edn. International Civil Aviation Organisation, Montreal (Canada). Doc. 8168. 3, 15, 30, 31, 57, 111

ICAO. 2006b. *Procedures for air navigation services - aircraft operations (PANS-OPS) - volume II, construction of visual and instrument flight procedures*. Fifth edn. International Civil Aviation Organisation, Montreal (Canada). Doc. 8168. 16, 44, 111

ICAO. 2008 (Apr). *Guidance on the balanced approach to aircraft noise management*. 2 edn. International Civil Aviation Organisation, Montreal (Canada). Doc 9829. 4

ICCAIA. 2005. *Report on the progress in noise reducttion submitted to ICAO*. International Coordinating Council of Aerospace Industries Associations. 3

IEC. 2003 (Apr). *Electroacoustics - sound level meters - part 2: Pattern evaluation tests*. International Electrotechnical Commission – Comittee 29, Geneve, Switzerland. Doc. IEC-61672. 116

INTERGOVERNMENTAL PANEL ON CLIMATE CHANGE. 1999. Aviation and the global atmosphere. *In:* PENNER, J.E., LISTER, D.H., GRIGGS, D.J., DOKKEN, D.J., & MCFARLAND, M. (eds), *Special report of IPCC Working Groups I and II*. Cambridge (UK): Cambridge University Press. 1

ISO. 2003. *Acoustics – normal equal-loudness-level contours*. Second edn. International Organization for Standarization, Genève, Switzerland. ISO 226:2003. 116

JAA. 2003. *Joint aviation requirements. JAR-OPS: Airplane operations*. Joint Aviation Authorities, Hoofddorp (The Netherlands). 30

JAA. 2005 (Feb). *JAA administrative & guidance material. Section one: General part 3: Temporary Guidance Leaflets LEAFLET No 10 Rev 1: Airworthiness and operational approval for precision RNAV operations in designated European airspace*. Joint Aviation Authorities, Hoofddorp (The Netherlands). JAA TGL-10. Available at `http://www.ecacnav.com/Document_Library`. 14

JANSCH, C., & PAUS, M. 1990 (May). Aircraft trajectory optimization with direct collocation using movable gridpoints. *Pages 262–267 of: Proceedings of the American control conference*. 46

KALMAN, R. E. 1963. Mathematical description of linear dynamical systems. *J.S.I.A.M. control series*, **1**(2), 152–192. Ser. A. 121

KAYTON, MYRON, & FRIED, WALTER R. 1997. *Avionics - navigation systems*. 2 edn. London (UK): John Wiley and Sons. Inc. 108

KERRIGAN, E., & MACIEJOWSKI, J. 2002 (Sep). Designing model predictive controllers with prioritised constraints and objectives. *Pages 33–38 of: Proceedings of the IEEE international symposium on computer aided control system design*. 53, 54

KOENIG, R., & MACKE, O. 2008 (Sep). Evaluation of simulator and flight tested noise abatement approach procedures. *In: Proceedings of the 26th international congres of the aeronautical sciences (ICAS)*. AIAA/ICAS, Anchorage, Alaska (USA). 17

KOVACIC, ZDENKO, & BOGDAN, STJEPAN. 2005. *Fuzzy controller design: Theory and applications*. Control Engineering Series. Boca Raton, Florida (USA): CRC Press. Taylor & Francis Group. 141

KRYTER, KARL D. 1994. *The handbook of hearing and the effects of noise: Physiology, psychology, and public health*. New York (USA): Academic Press. 21

KUENZ, ALEXANDER, MOLLWITZ, VILMAR, & KORN, BERND. 2007. Green trajectories in high traffic TMAs. *In: Proceedings of the 26th digital avionics systems conference (DASC)*. IEEE/AIAA, Dallas, Texas (USA). 18

KUENZ, ALEXANDER, BECKER, HAYUNG, EDINGER, CHRISTIANE, & KORN, BERND. 2008 (Sep). Performance-based TMA handling for mixed traffic using a ground based 4D-guidance for unequipped aircraft. *In: Proceedings of the 26th international congres of the aeronautical sciences (ICAS)*. AIAA/ICAS, Anchorage, Alaska (USA). 6

KUWANO, SONOKO, & NAMBA, SEIICHIRO. 1996. Evaluation of aircraft noise: effects of number of flyovers. *Environment international*, **22**(1), 131–144. 34

LCACC. 2009. http://www.lcacc.org/operations/operations.html. London City Airport Consultative Committee. Last visited: February 2009. 16

LE TALLEC, CLAUDE, & JOULIA, ANTOINE. 2007 (May). IFATS: 4D contracts in 4D airspace. *In: Proceedings of the infotech and aerospace conference and exhibit*. AIAA, Rohnert Park, California (USA). 6

LEWIS, L. FRANK, & SYRMOS, L. VASSILIS. 1995. *Optimal control*. Second edn. New York: John Wiley & Sons, Inc. 46

LIGHTHILL, M.J. 1954. On sound generated aerodynamically. II. turbulence as a source of sound. *Royal society of london proceedings series A*, **222**(1148), 1–32. 118

LIM, CHANGWOO, KIM, JAEHWAN, HONG, JIYOUNG, LEE, SOOGA, & LEE, SOOJOO. 2007. The relationship between civil aircraft noise and community annoyance in Korea. *Journal of sound and vibration*, **299**(3), 575–586. 34

LUCAS, R., GALBO, P. LO, MATEO, M.L. DE, STECIW, A., & ASHFORD, E. 1996. The ESA contribution to the European satellite navigation programme. *Acta astronautica*, **38**(4-8), 605–611. 109

LUSS, HANAN. 1999. On equitable resource allocation problems: a lexicographic minmax approach. *Operations research journal*, **47**(3), 361–378. 56, 68

MACKE, O., & KOENIG, R. 2007 (Aug). Comparison of different aircraft noise analysis methods for noise abatement flight procedures. *In: Proceedings of the 36th congress and exposition on noise control engineering*. Turkish AcoTurkish Acoustical Society; IZOCAM, Istanbul (Turkey). 17

MARLER, R.T., & ARORA, J.S. 2004. Survey of multi-objective optimization methods for engineering. *Structural multidisciplinary optimization*, **26**(6), 369–395. 50

MARTIN-HOUSSART, GÉRALDINE, & RIZK, CYRIL. 2002 (Oct). *Mesurer la qualité de vie dans les grandes agglomérations*. INSEE Première. Numéro 868. Institut National de la Statistique et des études économiques. (in French). 1

MASUI, KAZUYA, TOMITA, HIROSHI, & YANAGIDA, AKIRA. 2008 (Sep). Research and development for fault tolerant flight control system - Part 2. Flight experiments. *In: Proceedings of the 26th international congress of the aeronautical sciences (ICAS)*. AIAA/ICAS, Anchorage, Alaska (USA). 20

MIEDEMA, HENK M. E., & OUDSHOORN, CATHARINA G.M. 2001. Annoyance form transportation noise: relationships with exposure metrics DNL and DENL and their confidence intervals. *Environmental health perspectives*, **109**(4), 409–416. 21

MIEDEMA, HENK M. E., & VOS, J. 1998. Exposure-response relationships for transportation noise. *Journal of the acoustical society of America*, **104**(6), 3432–3445. 21

MIETTINEN, K.M. 1999. *Nonlinear multiobjective optimization*. Boston - London -Dordrecht: Kluwer Academic Publishers. 50, 52, 53, 56, 75, 82

MUZET, A. 2007. Environmental noise, sleep and health. *Sleep medecine reviews*, **11**(2), 135–142. 21

NAKAYAMA, HIROTAKA. 2005. Multi-objective optimization and its engineering applications. *In:* BRANKE, JÜRGEN, DEB, KALYANMOY, MIETTINEN, KAISA, & STEUER, RALPH E. (eds), *Practical approaches to multi-objective optimization*. Dagstuhl Seminar Proceedings, no. 04461. Schloss Dagstuhl (Germany): Internationales Begegnungs- und Forschungszentrum für Informatik (IBFI). Available online at http://drops.dagstuhl.de/opus/volltexte/2005/234. 50

NETJASOV, FEDJA. 2006 (Jun). Air traffic assignment as a noise abatement measure case study: Zurich airport, Switzerland. *Pages 13–18 of: Proceedings of the 2nd international congress on research in air transportation (ICRAT)*. EUROCONTROL / Faculty of Transport and Traffic Engineering of Belgrade University, Belgrade (Serbia). 18

NORGIA, L. 1999. A graphical optimization of take-off noise abatement procedures for subsonic aircraft. *Journal of sound and vibration*, **222**(3), 489–501. Article No: jsvi.1998.2100. 19

OCAMPO-MARTÍNEZ, C., BEMPORAD, A., INGIMUNDARSON, A., & PUIG, V. 2007. On hybrid model predictive control of sewer networks. *In:* SANCHEZ-PEÑA, R., PUIG, V., & QUEVEDO, J. (eds), *Identification & control: The gap between theory and practice*. Springer-Verlag. 45

OCAMPO-MARTÍNEZ, C., INGIMUNDARSON, A., PUIG, V., & QUEVEDO, J. 2008. Objective prioritization using lexicographic minimizers for MPC of sewer networks. *IEEE transactions on control systems technology*, **16**(1), 113–121. 54

ÖHRSTRÖM, E, & GRIEFAHN, B. 1993. Summary of team 5: Effects of noise on sleep. *In:* VALLET, M. (ed), *Proocedings of the 6th international congress on noise as a public health problem. Noise and man.* 21

OLMSTEAD, JEFFREY R., FLEMING, GREGG G., GULDING, JOHN M., ROOF, CHRISTOPHER J., GERBI, PAUL J., & RAPOZA, AMANDA S. 2002 (Jan). *Integrated noise model (INM) version 6.0 technical manual*. Federal Aviation Administration. Office of Environment and Energy., Washington, DC. USA. FAA-AEE-02-01. 32

OVCHINNIKOV, SERGEI. 2002. Max-min representation of piecewise linear functions. *Beiträge zur Algebra und Geometrie - Contributions to Algebra and Geometry*, **43**(1), 297–302. 45

PARKINSON, BRADFORD W., & SPILKER, JAMES J. (eds). 1996. *Global Positioning System: Theory and applications*. Progress in astronautics and aeronautics. Volume 164, vol. 2. Washington DC (USA): American Institute of Aeronautics and Astronautics Inc. 109

PAULLIN, R.L. 1970. Capacity and noise relationships for major hub airports. *Proceedings of the IEEE*, **58**(3), 307–313. 12

PEPPER, CHRISTOPHER B., NASCARELLA, MARC A., & KENDALL, RONALD J. 2003. A review of the effects of aircraft noise on wildlife and humans, current control mechanisms, and the need for further study. *Environmental management*, **32**(4), 418–432. 22

PRATT, ROGER W. (ed). 2000. *Flight control systems: Practical issues in design and implementation*. IEE Control Engineering Series. Institution of Engineering and Technology. 31

RAWLS, JOHN. 2005. *A theory of justice*. Belknap Press of Harvard University Press. 56

REN, LILING, & CLARKE, JOHN-PAUL. 2007 (Jun). Flight demonstration of the separation analysis methodology for continuous descent arrival. *In: Proceedings of the 7th USA/Europe air traffic management R&D seminar*. FAA/Eurocontrol, Barcelona (Spain). 17

REN, LILING, CLARKE, JOHN-PAUL, & HO, NHUT TAN. 2003 (Oct). Achieving low approach noise without sacrificing capacity. *In: Proceedings of the 22nd digital avionics systems conference*. AIAA, Indianapolis, Indiana (USA). 18

RENTMEESTERS, MARK J., TASI, WEI K., & LIN, KEW-JAY. 1996 (Oct). A theory of lexicographic multi-criteria optimiszation. *Pages 76–79 of: Proceedings of the second IEEE international conference on engineering of complex computer systems*. 53

REYNOLDS, TOM. G., REN, LILING, & CLARKE, JOHN-PAUL. 2007 (Jul). Advanced noise abatement approach activities at Nottingham East Midlands airport, UK. *In: Proceedings of the 7th USA/Europe air traffic management R&D seminar*. FAA/Eurocontrol, Barcelona (Spain). 19

ROSKAM, JAN. 2001. *Airplane flight dynamics and automatic flight controls*. Third edn. Vol. 1. Lawrence, Kansas (USA): DARcorporation. 26, 131

ROSS, I.M., & FAHROO, F. 2002a (Jul). A direct method for solving nonsmooth optimal control problems. *In: Proceedings of the 2002 IFAC World Congress*. 47

ROSS, I.M., & FAHROO, F. 2002b (Aug). A perspective on methods for trajectory optimization. *In: Proceedings of the AIAA/ASS astrodynamics conference*. Invited Paper no. AIAA 2002-4727. 46

ROSS, TIMOTHY J. 1995. *Fuzzy logic with engineering applications*. McGraw-Hill. 138, 140, 141

ROY, ALEXIS. 2003 (Aug). *La sensibilité des français à leur environnement de proximité.* Société – Les données de l'environnement. Numéro 85. Institut Français de l'Environnement (IFEN), Orléans (France). (In French). 1

RYLANDER, R. 2004. Physiological aspects of noise-induced stress and annoyance. *Journal of sound and vibration*, **277**(3), 471–478. 34

RYLANDER, R., & BJÖRKMAN, M. 1997. Annoyance by aircraft noise around small airports. *Journal of sound and vibration*, **205**(4), 533–537. 22

SAE – COMITEE A-21, AIRCRAFT NOISE. 1981 (Jun). *Prediction method of lateral attenuation of airplane noise during takeoff and landing*. Tech. rept. Society of Automotive Engineers, Warrendale, PA (USA). Aerospace Information Report (AIR) No. 1751. 32

SAE – COMITEE A-21, AIRCRAFT NOISE. 1986. *Procedure for the calculation of airplane noise in vicinity of airports*. Tech. rept. Society of Automotive Engineers, Warrendale, PA (USA). Aerospace Information Report (AIR) No. 1845. 32

SAE. COMITEE A-21, AIRCRAFT NOISE. 1975 (Mar). *Standard values of atmospheric absorption as a function of temperature and humidity*. Tech. rept. Society of Automotive Engineers, Warrendale, PA (USA). Aerospace Research Report (ARR) No. 866A. 32

SALLES, R.M., & BARRIA, J.A. 2004 (Aug). Fair bandwidth allocation for the integration of adaptive and non-adaptive applications. *Pages 1–12 of: Proceedings of the service assurance with partial and intermittent resources SAPIR*. 56

SALLES, RONALDO M., & BARRIA, JAVIER A. 2008. Lexicographic maximin optimisation for fair bandwidth allocation in computer networks. *European journal of operational research*, **185**, 778–794. 82

SARKAR, SASWATI, & TASSIULAS, LEANDROS. 2000. Fair allocation of discrete bandwidth layers in multicast networks. *Pages 1491–1500 of: Proceedings of the nineteenth annual joint conference of the IEEE computer and communications societies: INFOCOM 2000*. IEEE. 56

SCHOMER, PAUL. 2001 (Apr). *A white paper: Assessment of noise annoyance*. Tech. rept. Schomer and Associates. 34, 60

SCHULTZ., T. J. 1978. Synthesis of social surveys on noise annoyance. *Journalof the acoustical society of America*, **64**(2), 377–405. 21

SESAR CONSORTIUM. 2006 (Dec). *Air transport framework-the performance target*. Single European Sky ATM Research Consortium, Brussels (Belgium). SESAR Definition Phase. Milestone Deliverable 2 (D2). 6

SKÅNBERG, A., & ÖHRSTRÖM, E. 2002. Adverse health effects in relation to urban residential soundscapes. *Journal of sound and vibration*, **250**(1), 151–155. 6

SOURDINE I CONSORTIUM. 2001. *Final report*. Tech. rept. Study of Optimisation procedURes for Decreasing the Impact of NoisE (SOURDINE) I. Report D5. 16, 19

SOURDINE II CONSORTIUM. 2003. *Identification document*. Tech. rept. Study of Optimisation procedURes for Decreasing the Impact of NoisE (SOURDINE) II. Report D1-1. Available at `http://www.sourdine.org/pub-documents.html`. 13, 17

SOURDINE II CONSORTIUM. 2006. *Final report*. Tech. rept. Study of Optimisation procedURes for Decreasing the Impact of NoisE (SOURDINE) II. Report D9-1. Available at `http://www.sourdine.org/pub-documents.html`. 19

SOUTHGATE, DAVE, AKED, ROB, FISHER, NICK, & RHYNEHART, GREG. 2000 (Mar.). *Expanding ways to describe and assess aircraft noise*. Discussion Paper. Department of Transport and Regional Services. Airports Operations area. Sydney Environment Section., Canberra (Australia). Available at `http://www.infrastructure.gov.au/aviation/environmental/transparent_noise/expanding/pdf/sepb_discussion_paper.pdf`. 119

SPALL, JAMES C. 2003. *Introduction to stochastic search and optimization: Estimation, simulation, and control*. New York (USA): Wiley-Interscience. 20

STEVENS, BRIAN L., & LEWIS, FRANK L. 1992. *Aircraft control and simulation*. London, UK: John Wiley and Sons, INC. 26, 129

SURYANARAYANA RAO, K.N., & PAL, S. 2004 (June). The indian SBAS system - GAGAN. *In: India-United States conference on space science, applications, and commerce*. AIAA, Bangalore (India). 109

SUZUKI, SHINJI, & YANAGIDA, AKIRA. 2008 (Sep). Research and development for fault tolerant flight control system - Part 1. Intelligent flight control system. *In: Proceedings of the 26th international congress of the aeronautical sciences (ICAS)*. AIAA/ICAS, Anchorage, Alaska (USA). 20

SUZUKI, SHINJI, TSUCHIYA, TAKESHI, & ANDREEVA, A. 2009 (Mar). Trajectory optimization for safe, clean and quiet flight. *In: Proceedings of the 1st ENRI International Workshop on ATM/CNS (EIWAC)*. Electronic Navigation Research Institute (ENRI), Tokyo, Japan. 20

SÁEZ NIETO, F.J., & SALAMANCA BUENO, M.A. 1995. *Sistemas y equipos para la navegación y circulación aérea*. Madrid (Spain): Fundación General UPM. (In Spanish). 108

TANAKA, KAZUO. 1997. *An introduction to fuzzy logic for practical applications*. Berlin - New York: Springer-Verlag. 36, 139

THE PARLIAMENTARY OFFICE OF SCIENCE AND TECHNOLOGY. 2003 (Apr). *Postnote – Aviation and the environment*. Report Summary Number 195, London, England (United Kingdom). www.parliament.uk/post. 2

THOMAS, GEOFFREY. 2008. Making engines greener. *Air transport world*, **45**(12), 47–48. 2

TSUCHIYA, TAKESHI, ISHII, HIROKAZU, UCHIDA, JUNICHI, IKAIDA, HIROSHI, GOMI, HIROMI, MATAYOSHI, NAOKI, & OKUNO, YOSHINORI. 2009. Flight trajectory optimization to minimize ground noise in helicopter landing approach. *Journal of guidance, control and dynamics*, **32**(2), 605–615. 20

VAJDA, S. 1974. *Theory of linear and non-linear programming*. London (UK): Longman. 19

VALLET, M. 2006 (Jun). Specificity of aircraft noise compared to other transport sources. *In: Proceedings of the 6th european conference on noise control (EURONOISE)*. European Acoustics Association (EAA), Acoustical Society of Finland, VTT (Technical Research Centre of Finland). 21

VANDERBEI, ROBERT J. 2000. *A case study in trajectory optimization: Range maximiation for a hang glider*. Who's Who Case Studies. Available on-line at `http://www.e-optimization.com`. 46

VENTURA-TRAVESSET, JAVIER, MICHEL, P., & GAUTHIER, L. 2001 (Oct.). Architecture, mission and signal processing aspects of the EGNOS system: the first european implementation of GNSS. *In: 7th international workshop on digital signal processing techniques for space communications*. 109

VERKEYN, ANDY. 2004 (Feb). *Fuzzy modeling of noise annoyance*. Ph.D. thesis, Gent Universsity, Gent (Belgium). 21, 22, 36, 39

VERKEYN, ANDY, & BOTTELDOOREN, DICK. 2004. Fuzzy translation tool for linguistic terms. *Pages 1065–1071 of: Proceedings of the IEEE international conference on fuzzy systems*. 22

VIRTANEN, KAI, EHTAMO, HARRI, RAIVIO, TOMAS, & HÄMÄLÄINEN, RAIMO P. 1999. VIATO - visual interactive aircraft trajectory optimization. *IEEE Transactions of systems, man, and cybernetics - Part C: Applications and reviews*, **29**(3), 409–421. 46, 133

VISSER, HENDRIKUS G. 1990 (Sep). Four-dimensional fuel-optimal flights into and out of the terminal area. *Pages 1468–1478 of: Proceedings of the 17th ICAS congress*, vol. 2. ICAS. A91-24301 09-01. 18

VISSER, HENDRIKUS G. 2005. Generic and site spacific criteria in the optimization of noise abatement procedures. *Transportation research part D: Transportation and environment*, **10**(5), 405–419. 20, 53

VISSER, HENDRIKUS G., & WIJNEN, ROLAND A.A. 2001. Optimization of noise abatement departure trajectories. *Journal of aircraft*, **38**(4), 620–627. 19, 23

VISSER, HENDRIKUS G., & WIJNEN, ROLAND A.A. 2003. Optimization of noise abatement arrival trajectories. *The aeronautical journal*, **107**(1076), 607–615. 20, 23

VORMER, F. J., MULDER, M., VAN PAASSEN, M. M., & MULDER, J. A. 2006. Optimization of flexible approach trajectories using a genetic algorithm. *Journal of aircraft*, **43**(4), 941–952. 20

VORMER, FRIZO JAN-PETER. 2005 (Dec). *Theoretical and operational aspects of optimal airport arrival trajectories*. Ph.D. thesis, TU Delft, Delft (The Netherlands). 20

VOS, J. 2000. On total annoyance caused by different environmental sounds: a review and suggestions for additional research. *Pages 3556–3561 of:* D, CASSEREAU (ed), *Proceedings of the 29th international congress and exhibition on noise control engineering. internoise 2000.*, vol. 6. Societe Francaise d'Acoustique (S.F.A.), Nice (France). 21

WEBER, E., RIZZOLI, A.E., R., SONCINI-SESSA, & CASTELLETTI, A. 2002. Lexicographic optimisation for water resources planning: The case of lake Verbano, Italy. *In:* RIZZOLI, A. E., & JAKEMAN, A. J. (eds), *Proceedings of the 1st biennial meeting of IEMSS. Integrated assessment and decision support.* 54

WELLS, D. 1967. *Theory and problems of Lagrangian dynamics.* New York - London: McGraw-Hill Science/Engineering/Math. Schaum's Outline Series. 126

WIJNEN, ROLAND A.A., & VISSER, HENDRIKUS G. 2003. Optimal departure trajectories with respect to sleep disturbance. *Aerospace science and technology*, **7**, 81–91. 23

WILLIAMS, VICTORIA. 2007. European ATM and the environment. *Chap. 5, pages 123–149 of:* COOK, ANDREW (ed), *European air traffic management. principles, practice and research.* Aldershot, England: Ashgate Publishing Limited. 4

WILSON, IAN A. B. 2007 (Apr). 4-dimensional trajectories and automation connotations and lessons learned from past research. *In: Proceedings of the integrated communications, navigation and surveillance conference (ICNS).* IEEE, Herndon, Virginia (USA). 6

WUBBEN, F.J.M., & BUSINK, J.J. 2000 (May). *Environmental benefits of continuous descent approaches at Schiphol airport compared with conventional approach procedures*. Tech. rept. Nationaal Lucht- en Ruimtevaartlaboratorium (NLR). Document No: NLR-TP-2000-275. 17

XUE, MIN. 2006 (Feb). *Real time terminal area trajectory planning for runway independent aircraft*. Ph.D. thesis, University of Maryland, College Park, Maryland (USA). 20, 23, 53

XUE, MIN, & ATKINS, ELLA M. 2003 (Aug). Noise-sensitive final approach trajectory optimization for runway-independent aircraft. *In: Proceedings of the AIAA guidance, navigation, and control conference*. American Institute of Aeronautics and Astronautics, Austin, Texas (USA). 20

XUE, MIN, & ATKINS, ELLA M. 2006a. Noise-minimum runway-independent aircraft approach design for Baltimore-Washington international airport. *Journal of aircraft*, **43**(1), 39–51. 20

XUE, MIN, & ATKINS, ELLA M. 2006b (Jan). Terminal area trajectory optimization using simulated annealing. *In: Proceedings of the 44th AIAA aerospace sciences meeting and exhibit*. American Institute of Aeronautics and Astronautics, Reno, Nevada (USA). 20

ZADEH, LOFTI A. 1965. Fuzzy sets. *Information and control*, **8**, 338–353. 137

ZADEH, LOFTI A. 1975a. The concept of a linguistic variable and its application to approximate reasoning. Part I. *Journal of information sciences*, **8**, 199–249. 137

ZADEH, LOFTI A. 1975b. The concept of a linguistic variable and its application to approximate reasoning. Part II. *Journal of information sciences*, **8**, 301–357. 137

ZADEH, LOFTI A. 1975c. The concept of a linguistic variable and its application to approximate reasoning. Part III. *Journal of information sciences*, **9**, 43–80. 137

ZADEH, LOFTI A. 1978. Fuzzy sets as a basis for a theory of possibility. *Fuzzy sets and systems*, **1**, 3–28. 137

ZADEH, LOFTI A. 1983. The role of fuzzy logic in the management of uncertainty in expert systems. *Fuzzy sets and systems*, **11**, 199–227. 137

ZAHEERUDDIN, & VINOD, JAIN K. 2006. A fuzzy expert system for noise-induced sleep disturbance. *Expert systems with applications*, **30**, 761–771. 23

ZAHEERUDDIN, JAIN, V. K., & SINGH, G.V. 2003. Fuzzy modelling of human work efficiency in noisy environment. *In: Proceedings of the IEEE international conferenceon fuuy systems*. IEEE. 23

ZAHEERUDDIN, VINOD, JAIN K., & GURU, SINGH V. 2006. A fuzzy model for noise-induced annoyance. *IEE Transactions on systems man and cyberetics - part A: Systems and humans*, **36**(4), 697–705. 23

ZALOVCIK, JOHN A., & SHAEFER, WILLIAM T. 1967 (Jun). *NASA research on noise abatement approach profiles for multiengine jet transport aircraft*. Tech. rept. NASA - Langley Research Center. Technical note: TN-D-4044. 11

ZAPOROZHETS, OLEKSANDER I., & TOKAREV, VADIM I. 1998a. Aircraft noise modelling for environmental assessment around airports. *Journal of applied acoustics*, **55**(2), 99–127. 32, 119

ZAPOROZHETS, OLEKSANDER I., & TOKAREV, VADIM I. 1998b. Predicted flight procedures for minimum noise impact. *Journal of applied acoustics*, **55**(2), 129–143. 18

ZOU, KATHERINE FENG. 2004 (Jun). *Real-time trajectory optimization and air traffic control simulation for noise abatement approach procedures*. M.Phil. thesis, Massachusetts Institute of Technology (MIT), Boston, Massachusets (USA). 20

ZOU, KATHERINE FENG, & CLARKE, JOHN-PAUL. 2003. Adaptative real-time optimization algorithm for noise abatement approach procedures. *In: Proceedings of the 3rd AIAA aviation technology, integration, and operations (ATIO) conference*, vol. 1. Denver, Colorado (USA): American Insitute of Aeronautics and Astronautics. AIAA paper No 2003-6771. 20

Avinguda del Parc Logístic, 12-20
08040 Barcelona
Tel: +34 93 230 50 00
www.abertis.com

Contributions to the optimisation of aircraft noise abatement procedures

Author: **Xavier Prats i Menéndez**

Directors: **Dr. Joseba Quevedo Casin**
Dr. Vicenç Puig Cayuela

Castelldefels (Barcelona), January 2010